Advancements in site-directed incorporation of rigid spin-labels into nucleic acids

Haraldur Yngvi Júlíusson

Faculty of Physical Sciences

School of Engineering and Natural Sciences

University of Iceland

Advancements in site-directed incorporation of rigid spin-labels into nucleic acids

Haraldur Yngvi Júlíusson

Dissertation submitted in partial fulfillment of a

Philosophiae Doctor degree in Chemistry

Advisor

Prof. Snorri Th. Sigurdsson

PhD Committee

Prof. Guðmundur G. Haraldsson

Prof. Már Másson

Assistant Professor Benjamín Ragnar Sveinbjörnsson

Opponents

Dr. Stefán Jónsson

Associate Professor Stefan Vogel

Faculty of physical sciences

School of Engineering and Natural Sciences

University of Iceland

Reykjavik, February 2020

Advancements in site-directed incorporation of rigid spin-labels into nucleic acids

Advancements in spin-labeling of nucleic acids.

Dissertation submitted in partial fulfillment of a *Philosophiae Doctor* degree in Chemistry

Faculty of physical sciences
School of Engineering and Natural Sciences
University of Iceland
Dunhagi 3
107, Reykjavik
Iceland

Telephone: 525 4000

Bibliographic information:
Haraldur Yngvi Júlíusson, 2020, *Advancements in site-directed incorporation of rigid spin-labels into nucleic acids*, PhD dissertation, Faculty of physical sciences, University of Iceland, XX pp.

Author ORCID:XX

Printing: XX
Reykjavik, Iceland, XXmonth 20XX

Abstract

Electron paramagnetic resonance (EPR) spectroscopy is routinely used to study the structure and dynamics of nucleic acids to obtain information about their functions. Incorporation of a paramagnetic center into nucleic acids is necessary prior to EPR measurements. This doctoral dissertation focuses on improvements in nitroxide spin-labeling of nucleic acids for structure determination using rigid spin labels. The first part of this thesis describes the development of a protecting group strategy for nitroxide radicals to circumvent their reduction during the chemical synthesis of DNA. Specifically, a benzoylated hydroxylamine was used as a protected form of the nitroxide. This method was used to incorporate the rigid spin label **Ç** into DNA oligonucleotides and represents a general strategy for spin labeling nucleic acids using the phosphoramidite method.

In the second part of the thesis, the synthesis of the reduction-resistant spin labels **EÇ** and **EÇm** is described, nitroxides that will facilitate application of EPR spectroscopy for the investigation of nucleic acids within cells. Both labels possess rigidity for extracting detailed information about structure and dynamics by EPR. **EÇ** and **EÇm** were incorporated into DNA and RNA, respectively, by oligonucleotide synthesis. Partial reduction of **EÇm** during RNA synthesis was observed but was circumvented by using the aforementioned benzoyl protecting group strategy. **EÇ** and **EÇm** were shown to be non-perturbing of duplex DNA and RNA structures, respectively.

The third part of this thesis describes the synthesis of *o*-benzoquinone derivatives of isoindoline and their condensation with *o*-phenylenediamines to form isoindoline-phenazines. Subsequent oxidation gave phenazine-di-*N*-oxide radicals that were evaluated for noncovalent spin-labeling of duplex DNA and RNA containing abasic sites. No specific binding was observed for RNA, but an unsubstituted phenazine-*N*,*N*-dioxide tetramethyl isoindoline nitroxide showed

high binding affinity and specificity towards abasic sites in duplex DNA opposite to C.

Útdráttur

Rafeindasegullitrófsgreiningu (e. Electron Paramagnetic Resonance, EPR) er reglubundið beitt í rannsóknum á byggingu og hreyfingu kjarnsýra til að fá upplýsingar um starfsemi þeirra og hlutverk. Innleiðing meðseglandi kjarna á ákveðinn stað í kjarnsýrum er nauðsynleg fyrir EPR mælingar og er það gert með aðferð sem kallast staðbundin spunamerking. Þessi doktorsritgerð lýsir betrumbótum á staðbundinni spunamerkingu á kjarnsýrum með notkun stífra spunamerkja. Fyrsti hluti ritgerðarinnar lýsir þróun á aðferð til verndunar nítroxíð stakeinda til að koma í veg fyrir afoxun þeirra þegar spunamerktar kjarnsýrur eru útbúnar með efnasmíði. Notast var við bensóylverndað hýdroxylamín til verndunar á nítroxíðinu. Þessi aðferð var notuð til að innleiða stífa spunamerkið **Ç** inn í DNA kjarnsýrur og lofar góðu sem almenn aðferð til þess að innleiða spunamerki í kjarnsýrur með fosfóramíðít efnasmíði.

Í öðrum hluta ritgerðarinnar er efnasmíði á spunamerkjunum **EÇ** og **EÇm** lýst, en bæði eru stöðug við afoxandi aðstæður. Þessi spunamerki eru ætluð til notkunar við innan-fruma EPR mælingar á kjarnsýrum. Bæði spunamerkin eru stíf, sem gerir mögulegt að fá nákvæmar upplýsingar um byggingu og hreyfingu kjarnsýra með EPR. **EÇ** var innleitt í DNA og **EÇm** í RNA með kjarnsýruefnasmíði. **EÇm** afoxaðist að hluta til á meðan á RNA smíðinni stóð en þá afoxun var unnt að koma í veg fyrir með fyrrnefndri bensóyl verndun nítroxíðsins. Sýnt var fram á að **EÇ** og **EÇm** breyttu ekki byggingu DNA og RNA tvíliða.

Þriðji hluti ritgerðarinnar lýsir efnasmíðum á *o*-bensókvinón afleiðum af ísóindólíni og þéttingu þeirra með *o*-fenýlentvíamínum til að mynda ísóindólín-fenasín afleiður. Í kjölfarið voru þær oxaðar í fenasín-tví-*N*-oxíð nítroxíð og kannað hvort unnt væri að nota þær til spunamerkinga án samgildra tengja á tvístrendum DNA og RNA kjarnsýrum sem innihalda basalausar stöður. Ósetið fenasín-*N*,*N*-

tvíoxíð tetrametýlísóindólín nítroxíð sýndi mikla sækni í basalausa stöðu í DNA á móti basanum C.

Dedicated to Arna Albertsdóttir

and

my children Stefanía and Ágúst

Table of Contents

List of Figures

List of Schemes

List of Tables

Abbreviations

A	adenine
C	cytosine
Ç	rigid spin-labeled nucleoside “C-spin” for DNA
Çm	rigid spin-labeled nucleoside “C-spin” for RNA
CD	circular dichroism
CW	continuous wave
DEER	double electron-electron resonance
DMAP	dimethyl amino pyridine
DMF	*N,N*-dimethylformamide
DMTCl	4,4′-dimethoxytrityl chloride
DMSO	dimethylsulfoxide
DNA	deoxyribonucleic acid
EPR	electron paramagnetic resonance
FRET	fluorescence resonance energy transfer
G	guanine
K_D	dissociation constant
kDa	kilodalton
mRNA	messenger ribonucleic acid
m-CPBA	*meta*-chloroperbenzoic acid
NC-SDSL	noncovalent site-directed spin labeling
NMR	nuclear magnetic resonance
μM	Micromolar
PELDOR	pulsed electron-electron double resonance
RNA	ribonucleic acid
rRNA	ribosomal ribonucleic acid
SDSL	site-directed spin labeling
T	Thymine
TBAF	tetrabutylammonium fluoride
TBDMS	*tert*-butyldimethyl silyl
TEMPO	2,2,6,6-tetramethylpiperidine-1-oxyl
TLC	thin layer chromatography
tRNA	transfer ribonucleic acid
T_M	melting temperature
DPAGE	denaturing polyacrylamide gel electrophoresis

Acknowledgements

Firstly, I would like to express my sincere gratitude to my doctoral supervisor Prof. Snorri. Th. Sigurdsson for offering me the opportunity to do a PhD in organic chemistry and to be a part of his research group which has been an enriching professional and personal experience. I thank him for the constructive discussions and his patience.

I want to take this opportunity to thank my doctoral committee members, Prof. Guðmundur G. Haraldsson, Prof. Már Másson and Assistant Professor Benjamín Ragnar Sveinbjörnsson for their encouragements and guidance. I would also like to thank my distinguished opponents, Dr. Stefán Jónsson and Associate Professor Stefan Vogel for being willing to review this dissertation and my work.

I am highly grateful to Anna-Lena Johanna Segler for an in-house collaboration. I would like to thank the present members of the Sigurdsson research group, Sucharita Mandal, Thomas Halbritter and Anna-Lena Johanna Segler, for all their help, friendship and support along with helpful discussions.

Last but not least, I would like to thank, my family and friends for their love and support. Especially, I would like to thank Arna Albertsdóttir, for her support, patience and love and our children, Stefanía and Ágúst for their love and patience.

1 Objects and scope of the PhD thesis

The functions of biopolymers are governed by their structure and dynamics. Therefore, to help us gain insights and understand their functions it is essential to investigate their structure and dynamics. Electron paramagnetic resonance (EPR) spectroscopy has emerged as a valuable technique for that purpose. In order to perform EPR studies on biopolymers, paramagnetic centers, called spin labels, need to be incorporated at chosen positions. This can be accomplished with a technique called site-directed spin-labeling (SDSL).

This doctoral dissertation focuses on three separate objectives, but their common goal is to improve nitroxide spin-labeling of nucleic acids for structure determination through electron paramagnetic resonance (EPR) spectroscopy, with a focus on rigid spin labels. The first objective, described in **Chapter 3**, focuses on a protecting group strategy for improved spin-labelling efficiency of nucleic acids through the phosphoramidite approach. The second objective, delineated in **Chapter 4**, describes the design, synthesis and incorporation of reduction-resistant tetraethyl-derived rigid spin labels into DNA and RNA. The third objective, delineated in **Chapter 5**, describes the design and synthesis of *o*-quinone isoindoline derivatives that, through condensation with o-phenylenediamines, allow for easy access to various diversely substituted phenazine structures carrying the isoindoline moiety.

Chapter 2 contains a brief introduction into biomolecules with the focus on nucleic acids and their biological importance. It covers the important spectroscopic techniques that have been used for structural studies of nucleic acids with the main focus on the use of EPR spectroscopy. The chapter also briefly outlines the different approaches used for spin-labeling of nucleic acids.

In the first part of **Chapter 3**, detailed introduction is given for solid phase synthesis of oligonucleotides through the phosphoramidite approach, including advantages and disadvantages of the method along with previous attempts at rectifying them. Detailed design and synthesis of a benzoyl-protected hydroxylamine of **Ç**, called **Ç-Bz** (**Figure 1.1**), is given in the later part of the chapter along with its incorporation into DNA though the phosphoramidite approach. The benzoyl protecting group was shown to be stable through the oligonucleotide synthesis and that it could be completely removed using standard oligonucleotide deprotection conditions, returning **Ç** in quantitative yields. This method circumvented one of the biggest problems that has plagued nitroxide radicals when used as spin-labels in the solid-phase synthesis of oligonucleotides, namely reduction of the radical to its corresponding EPR-silent amine.

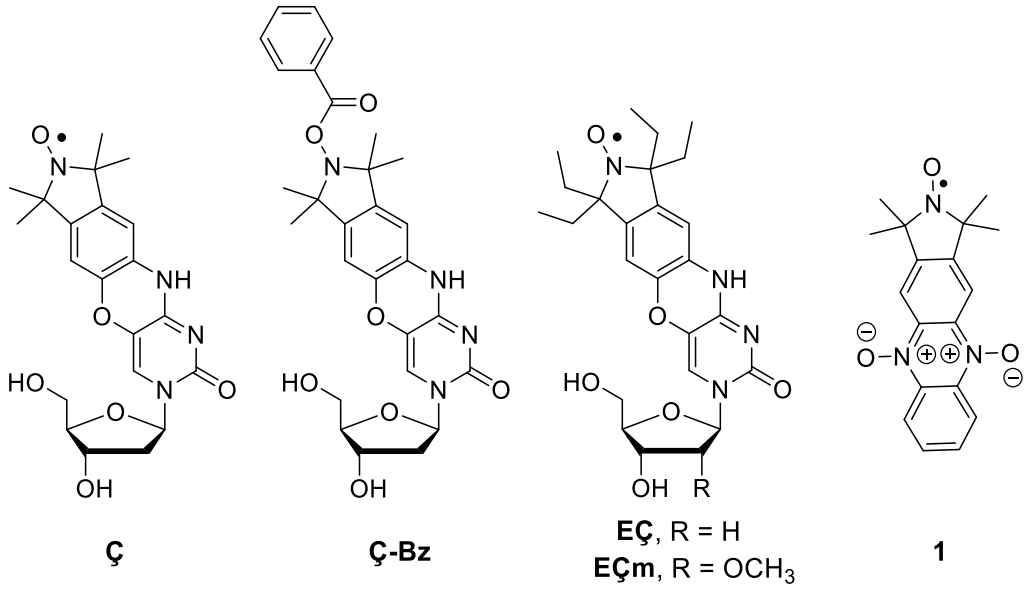

Figure 1.1. Structures of the rigid spin-labels **Ç**,[1] its benzoylated form **Ç-Bz**, **EÇ**, **EÇm**, and isoindoline-phenazine-N-oxide spin-label **1**.

The beginning of the **Chapter 4** contains a brief discussion of flexibility vs. rigidity of spin-labels along with a detailed introduction of the study of biomolecules in cells with the focus on the use of EPR spectroscopy. The latter part of the chapter describes the design, synthesis, and incorporation of the ethyl-derived spin labels **EÇ** and **EÇm** (**Figure 1.1**) into DNA and RNA, respectively. The

labels were shown to have a negligible effect on the stability and conformation of both DNA and RNA duplexes, indicating that they are nonperturbing of duplex structures. Substantial reduction of **EÇm** took place during the synthesis of **EÇm**-labeled RNA and that reduction was circumvented by using the benzoyl protecting method previously described in **Chapter 3**. **EÇ** and **EÇm** possess both the rigidity and the reduction resistance needed for extracting detailed structural information *in-cell* by EPR spectroscopy.

Chapter 5 begins with a brief introduction into rigid 5,6-locked nucleosides and their uses as spectroscopic labels for nucleic acids. The design and synthesis of *o*-quinone isoindoline derivatives are described and attempts at using them to obtain 5,6-locked spin-labeled nucleosides. Later in the chapter the condensation of the previously synthesized *o*-quinone isoindoline derivates with a number of *o*-phenylenediamines to obtain various diversely substituted phenazine structures carrying the isoindoline moiety are described. Oxidation of the isoindoline-phenazines gave phenazine di-*N*-oxide nitroxide radicals that were evaluated as noncovalent spin labels for DNA and RNA containing abasic sites. Spin label **1** (**Figure 1.1**) showed high binding affinity and specificity towards abasic sites opposite to cytidine (C) in DNA and is, therefore, a promising spin label for future EPR studies of DNA.

2 Introduction

All life on Earth shares a common chemistry which provides indirect evidence for evolution. Despite the great variety of cells that exist, all living organisms contain only a few groups of carbon-based compounds, called biomolecules.[2] The four major groups of macromolecules within cells are carbohydrates, proteins, lipids and nucleic acids (**Figure 2.1)**.[3] Each group is an important component of the cell and performs a wide array of functions. Combined, these molecules make up the majority of a cell's mass.

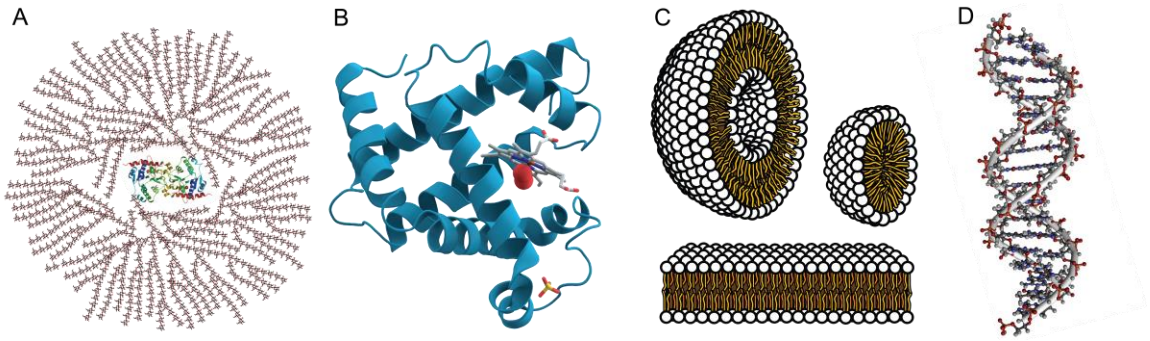

Figure 2.1. The four major groups of biomolecules. **A**. Carbohydrates (glycogenin surrounded by branches of glucose units as an example[4]). **B**. Proteins (myoglobin as an example). **C**. Lipids (phospholipids as an example). **D**. Nucleic acids (DNA duplex as an example).

Carbohydrates are comprised of the elements carbon (C), hydrogen (H), and oxygen (O) and are more commonly known as sugars.[5] They are used by cells as respiratory substrates but also carry a variety of other functions, such as the formation of structural components in plasma membranes and cell walls.[6] Lipids have many functions such as making up the bilayer of plasma membranes,[6, 7] as certain hormones[8], and as respiratory substrates.[9] Proteins form many cell structures and are also important as enzymes,[10] chemical messengers[11], and components of the blood.[12] Nucleic acids carry the genetic code for the production of proteins and as such they are the hereditary material for storage and transmission

of genetic information in all living organisms from one generation to the next.[13] This last group of biomolecules, nucleic acids, is the main focus of this thesis and will be described in more detail in the following section.

2.1 Nucleic acids

Friedrich Miescher, a Swiss scientist, isolated a precipitate of an unknown substance in 1869, which contained a large amount of phosphorous and lacked sulphur. Miescher named the precipitate "nuclein", as he had isolated it from the cell nuclei of leukocytes, a name that has been preserved in today's designation as nucleic acids.[14-16] Albrecht Kossel discovered the four bases, adenine, thymine, guanine and cytosine in 1896.[17] For a long time the three-dimensional structure of DNA was unknown and it was the subject of an intensive research effort in the late 1940s to early 1950s.[18] Initial work revealed that the polymer had a regular repeating structure. Rosalind Franklin came very close to elucidating the correct structure of DNA in 1952, by producing the first ever high-resolution crystallographic photographs of DNA fibers. She deduced the basic dimensions of DNA strands, and that the phosphates were on the outside of what was probably a helical structure.[19] It wasn't until almost a century after the first isolation of DNA that its structure was solved, in 1953, by James Watson and Francis Crick.[20] A discovery that marked a milestone in the history of science and gave rise to modern molecular biology.

The two main types of nucleic acids are deoxyribonucleic acid (DNA) and ribonucleic acid (RNA). DNA functions as a long-term storage of genetic information.[21] The presence of a 2'-hydroxyl group on the sugar moieties of RNA leads to much more diverse structural and chemical properties. DNA is transcribed into messenger RNA (mRNA) which carries genetic sequence information to a ribonucleoprotein machinery, made from proteins and ribosomal RNA (rRNA), called the ribosome.[22-24] The third type of RNA that is involved in the process of

translation into proteins, along with mRNA and rRNA, is transfer RNA (tRNA) which binds to mRNAs within the ribosome and transfers a specific amino acid to a growing polypeptide chain at the ribosomal site.[22, 24]

It has been revealed recently that RNA does much more than simply play a role in transferring genetic data to protein production. For example, many types of RNA have been found to have complex regulatory roles in cells such as gene expression or suppression. Small nuclear RNAs (snRNA) are involved in important processes of gene regulation through RNA splicing, which is performed by a complex of specialized RNA and protein subunit called the spliceosome.[25, 26] Micro RNA (miRNA) plays a role in gene expression and consists of small single-stranded RNAs that have been shown to silence translation of mRNA, or directly leading to mRNA degradation.[27-29] Small interfering RNAs (siRNA), also called short interfering RNAs, are yet another class of RNAs that lead to inhibition of gene expression.[30-32]

Another class of RNAs, referred to as ribozymes, have been found to be catalytic, similar to enzymes,[33, 34] and carry out biochemical reactions such as the cleavage of phosphodiester bonds in the absence of proteins.[35] An example of a ribozyme can be found in the aforementioned ribosome, responsible for peptide bond formations.[36] Of note it that there are several deoxyribozymes, called DNAzymes, that have been discovered and are capable of performing specific chemical reactions like ribozymes.[37, 38]

To gain insights into the variety of functions of nucleic acids collecting information about their structure and dynamics has become of great importance.

2.2 Structure determination of nucleic acids

Over the last few decades a variety of biochemical and biophysical techniques have been employed, and are still routinely used, to obtain structural information on

nucleic acids. X-ray crystallography is a high-resolution technique that can provide three-dimensional structural information on nucleic acids and other biomolecules, and is the most precise method as it gives precise arrangements of atoms in space.[39-41] However, this technique comes with some disadvantages as, to be able to study biomolecules with X-ray crystallography, a large and regular single crystal is required that diffracts well enough to get a high-resolution structure.[39] Obtaining such crystals can be labor-intensive, time-consuming and require large amounts of sample. Moreover, crystal structures of the biomolecules might not represent their biologically active conformation[41] and as the nucleic acid is in a crystalline state, conformational changes cannot be studied.

Nuclear magnetic resonance (NMR) spectroscopy is another widely used high-resolution technique that provides structural information about nucleic acids under biologically relevant conditions as well as information on dynamics.[42-45] Although NMR is highly effective for studying structure and dynamics of nucleic acids, it suffers from lack of sensitivity. Therefore, relatively large amounts of isotopically labeled samples of nucleic acids is required, which is a tedious work and expensive. Another limitation is that the molecular weight of the nucleic acids cannot exceed approximately 50 kDa.[46]

Fluorescence resonance energy transfer (FRET) is another technique that is frequently used to study nucleic acids.[47-49] FRET is based on the energy transfer from a donor chromophore to an acceptor chromophore and can be used to measure distances between two or more chromophores in the range of 10-100 Å. FRET has been used extensively to study tertiary structures of nucleic acids and has enabled studies of single-molecule studies.[50, 51] Although FRET is not considered as a high-resolution technique, it is highly sensitive and, therefore, requires small amounts of sample and can be carried out under biologically-relevant conditions. However, FRET also has disadvantages as it requires the incorporation of at least two different chromophores that are compatible (one donor, the other acceptor) with each other.

These chromophores can be rather bulky and can perturbate the nucleic acid duplex structures in question.

There are several other techniques that are useful for studying nucleic acids and provide low-resolution structural information. Examples of these methods are circular dichroism (CD) which provides information of secondary structures such as A, B and Z forms of helical structures,[52] non-denaturing gel electrophoresis[53, 54] and Raman spectroscopy.[55-57]

Electron paramagnetic resonance (EPR) spectroscopy is another method to study the structure and dynamics of nucleic acids, which will be described in detail in the following section and is the method that this thesis focuses on.

2.3 Electron paramagnetic resonance (EPR) spectroscopy

EPR spectroscopy, also known as electron spin resonance (ESR), was developed by the physicist Yevgeny Zavoisky in 1945.[58, 59] EPR spectroscopy detects paramagnetic centers such as free radicals and many transition metal ions. EPR has proven to be highly effective to study structure and dynamics of nucleic acids[60, 61] and other biomolecules, such as proteins.[62] EPR spectroscopy detects electron spins by monitoring transitions of unpaired electrons in an applied magnetic field and is in principle very similar to NMR, which detects transitions of nuclear spins. EPR detects the transition of electron spins from a lower to a higher energy level, which is induced by absorption of microwave radiation.[63]

Continuous wave (CW) EPR spectroscopy can provide information about structure and dynamics of specific sites of a biomolecule through line-broadening of the EPR spectra.[64-66] CW-EPR spectra are obtained by measuring a paramagnetic sample at a field microwave frequency while sweeping the external magnetic field. CW-EPR can be used for distance measurements in the range of 5 to 25 Å, based on the line-broadening due to dipolar coupling between two spin centers.[67] For longer

distance measurements pulsed EPR methods such as pulsed electron-electron double resonance (PELDOR), also called double electron-electron resonance (DEER), can be used and are able to measure distances in the range of 15-160 Å.[68, 69]

EPR spectroscopy possesses some desirable qualities and advantages over other spectroscopic methods. EPR spectra can be recorded under physiological conditions with high sensitivity. This requires less amounts of sample compared to NMR spectroscopy and X-ray crystallography and furthermore EPR spectroscopy has no molecular size limitation, unlike NMR spectroscopy.[70] One of the major disadvantages of EPR studies of nucleic acids and other biopolymers is that they are inherently diamagnetic. Therefore, it is necessary to modify the biopolymers of interest, prior to the EPR measurements, with paramagnetic molecules or groups, referred to as spin labels.[70, 71] There is a wide variety of paramagnetic compounds used for EPR spectroscopy as spin probes, for example metal ions, such as Gd(III) (**Figure 2.2 A**)[72] and Mn(II),[73] and carbon-based radicals[74, 75] (**Figure 2.2 B**) but the paramagnetic entities that are most commonly used for EPR applications are nitroxide radicals.[76] Nitroxides are usually small organic molecules that possess an unpaired electron which resonates between a nitrogen atom and an oxygen atom, flanked by sterically demanding side groups (**Figure 2.2 C**).

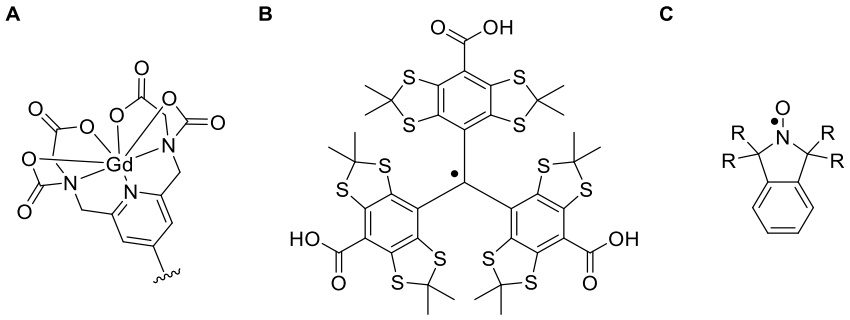

Figure 2.2. Examples of paramagnetic compounds used for EPR applications. **A.** PyMTA-Gd(III). **B.** A carbon-based trityl radical. **C.** An isoindoline nitroxide radical.

Radicals are usually known for their instability and reactivity but these nitroxides are stable because of the shielding that the bulky side groups provide along with the resonance of the radical.[77, 78] Spin labeling of biopolymers can be achieved with several methods and the major ones are described in the following section.

2.4 Site-directed spin-labeling (SDSL) of nucleic acids

For investigation of nucleic acids by EPR spectroscopy, a spin label must be incorporated at specific sites. That is accomplished with a method known as site-directed spin-labeling (SDSL).[60, 64, 79, 80] Attaching the spin-labels to nucleic acids can either be performed covalently or noncovalently (**Figure 2.3**). The first spin-labeling method, most often referred to as the phosphoramidite approach, involves spin-labeled phosphoramidite building blocks that are incorporated at specific sides during automated solid-phase synthesis of oligonucleotides (**Figure 2.3 A**). The second SDSL approach is post-synthetic spin-labeling (**Figure 2.3 B**). This method requires oligonucleotides that have reactive groups at specific sites for modification with the spin label after the oligonucleotide synthesis. These two methods are approaches that attach spin labels covalently to nucleic acids. The third SDSL strategy is noncovalent spin-labeling (**Figure 2.3 C**), which utilizes noncovalent interactions, specifically hydrogen bonding and π-stacking between spin labels and nucleic acids. The phosphoramidite method and the noncovalent spin-labeling method will be covered in more detail later in the thesis.

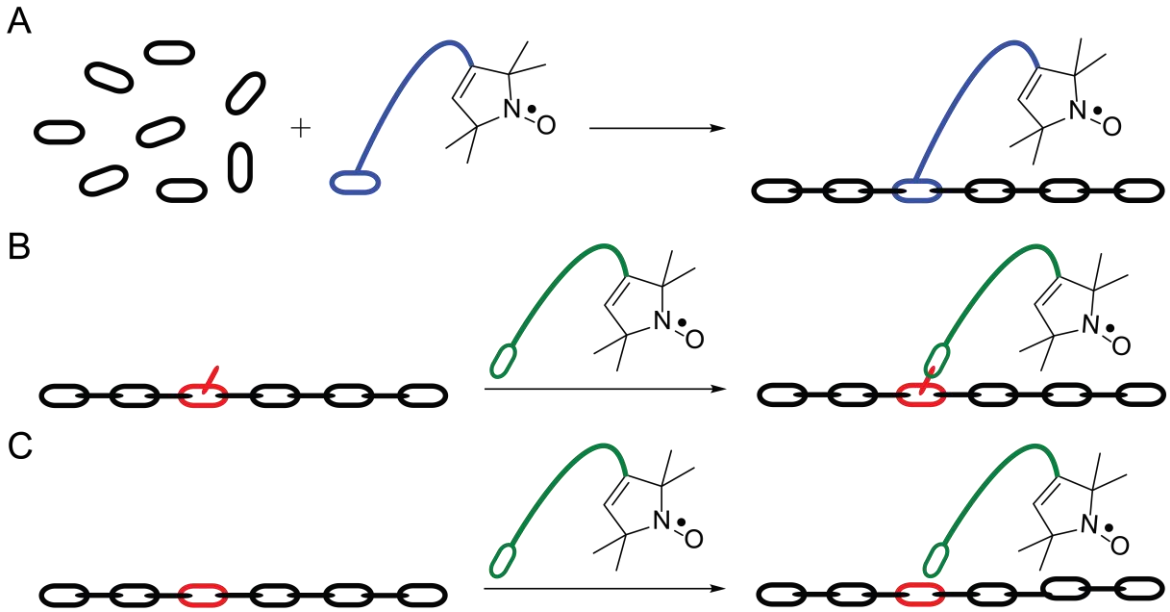

Figure 2.3. A general scheme of the main strategies used for site-directed spin labeling (SDSL) of nucleic acids, using a pyrrolidine-based spin-label as a representative nitroxide and nucleotides are represented by links that form oligonucleotide chains. **A**. The phosphoramidite approach. **B**. Post-synthetic spin-labeling. **C**. Noncovalent spin labeling.

2.5 Contribution of this thesis to the studies of nucleic acids by EPR spectroscopy

The work presented within this thesis focuses on new rigid nitroxide spin-labels and improved methods for incorporation of spin labels into nucleic acids.

Chapter 3 describes a new protecting group strategy for nitroxide radicals suitable for oligonucleotide synthesis by the phosphoramidite approach. This approach greatly improves the chemical synthesis of oligonucleotides containing nitroxide spin-labels. The method involves protection of the hydroxylamine of the corresponding nitroxide with a benzoyl group. The benzoyl group is stable through the oligonucleotide synthesis and is readily removed under standard oligonucleotide deprotection conditions, yielding a hydroxylamine that is oxidized *in situ* to the nitroxide. This protecting group strategy facilitates the high-yielding synthesis of spin-labeled DNA and RNA oligonucleotides using the phosphoramidite method and made it possible to synthesize a doubly labeled 36-

nucleotide long DNAzyme. **Chapter 4** describes the design, synthesis and incorporation of tetraethyl-derived rigid spin labels **EÇ** and **EÇm** into DNA and RNA, respectively, that possess the reduction resistance needed along with the rigidity for extracting detailed structural information by *in-cell* EPR spectroscopy. It was shown that **EÇ** and **EÇm** had minimal effect on conformation and stability of B-DNA and A-RNA duplexes, respectively. **Chapter 5** describes the design and synthesis of *o*-quinone isoindoline derivatives that allow easy access to various substituted isoindoline-phenazine structures through the condensation with *o*-phenylenediamines. Oxidation of the isoindoline-phenazine structures yielded phenazine di-*N*-oxide nitroxide radicals that were evaluated as noncovalent spin labels for DNA and RNA containing abasic sites. One of those labels, spin label **1** (**Figure 1.1**), showed high binding affinity and specificity towards abasic sites opposite to C in DNA and is, therefore, a promising spin label for future EPR studies of DNAs.

3 A protecting group strategy for nitroxide radicals suitable for chemical synthesis of oligonucleotides

3.1 Introduction

The spin labeling approach that completely changed the use of modified nucleic acids for structural determination and various applications is the aforementioned phosphoramidite approach, which utilizes automated chemical synthesis of nucleic acids on a solid support. The phosphoramidite method, developed by Caruthers,[81-84] describes the step wise synthesis of polynucleotides and allows incorporation of modified nucleotides into predetermined positions in the nucleic acid. This is currently the only method that allows for incorporation of intricate nitroxide spin-labels with unique structural features, such as rigid labels, into nucleic acids.

3.1.1 Principles of solid-phase synthesis of nucleic acids

The synthesis of DNA by the phosphoramidite approach is shown schematically in **Figure** 3.1. Prior to the automated solid-phase synthesis of oligonucleotides, preparation of phosphoramidite building blocks is needed. The exocyclic amino groups of nucleobases A, C and G are protected as amides, the 5′-hydroxy group is protected as a dimethoxytrityl ether (DMT) and the 3′-hydroxy group is phosphitylated to give a phosphoramidite (**Figure 3.1 A**). The oligonucleotide synthesis is directed from the 3′- to the 5′-terminus in which the first base of the desired oligomer is attached to a solid support. After coupling of the first

phosphoramidite through a tetrazole-catalyzed reaction with deprotected 5′-hydroxyl group on the oligomer, which adds a new nucleotide to the growing oligomer chain (**3**, **Figure 3.1 B**), any unreacted 5′-deprotected oligomer is capped with an acetyl group (**4**, **Figure 3.1 B**) to prevent the formation of N-1 oligonucleotides. Next, the phosphorus atom is oxidized from a trivalent to pentavalent state (**5**, **Figure 3.1 B**), and the 5-hydroxy group is deprotected (**6**, **Figure 3.1 B**), setting the stage for the next coupling reaction. After the desired sequence of the oligomer has been synthesized, the exocyclic amino groups and the phosphates are deprotected and the oligomer is cleaved from the resin, all in one step, by heating in aqueous ammonia (**7**, **Figure 3.1 B**). RNA has also been synthesized by this approach, with use of a protecting group for the 2′-hydroxy group.[85-87]

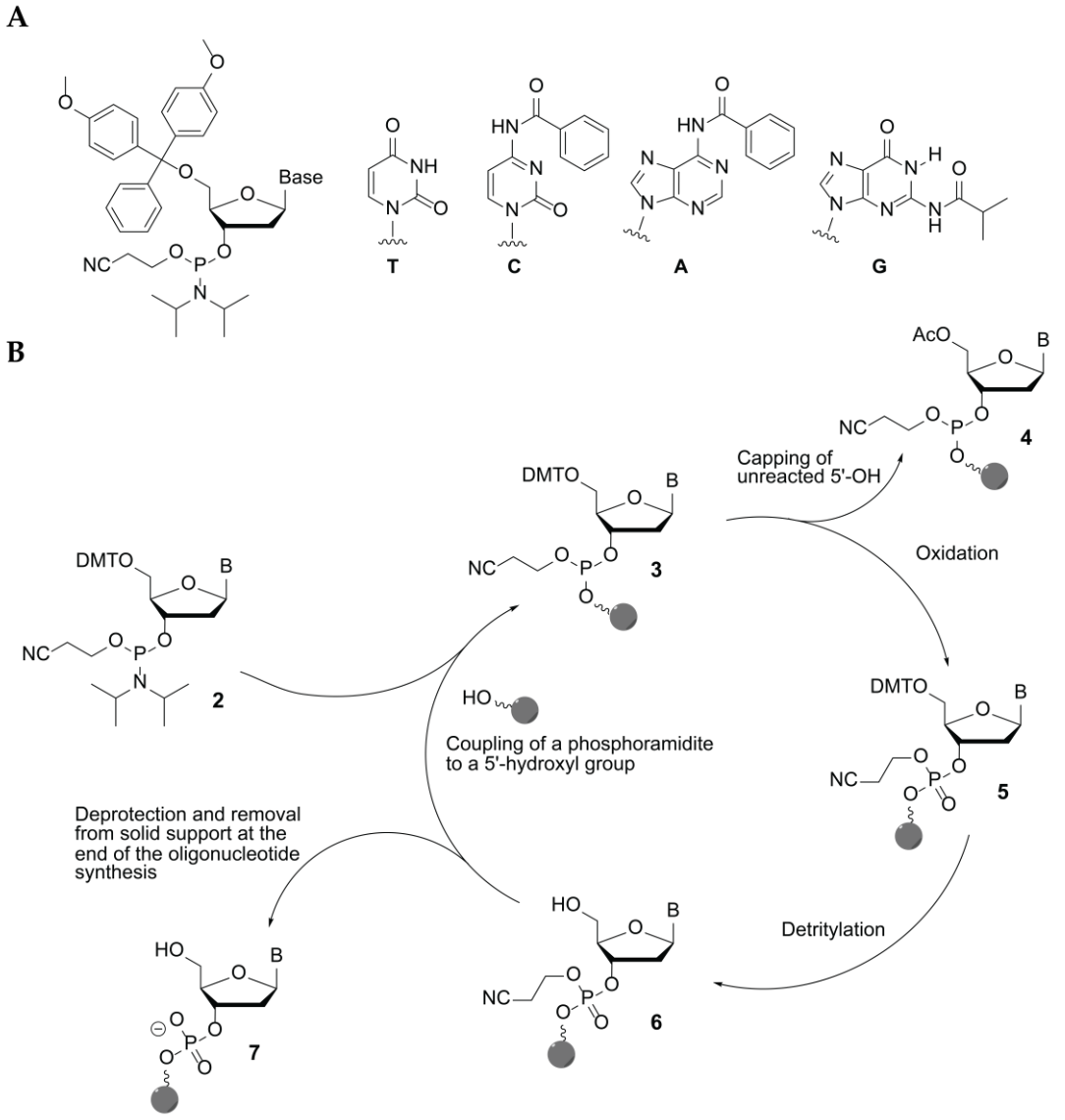

Figure 3.1. **A.** Structure of phosphoramidites used for an automated DNA synthesis. **B.** Automated chemical synthesis of DNA oligonucleotides with the phosphoramidite approach.

3.1.2 Solid-phase synthesis of spin-labeled nucleic acids

The first report of site-directed spin-labeling of nucleic acids using automated chemical synthesis by the phosphoramidite approach was by Hopkins *et al.* His group prepared the spin-labeled nucleosides **8**[88] and **9**[89] (**Figure 3.2**), 2′-deoxy uridine and 2′-deoxy cytidine derivatives, respectively, and incorporated into DNA, where they were found to be well tolerated in the major groove of the DNA duplex and showed limited motion relative to the nucleic acid. Gannet *et al.* prepared spin label **10**[90] which is another example of a spin label that has restricted motion

relative to the nucleic acid. The spin label was successfully incorporated into oligonucleotides and used to probe the structural changes during DNA duplex and triplex formation by CW-EPR[91] as well as studying G-quadruplex conformations in human telomeric DNA by PELDOR.[92] Nucleosides **11** and **12**[93] as well as **13** and **14**,[94] (**Figure 3.2**) all of which contain spin-labels on their exocyclic amino groups, have also been incorporated site-specifically into nucleic acids by the phosphoramidite approach. These labels have been used for detection of mismatches and to identify its base-pairing partner[95, 96] in duplex DNA along with distance measurements.

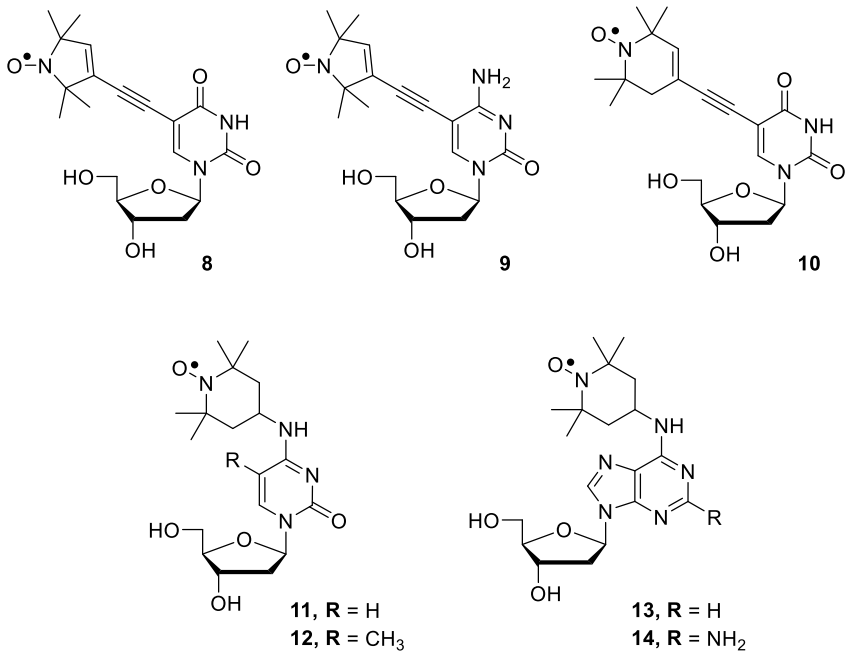

Figure 3.2. Examples of nucleosides containing spin labels that have been incorporated into oligonucleotides by the phosphoramidite approach.

A different strategy for incorporation of spin labels **15**[97] and **16**-**18**[98] (**Figure 3.3 A**) into oligonucleotides was reported by Engels and co-workers, by utilization of an on-column coupling method during the solid phase synthesis of the oligonucleotides, where the spin-label is coupled to the nucleobase during the oligonucleotide synthesis (**Figure 3.3 B**). These labeled nucleotides enabled the measurement of accurate long-range distances in DNA and RNA by PELDOR.[97-99]

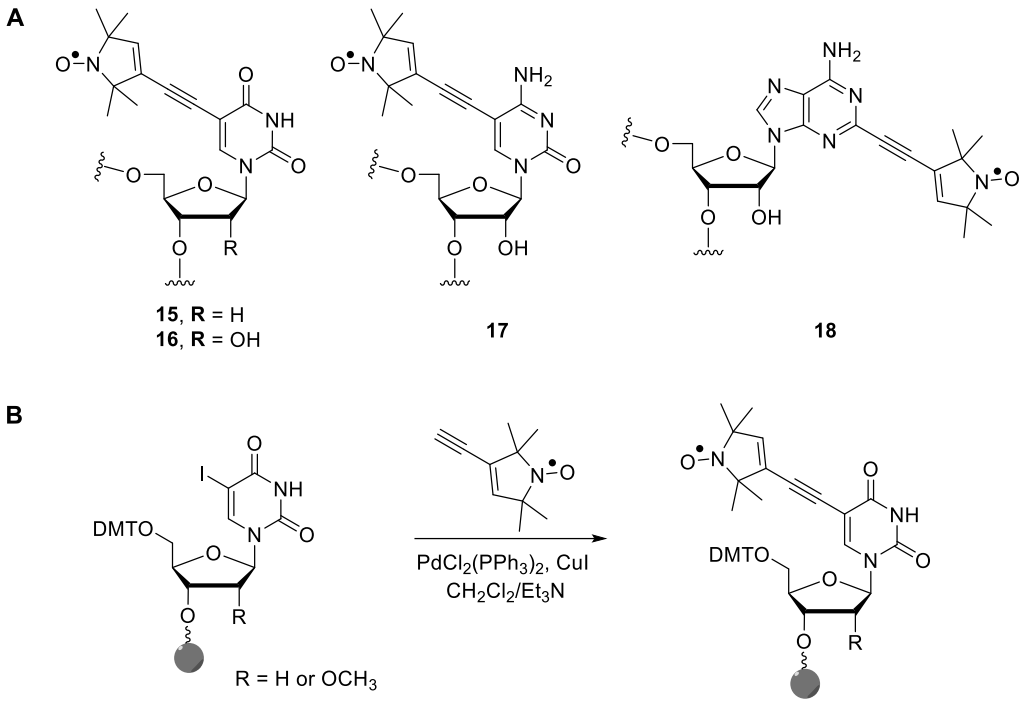

Figure 3.3. **A**. Examples of spin labeled nucleosides where the spin label was incorporated with the on-column coupling during the solid phase synthesis. **B**. An example of the on-column coupling method during the solid phase synthesis of the oligonucleotides, reported by Engels *et al*.[97]

Sigurdsson and co-workers have reported several different spin-labels that were used to label nucleic acids through the phosphoramidite approach, many of them possessing desirable qualities. Of note are the rigid spin labels **Ç**[1] and **Çm**[100] (**Figure 3.4**), analogues of cytidine (C), that can base-pair with guanine (G). Both **Ç** and **Çm** have been incorporated into DNA and RNA, respectively, allowing accurate distance measurements in duplex oligonucleotides. The rigidity also enabled determination of relative orientations of two labels by PELDOR, which provides further insights into structure and dynamics of nucleic acids.[101-105] An interesting feature of **Ç** and **Çm** is that upon reduction of the nitroxide functional group to the corresponding amines **Çf** and **Çmf** (**Figure 3.4**) the nucleosides become fluorescent. Sigurdsson and co-workers have also reported the semi-rigid spin-labels ^{Ox}**U,** ^{Im}**U** and ^{Im}**Um** (**Figure 3.4**) that have been used to label oligonucleotides through the phosphoramidite approach. The spin labels ^{Im}**U** and ^{Im}**Um** are less mobile than ^{Ox}**U** due to intramolecular hydrogen-bonding of the NH on benzimidazole and O4 of the uracil base.[66, 106, 107]

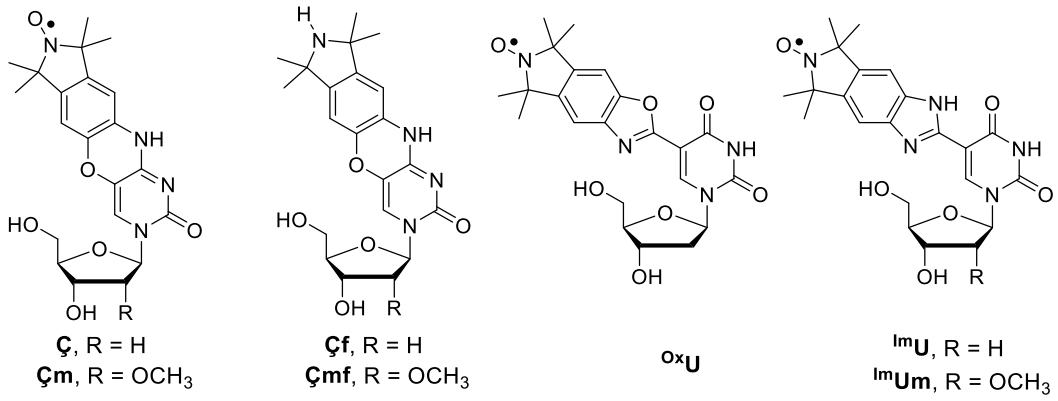

Figure 3.4. Structures of rigid and semi-rigid spin-labels reported by Sigurdsson *et al*.[1, 66, 100]

The main disadvantage of the phosphoramidite approach for incorporation of nitroxide spin labels into nucleic acids is that the nitroxides get partially reduced to their corresponding EPR silent amine.[108] This reduction happens during the iodine oxidation, the stepwise trityl deblocking and by tetrazolide activation during the phosphoramidite coupling. For oligonucleotides shorter than ca. 15-nucleotide (nt) long, the desired spin-labeled product can be readily separated from the reduced material by denaturing polyacrylamide gel electrophoresis (DPAGE). For longer oligonucleotides, on the other hand, the separation is usually a tedious and non-trivial task that often results in a mixture of spin-labeled and reduced material in low yields. Attempts have been made to prevent or minimize the reduction by exchanging the reagents used for oligonucleotide synthesis, for example by replacing trichloroacetic acid (TCA) with dichloroacetic acid (DCA) and the iodine oxidation solution with *tert*-butylperoxide.[98, 101] Protecting groups have also been implemented and will be listed in detail in the following section.

3.1.3 Protecting groups for nitroxides

During the course of this PhD work the reduction of the nitroxide spin-labels during oligonucleotide synthesis became a major issue as one of the objectives was to synthesize longer spin-labeled oligonucleotides. As separation of the reduced oligonucleotides from the spin labeled ones was almost impossible, other solutions were considered. Protecting the nitroxide with a group that would be stable through

the oligonucleotide synthesis and could be removed after the synthesis would eliminate this drawback of spin-labeling nucleic acids by the phosphoramidite method.

Several methods have been used for the protection of nitroxides, such as *O*-methyl hydroxylamines[109] under reaction conditions that would otherwise reduce the nitroxide (**19**, **Figure 3.5**). The methyl group can be removed by treatment with *meta*-chloroperbenzoic acid (*m*-CPBA), but since this reagent can also oxidize nitrogen atoms in the heterocyclic nucleobases present in nucleic acids it was deemed unsuitable. The *tert*-butyldimethylsilyl (TBDMS) group has been used to protect the hydroxylamine of 2,2,6,6-tetramethylpiperidyl-1-oxyl (TEMPO) for the synthesis of a nitroxide-nitroxide biradical[110] (**20**, **Figure 3.5**), however, less than 50% of the nitroxide was recovered after removal of the TBDMS group.

Some methods have been employed specifically to protect the nitroxides from the reagents used in the oligonucleotide synthesis. A photolabile protecting group has been used to protect TEMPO (**21**, **Figure 3.5**) for both DNA and RNA; irradiation with light and heating gave high yields of spin-labeled oligonucleotides.[111-114] However, additional synthetic effort is required to prepare and incorporate the photolabile protecting group and specialized equipment is needed to irradiate the oligomers with the right wavelength for deprotection. An ideal protecting group for routine preparation of spin-labeled oligonucleotides would be removed by using standard oligonucleotide deprotecting conditions, returning the radical without having an additional deprotection step. An acetyl group has been used to protect a TEMPO moiety attached to a deoxyuridine **22** (**Figure 3.5**) phosphoramidite during incorporation into DNA.[115] After oligomer deprotection using standard conditions complete removal of the acetyl group required additional incubation with aqueous NaOH (0.5 M), conditions that are not compatible with RNA. Incorporation of 2-*N*-*tert*-butylaminoxyl-2′-deoxyadenosine (**23**, **Figure 3.5**) into DNA utilizing acetylated hydroxylamine has also been

reported,[116] however, the structure of this nitroxide is very different from the nitroxides that are normally used for spin labeling.

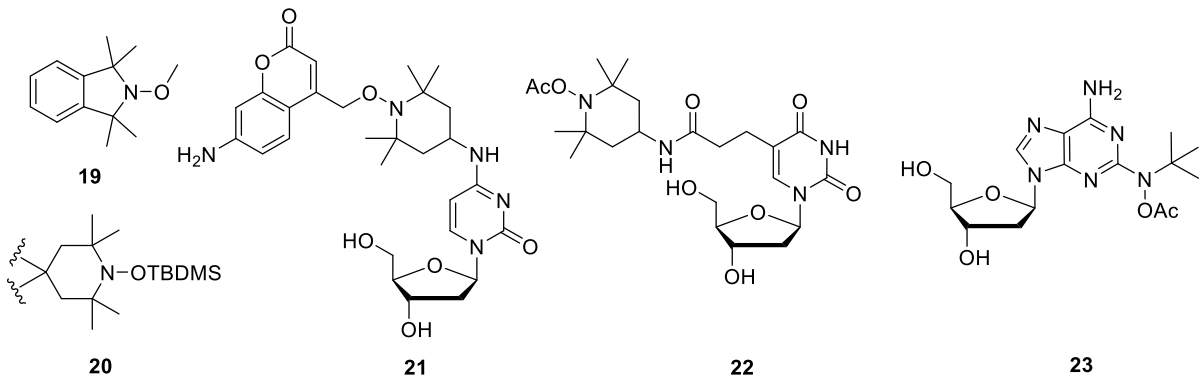

Figure 3.5. Protecting groups that have been utilized for **19**,[109] **20**,[110] **21**,[111] **22**[115] and **23**.[116]

3.2 Selection of a protecting group and its incorporation

There were three requirements the protecting group for nitroxides should possess. First, it should be applicable for the synthesis of both DNA and RNA. Second, it should be stable though the oligonucleotide synthesis. Third, it should be removable using the standard deprotection conditions for oligonucleotides, without adding an additional processing step of the oligonucleotides and returning the radical in quantitative yields. As the exocyclic amino groups of unmodified phosphoramidites A, C and G are already protected as amides, we evaluated acyl groups as protecting groups for the nitroxide radical. The most common protecting groups for the amines of the nucleobases are acetyl (Ac), benzoyl (Bz), isobutyryl (iBu) and phenoxyacetyl (PAC) (**Figure 3.6**). The acetyl group had already been deemed unsuitable for RNA. Therefore, the Bz group was chosen as it is the most common protecting group used for the oligonucleotide synthesis.

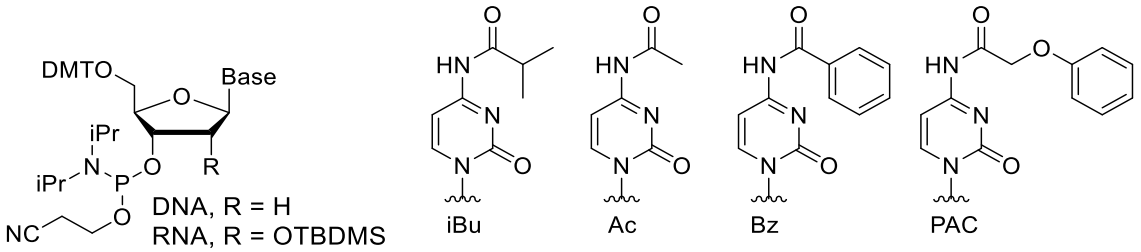

Figure 3.6. Protecting groups used for protection of amines on the nucleobases during the solid-phase synthesis of oligonucleotides. A, G and C are all protected but only C is shown as an example.

Two different methods were tested for the incorporation of the Bz group into compound **24**, used as a model compound. The first method was a reaction of a benzaldehyde with **24** (**Scheme 3.1**) which gave the benzoyl protected nitroxide **26** in quantitative yields. However, when the same reaction conditions were used with **Ç** instead of **24**, it only gave traces of the desired **Ç-Bz** along with a complex mixture of various compounds. Protecting the hydroxyl groups of **Ç** with acetyl groups of TBDMS groups prior to the reaction also led to a complex mixture of compounds.

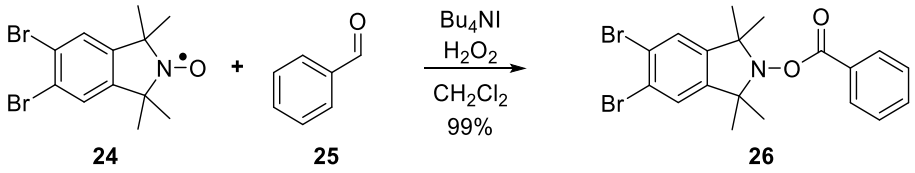

Scheme 3.1. Benzoyl protection of compound **24** using benzaldehyde.

The second method that was evaluated for incorporation of the Bz group into compound **24** was the reduction of the nitroxide radical with ascorbic acid to the corresponding hydroxylamine **27**, which was subsequently benzoylated with benzoyl chloride to give the benzoyl protected nitroxide **26** in quantitative yields (**Scheme 3.2**). The incorporation of the benzoyl group into **Ç** was also successful using this method and is described in detail in the following section.

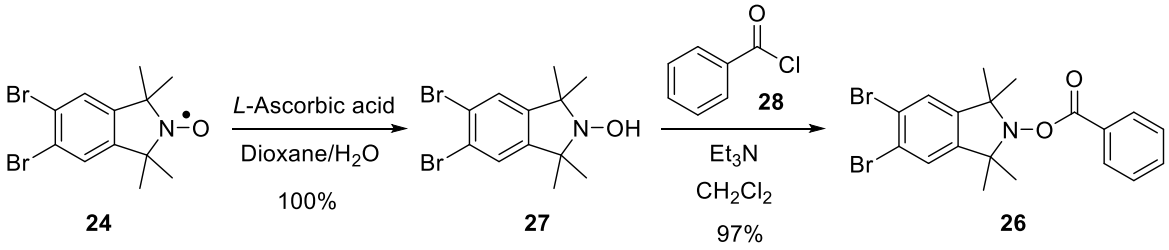

Scheme 3.2. Benzoyl protection of compound **24** through ascorbic acid reduction and benzoylation.

3.3 Synthesis of Ç-Bz

After optimizing the reaction conditions needed for the benzoyl protection of compound **24**, the synthesis of **Ç-Bz** (**Scheme 3.3**) began by protecting the 5′- and 3′-hydroxyl groups of **Ç** with TBDMS to prevent benzoylation of the hydroxyl groups. The resulting nitroxide radical **29** was reduced with ascorbic acid to yield the corresponding hydroxylamine that was subsequently benzoylated to give **30**. The TBDMS groups on **30** were removed using TBAF to give **Ç-Bz** in excellent yields.

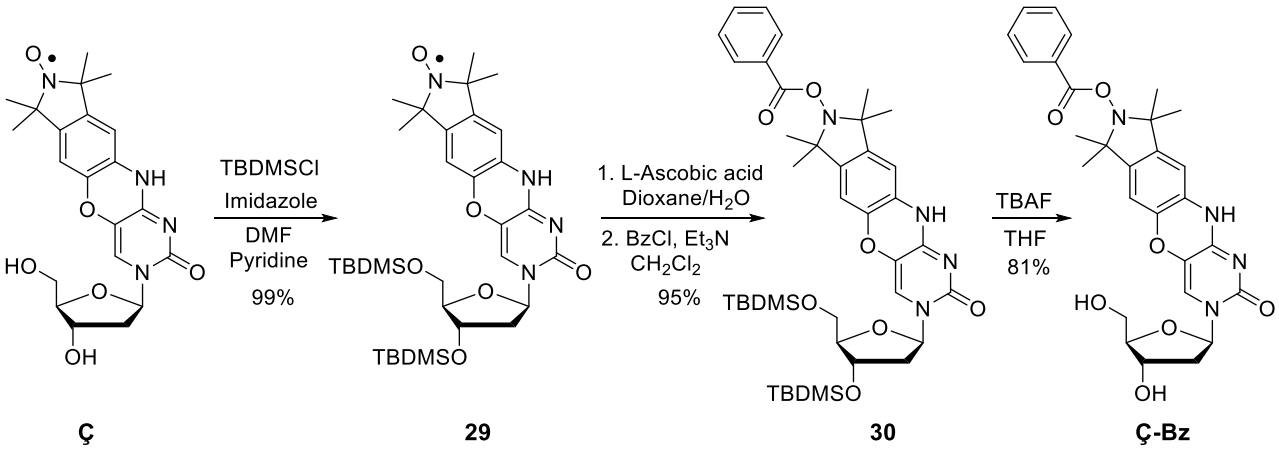

Scheme 3.3. Synthesis of **Ç-Bz** through reduction of the nitroxide radical with ascorbic acid and subsequent benzoylation.

The stability of the Bz group on **Ç-Bz** was tested under the reaction conditions that are used for the oligonucleotide synthesis. The benzoyl group was shown to be stable under all reaction conditions for more than five days, except when exposed to either 5-ethylthio tetrazole or 5-benzylthio tetrazole, present in the activation solutions, where around 10% removal of the benzoyl group was observed after 24 h (data not shown). The deprotection of the benzoyl protecting group under standard DNA deblocking conditions (satd. aq. NH_3, 55 °C) was monitored by HPLC (**Figure 3.7**) and it showed that the benzoyl protecting group on **Ç-Bz** (**Figure 3.7**, peak around 26.6 min) was readily removed after two hours, returning the spin label **Ç** (**Figure 3.7**, peak around 20.8 min). Some additional peaks were observed

using HPLC analysis after 30 min of deblocking that had disappeared after 2 h. We postulate that this may have been due to migration of the benzoyl group, that was slowly deprotected as the reaction moved forward. The deprotection of the benzoyl group was even faster under standard RNA deblocking conditions ($MeNH_2/NH_3$ in H_2O/EtOH, 65 °C) (data not shown).

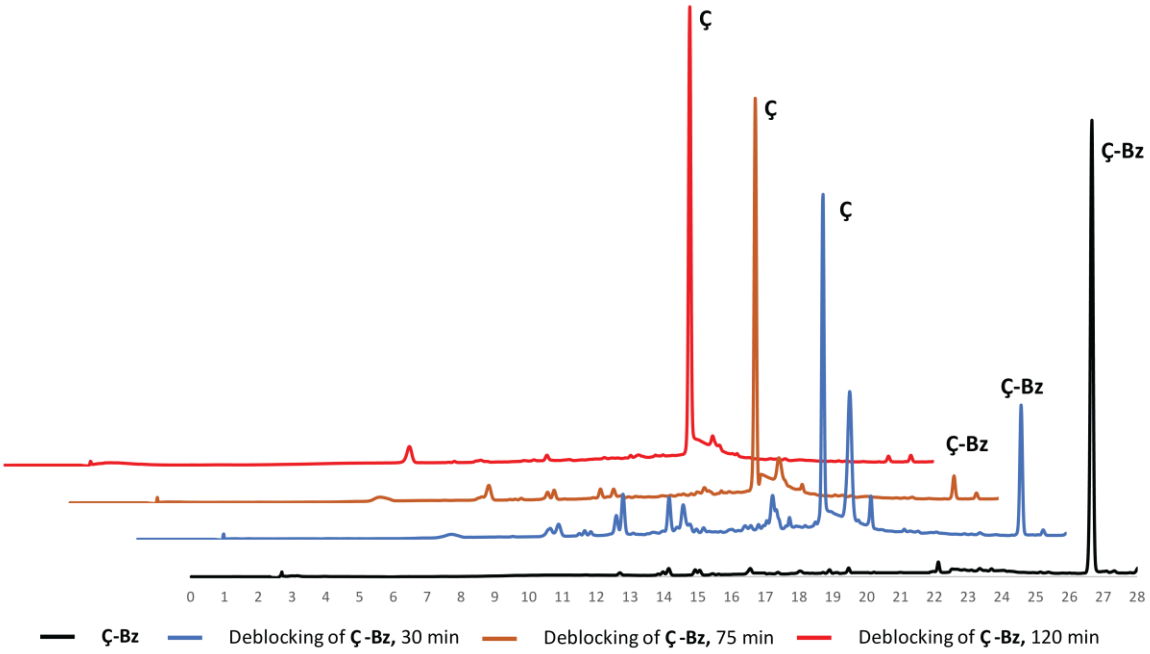

Figure 3.7. Deblocking of **Ç-Bz** using standard DNA deblocking conditions monitored by HPLC.

These results showed that the benzoyl protecting group was a promising candidate as a nitroxide protecting group for incorporation of spin labels into both DNA and RNA. Therefore, the phosphoramidite of **Ç-Bz** was synthesized. The 5′-hydroxyl group of **Ç-Bz** was protected as a DMT ether to give **31** and the 3′-hydroxyl group was subsequently phosphitylated to give phosphoramidite **32** in excellent yields (**Scheme** 3.4).

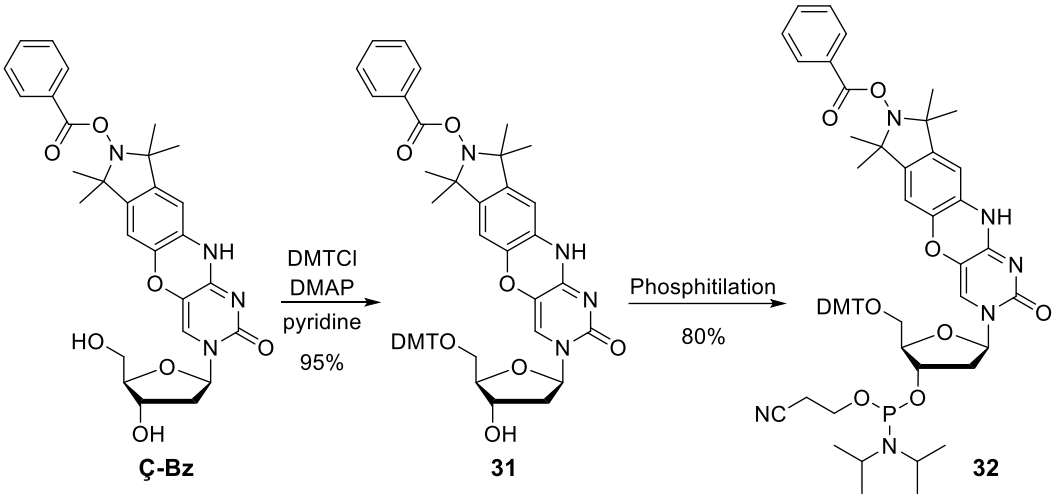

Scheme 3.4. Synthesis of phosphoramidite **32** from **Ç-Bz.**

3.4 Synthesis of oligonucleotides using Ç-Bz and their characterization

To test the scope and viability of the benzoyl protecting strategy, phosphoramidite **32** was used to synthesize seven different DNA oligonucleotides, that varied in length and in position of the spin label (**Table 3.1**), by automated chemical synthesis using the optimized reaction conditions.[101] For comparison some of the same sequences were also synthesized using a phosphoramidite of an unprotected **Ç**.

Table 3.1. Sequences, Monoisotopic masses and spin-labeling efficiency of spin-labeled oligonucleotides. Oligonucleotides **II** and **IV** and **VI** were synthesized with the unprotected phosphoramidite of **Ç**. PHO is a phosphate.

No.	Sequence	Calculated Mass	Measured Mass	Radical (%)
I	5′-d(TGCAT**Ç**TT)-3′	2576.5	2574.9	99
II	5′-d(TGCAT**Ç**TT)-3′	2576.5	2573.7	48
III	5′-PHO-d(TGAGGTAGTAGGTTGTATA**Ç**T)-3′	6809.2	6807.7	96
IV	5′-PHO-d(TGAGGTAGTAGGTTGTATA**Ç**T)-3′	6809.2	6808.0	5
V	5′-PHO-d(GGAGGTAGTAGGTTGTATA**Ç**T)-3′	6835.2	6834.5	97
VI	5′-PHO-d(GGAGGTAGTAGGTTGTATA**Ç**T)-3′	6835.2	6832.5	3
VII	5′-d(TATA**Ç**AACCTACTACCTCGT)-3′	6195.1	6194.3	98
VIII	5′-d(TAGGGTACGTGCTGAGG**Ç**TT)-3′	6403.1	6402.5	100
IX	5′-d(GC**Ç**TCAGCACGTACCTCTATT)-3′	6516.2	6515.2	99
X	5′-d(TGTAA**Ç**GCACTACCAGCGGCTGGAAATCT**Ç**TCTCGT)-3′	11400.4	11400.1	99

An advantage of using **Ç** for developing this nitroxide protecting group strategy is that reduction of the nitroxide yields the fluorescent amine **Çf**. The oligonucleotides were purified by denaturing polyacrylamide gel electrophoresis (DPAGE) and were visually evaluated. **Figure 3.8A** shows a denaturing polyacrylamide gel of crude DNA **IV** (lane 1), DNA **III** (lane 2), DNA **VI** (lane 3), DNA **V** (lane 4). No fluorescent band was detected for DNAs **III** and **V** (**Figure 3.8A**, lane 2 and 4), synthesized with **Ç-Bz**. In contrast, DNA **IV** and **VI** (**Figure 3.8A**, lane 1 and 3), synthesized with the unprotected **Ç**, contained a strong fluorescent band that overlapped with the band of the spin-labeled oligonucleotide, which indicates reduction of the nitroxide to the corresponding **Çf**. **Figure 3.8B** shows an analytic denaturing polyacrylamide gel of purified DNA oligonucleotides **VII** (lane 1), **VIII** (lane 2), **IX** (lane 3), **X** (lane 4), **III** (lane 5) and **V** (lane 6), all synthesized using phosphoramidite **32**. No fluorescence was observed for any of them, not even for the doubly labeled 36-mer DNAzyme **X** (lane 4).

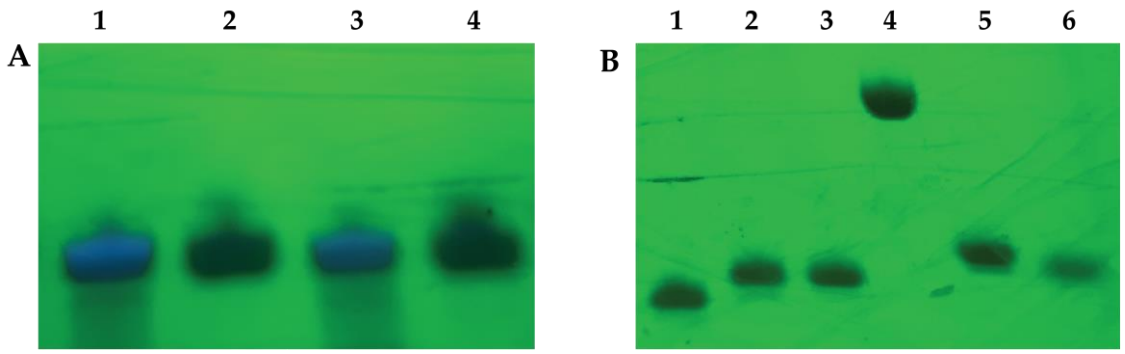

Figure 3.8. Analysis of spin-labeled oligonucleotides by DPAGE. **A**. Crude 21-mer DNA oligonucleotides **IV** (lane 1) and **III** (lane 2) (5'-PHO-d(TGAGGTAGTAGGTTGTATA**Ç**T)-3'), synthesized using the phosphoramidite of unprotected **Ç** and **32**, respectively. **VI** (lane 3) and **V** (lane 4) (5'-PHO-d(GGAGGTAGTAGGTTGTATA**Ç**T)-3'), synthesized using the phosphoramidite of unprotected **Ç** and **32**, respectively. **B**. Analytical gel of DNA oligonucleotides **VII** (lane 1), **VIII** (lane 2), **IX** (lane 3), **X** (lane 4), **III** (lane 5) and **V** (lane 6) all synthesized using **32**. PHO is a phosphate.

All synthesized oligonucleotides were analyzed by EPR spectroscopy where spin-count was performed for quantification of the amount of spin label within each oligonucleotide. A stock solution of 4-hydroxy-TEMPO was prepared and diluted into samples of different concentrations (0-0.5 mM) and each sample was measured by EPR spectroscopy. The area under the peaks of each sample, obtained by double integration, was plotted against the concentration of the sample to yield a standard curve that was used to determine the spin-labeling efficiency. The amount of radical was compared between the same sequences synthesized using the unprotected **Ç** and phosphoramidite **32** (**Table 3.1**). A dramatic increase of radical was observed for the oligonucleotides synthesized using **32** as compared to the oligonucleotides with the unprotected **Ç**. For example, the 8-mer DNA **I** (prepared with **32**) had quantitative spin count while **II** (synthesized with unprotected **Ç**) had 48% (**Table 3.1**). A more dramatic difference was observed between 21-mer DNAs **III** and **V** that were synthesized using **32** (quantitative spin count) while the same sequences synthesized with unprotected **Ç** (**IV** and **VI**) had only 5% and 3% spin count, respectively (**Table 3.1**).

3.4.1 HPLC analyses of enzymatic digests of the spin-labeled oligonucleotides

For further analysis, all oligonucleotides were enzymatically digested, and their digests analyzed by HPLC. Crude DNAs **I**, **II**, **III**, **IV**, **V** and **VI** were digested with snake venom phosphodiesterase, nuclease P1 and calf spleen alkaline phosphatase (**Figure 3.9**).[117] The HPLC chromatograms for the digests of DNAs **I**, **III** and **V** (synthesized with **32**) (**Figure 3.9 A**, **C** and **E**) contained one peak for each natural nucleoside within its sequence and a strongly retained peak that was shown by co-injection to be **Ç**. In contrast DNA **II,** synthesized with unprotected **Ç**, contained a much smaller peak for **Ç** along with a large peak for **Çf**. The digests of DNAs **IV** and **VI** (**Figure** 3.9 **B**, **D** and **F**) also contained a very small peak for **Ç** along with some strongly retained impurities. The chromatograms of digests of oligonucleotides **VII**-**X** contained five peaks, one for each natural nucleoside and one for **Ç** (**Figure 3.9 G**, **H**, **I** and **J**).

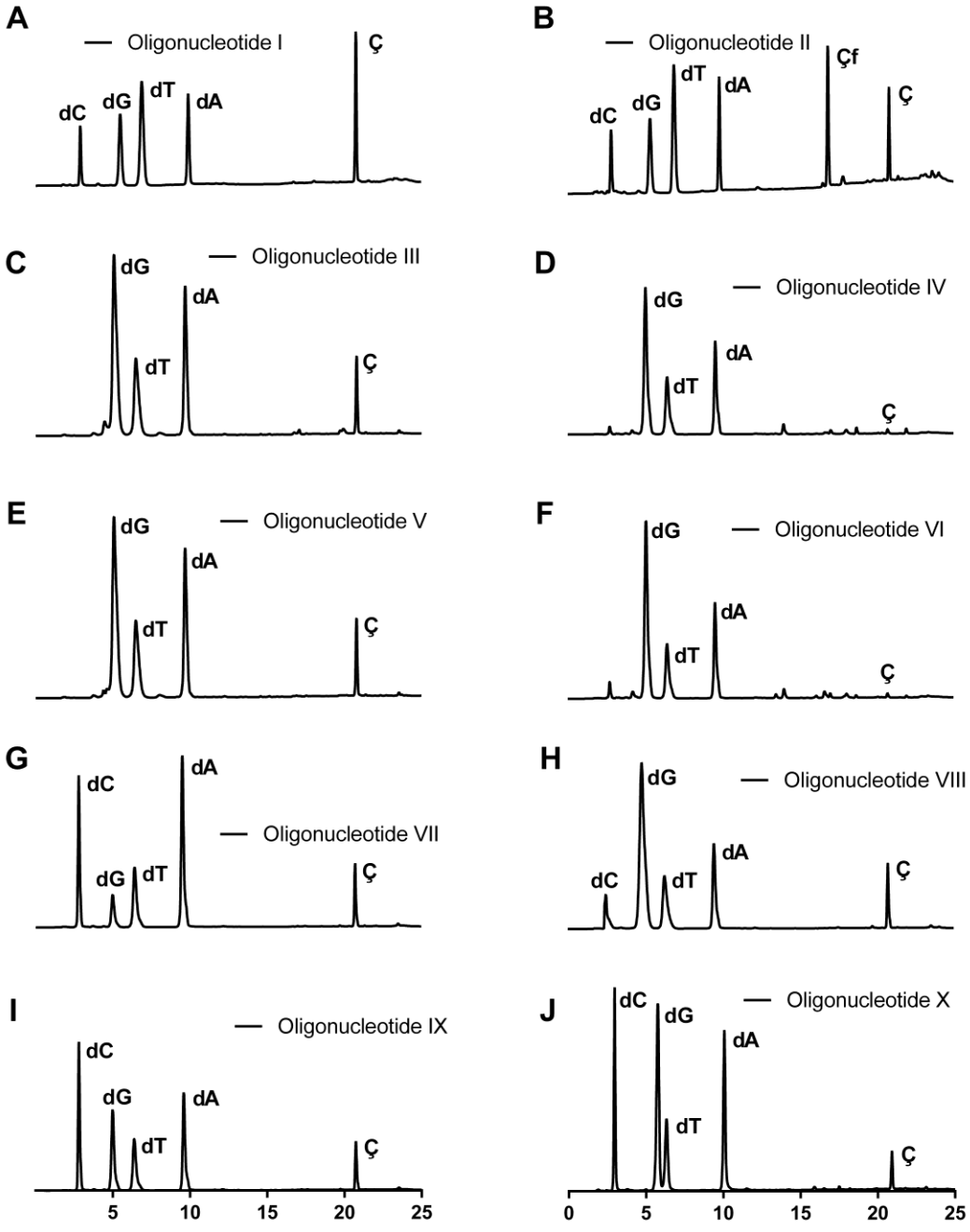

Figure 3.9. HPLC chromatograms of DNA oligonucleotides after enzymatic digestion with snake venom phosphodiesterase, nuclease P1, and alkaline phosphatase. **A**. Crude DNA **I** [5′-d(TGCAT**Ç**TT)-3′] synthesized using **32**. **B**. Crude DNA **II** [5′-d(TGCAT**Ç**TT)-3′] synthesized using unprotected **Ç**. **C**. Crude DNA **III** [5′-PHO-d(TGAGGTAGTAGGTTGTATA**Ç**T)-3′] synthesized using **32**. **D**. Crude DNA **IV** [5′-PHO-d(TGAGGTAGTAGGTTGTATA**Ç**T)-3′] synthesized using unprotected **Ç**. **E**. Crude DNA **V** [5′-PHO-d(GGAGGTAGTAGGTTGTATA**Ç**T)-3′] synthesized using **32**. **F**. Crude DNA **VI** [5′-PHO-d(GGAGGTAGTAGGTTGTATA**Ç**T)-3′] synthesized using unprotected **Ç**. **G**. DNA **VII** [5′-d(TATA**Ç**AACCTACTACCTCGT)-3′] synthesized using **32**. **H**. DNA **VIII** [5′-d(TAGGGTACGTGCTGAGG**Ç**TT)-3′] synthesized using **32**. **I**. DNA **IX** [5′-d(GC**Ç**TCAGCACGTACCTCTATT)-3′] synthesized using **32**. **J**. DNA **X** [5′-d(TGTAA**Ç**GCACTACCAGCGGCTGGAAATCT**Ç**TCTCGT)-3′] synthesized using **32**. PHO is a phosphate.

3.5 Conclusions

The nitroxide functional group of **Ç** was protected by benzoylation of the corresponding hydroxylamine. The resulting **Ç-Bz** was converted into a phosphoramidite and used for oligonucleotide synthesis of DNAs of various lengths. The benzoyl protecting group was shown to be stable through the chemical synthesis of the oligonucleotides and was readily removed by standard oligonucleotide deprotection conditions to give nitroxide-labeled oligonucleotides; gel electrophoresis was used to visually evaluate the oligomers and EPR spin count and enzymatic digestion, followed by HPLC analysis, were used to quantify the spin label in the samples. To demonstrate the use of this protecting group strategy for longer oligonucleotide syntheses, a 36-nt DNAzyme (**X**, **Table 3.1**) containing **Ç** at two positions (6 and 31) was prepared, giving a fully spin-labeled oligonucleotide. The benzoyl protecting-group strategy was also implemented for the 2'-O-methoxy derivative of **Ç** (**Çm**) and was used for incorporation into RNA oligonucleotides of various lengths. That work was done by Anna-Lena Johanna Segler. Combined, these results show that this protecting group strategy for nitroxides can be used as a general method to prepare spin-labeled nucleic acids using the phosphoramidite approach.

4 Rigid spin labels for *in-cell* EPR

4.1 Introduction

Biomolecules have over the years been extensively studied *in vitro* but in recent years the focus has shifted more towards studying them in cells. This shift has been taking place to answer the question of whether the structure and dynamics of biomolecules are different in cells, since the intracellular environment may be impossible to reproduce *in vitro*, in particular factors such as viscosity, molecular crowding, interactions with other macromolecules, and concentration of ions.[118] A few different techniques have been employed for *in-cell* studies,[118-121] but EPR spectroscopy has in recent years become a technique of interest. For *in-cell* EPR, the design of the spin labels needs to take into account factors such as position, size, rigidity and reduction resistance of the label to obtain the most accurate structural data possible, described in the following sections.

4.1.1 Rigid versus flexible spin labels

The majority of nitroxide-based spin labels that have been reported for nucleic acids thus far, are flexible or semi-flexible (**Figure 4.1**). These labels are attached to nucleic acids with a tether that has some degree of flexibility and therefore have movement independent of the biopolymer to which they are attached. This inherent mobility of the spin labels complicates the EPR analysis and are therefore, not optimal probes to study the structure and dynamics of nucleic acids.

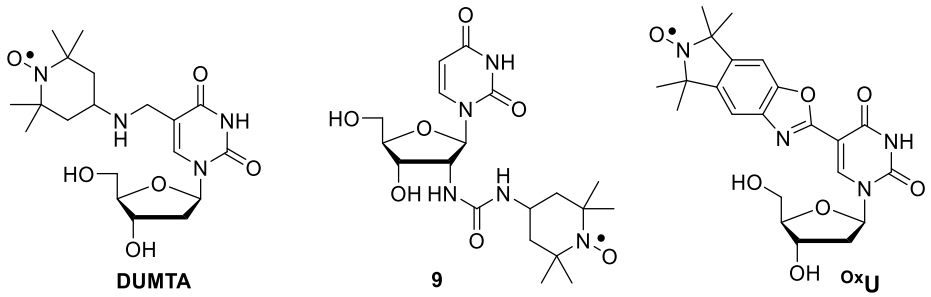

Figure 4.1. Example of a flexible label (**DUMTA**)[122] and semi-flexible spin-labels (**9**[123] and ^{Ox}**U**[66]).

Rigid spin labels are fused to the nucleoside of interest and do not move independently of the nucleic acid that they are attached to. They yield more precise structural information by pulsed EPR, through accurate distance measurements and by giving information about orientation of the labels within nucleic acids. Hopkins *et al*. reported the rigid spin label **Q** (**Figure 4.2 A**) which is the first reported rigid spin label.[124, 125] This non-natural nucleobase forms a base pair with 2-aminopurine (**2AP**) in duplex DNA and has been used to study sequence-dependent dynamics of DNA.[126] Sigurdsson *et al*. developed and reported the previously aforementioned rigid spin label **Ç** (**Section 3.1.2**). The phenoxazine-derived nucleoside **Ç** forms a stable and non-perturbing base pair with the natural base G[127] (**Figure 4.2 B**) and its rigidity enabled the measurement of accurate distances as well as orientation of the labels in duplex DNA.[102, 128] **Çm**, a 2′-O-methoxy derivative of **Ç**, has also been synthesized and incorporated into RNA. CW-EPR measurements on a series of RNAs spin-labeled with **Çm** demonstrated that the rigid spin label can yield information on RNA folding.[100]

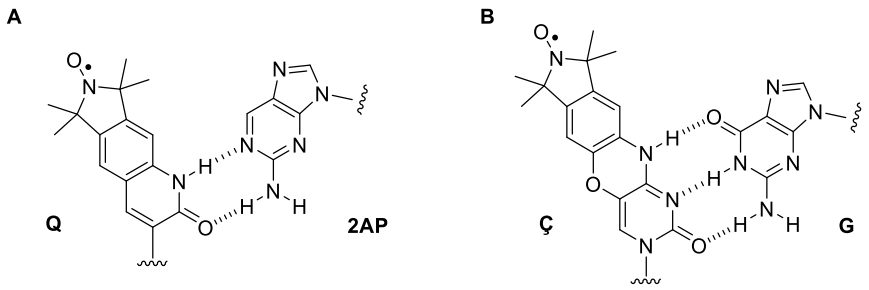

Figure 4.2. **A**. The rigid spin label **Q** base-paired to **2AP**. **B**. The rigid spin label **Ç** base-paired to **G**.

4.1.2 Study of biomolecules *in-cell*

There are three spectroscopic techniques that have been utilized for studying biomolecules in cells, NMR, FRET and EPR.[118-121] *In-cell* NMR has been used to study the structure and dynamics of nucleic acids in several cell types, along with membranes and disordered proteins.[118, 120, 121, 129-131] *In-cell* NMR has mostly been used to monitor enzymatic or "nonspecific" interactions,[129] and requires isotopic labeling of molecules to overcome cellular background signals. *In-cell* NMR has been used to obtain the first insights into possible conformations of G-quadruplexes in the cellular environment of *X. laevis* oocytes[132] and their results show different G-quadruplex conformations as compared to the same G-quadruplexes measured in a so-called intraoocyte buffer, which was designed to emulate the intracellular space in terms of both ion composition and ionic strength.[133]

In-cell FRET has been used to study inter- and intra-molecular interactions through distance measurements between two fluorescent tags.[134, 135] Fessl *et al*. also used *in-cell* smFRET to assess the helical geometry of double-stranded DNA in living *Escherichia coli* cells and their results showed that double-stranded DNA constructs of variable lengths (8–16 bp) adopted B-DNA geometry. [136]

EPR spectroscopy has also been used to measure distances within biomolecules in cells and recent studies have highlighted its advantages.[119, 137, 138] EPR requires small amounts of material and it is not limited by molecular size. Structural information can be readily obtained through distance measurements by dipolar EPR-experiments, such as pulsed electron-electron double resonance (PELDOR/DEER).[137, 139-141] Two types of spin labels have been used for EPR measurements in cells, namely Gd(III) complexes and nitroxide radicals. Gd(III) complexes have been used for distance measurements in proteins, such as a doubly labeled ubiquitin protein using 4PS-PyMTA-Gd(III) (**Figure** 4.3 **A**).[142-144] Nitroxide radicals have also been used for *in-cell* distance measurements.[119, 137, 139-141, 145-147] Krstic *et al*. were the first to report the use of *in-cell* EPR for nucleic acids in *X. laevis*

oocytes in 2011 and performed *in-cell* DEER spectroscopy on a 12-bp DNA duplex, a 14-mer cUUCGq tetraloop RNA hairpin and a 27-mer neomycin-sensing riboswitch double-labeled with 2,2,5,5-tetramethylpyrrolinyl-*N*-oxyl-3-acetylene (TPA) (**Figure 4.3 B**).[140] The distance distribution obtained for the double-stranded DNA was found to be distinct from that observed under *in vitro* conditions. Later, Azarkh *et al*.[139] employed *in-cell* DEER to probe an antiparallel double-helical DNA terminally labeled with TEMPA (**Figure 4.3 C**).

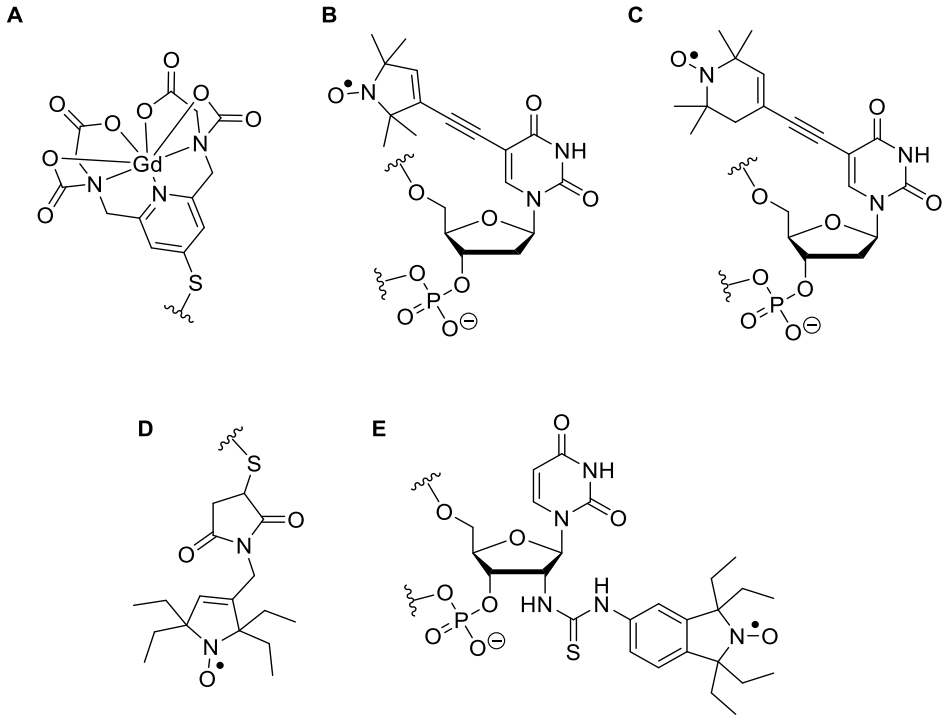

Figure 4.3. Different spin labels used for *in-cell* EPR measurements. **A**. 4PS-PyMTA-Gd(III) linked to a protein.[72] **B**. 2,2,5,5-Tetramethylpyrrolinyl-*N*-oxyl-3-acetylene (TPA) labeled thymidine. **C**. TEMPA labeled thymidine. **D**. M-TETPO linked to a protein.[148] **E**. A tetraethyl-derived spin label conjugated to a 2′-amino labeled uridine through a thiourea linkage.[149]

The limitation of most nitroxides is that they are rapidly reduced in the reducing environment encountered within cells, making the time-window of the experiment short.[145, 150, 151] However, sterically-shielded nitroxide radicals, in particular tetraethyl-derived nitroxides, are resistant towards reduction.[150] For example, a tetraethyl-derived pyrrolidine nitroxide has been used to spin label a chaperone protein for *in-cell* EPR (**Figure 4.3 D**). Only minimal reduction of the

radical was observed, which enabled the EPR study of structural features of the chaperone protein through determination of inter-spin distances.[148] A tetraethyl-derived isoindoline spin label has recently been used for post-synthetic labeling of 2'-amino groups of RNA (**Figure 4.3 E**) and shown to be stable in the presence of ascorbic acid.[149] Preliminary *in-cell* EPR measurements with this label have revealed structural changes in duplex RNAs (unpublished data). However, the semi-flexible nature of the linker attaching the spin label to the RNA limited the structural information that could be obtained.

4.2 The reduction resistant tetraethyl-derived rigid spin-labels EÇ and EÇm

The rigid spin labels **Ç**[1] and **Çm**[100] (**Figure 4.4**) have been shown to provide more detailed information on structural changes and dynamics in nucleic acids[105, 152, 153] than flexible and semi-flexible labels, which makes them optimal spin labels for EPR measurements in cells. However, they lack the stability necessary for the measurements in the intracellular environment. Here we describe the synthesis and characterization of the corresponding tetraethyl nitroxide spin labels **EÇ** and **EÇm** (**Figure 4.4**) that combine two characteristics necessary for obtaining detailed structural information on nucleic acids in cells by EPR spectroscopy, namely rigidity and reduction resistance.

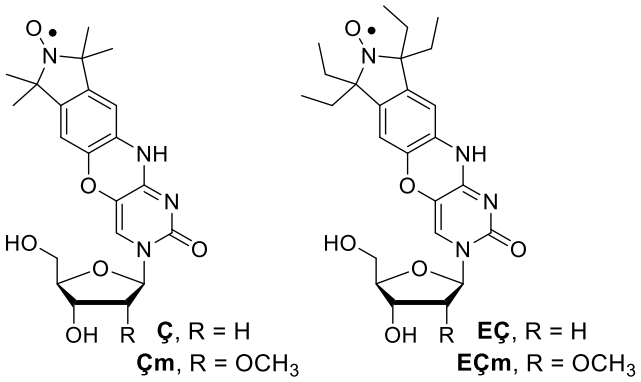

Figure 4.4. The rigid spin labels **Ç** and **Çm** and their corresponding tetraethyl-derivatives **EÇ** and **EÇm**.

A molecular model of **EÇ** within a B-form DNA duplex (**Figure 4.5 A**) shows that the spin label is well accommodated in the major groove of the DNA duplex and a molecular model of **EÇm** within an A-form RNA duplex (**Figure 4.5 B**) shows that the spin label fits tightly into the major groove of the RNA duplex.

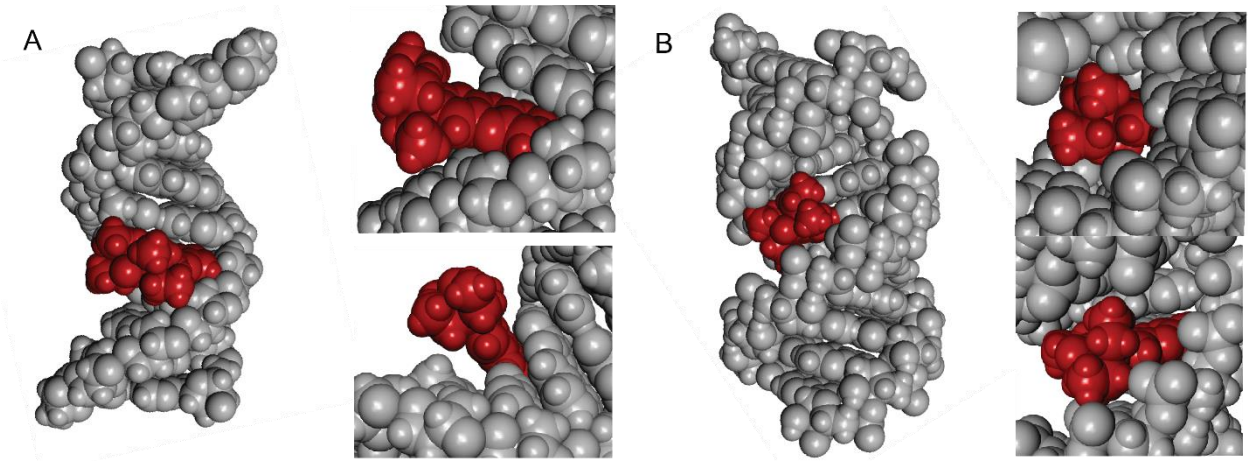

Figure 4.5. **A**. Space-filling model of **EÇ** labeled B-form DNA duplex with **EÇ** projected into the major groove with close-ups from two different angles. **B**. Space-filling model of **EÇm** labeled A-form RNA duplex with **EÇm** projected into the major groove with close-ups from two different angles. The oligonucleotide constituents are shown in grey and the spin-labeled nucleotides in red.

4.2.1 Synthesis of EÇ and EÇm

The first stage in the synthesis of the rigid spin labels **EÇ** and **EÇm** was the preparation of the tetraethyl isoindoline **33** (**Scheme 4.1**). The synthesis of **33** started with the amination[154] of compound **34**[155] to give amino-nitro derivative **35** in 70%

yield. Subsequent hydrolysis of **35** afforded compound **36** in 72% yield. Here the hydrolysis is usually accomplished in water but that was unsuccessful for compound **35** as it is completely insoluble under these conditions. Therefore, a mixture of MeOH and water was necessary for the reaction to proceed. Hydrogenation of the nitro group gave ethyl isoindoline-derived aminophenol **33**.

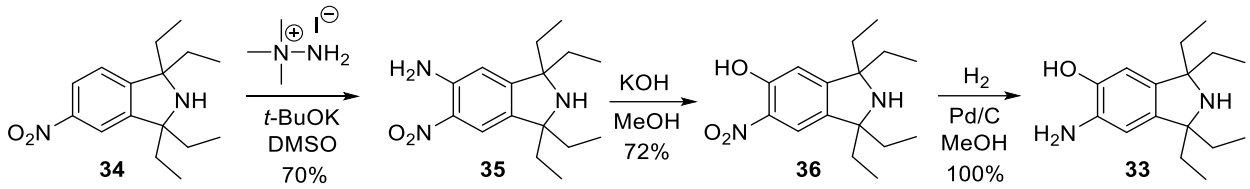

Scheme 4.1. Synthesis of tetraethyl isoindoline **33**.

To incorporate the ethylisoindoline moiety into nucleosides, the dihalogenated nucleosides **37**[1] and **38**[100] needed to be prepared by the previously reported procedure. **37** and **38** were coupled with **33** in the presence of Et_3N to give intermediates **39** and **40**, respectively, followed by ring-closure[1, 100, 156] to yield phenoxazine derivatives **EÇf** and **EÇmf** (**Scheme 4.2**). Direct oxidation of **EÇf** and **EÇmf** proved troublesome as the ethyl groups render the amine much less prone to oxidation as compared to the tetramethyl derivative. Using either hydrogen peroxide and Na_2WO_4[1] or *m*-CPBA[157] under a variety of conditions gave very low yields of the desired product along with multiple other products. We noticed that almost all *m*-CPBA oxidations are done in chlorinated solvents but **EÇf** and **EÇmf** are not soluble in those solvents. Therefore, the 5′ and 3′ hydroxyl groups were TBDMS-protected to give **41** and **42**. Oxidation of **41** and **42** in CH_2Cl_2 with *m*-CPBA in the presence of NaN_3[154] gave **43** and **44** in excellent yields. Here the NaN_3 was also necessary to avoid multiple other products to form.

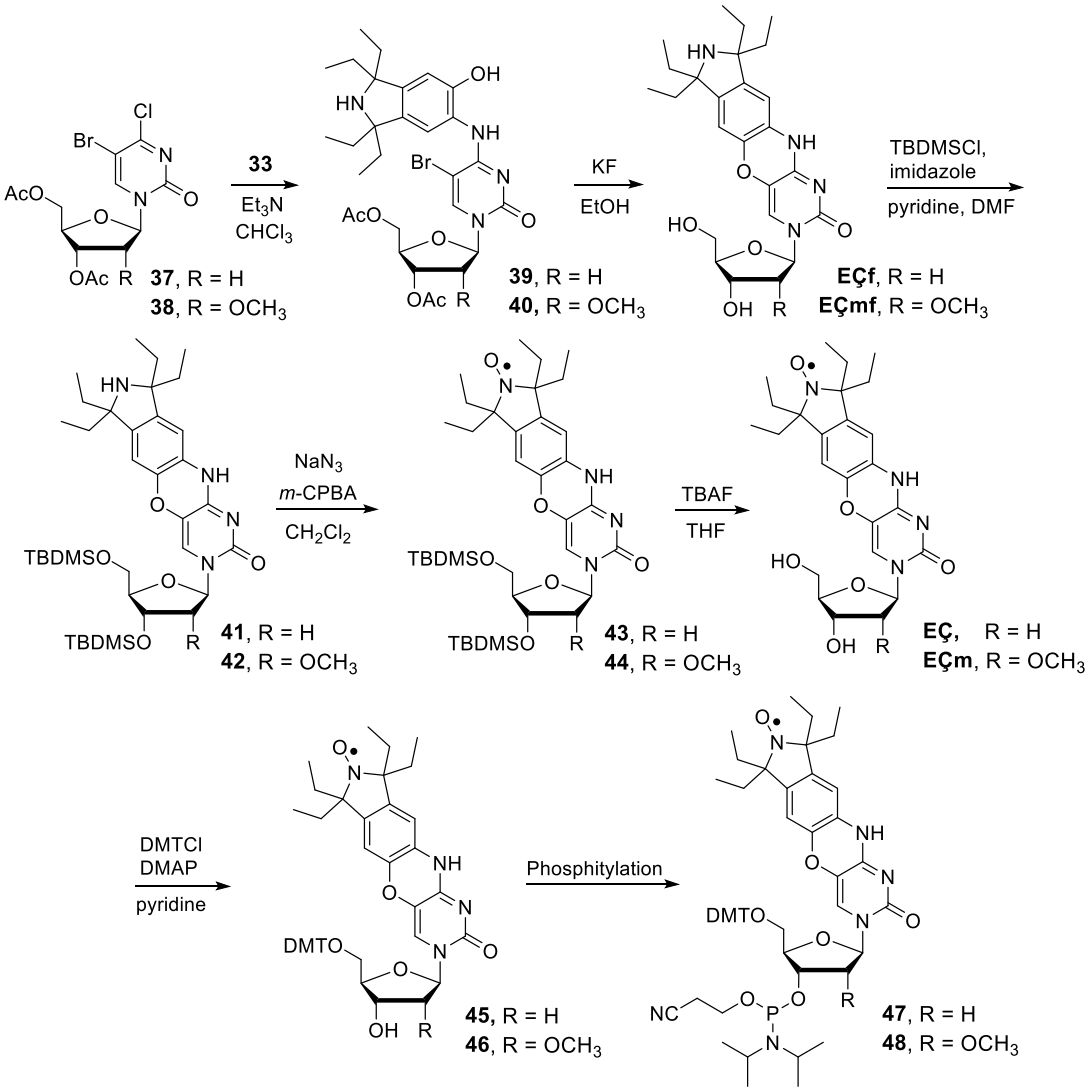

Scheme 4.2. Synthesis of spin-labeled nucleosides **EÇ** and **EÇm** and their corresponding phosphoramidites. Yields were as follows: **EÇf** (56%, over 2 steps), **EÇmf** (60%, over 2 steps), **41** (95%), **42** (93%), **43** (71%), **44** (68%), **EÇ** (91%), **EÇm** (94%), **45** (92%), **46** (93%), **47** (71%), and **48** (63%).

The TBDMS groups were subsequently removed with TBAF to give nucleosides **EÇ** and **EÇm**. The 5′-hydroxyl groups of **EÇ** and **EÇm** were protected as DMT ethers to give **45** and **46**, followed by a 3′-phosphitylation to yield phosphoramidites **47** and **48** (**Scheme 4.2**). It was discovered while working with **45**, **46** and phosphoramidites **47** and **48**, that the DMT groups were unusually labile. Even dissolving these compounds in polar and/or protic solvents, such as CH_3CN or MeOH, led to rapid loss of the DMT group. The use of nonpolar or chlorinated solvents such as CH_2Cl_2 or 1,2-dichloroethane circumvented this decomposition.

4.2.2 Stability of nitroxides EÇm and Çm in the presence of ascorbic acid

The resistance of **EÇm** towards reduction in presence of ascorbic acid, frequently used to evaluate the stability of nitroxides,[150] was investigated and compared to its tetramethyl derivative **Çm**.[100] The normalized EPR signal intensity was plotted as a function of time and showed that the tetramethyl derived **Çm** was almost fully reduced within 1 h, while ca. 90% of the **EÇm** nucleoside was still intact after 16 h (**Figure 4.6 A**). The stability of **EÇm** towards reduction in presence of ascorbic acid was also investigated in an organic solvent (MeOH) and compared to its stability in aqueous media (phosphate buffer) (**Figure** 4.6 **B**) and it shows that **EÇm** gets reduced at a much faster rate in the organic solvent as compared to the phosphate buffer. We postulate the reason being the hydrophobic properties of the tetraethyl-groups.

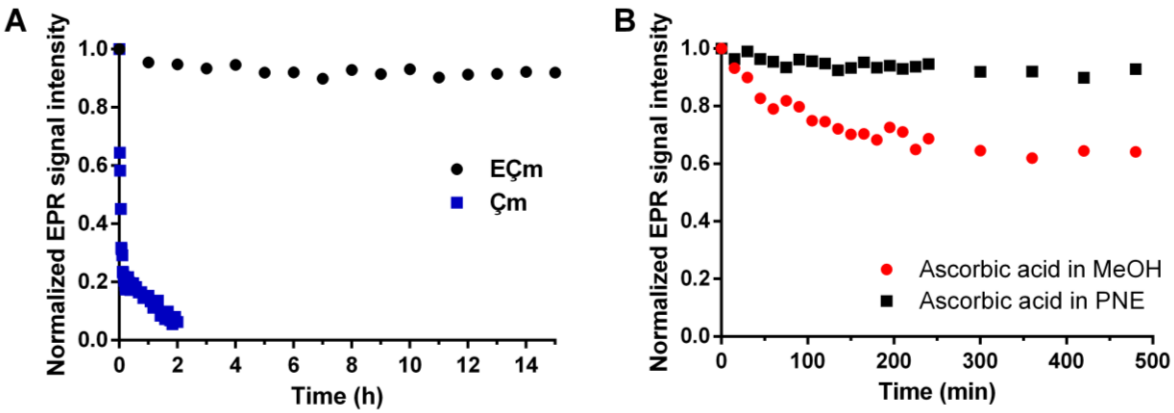

Figure 4.6. **A**. Stability of **EÇm** and **Çm** against ascorbic acid (5 mM) in phosphate buffer (10 mM $NaHPO_4$, 100 mM NaCl, 0.1 mM Na_2EDTA, pH 7.0). **B**. Stability of **EÇm** against ascorbic acid (5 mM) in phosphate buffer and in MeOH.

The stability of **EÇm** was also tested under reaction conditions that are present during the oligonucleotide synthesis. **EÇm** proved to be stable in the *tert*-butyl hydroperoxide oxidation solution for more than a week. However, when the stability was investigated in 5-ethylthio tetrazole, present in the DNA activation solution, and dichloroacetic acid, present in the oligonucleotide deblocking

solution, no decomposition was observed after 135 min but after 72 h significant decomposition of **EÇm** had occurred (**Figure 4.7**).

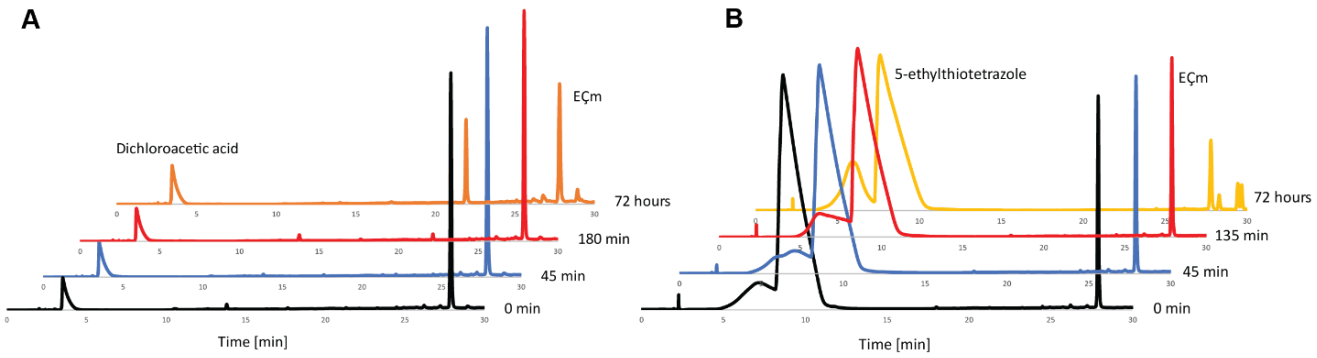

Figure 4.7. **A**. Stability of **EÇm** in 3% dichloroacetic acid. **B**. Stability of **EÇm** in 0.25 M 5-ethylthiotetrazolide solution.

4.3 Oligonucleotide spin-labeling using EÇ and EÇm

The phosphoramidites **47** and **48** were used for incorporation of **EÇ** and **EÇm** into DNA and RNA oligonucleotides, respectively, by automated solid phase synthesis.

4.3.1 Synthesis and characterization of DNA oligonucleotides containing EÇ.

Phosphoramidite **47** was used for the synthesis of seven different oligodeoxynucleotides containing **EÇ** (**Table 4.1**). The DNAs varied in length and position of the spin-label. Spin-labeled phosphoramidite **47** coupled well during the solid-phase synthesis, as indicated by a strong orange color of the trityl cation that appears during removal of the DMT group. Analysis of the crude oligodeoxynucleotides by denaturing polyacrylamide gel electrophoresis (DPAGE) did not reveal any failure bands that would have resulted for partial coupling of **47**. The **EÇ**-modified oligomers migrated slightly slower than the unmodified strands of the same sequence by DPAGE, consistent with incorporation of the spin label, which was confirmed by mass spectrometry (**Table 4.1**).

Table 4.1. DNA sequences synthesized, their monoisotopic masses and percentage of nitroxide radical within each sequence determined by EPR spin-counting.

No.	DNA Sequence	Calculated Mass	Measured Mass	Radical content (%)
I	5′-d(CGCGAATTCGCG)-3′	3646.4	3643.1	
II	5′-d(CGCGAATT**EÇ**GCG)-3′	3904.8	3901.2	99
III	5′-d(GACCTCGCATCGTG)-3′	4239.8	4236.1	
IV	5′-d(GACCTCG**EÇ**ATCGTG)-3′	4497.9	4494.2	96
V	5′-d(AGTGGACGCTTGGGGTGTA)-3′	5939.9	5934.6	
VI	5′-d(AGTGGA**EÇ**GCTTGGGGTGTA)-3′	6198.1	6192.6	82
VII	5′-d(ATACACCCCAAGCGTCCAC)-3′	5686.7	5682.0	
VIII	5′-d(ATACA**EÇ**CCCAAGCGTCCAC)-3′	5944.9	5939.7	81
IX	5′-d(ATACAC**EÇ**CCAAGCGTCCAC)-3′	5944.9	5939.7	100
X	5′-d(ATACACC**EÇ**CAAGCGTCCAC)-3′	5944.9	5939.7	82
XI	5′-d(ATACACCC**EÇ**AAGCGTCCAC)-3′	5944.9	5939.7	94
XII	5′-d(CACGATGCGAGGTC)-3′	4288.8	4285.1	

After purification by DPAGE, spin-counting of DNAs **II, IV, VI** and **VIII-XI** was performed by EPR spectroscopy, giving 81-100% spin labeling (**Table 4.1**), which indicated that some reduction might have occurred. The DNA oligomers were enzymatically digested and the digests were analyzed by HPLC (**Figure 4.8**).[101, 158] The HPLC chromatograms for digests of DNAs **II, IV, VI** and **VIII-XI** each showed five peaks, one for each natural nucleoside and a strongly retained nucleoside that was shown by co-injection[1] to be **EÇ**. Chromatograms for the longer oligonucleotides (**VI, VIII, X** and **XI**) also contained an additional small peak around 20.5 minutes that was shown by co-injection to be **EÇf**, which **EÇ** corresponding amine that appears when the nitroxide radical is reduced during the oligonucleotide synthesis. The amounts of **EÇf** and **EÇ** was quantified, showing that ca. 6-18% of the spin-labels had been reduced. It should be noted that more extensive reduction was observed in oligodeoxynucleotides of similar length that

were synthesized using the phosphoramidite of the tetramethyl derived **Ç**, as was described in **Chapter 3**.

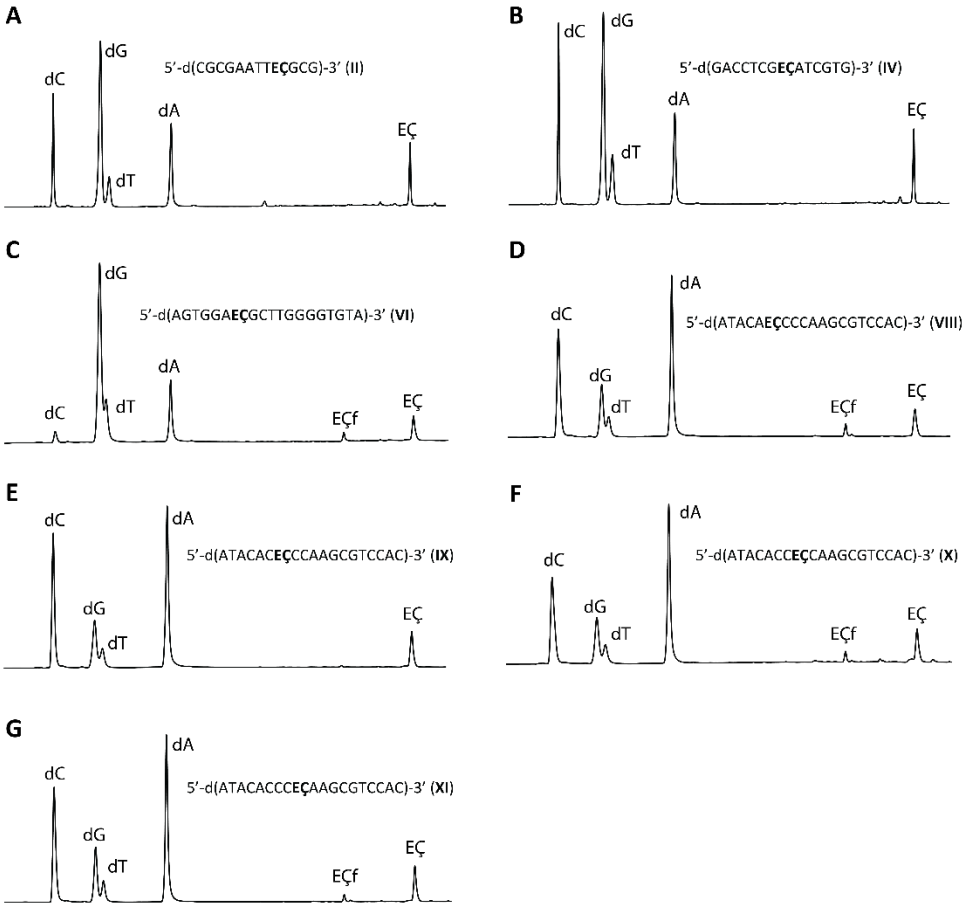

Figure 4.8. HPLC chromatograms of enzymatic digests of DNAs**.**

It is well known that nitroxide radicals get partially, or even fully,[108] reduced during oligonucleotide synthesis using the phosphoramidite approach. Even though we showed (in the section before) that the tetraethyl groups on **EÇ** render the nitroxide significantly more resistant to reduction by common reducing agents and that the **EÇ** spin-label is unchanged even after 180 min under the reaction conditions used on the oligonucleotide synthesizer (**Section 4.2.2**), they do not provide full protection against reduction (through disproportionation)[159] by the acids used for oligonucleotide synthesis (dichloroacetic acid and ethylthiotetrazole).

To determine experimentally whether the **EÇ** spin-label caused a structural perturbation of the B-DNA, circular dichroism (CD) spectra of the **EÇ**-labeled duplexes were recorded (**Figure 4.9**). The CD spectra of the modified and unmodified DNA duplexes were almost identical, all possessing negative and positive molar ellipticities at ca. 250 and 280 nm, respectively, characteristic of a right-handed B-DNA duplex.

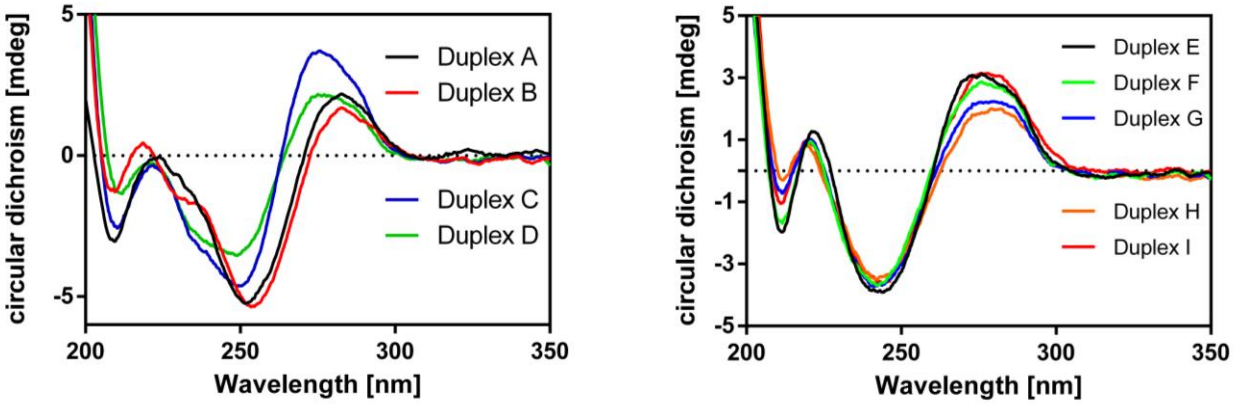

Figure 4.9. CD spectra of DNA duplexes **A, B, C, D, E, F, G, H** and **I** (see sequences in **Table 4.2**).

Thermal denaturation data was also collected to see if the **EÇ** modification caused any destabilization of the helix (**Table 4.2**). In general, the thermal denaturation experiments showed that the spin labels did not result in a significant decrease in the melting temperature, with ΔT_Ms ranging from -0.8 to -2.8 °C. Increased stability was observed for duplexes **B** and **I**. The increase of the T_M for duplex **B** of +5.6 °C and decrease for duplex **D** of -1.5 °C, is nearly identical to what has been observed for **Ç** in the same location of the same sequence (ΔT_M +5.7 °C and ΔT_M -1.1 °C, respectively).[101]

Table 4.2. Sequences of spin-labeled DNA duplexes and their thermal denaturation analysis.

	DNA sequences	T_M (°C)	ΔT_M
A	5'-d(CGCGAATTCGCG)-3' 3'-d(GCGCTTAAGCGC)-5'	58.2	
B	5'-d(CGCG AATT**EÇ**GCG)-3' 3'-d(GCG**EÇ**TTAAG CGC)-5'	63.8	+5.6
C	5'-d(GACCTCGCATCGTG)-3' 3'-d(CTGGAGCGTAGCAC)-5'	60.8	
D	5'-d(GACCTCG**EÇ**ATCGTG)-3' 3'-d(CTGGAGCG TAGCAC)-5'	59.3	-1.5
E	5'-d(AGTGGACGCTTGGGGTGTA)-3' 3'-d(CACCTGCGAACCCCACATA)-5'	66.6	
F	5'-d(AGTGGA**EÇ**GCTTGGG GTGTA)-3' 3'-d(CACCT GCGAACCC**EÇ**ACATA)-5'	63.8	-2.8
G	5'-d(AGTGGA**EÇ**GCTTGG GGTGTA)-3' 3'-d(CACCT GCGAACC**EÇ**CACATA)-5'	65.0	-1.6
H	5'-d(AGTGGA**EÇ**GCTTG GGGTGTA)-3' 3'-d(CACCT GCGAAC**EÇ**CCACATA)-5'	65.8	-0.8
I	5'-d(AGTGGA**EÇ**GCTT GGGGTGTA)-3' 3'-d(CACCT GCGAA**EÇ**CCCACATA)-5'	67.4	+0.8

The formation of the DNA duplexes was also confirmed by continuous-wave (CW) EPR spectroscopy. **Figure 4.10** shows a comparison of the CW-EPR spectra of **EÇ**, the **EÇ**-labeled 19-mer DNA single strand **VI** and the corresponding 19-mer DNA duplex **F**. **EÇ** showed three sharp lines (**Figure 4.10** A) that broadened after incorporation into the 19-mer oligoribonucleotide 5′-d(AGTGGA**EÇ**GCTTGGGGTGTA)-3′ (**Figure 4.10 B**). Upon annealing to its complementary strand 5′-d(ATACA**EÇ**CCCAAGCGTCCAC)-3′, the CW-EPR spectrum broadened further, showing a splitting of the high- and low-field components (**Figure 4.10 C**). Such broadening is characteristic for the formation of a spin labeled duplex containing a rigid spin label.[1, 100] All the DNA oligonucleotides that were characterized by CW-EPR spectroscopy showed broadening once a duplex had been formed (**Figure 4.11**).

Figure 4.10. **A**. EPR spectrum of **EÇ**. **B**. EPR spectrum of a **EÇ**-labeled 19-mer DNA single strand 5′-d(AGTGGA**EÇ**GCTTGGGGTGTA)-3′. **C**. EPR spectrum of a **EÇ**-labeled duplex 5′-d(AGTGGA**EÇ**GCTTGGGGTGTA)-3′·5′-d(ATACA**EÇ**CCCAAGCGTCCAC)-3′. EPR spectra were recorded at 20 °C in a phosphate buffer (2 nmol of DNA; 10 mM phosphate, 100 mM NaCl, 0.1 mM Na_2EDTA, pH 7.0).

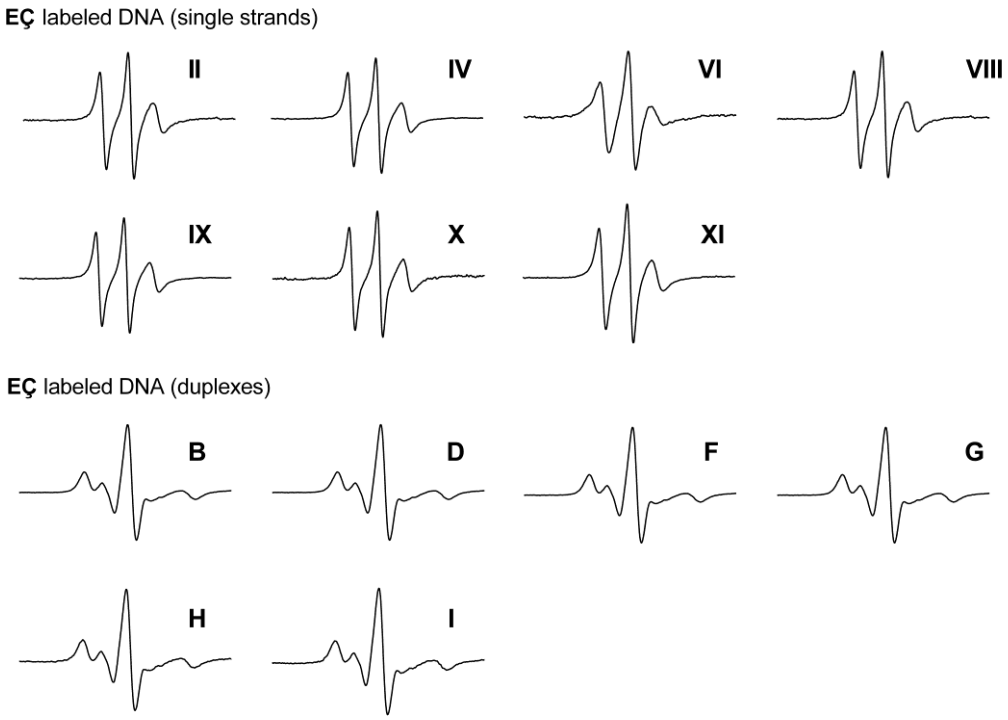

Figure 4.11. EPR spectra of spin-labeled DNA oligonucleotides.

4.3.2 Syntheses of RNA oligonucleotides containing EÇm

Phosphoramidite **48** was used for the synthesis of five 21-nucleotide long **EÇm**-labeled RNAs (**Table 4.3**). Upon completion of the oligomer synthesis, treatment with methylamine cleaved the oligoribonucleotides from the solid support and deprotected the nucleobases and the phosphodiester groups. The 2′-*O*TBDMS

groups were removed by treatment with $NEt_3 \cdot 3HF$ and the oligomers were purified by DPAGE. A bright fluorescent band that overlapped with a non-fluorescent band was observed for some of the oligomers, which indicated that partial reduction of the spin-labels had occurred. After purification by DPAGE, spin-counting by EPR was performed giving 52-98% spin labeling (**Table 4.3**), further confirming reduction of the spin-labels.

Table 4.3. RNA sequences synthesized, their monoisotopic masses and percentage of nitroxide radical within each sequence.

No.	RNA sequence	Calculated Mass	Measured Mass	Radical content (%)
XIII	5′-AGUGGACGCUUGUGGGGUGUA-3′	6825.1	6819.4	
XIV	5′-AGUGGA**EÇm**GCUUGUGGGGUGUA-3′	7097.1	7056.5	52
XV	5′-AUACACCCCACAAGCGUCCAC-3′	6597.09	6591.5	
XVI	5′-AUACA**EÇm**CCCACAAGCGUCCAC-3′	6869.1	6863.6	71
XVII	5′-AUACAC**EÇm**CCACAAGCGUCCAC-3′	6869.1	6863.6	98
XVIII	5′-AUACACC**EÇm**CACAAGCGUCCAC-3′	6869.1	6860.6	64
XIX	5′-AUACACCC**EÇm**ACAAGCGUCCAC-3′	6869.1	6863.6	94

HPLC chromatograms of enzymatic digests of RNAs **XIV** and **XVI**-**XIX** (**Figure** 4.12) showed five peaks, one for each natural nucleoside and one for **EÇm**. An additional peak or two were observed in digests of five oligonucleotides, one corresponding to inosine (from partial enzymatic hydrolysis of A by an adenosine deaminase-contamination in phosphodiesterase I)[117] (**Figure 4.12 B, C, D** and **E**) and the other corresponding to **EÇmf** (**Figure 4.12 A, B** and **D**). The reduction of **EÇm** to **EÇmf** was determined from the chromatograms to be 30-49%.

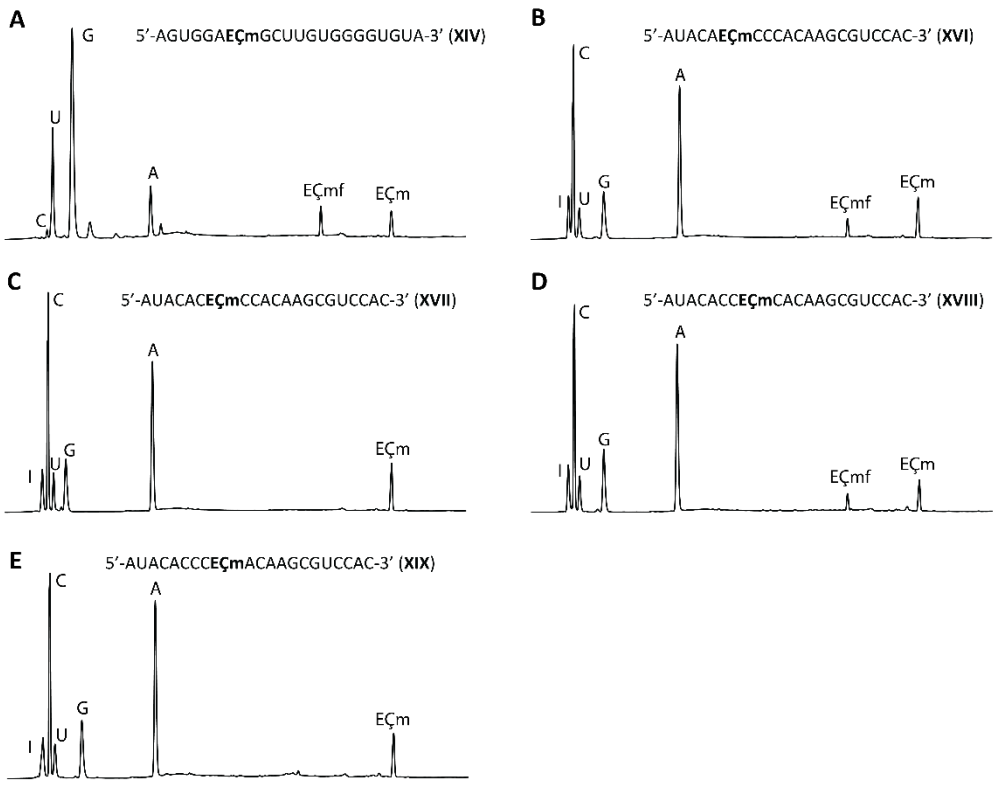

Figure 4.12. HPLC chromatograms of enzymatic digest of RNAs **XIV** and **XVI-XIX**.

The more extensive reduction of **EÇm** compared to reduction of **EÇ** during DNA synthesis can be explained by longer exposure of the spin label to oligonucleotide reagents during RNA synthesis. Since ca. 75% spin labeling is necessary for distance measurements by dipolar EPR spectroscopy, the benzoyl protecting group strategy for nitroxide radicals, previously described in **Chapter 3**, was employed for **EÇm** during the RNA synthesis and **Bz-EÇm** was synthesized.

4.4 Synthesis of Bz-EÇm and its phosphoramidite

The synthesis of **Bz-EÇm** (**Scheme 4.3**) began with reduction of the TBDMS-protected nitroxide **44** to yield the corresponding hydroxylamine, which was subsequently benzoylated to give **49**. Reducing this structurally hindered nitroxide on **EÇm** to give the corresponding hydroxyl amine proved quite difficult and

heating **44** at 60 °C for 24 h with 20 eq. of ascorbic acid was required. Subsequent removal of the TBDMS groups of **49** gave **Bz-EÇm**. The benzoyl protecting group was shown to be stable under all conditions used for oligonucleotide synthesis for more than a week. Removing the benzoyl protecting group under our standard RNA deblocking conditions (1:1, 8 M $MeNH_2$ in EtOH:33% NH_3 w/w in H_2O) proved difficult and needed optimization. In the end, the benzoyl group was efficiently removed in 2.5 h using previously reported deprotecting conditions for RNA (1:1, 40% $MeNH_2$:40% NH_3 in H_2O), returning **EÇm** in quantitative yields. The 5′-hydroxyl group of **Bz-EÇm** (**Scheme 4.3**) was protected as 4,4′-dimethoxytrityl (DMT) ether and subsequently phosphitylated to give phosphoramidite **50** in good yields.

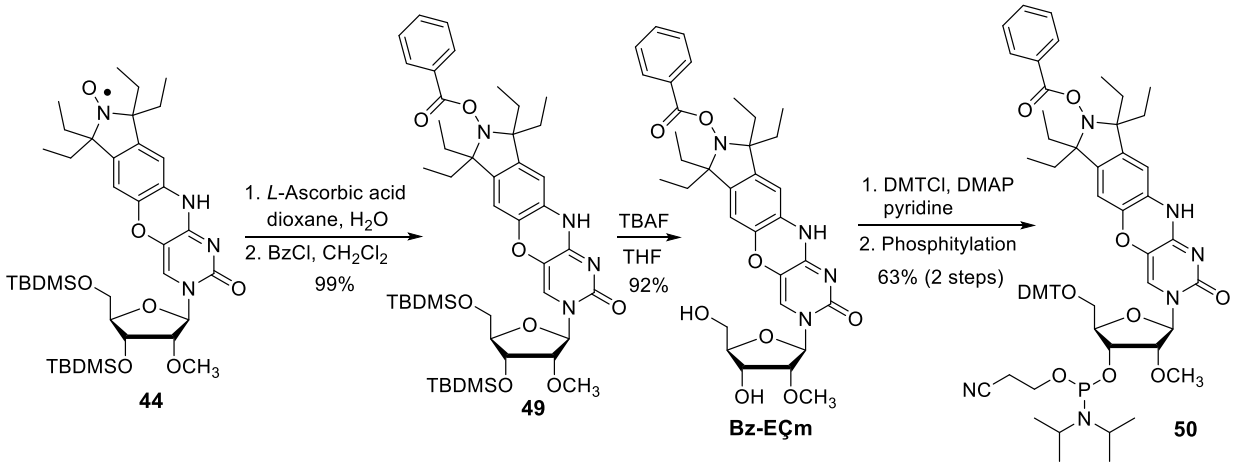

Scheme 4.3. Synthesis of **Bz-EÇm** and its corresponding phosphoramidite.

4.5 RNA spin-labeling using Bz-EÇm

Phosphoramidite **50** was used to repeat the syntheses of oligonucleotides **XIV**, **XVI** and **XVIII** (**Table 4.4**), the oligonucleotides in which extensive reduction of the spin label had been observed when using the phosphoramidite of **EÇm**. As before, the protected spin label coupled well during the solid-phase synthesis. After completion of the oligomer synthesis, treatment with 1:1, 40% $MeNH_2$:40% NH_3 in H_2O cleaved the oligoribonucleotides from the solid support and deprotected the

Bz-EÇm, the nucleobases and the phosphodiester groups. The 2′-*O*TBDMS groups were removed by treatment with $NEt_3 \cdot 3HF$ and the oligonucleotides were purified by DPAGE. No fluorescence was observed during the purification and spin counting by EPR spectroscopy after purification showed 98-100% spin labeling, indicating that little or no reduction of the spin label had occurred during the synthesis (**Table 4.4**).

Table 4.4. RNA sequences, their monoisotopic masses and percentage of nitroxide radical within each sequence as determined by EPR spin-counting.

No.	RNA Sequence	Calculated Mass	Measured Mass	Radical content (%)
XX	5′-AGUGGA**EÇm**GCUUGUGGGGUGUA-3′	7097.1	7096.5	99
XXI	5′-AUACA**EÇm**CCCACAAGCGUCCAC-3′	6869.1	6863.6	100
XXII	5′-AUACACC**EÇm**CACAAGCGUCCAC-3′	6869.1	6863.6	98

The fact that no reduction of the spin label occurred was further confirmed by HPLC analysis of the enzymatic digests of RNAs **XX**, **XXI** and **XXII** (**Figure 4.13**), that showed complete absence of **EÇmf**. The HPLC analyses also showed that the benzoyl protecting group had been completely removed during the RNA deprotection.

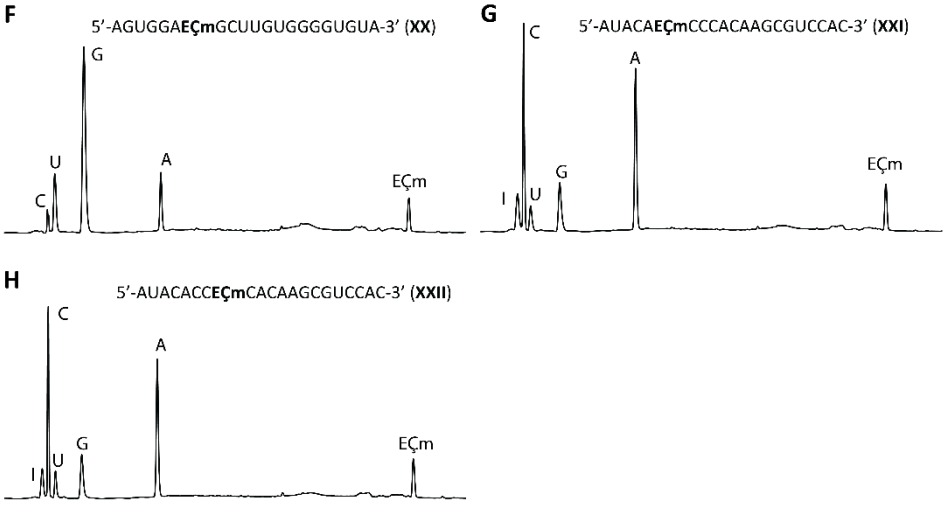

Figure 4.13. HPLC chromatograms of enzymatic digest of RNAs **XX**-**XXII**.

To determine experimentally whether the **EÇm** spin-label caused a structural perturbation of the A-RNA, circular dichroism (CD) spectra were recorded of the RNA duplexes (unmodified and modified) which showed negative and positive molar ellipticities at ca. 210 nm and 263 nm, respectively, as expected for A-form RNA (**Figure 4.14**).

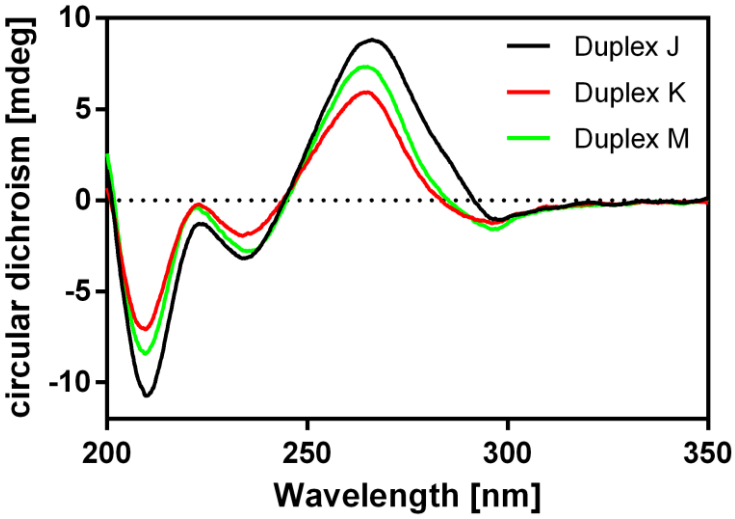

Figure 4.14. CD spectra of RNA duplexes **J**, **K** and **M**.

Thermal denaturation data (**Table 4.5**) of **EÇm**-modified RNA duplexes was collected and showed only minor destabilization of the duplexes**,** with the ΔT_{MS} ranging from -1.1 to -3.0 °C. Since each duplex contains two labels, the change in T_m caused by **EC̦m** was less than -2.0 °C per modification, relative to the unmodified RNA, which are a similar results as obtained for **C̦m** modified RNA duplexes of similar length.[100] All these RNA duplexes have one strand in common (**Table 4.3**, **XIV**) which is complimentary to all the other strands (**Table 4.3**, **XVI**, **XVII**, **XVIII** and **XIX**). Thus, the only difference between the spin-labeled duplexes is the position of **EC̦m** in the complementary strand. Therefore, the minor differences in the melting temperatures are likely due to flanking-sequence dependence, as has

been observed with both phenoxazine-derived spin labels[100, 101] and fluorophores[160, 161] in DNA.

Table 4.5. Sequences of spin-labeled RNA duplexes and their thermal denaturation analysis.

	RNA sequences	T_M (°C)	ΔT_M
J	5'- AGUGGACGCUUGUGGGGUGUA -3' 3'- CACCUGCGAACACCCCACAUA-5'	77.0	
K	5'- AGUGGA**EÇm**GCUUGUGGGG UGUA -3' 3'- CACCUG CGAACACCC**EÇm**ACAUA-5'	74.0	-3.0
L	5'- AGUGGA**EÇm**GCUUGUGGG GUGUA -3' 3'- CACCUG CGAACACC**EÇm**CACAUA-5'	76.0	-1.1
M	5'- AGUGGA**EÇm**GCUUGUGG GGUGUA -3' 3'- CACCUG CGAACAC**EÇm**CCACAUA-5'	75.6	-1.4
N	5'- AGUGGA**EÇm**GCUUGUG GGGUGUA -3' 3'- CACCUG CGAACA**EÇm**CCCACAUA-5'	74.6	-2.4

As for the DNA oligonucleotides, the RNA oligonucleotides were characterized by continuous-wave (CW) EPR spectroscopy which, also, showed broadening once a duplex had been formed for all duplexes (**Figure 4.15**).

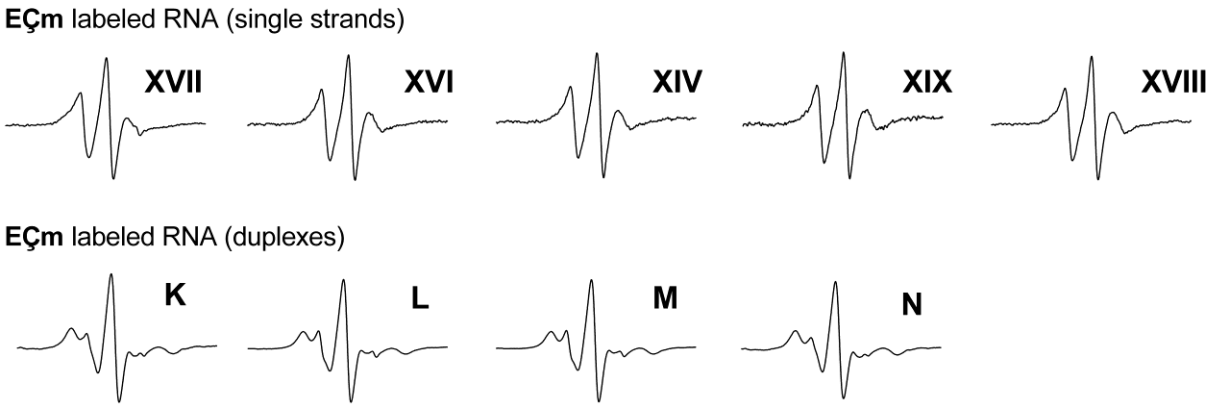

Figure 4.15. EPR spectra of spin-labeled RNA oligonucleotides and their corresponding duplexes.

4.6 Conclusions

The tetraethyl-derived rigid spin-labels **EÇ** and **EÇm** were synthesized and incorporated into DNA and RNA, respectively. The spin-labeled oligonucleotides were analyzed by UV-vis, CD and EPR spectroscopy as well as enzymatic digestion

followed by HPLC analysis. Together this data verified incorporation of the spin labels and showed them to be non-perturbating of duplex structures. A minor reduction of the **EÇ** spin label was observed during the automated synthesis of **EÇ**-labeled DNA, but substantial reduction of **EÇm** took place during the synthesis of **EÇm**-labeled RNA. This reduction was circumvented by using a benzoyl protecting group for the hydroxylamine prepared from **EÇm**.[158] The new tetraethyl-derived rigid labels **EÇ** and **EÇm** showed dramatically increased resistance towards reduction by *L*-ascorbic acid, when compared to its tetramethyl derivatives **Ç**[1] and **Çm**,[100] which will enable the investigation of structure and dynamics of DNA and RNA by *in-cell* EPR spectroscopy. These **EÇ** and **EÇm** labeled oligonucleotides that we synthesized are currently being used for *in-cell* measurements at our collaborator Prof. Thomas Prisner's research group at the University of Frankfurt.

5 *o*-Quinone-derived isoindolines for the synthesis of nitroxide spin labels

5.1 Introduction

The advantages of rigid spin labels over flexible labels were discussed in **Chapter 4**, using the example of the spin label **Ç**, which is able to provide more accurate and detailed structural data as compared to flexible or semi-flexible spin labels.[105, 152] One drawback of **Ç** is that its synthesis is non-trivial, it requires a ring-fusion of the isoindoline to the nucleobase, all of which entails a labor intensive 17-step synthesis with a low overall yield. Therefore, it is of interest to discover new simpler ways to synthesize rigid spin-labels that possess similar properties as **Ç**.

Sigurdsson and co-workers have previously reported the 1,10-phenanthrolinecontaining 5′-6-locked nucleoside **51**[162] (**Figure 5.1**) along with a series of other 5′-6-locked fluorophores[163, 164] which are all fused to the nucleobase through a pyrazine ring, a strategy based on a nucleoside derivative prepared by Kalman and co-workers in search of new anticancer drugs.[165, 166] Nucleoside **51** was simply prepared by the condensation reaction of a 5-amino-2′-deoxycytidine (**52**) with 1,2-diketone **53** (**Figure 5.1**). During the synthesis, an ether linkage was formed between 5′-hydroxyl group of the sugar and 6-C of the nucleobase. These rigid 5′-6-locked nucleosides are readily accommodated at the end of DNA duplexes.[162-164] Nucleoside **51** is a T-analog, forming a base-pair with A, where one of the nitrogens in the pyrazine ring replaces the 4-carboxy oxygen of T as a hydrogen bond acceptor (**Figure 5.1**).

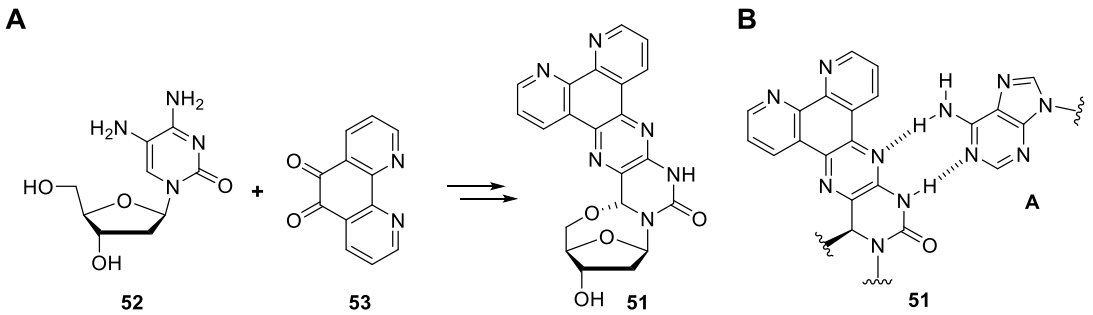

Figure 5.1. **A**. Condensation of **52** with **53** to form 5′-6-locked nucleoside **51**. **B**. Base-pairing of **51** with adenosine.

Our original aim was to devise a simple synthesis of a rigid spin label, but this time utilizing the chemistry of an *o*-substituted diketone derivative of isoindoline (**54**) and the modified diamine cytosine nucleobase (**52**) (**Figure 5.2**). We intended to use this chemistry to immobilize spin label on the modified DNA base cytosine by fusing it to the nucleobase through a pyrazine ring (**Figure 5.2**).

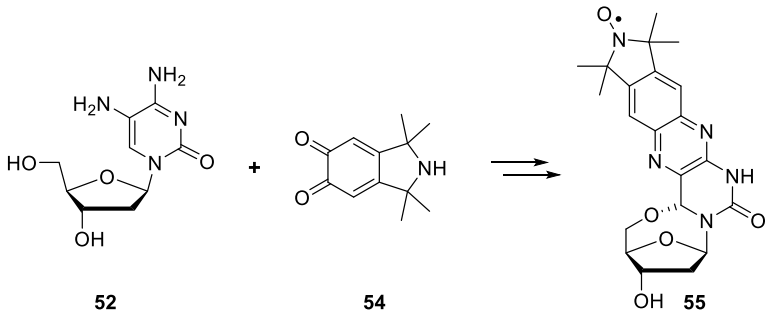

Figure 5.2. Synthetic route to obtain an isoindoline spin labeled 5′-6-locked nucleoside.

Due to unexpected results the project evolved into noncovalent spin-labeling which will be covered later in this chapter (**section 5.6**).

5.2 Synthesis of *o*-quinone isoindolines

For the synthesis of *o*-quinone isoindoline **54**, the plan was to go through 5,6-diamine-1,1,3,3-tetramethylisoindoline (**56**) (**Scheme 5.1**) and obtain **57** by

diazotization using sodium nitrite followed by hydrolysis. This route proved to be infeasible and the reaction from **56** to **57** provided a very complex mixture of condensed products.

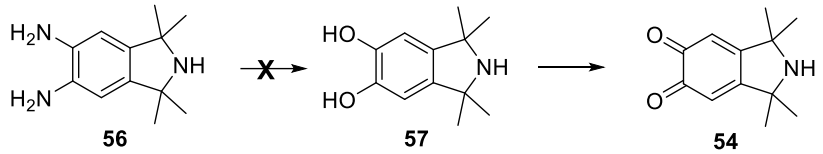

Scheme 5.1. Unsuccessful synthetic route to **54** through **56**.

The next route that was attempted was to use 5,6-dibromo-1,1,3,3-tetramethylisolindoline **58**[167] instead of **56** (**Scheme 5.2**). The ethyl derivative of *o*-quinone isoindoline (**63**) was synthesized alongside the methyl derivative, as ethyl derived nitroxide radicals show higher stability under reductive conditions. The synthesis of **54** and **63** (**Scheme 5.2**) started with substitution of the bromines on tetramethyl isoindoline **58**[167] and tetraethyl isoindoline **59**[168] with methoxide to yield compounds **60**[169] and **61**, respectively. Initial attempts to prepare *o*-quinone derivatives **54** and **63** from **60** and **61**, respectively, by AgO and nitric acid-assisted oxidation[170] gave **54** and **63** only in very low yields. These reaction conditions are rather harsh and **60** is reported to have limited stability.[169] Therefore, dihydroxyl derivatives **57** and **62** were first prepared by demethylation of **60** and **61**, respectively. Reactions of **60** and **61** with boron tribromide or iodotrimethylsilane, commonly used for demethylation of methyl ethers,[171] under a variety of conditions led to complex mixtures of products, which at best resulted in very low yields of **57** and **62**. However, demethylation with iodotrimethylsilane, followed by a water-free workup and precipitation gave **57** and **62** in excellent yields. *o*-Quinones **54** and **63** were subsequently obtained in excellent yields by oxidation of **57** and **62** with MnO_2 in the presence of air.[172]

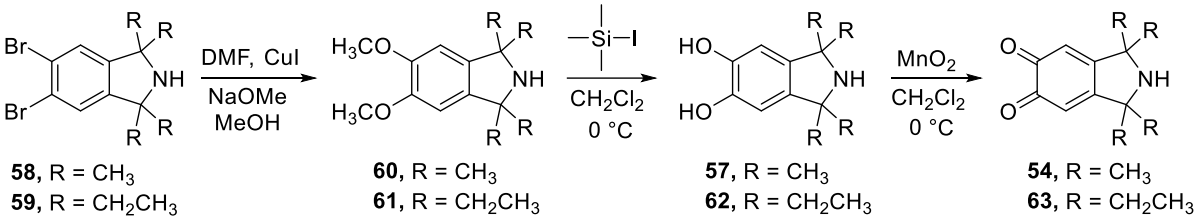

Scheme 5.2. Synthesis of *o*-quinone isoindolines **54** and **63**. Yields were as follows: **60** (95%), **61** (62%), **57** (91%), **62** (77%), **54** (88%) and **63** (93%).

5.3 Attempts at making the 5,6-locked rigid spin label 55

The synthesis of **55** started with the preparation of 5-amino-2-deoxycytidine (**52**) by a previously reported protocol.[162] Condensation of **54** with **52** (**Scheme 5.3**) to obtain **64**, under previously reported conditions for **51**, which is heating in ethanol[162] or any other alcohol-water mixture,[163] was unsuccessful. *O*-quinone **54** had limited stability in solution at room-temperature (complete decomposition in 1-2 h) and the rate of decomposition increased with heating. There seemed to be no reaction occurring between **54** and **52**. Therefore, effort was put into optimizing the condensation conditions between **54** and *o*-phenylenediamine (**65**), a model compound, to obtain **66**, before proceeding further with the synthesis of **64**.

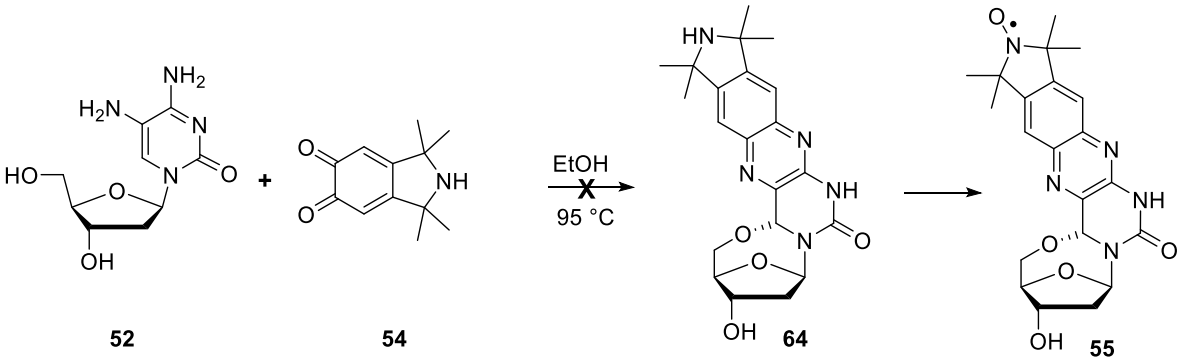

Scheme 5.3. Condensation between **52** and **54** under previously reported conditions in attempts at obtaining **64.**

Several conditions were evaluated for condensation of **54** with *o*-phenylenediamine **65** (**Table 5.1**) to obtain **66**. Most of the solvents that were evaluated resulted in moderate to excellent yields which showed that *o*-phenylenediamine is more reactive than **52**. Acetic acid (**Table 5.1**, entry 3) and

EtOH (70% in H_2O) (**Table 1**, entry 5) proved to be the best solvents. Using catalytic amount of a base led only to rapid decomposition of the diketones (**Table 5.1**, entry 6-8). In contrast, acetic acid was very effective as a catalyst. The optimal conditions proved to be 70% EtOH (aq.) with a catalytic amount of acetic acid (**Table 5.1**, entry 11).

Table 5.1. Evaluation of reaction conditions for the synthesis of phenazine **66** from *o*-quinone **54** and *o*-phenylenediamine **65**.

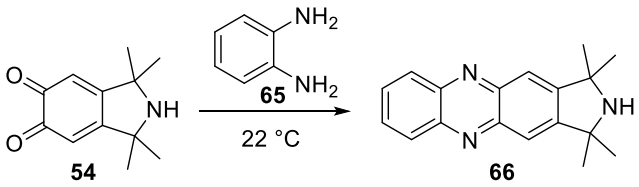

No.	Solvent	Catalyst	Time	Yield (%)
1	EtOH	-	40 min	90
2	CH_2Cl_2	-	60 min	70
3	AcOH	-	<1 min	95
4	CH_3CN	-	50 min	83
5	70% EtOH	-	30 min	94
6	70% EtOH	KOH	<5 min	0
7	EtOH	Pyridine	10 min	<1%
8	EtOH	Et_3N	10 min	<5%
9	CH_3CN	AcOH	10 min	95
10	CH_2Cl_2	AcOH	10 min	95
11	70% EtOH	AcOH	<1 min	99
12	EtOH	AcOH	5 min	95

After optimizing the condensation reaction of *o*-quinone **54** with 1,2-diamines, we proceeded with the nucleoside synthesis. The condensation of **52** with **54** under the optimized acetic acid catalyzed conditions (**Scheme 5.4**) yielded a single very polar product in near quantitative yields. Based on NMR and HRMS data, we postulated that the structure of the condensation product was **67**, resulting from reaction of one amino group with one ketone in the o-quinone. Attempts at

completing the condensation of **67** to obtain **64** under several different conditions (acidic, basic, different solvents and temperatures) were unsuccessful and instead resulted in decomposition.

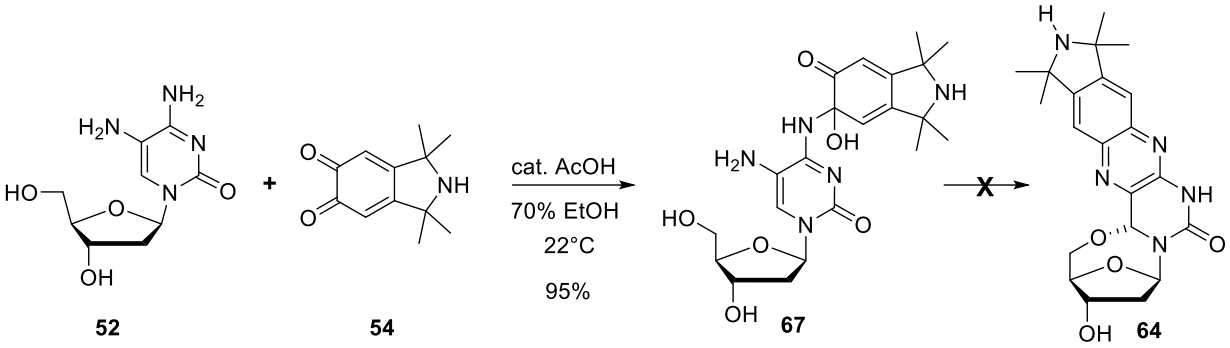

Scheme 5.4. Reaction between **52** and **54** under optimized conditions and attempted condensation of **67** to obtain **64**.

We hypothesized that prolonged heating, as was used in the synthesis of **51**, was necessary for complete condensation of **52** with a *o*-quinone to obtain a 5′-6 locked nucleoside. However, we were able to synthesis **51**[162] under the same optimized acid catalyzed conditions at 22 °C in near quantitative yields within 15 min. (**Scheme 5.5**). Therefore, heating is not necessary for the complete condensation between **52** and an *o*-quinone and that other factors may be in play in preventing the complete condensation of **52** with **54** to give **64**.

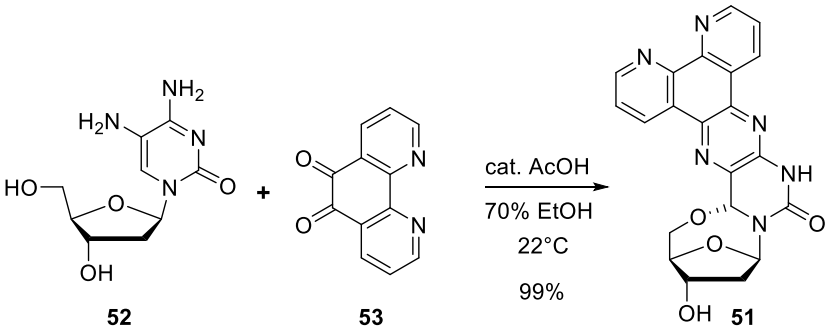

Scheme 5.5. Condensation of **52** with **53** to obtain **51** under optimized conditions.

As condensation of **52** with **54** proved to be unsuccessful, a number of commercially available *o*-phenylenediamines with different functional groups were

purchased and condensed with *o*-benzoquinones **54** and **63** to investigate the scope of their condensation reactions with diamines, as described in the next section.

5.4 Condensation of *o*-quinone isoindolines 54 and 63 with a series of diamines

Numerous commercially available *o*-phenylenediamines with different functional groups were condensed with *o*-benzoquinones **54** and **63** (**Table 5.2**). All the selected *o*-phenylenediamines condensed readily with the diketones to give the desired products in near quantitative yields (≥90%) (**Table 5.2**, entry 1-6), except for **76** (**Table 5.2**, entry 7) which did not give the desired product using any of the reaction conditions listed in **Table 5.1**. We postulated that the low solubility of **76** was the cause; low rate of condensation led to decomposition of *o*-quinones **54** and **63**. However, compound **76** was soluble in DMSO but did not yield any condensed products upon incubation with **54** (in the presence or absence of a catalytic amount of acetic acid).

Table 5.2. Condensation of **54** or **63** with various derivatives of *o*-diamines using 70% EtOH (aq.) with catalytic amount of acetic acid at 22 °C.

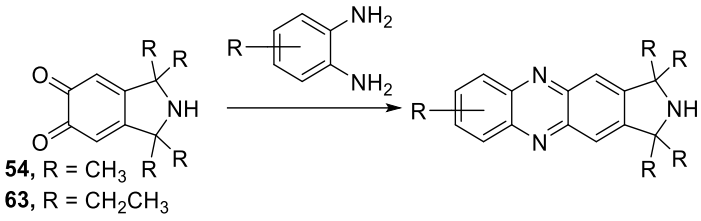

Diamine	*O*-quinone	Product	Yield (%)
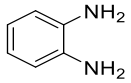 **65**	**54**	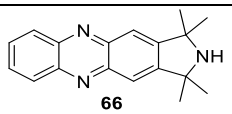 **66**	99
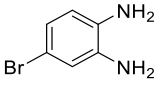 **68**	**54**	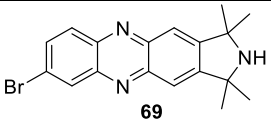 **69**	95
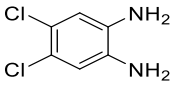 **70**	**54**	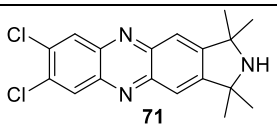 **71**	95
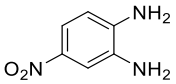 **72**	**54**	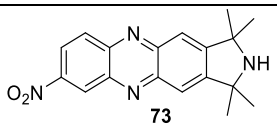 **73**	93
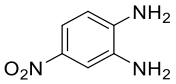 **72**	**63**	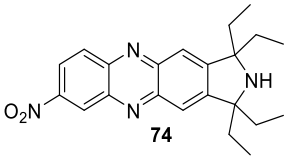 **74**	90
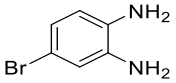 **68**	**63**	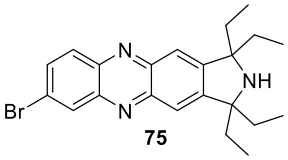 **75**	96
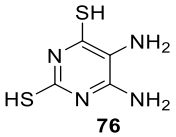 **76**	**54**	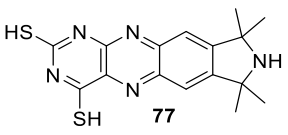 **77**	0

5.5 Oxidation of isoindoline-phenazines

The next step was the oxidation of the different derivatives of isoindoline-phenazine compounds, that were obtained from condensation (**Table 5.2**), to the nitroxide radical. While oxidizing the phenazines with *m*-CPBA to receive the corresponding nitroxide radical, it became apparent that the level of oxidation of the phenazine skeleton could be controlled by the number of equivalents of the oxidizing agent used in the reaction. When **66** was treated with one equivalent of *m*-CPBA, only nitroxide radical **78** was obtained (**Scheme 5.6**). The mono-*N*-oxide aminoxyl radical **79** was obtained with 2.2 eq. of the oxidizing agent and 5.5 eq. gave the di-*N*-oxide radical **1** (**Scheme 5.6**), all in good to excellent yields.

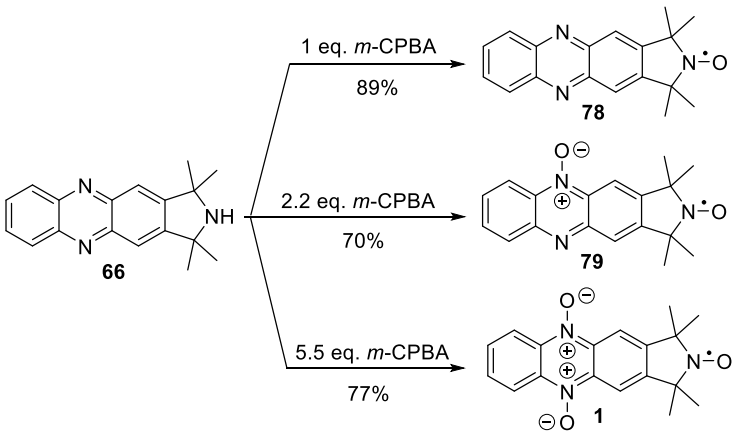

Scheme 5.6. Reaction of phenazine **66** with different amounts of oxidizing agent.

While working with **1** it was discovered that it was water-soluble, which makes it possible to evaluate the isoindoline nitroxide-derived phenazines as noncovalent spin labels for duplex DNA and RNA containing abasic sites. Noncovalent spin labeling will be discussed in detail in the next section. In contrast, **78** and **79** had limited or no solubility in water and, therefore, only the di-*N*-oxides of the other isoindoline derived phenazines were prepared. Oxidation of compounds **66**, **69**, **71**, **73** and **75** gave the desired phenazine di-*N*-oxide radicals **1** and **80**-**83** in very good yields (**Table 5.3**).

Table 5.3. Oxidation of isoindoline-phenazines to the corresponding isoindoline-phenazine di-*N*-oxide nitroxide radicals.

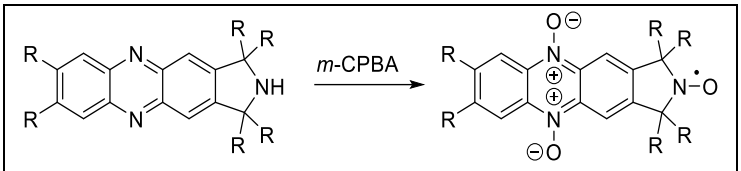

Starting compound	Product	Yield (%)
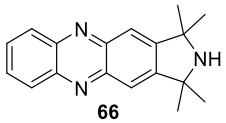 **66**	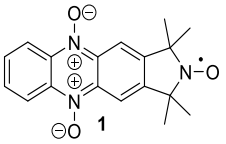 **1**	77
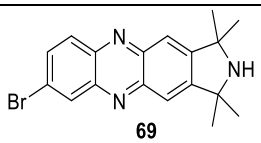 **69**	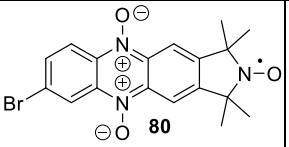 **80**	72
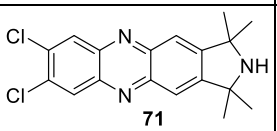 **71**	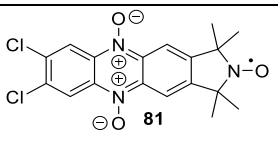 **81**	70
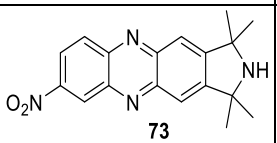 **73**	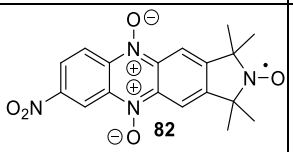 **82**	78
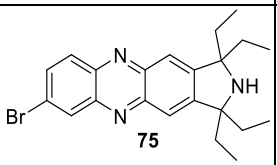 **75**	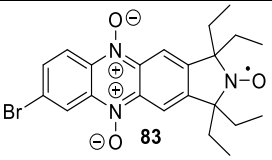 **83**	75

Since NMR spectra of the paramagnetic phenazine di-*N*-oxide radicals give limited information due to peak-broadening and even loss of NMR signals, UV-vis spectroscopy was used for spectroscopic characterization of the di-*N*-oxides (**Figure 5.3**), in addition to HRMS. Absorption peaks at 250 and 370 nm for the phenazine derivatives were red-shifted to 290 and 490 nm upon oxidation to the di-*N*-oxide radicals.

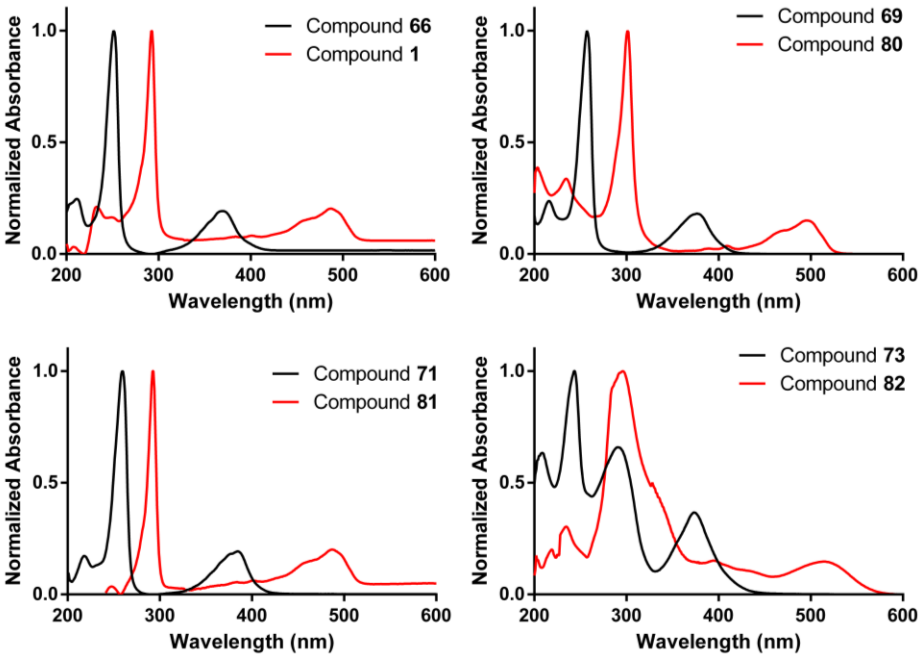

Figure 5.3. UV-vis spectra of the phenazine derivatives, compared to their oxidized counterparts.

5.6 Noncovalent spin labeling of nucleic acids

The third strategy for site-directed spin labeling of nucleic acids that was briefly described in **Chapter 2** is noncovalent spin-labeling, which utilizes binding through van der Waals interactions, hydrogen bonding and π-stacking between the spin labels and the nucleic acid. Attaching a spin label noncovalently to a nucleic acid avoids the various challenges associated with connecting the label via a covalent bond. Noncovalent labeling is a more straightforward and a less labor-intensive labeling strategy than other methods as the respective spin label is simply mixed with the nucleic acid prior to EPR measurements, requiring no purification of thee spin labeled nucleic acid. There are reports of spin-labeled intercalators and groove binders that bind to nucleic acids noncovalently, but most of them lack the sequence specificity that is usually required for EPR studies.[173, 174] Sigurdsson *et al*. recently reported the noncovalent site-directed spin-labeling of the malachite green (MG) RNA aptamer, which utilized a spin-labeled derivative of tetramethylrosamine (**84**) (TMR) (**Figure 5.4**), and is the first example of site-specific spin labeling of a

completely unmodified RNA.[175] Abasic sites in duplex nucleic acids have also been used as binding sites for noncovalent binding of small molecules. For example, fluorescent compounds that bind to abasic sites have been used for the detection of single nucleotide polymorphisms (SNPs).[176-178] An adenine acridine-derived spin-label (**85**) (**Figure 5.4**) was incorporated into a DNA duplex containing an abasic site.[179, 180] Although the adenine directs the spin label into the vicinity of an abasic site, the spin label is attached with a long flexible tether to the adenine and has only limited sequence selectivity. Sigurdsson *et al*. reported the spin label **ç** (**Figure** 5.4), a cytosine-based spin label, that bound specifically to abasic sites in duplex DNA opposite guanine (G).[127, 181-183] This spin label showed negligible binding at 25 °C but upon cooling to -30 °C the spin label was fully bound to the abasic site which enabled distance measurements in duplex DNA by PELDOR.[184] The semi-flexible G-spin (**Ǵ**) (**Figure 5.4**), a guanine-based spin label also reported by Sigurdsson *et al*., was found to bind to abasic sites in duplex RNA opposite cytosine (C) with very high affinity.[185, 186] Ǵ was prepared in a single step from readily available starting materials and showed significant binding to RNA duplexes at 20 °C allowing for accurate measurement of inter-spin distances between two spin labels using PELDOR.[185, 187]

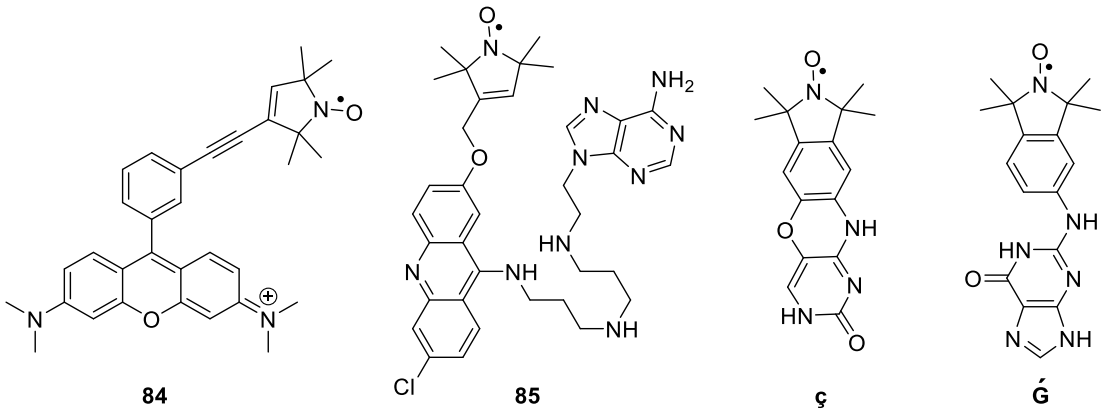

Figure 5.4. Structures of noncovalent spin labels.

Two requirements need to be met for noncovalent spin-labels. First, it needs to be EPR active and second, it needs to be water-soluble. The phenazine di-*N*-oxide isoindoline nitroxide derivatives **1** and **80**-**82** were water soluble which made it possible to evaluate them as noncovalent spin labels. The tetraethyl derivative **83** was not water-soluble and was not studied further.

5.7 Binding of isoindoline-phenazine-*N*-oxide spin labels to abasic sites in duplex nucleic acids monitored by EPR spectroscopy

Binding of **1**, **80**, **81** and **82** to abasic sites in DNA duplexes was evaluated by EPR spectroscopy.[181] Each spin label was incubated with a 14-mer duplex DNA containing an abasic site with either G, T, A or C as the orphan base at -30 °C (**Figure 5.5**). The EPR spectrum of each spin label in the absence of DNA (**Figure 5.5**, top row, spectra **a**, **g**, **m** and **s**) showed comparatively narrow lines, consistent with fast tumbling of the radical in solution. In contrast, an EPR spectrum of a spin label bound to a DNA duplex is wider due to a longer rotational correlation time,[181] that manifest in generation of a slow-moving component, as observed for spin label **1**, which showed high binding affinity and specificity towards abasic sites opposite to C (**Figure 5.5**, spectrum **b**). Nitroxide **1** also showed nearly full binding (ca. 90%) opposite to A (**Figure 5.5**, spectrum **c**), but a moderate to low binding opposite to T (**Figure 5.5**, spectrum **d**), represented by the mixture of slow- and fast-moving components in its EPR spectrum. No binding of **1** was observed to abasic sites opposite to G (**Figure 5.5**, spectrum **e**). Spin label **80** showed slight binding to abasic sites opposite to C and A (**Figure 5.5**, spectra **h** and **i**), whereas **81** showed no binding to any of the DNA duplexes. Spin labels **1**, **80** and **81** did not exhibit any nonspecific binding to an unmodified duplex (**Figure 5.5**, spectra **f**, **l** and **r**, respectively). Spin label **82** showed extensive binding to abasic sites opposite to all

the nucleobases (C, A, G and T) (**Figure 5.5**, spectra **t**-**w**), however, substantial binding was also observed to the unmodified duplex to an extent of ca. 85% (**Figure 5.5**, spectrum **x**). Spin label **82** has a strong dipole moment owed to the nitro group therefore making the label favorable for intercalation[188] which may explain the extensive nonspecific binding.

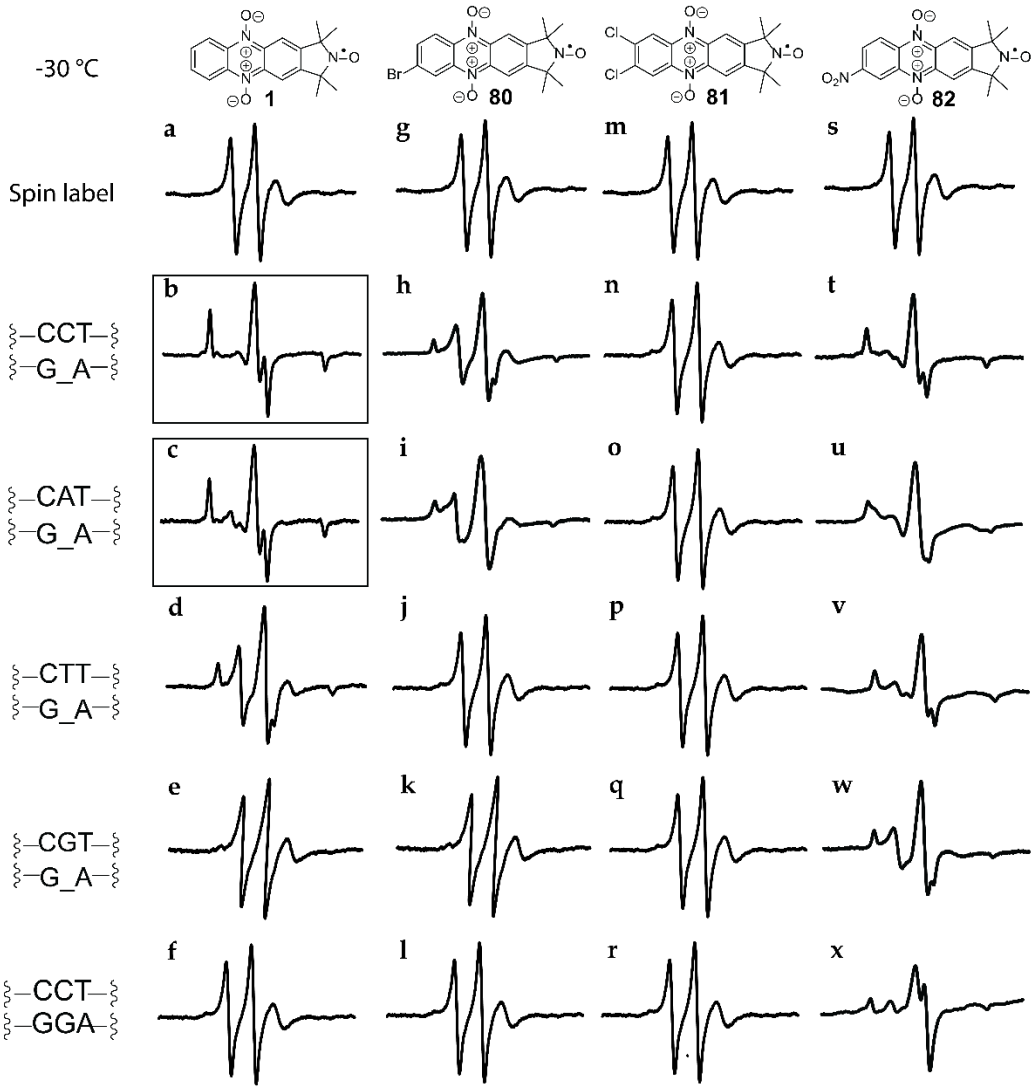

Figure 5.5. Evaluation of noncovalent spin labeling of abasic sites in DNA duplexes by EPR spectroscopy at -30 °C. EPR spectra of the labels without DNA (**a**, **g**, **m** and **s**) and in the presence of unmodified DNA (**f**, **l**, **r** and **x**) is shown for comparison. The central four rows show the spin labels in the presence of DNA duplexes containing an abasic site (denoted by "_") opposite to the orphan bases G, T, A and C. Only a part of the DNA construct is shown to the left; the complete sequence is 5′-d(GACCTCG_ATCGTG)-3′·5′-d(CACGATXCGAGGTC)-3′, where X represents the orphan base. EPR spectra of the spin-labels (100 μM) in the presence of DNA duplexes (200 μM) were recorded in phosphate buffer (10 mM $NaHPO_4$, 100 mM NaCl, 0.1 mM Na_2EDTA, pH 7.0) containing 30% ethylene glycol and 2% DMSO at -30 °C.

As spin label **1** exhibited full binding to abasic sites opposite to C and almost full binding opposite to A, the temperature dependence was investigated to obtain information about the relative affinity of the spin label to the abasic sites in question (**Figure 5.6**). Significant binding was already observed for the abasic site opposite to C at 0 °C, while close to no binding was seen for A, and almost full binding was observed at -20 °C (>95%). Little to no binding was observed at +10 °C and no binding was seen at +20 °C (data not shown).

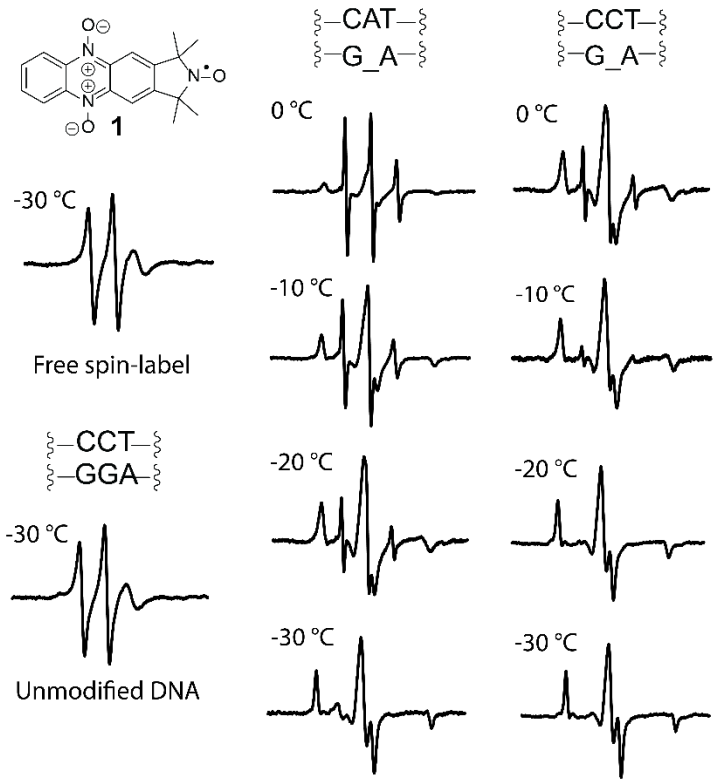

Figure 5.6. Evaluation of temperature-dependent noncovalent spin-labeling of spin label **1** to abasic sites in DNA duplexes opposite to A (middle column) and C (right column), by EPR spectroscopy. The EPR spectra of **1** alone and in the presence of an unmodified DNA at -30 °C are shown to the left.

Comparison with the binding affinity of the previously reported noncovalent spin labels **Ǵ** (K_d = 6.02 x 10^{-6} M at 0 °C)[186] and **ç** (K_d = 1.36 x 10^{-4} M at 0 °C)[181] to abasic sites in DNA opposite to C, shows that spin label **1** possesses higher affinity (K_d = 1.4 x 10^{-6} M at 0 °C).

To assess the binding of nitroxides **1** and **80**-**82** to abasic sites in RNA a combinatorial approach was used for the screening that enables the evaluation of the binding of each label to multiple oligonucleotides at once. Each sample contained the spin label along with four RNA duplexes, each of which contained an abasic site placed opposite to four different orphan bases, A, C, G and U. Each duplex was in twofold excess relative to the spin label. Each nitroxide would bind to the abasic site to which it has the highest affinity. Spin labels **1**, **80** and **81** did not show any binding to the four 14-mer RNA duplexes containing an abasic site opposite to either G, U, A or C at -30 °C (**Figure 5.7**). Spin label **82** shows only minor binding to RNA and was not investigated further.

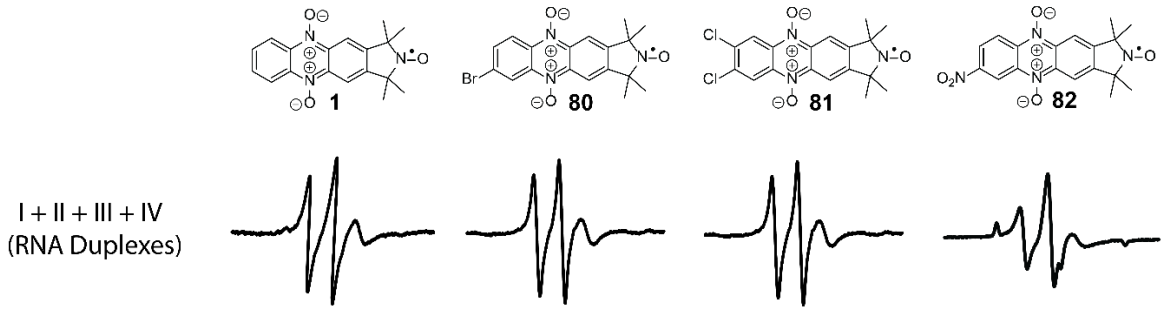

Figure 5.7. Evaluation of noncovalent spin labeling of abasic sites in RNA duplexes by EPR spectroscopy at -30 °C. The complete RNA sequence is 5′-GACCUCG_AUCGUG-3′·5′-CACGAUXCGAGGUC)-3′, where X represents the orphan base. Duplex I X=C, II X=A, III X=G, IV X=U. EPR spectra of the spin-labels (100 μM) in the presence of RNA duplexes (200 μM) were recorded in phosphate buffer (10 mM $NaHPO_4$, 100 mM NaCl, 0.1 mM Na_2EDTA, pH 7.0) containing 30% ethylene glycol and 2% DMSO at -30 °C.

5.8 Conclusions

We have demonstrated the synthesis of *o*-benzoquinone derivatives for both tetramethyl- and tetraethyl-isoindoline. Unfortunately, the *o*-benzoquinone derivatives did not condense with 5-amino-2′deoxycytidine (**52**) to afford a 5′-6-locked, spin-labeled nucleoside. However, the *o*-benzoquinone derivatives were readily condensed with a number of commercially available *o*-phenylenediamines in near quantitative yields. Oxidation of the isoindoline-phenazines gave phenazine

di-*N*-oxide nitroxide radicals that were evaluated as noncovalent spin labels for DNA and RNA containing abasic sites. Spin label **1** showed high binding affinity and specificity towards abasic sites opposite to C in DNA and is, therefore, a promising spin label for future EPR studies of DNAs. Moreover, the *o*-benzoquinone isoindoline derivatives give access to various diversely substituted phenazine structures carrying the isoindoline moiety and may thereby facilitate the incorporation of paramagnetic centers into other functional systems.

6 Conclusions

In this PhD thesis, advancements of nitroxide spin-labeling of nucleic acids using rigid spin labels is described. In the first part, the reduction of nitroxide radicals that occurs during oligonucleotide synthesis is addressed, which has a known and long-lasting problem. The development of a protecting group strategy is described in which the nitroxide functional group of **Ç** was protected by benzoylation of the corresponding hydroxylamine. The resulting **Ç-Bz** was converted into a phosphoramidite and used for oligonucleotide synthesis of DNA of various lengths. The protecting group was stable through the chemical synthesis of the oligonucleotides and was readily removed by standard deprotection conditions to give fully nitroxide-labeled DNA. A 36-nt DNAzyme containing **Ç** at two positions was prepared, giving a fully spin-labeled oligonucleotide, which would not have been possible without this protecting method. Combined, these results show that this protecting group strategy for nitroxides can be used as a general method to prepare spin-labeled nucleic acids using the phosphoramidite approach, thereby circumventing their reduction during the chemical synthesis of DNA.

The second part of the thesis focuses on the synthesis of reduction resistant rigid nitroxide spin labels for the purpose of studying the structure and dynamics of nucleic acids in cells. The synthesis of the tetraethyl-derived rigid spin labels **EÇ** and **EÇm** and their incorporation into DNA and RNA, respectively, is described. The spin-labels were shown to be non-perturbating of duplex structures by numerous methods. Some reduction of **EÇm** took place during the synthesis of **EÇm**-labeled RNA, which was circumvented by using the benzoyl protecting group strategy, described in **Chapter 3**. The new tetraethyl-derived rigid labels **EÇ** and

EÇm showed dramatically increased resistance towards reduction by ascorbic acid, when compared to its tetramethyl derivatives **Ç** and **Çm**, which will enable the investigation of structure and dynamics of DNA and RNA by *in-cell* EPR spectroscopy.

The third part of this thesis describes the synthesis of *o*-benzoquinone derivatives of both tetramethyl- and tetraethyl isoindoline. The *o*-benzoquinone derivatives were readily condensed with numerous commercially available *o*-phenylenediamines in near quantitative yields to obtain phenazine-isoindoline structures that were subsequently oxidized to give phenazine di-*N*-oxide nitroxide radicals. These radicals were evaluated as noncovalent spin labels for DNA and RNA duplexes containing abasic sites. One spin label showed high binding affinity and specificity towards abasic sites opposite to C in DNA and is, therefore, a promising spin label for future EPR studies of DNAs.

References

1. Barhate, N.; Cekan, P.; Massey, A. P.; Sigurdsson, S. T., A nucleoside that contains a rigid nitroxide spin label: A fluorophore in disguise. *Angew. Chem. Int. Ed.* **2007,** *46* (15), 2655-2658.
2. Myers, R. L., *The Basics of Chemistry*. Greenwood Press: 2003.
3. Alberts, B.; Johnson, A.; Lewis, J.; Walter, P.; Raff, M.; Roberts, K., *Molecular Biology of the Cell 4th Edition: International Student Edition*. Routledge: 2002.
4. Häggström, M., Medical gallery of Mikael Häggström. *WikiJournal of Medicine* **2014,** *1* (8).
5. Bhutani, S. P., Carbohydrates. In *Chemistry of Biomolecules, Second Edition*, Bhutani, S. P., Ed. CRC Press: 2019; pp 1-84.
6. Shan, Y.; Wang, H., The structure and function of cell membranes examined by atomic force microscopy and single-molecule force spectroscopy. *Chem. Soc. Rev.* **2015,** *44* (11), 3617-3638.
7. Karp, G., *Cell and Molecular Biology: Concepts and Experiments*. Wiley: 2004.
8. Strauss, J. F.; FitzGerald, G. A., Chapter 4 - Steroid Hormones and Other Lipid Molecules Involved in Human Reproduction. In *Yen and Jaffe's Reproductive Endocrinology (Eighth Edition)*, Strauss, J. F.; Barbieri, R. L., Eds. Content Repository Only!: Philadelphia, 2019; pp 75-114.e7.
9. Araújo, W. L.; Tohge, T.; Ishizaki, K.; Leaver, C. J.; Fernie, A. R., Protein degradation – an alternative respiratory substrate for stressed plants. *Trends Plant Sci.* **2011,** *16* (9), 489-498.
10. Berg, J. M.; Tymoczko, J. L.; Stryer, L., *Biochemistry, Fifth Edition*. W.H. Freeman: 2002.
11. Siegel, G. J.; Agranoff, B. W., *Basic Neurochemistry: Molecular, Cellular, and Medical Aspects*. Lippincott Williams & Wilkins: 1999.
12. Putnam, F., *The Plasma Proteins*. Elsevier Science: 2012.
13. Blanco, A.; Blanco, G., Chapter 6 - Nucleic Acids. In *Med. Biochem.*, Blanco, A.; Blanco, G., Eds. Academic Press: 2017; pp 121-140.
14. Miescher, F., Ueber die chemische Zusammensetzung der Eiterzellen. *Med.-Chem. Unters.* **1871,** (4), 441-460.
15. Dahm, R., Friedrich Miescher and the discovery of DNA. *Dev. Biol.* **2005,** *278* (2), 274-288.
16. Dahm, R., Discovering DNA: Friedrich Miescher and the early years of nucleic acid research. *Hum. Genet.* **2008,** *122* (6), 565-581.
17. Kossel, A., Ueber die basischen Stoffe des Zellkerns. In *Hoppe Seylers Z. Physiol. Chem.*, 1897; Vol. 22, p 176.
18. Olby, R. C., *The Path to the Double Helix: The Discovery of DNA*. Dover Publications: 1994.
19. Franklin, R. E.; Gosling, R. G., The structure of sodium thymonucleate fibres. I. The influence of water content. *Acta Crystallogr.* **1953,** *6* (8-9), 673-677.
20. Watson, J. D.; Crick, F. H. C., Molecular structure of nucleic acids: A structure for deoxyribose nucleic acid. *Nature* **1953,** *171* (4356), 737-738.

21. Travers, A.; Muskhelishvili, G., DNA structure and function. *FEBS J.* **2015,** *282* (12), 2279-2295.
22. Yusupova, G. Z.; Yusupov, M. M.; Cate, J. H. D.; Noller, H. F., The Path of Messenger RNA through the Ribosome. *Cell* **2001,** *106* (2), 233-241.
23. Steitz, T. A., A structural understanding of the dynamic ribosome machine. *Nat. Rev. Mol. Cell Biol.* **2008,** *9* (3), 242-253.
24. Dorman, J. S.; Schmella, M. J.; Wesmiller, S. W., Primer in Genetics and Genomics, Article 1:DNA, Genes, and Chromosomes. *Biol. Res. Nurs.* **2017,** *19* (1), 7-17.
25. Valadkhan, S.; Gunawardane, L. S., Role of small nuclear RNAs in eukaryotic gene expression. *Essays Biochem.* **2013,** *54*, 79-90.
26. Bohnsack Markus, T.; Sloan Katherine, E., Modifications in small nuclear RNAs and their roles in spliceosome assembly and function. In *Biol. Chem.*, 2018; Vol. 399, p 1265.
27. Valencia-Sanchez, M. A.; Liu, J.; Hannon, G. J.; Parker, R., Control of translation and mRNA degradation by miRNAs and siRNAs. *Genes Dev.* **2006,** *20* (5), 515-524.
28. Leigh-Ann, M.; Paul, R. M., MicroRNA: Biogenesis, Function and Role in Cancer. *Curr. Genomics* **2010,** *11* (7), 537-561.
29. O'Brien, J.; Hayder, H.; Zayed, Y.; Peng, C., Overview of MicroRNA Biogenesis, Mechanisms of Actions, and Circulation. *Front. Endocrinol.* **2018,** *9* (402).
30. Hamilton, A. J.; Baulcombe, D. C., A Species of Small Antisense RNA in Posttranscriptional Gene Silencing in Plants. *Science* **1999,** *286* (5441), 950-952.
31. Scherr, M.; Battmer, K.; Winkler, T.; Heidenreich, O.; Ganser, A.; Eder, M., Specific inhibition of bcr-abl gene expression by small interfering RNA. *Blood* **2003,** *101* (4), 1566-1569.
32. Hajiasgharzadeh, K.; Somi, M. H.; Shanehbandi, D.; Mokhtarzadeh, A.; Baradaran, B., Small interfering RNA–mediated gene suppression as a therapeutic intervention in hepatocellular carcinoma. *J. Cell. Physiol.* **2019,** *234* (4), 3263-3276.
33. Tanner, N. K., Ribozymes: the characteristics and properties of catalytic RNAs. *FEMS Microbiol. Rev.* **1999,** *23* (3), 257-275.
34. Weinberg, C. E.; Weinberg, Z.; Hammann, C., Novel ribozymes: discovery, catalytic mechanisms, and the quest to understand biological function. *Nucleic Acids Res.* **2019,** *47* (18), 9480-9494.
35. Lönnberg, H., Cleavage of RNA phosphodiester bonds by small molecular entities: a mechanistic insight. *Org. Biomol. Chem.* **2011,** *9* (6), 1687-1703.
36. Nissen, P.; Hansen, J.; Ban, N.; Moore, P. B.; Steitz, T. A., The Structural Basis of Ribosome Activity in Peptide Bond Synthesis. *Science* **2000,** *289* (5481), 920-930.
37. Hollenstein, M., DNA Catalysis: The Chemical Repertoire of DNAzymes. *Molecules* **2015,** *20* (11), 20777-20804.
38. Morrison, D.; Rothenbroker, M.; Li, Y., DNAzymes: Selected for Applications. *Small Methods* **2018,** *2* (3), 1700319.
39. Holbrook, E. L. H. S. R., Crystallisation of Nucleic Acids. In *eLS*, 2010.
40. McGregor, H. C. J.; Gunderman, R. B., X-Ray Crystallography and the Elucidation of the Structure of DNA. *Am. J. Roentgenol.* **2011,** *196* (6), W689-W692.
41. Holbrook, S. R., Structural Principles From Large RNAs. *Annu. Rev. Biophys.* **2008,** *37* (1), 445-464.
42. Kim, S.-G.; Lin, L.-J.; Reid, B. R., Determination of nucleic acid backbone conformation by proton NMR. *Biochemistry* **1992,** *31* (14), 3564-3574.

43. Katahira, M.; Mashima, T., Nucleic Acid NMR – Introduction. In *Encyclopedia of Biophysics*, Roberts, G. C. K., Ed. Springer Berlin Heidelberg: Berlin, Heidelberg, 2013; pp 1763-1772.
44. Al-Hashimi, H. M., NMR studies of nucleic acid dynamics. *J. Magn. Reson.* **2013,** *237*, 191-204.
45. Dračínský, M.; Hodgkinson, P., Solid-state NMR studies of nucleic acid components. *RSC Adv.* **2015,** *5* (16), 12300-12310.
46. Xu, Y.; Matthews, S., TROSY NMR Spectroscopy of Large Soluble Proteins. In *Modern NMR Methodology. Topics in Current Chemistry.*, Heise, H.; Matthews, S., Eds. Springer Berlin Heidelberg: Berlin, Heidelberg, 2013; Vol. 335, pp 97-119.
47. Roy, R.; Hohng, S.; Ha, T., A practical guide to single-molecule FRET. *Nat. Methods* **2008,** *5* (6), 507-516.
48. Sahoo, H., Förster resonance energy transfer – A spectroscopic nanoruler: Principle and applications. *J. Photochem. Photobiol., C* **2011,** *12* (1), 20-30.
49. Preus, S.; Wilhelmsson, L. M., Advances in Quantitative FRET-Based Methods for Studying Nucleic Acids. *ChemBioChem* **2012,** *13* (14), 1990-2001.
50. Blanchard, S. C., Single-molecule observations of ribosome function. *Curr. Opin. Struct. Biol.* **2009,** *19* (1), 103-109.
51. Sisamakis, E.; Valeri, A.; Kalinin, S.; Rothwell, P. J.; Seidel, C. A. M., Chapter 18 - Accurate Single-Molecule FRET Studies Using Multiparameter Fluorescence Detection. In *Methods Enzymol.*, Walter, N. G., Ed. Academic Press: 2010; Vol. 475, pp 455-514.
52. Kypr, J., Kejnovská, I., Bednářová, K. and Vorlíčková, M., Circular Dichroism Spectroscopy of Nucleic Acids. In *Comprehensive Chiroptical Spectroscopy*, N. Berova, P. L. P., K. Nakanishi and R.W. Woody, Ed. 2012; pp 575-586.
53. Offermans, M. T. C.; Sonneveld, R. D.; Bakker, E.; Deutz-Terlouw, P. P.; de Geus, B.; Rozing, J., Denaturing and non-denaturing gel electrophoresis as methods for the detection of junctional diversity in rearranged T cell receptor sequences. *J. Immunol. Methods* **1995,** *181* (1), 101-114.
54. Woodson, S. A.; Koculi, E., Chapter 9 - Analysis of RNA Folding by Native Polyacrylamide Gel Electrophoresis. In *Methods Enzymol.*, Academic Press: 2009; Vol. 469, pp 189-208.
55. Benevides, J. M.; Thomas, G. J., Jr., Characterization of DNA structures by Raman spectroscopy: high-salt and low-salt forms of double helical poly(dG-dC) in H2O and D2O solutions and application to B, Z and A-DNA *. *Nucleic Acids Res.* **1983,** *11* (16), 5747-5761.
56. George J. Thomas, J., RAMAN SPECTROSCOPY OF PROTEIN AND NUCLEIC ACID ASSEMBLIES. *Annu. Rev. Biophys. Biomol. Struct.* **1999,** *28* (1), 1-27.
57. Papadopoulou, E.; Bell, S. E. J., Label-Free Detection of Single-Base Mismatches in DNA by Surface-Enhanced Raman Spectroscopy. *Angew. Chem. Int. Ed.* **2011,** *50* (39), 9058-9061.
58. EK, Z., Spin-magnetic resonance in paramagnetics. *J Phys Acad Sci USSR* **1945,** *9*, 211–245.
59. Salikhov, K. M.; Zavoiskaya, N. E., Zavoisky and the discovery of EPR. *Resonance* **2015,** *20* (11), 963-968.
60. Shelke, S. A.; Sigurdsson, S. T., Site-directed spin labelling of nucleic acids. *Eur. J. Org. Chem.* **2012,** *2012* (12), 2291-2301.

61. Reginsson, G. W.; Schiemann, O., Spin Labeling of DNA and RNA. In *Encyclopedia of Biophysics*, Roberts, G. C. K., Ed. Springer Berlin Heidelberg: Berlin, Heidelberg, 2013; pp 2429-2431.
62. Roser, P.; Schmidt, M. J.; Drescher, M.; Summerer, D., Site-directed spin labeling of proteins for distance measurements in vitro and in cells. *Org. Biomol. Chem.* **2016,** *14* (24), 5468-5476.
63. Roessler, M. M.; Salvadori, E., Principles and applications of EPR spectroscopy in the chemical sciences. *Chem. Soc. Rev.* **2018,** *47* (8), 2534-2553.
64. Sowa, G. Z.; Qin, P. Z., Site-directed Spin Labeling Studies on Nucleic Acid Structure and Dynamics. In *Prog Nucleic Acid Res Mol Biol.*, Conn, P. M., Ed. Academic Press: 2008; Vol. 82, pp 147-197.
65. Zhang, X.; Cekan, P.; Sigurdsson, S. T.; Qin, P. Z., Chapter 15 - Studying RNA Using Site-Directed Spin-Labeling and Continuous-Wave Electron Paramagnetic Resonance Spectroscopy. In *Methods Enzymol.*, Academic Press: 2009; Vol. 469, pp 303-328.
66. Gophane DB, S. S., Hydrogen-bonding controlled rigidity of an isoindoline-derived nitroxide spin label for nucleic acids. *Chem. Commun.* **2013,** *49*, 999-1001.
67. Kim, N.-K.; Murali, A.; DeRose, V. J., A Distance Ruler for RNA Using EPR and Site-Directed Spin Labeling. *Chem. Biol.* **2004,** *11* (7), 939-948.
68. Reginsson, Gunnar W.; Schiemann, O., Studying biomolecular complexes with pulsed electron–electron double resonance spectroscopy. *Biochem. Soc. Trans.* **2011,** *39* (1), 128-139.
69. Schmidt, T.; Wälti, M. A.; Baber, J. L.; Hustedt, E. J.; Clore, G. M., Long Distance Measurements up to 160 Å in the GroEL Tetradecamer Using Q-Band DEER EPR Spectroscopy. *Angew. Chem. Int. Ed.* **2016,** *55* (51), 15905-15909.
70. Sahu, I. D.; McCarrick, R. M.; Lorigan, G. A., Use of Electron Paramagnetic Resonance To Solve Biochemical Problems. *Biochemistry* **2013,** *52* (35), 5967-5984.
71. Shelke, S. A.; Sigurdsson, S. T., Site-Directed Nitroxide Spin Labeling of Biopolymers. In *Structural Information from Spin-Labels and Intrinsic Paramagnetic Centres in the Biosciences*, Timmel, C. R.; Harmer, J. R., Eds. Springer Berlin Heidelberg: Berlin, Heidelberg, 2013; pp 121-162.
72. Yang, Y.; Yang, F.; Li, X.-Y.; Su, X.-C.; Goldfarb, D., In-cell EPR distance measurements on ubiquitin labeled with a rigid PyMTA-Gd(III) tag. *J. Phys. Chem. B* **2019,** *123* (5), 1050-1059.
73. Banerjee, D.; Yagi, H.; Huber, T.; Otting, G.; Goldfarb, D., Nanometer-Range Distance Measurement in a Protein Using Mn2+ Tags. *J. Phys. Chem. Lett.* **2012,** *3*, 157-160.
74. Shevelev, G. Y.; Krumkacheva, O. A.; Lomzov, A. A.; Kuzhelev, A. A.; Trukhin, D. V.; Rogozhnikova, O. Y.; Tormyshev, V. M.; Pyshnyi, D. V.; Fedin, M. V.; Bagryanskaya, E. G., Triarylmethyl Labels: Toward Improving the Accuracy of EPR Nanoscale Distance Measurements in DNAs. *J. Phys. Chem. B* **2015,** *119* (43), 13641-13648.
75. Krumkacheva, O.; Bagryanskaya, E., Trityl radicals as spin labels. In *Electron Paramagnetic Resonance: Volume 25*, The Royal Society of Chemistry: 2017; Vol. 25, pp 35-60.
76. Berliner, L. J., *Spin Labeling: Theory and Applications*. Elsevier Science: 2013.
77. Forrester, A. R.; Thomson, R. H., Stable Nitroxide Radicals. *Nature* **1964,** *203* (4940), 74-75.
78. Karoui, H., Moigne, F.L., Ouari, O. and Tordo, P., Nitroxide Radicals: Properties, Synthesis and Applications. In *Stable Radicals*, 2010; pp 173-229.

79. Shelke, S. A.; Sigurdsson, S. T., Site-Directed Spin Labeling for EPR Studies of Nucleic Acids. In *Modified Nucleic Acids*, Nakatani, K.; Tor, Y., Eds. Springer International Publishing: Cham, 2016; pp 159-187.
80. Haugland, M. M.; Lovett, J. E.; Anderson, E. A., Advances in the synthesis of nitroxide radicals for use in biomolecule spin labelling. *Chem. Soc. Rev.* **2018,** *47* (3), 668-680.
81. Matteucci, M. D.; Caruthers, M. H., Synthesis of deoxyoligonucleotides on a polymer support. *J. Am. Chem. Soc.* **1981,** *103* (11), 3185-3191.
82. Caruthers, M. H.; Barone, A. D.; Beaucage, S. L.; Dodds, D. R.; Fisher, E. F.; McBride, L. J.; Matteucci, M.; Stabinsky, Z.; Tang, J. Y., Chemical synthesis of deoxyoligonucleotides by the phosphoramidite method. In *Methods Enzymol.*, Academic Press: 1987; Vol. 154, pp 287-313.
83. Caruthers, M. H.; Beaton, G.; Wu, J. V.; Wiesler, W., Chemical synthesis of deoxyoligonucleotides and deoxyoligonucleotide analogs. In *Methods Enzymol.*, Academic Press: 1992; Vol. 211, pp 3-20.
84. Caruthers, M. H., The chemical synthesis of DNA/RNA: Our gift to science. *J. Biol. Chem.* **2013,** *288* (2), 1420-1427.
85. Damha, M. J.; Ogilvie, K. K., Oligoribonucleotide Synthesis. In *Protocols for oligonucleotides and analogs: Synthesis and properties*, Agrawal, S., Ed. Humana Press: Totowa, NJ, 1993; pp 81-114.
86. Muller, S.; Wolf, J.; Ivanov, S. A., Current strategies for the synthesis of RNA. *Curr. Org. Synth.* **2004,** *1* (3), 293-307.
87. Wachowius, F.; Höbartner, C., Chemical RNA modifications for studies of RNA structure and dynamics. *ChemBioChem* **2010,** *11* (4), 469-480.
88. Spaltenstein, A.; Robinson, B. H.; Hopkins, P. B., A rigid and nonperturbing probe for duplex DNA motion. *J. Am. Chem. Soc.* **1988,** *110* (4), 1299-1301.
89. Fischhaber, P. L.; Reese, A. W.; Nguyen, T.; Kirchner, J. J.; Hustedt, E. J.; Robinson, B. H.; Hopkins, P. B., Synthesis of duplex DNA containing a spin labeled analog of 2′-deoxycytidine. *Nucleosides Nucleotides* **1997,** *16* (4), 365-377.
90. Gannett, P. M.; Darian, E.; Powell, J. H.; Johnson, E. M., A short procedure for synthesis of 4-ethynyl-2,2,6,6-tetramethyl-3,4-dehydro-piperidine-1-oxyl nitroxide. *Synth. Commun.* **2001,** *31* (14), 2137-2141.
91. Gannett, P. M.; Darian, E.; Powell, J.; Johnson, E. M.; Mundoma, C.; Greenbaum, N. L.; Ramsey, C. M.; Dalal, N. S.; Budil, D. E., Probing triplex formation by EPR spectroscopy using a newly synthesized spin label for oligonucleotides. *Nucleic Acids Res.* **2002,** *30* (23), 5328-5337.
92. Azarkh, M.; Singh, V.; Okle, O.; Dietrich, D. R.; Hartig, J. S.; Drescher, M., Intracellular conformations of human telomeric quadruplexes studied by electron paramagnetic resonance spectroscopy. *ChemPhysChem* **2012,** *13* (6), 1444-1447.
93. Bannwarth, W.; Schmidt, D., Oligonucleotides containing spin-labeled 2′-deoxycytidine and 5-methyl-2′-deoxycytidine as probes for structural motifs of DNA. *Bioorg. Med. Chem. Lett.* **1994,** *4* (8), 977-980.
94. Giordano, C.; Fratini, F.; Attanasio, D.; Cellai, L., Preparation of spin-labeled-2-Amino-dA, dA, dC and 5-methyl-dC phosphoramidites for the automatic synthesis of EPR active oligonucleotides. *Synthesis* **2001,** *2001* (04), 0565-0572.
95. Cekan, P.; Sigurdsson, S. T., Identification of single-base mismatches in duplex DNA by EPR spectroscopy. *J. Am. Chem. Soc.* **2009,** *131* (50), 18054-18056.

96. Gophane, D. B.; Sigurdsson, S. T., TEMPO-derived spin labels linked to the nucleobases adenine and cytosine for probing local structural perturbations in DNA by EPR spectroscopy. *Beilstein J. Org. Chem.* **2015,** *11*, 219-227.
97. Schiemann, O.; Piton, N.; Mu, Y.; Stock, G.; Engels, J. W.; Prisner, T. F., A PELDOR-based nanometer distance ruler for oligonucleotides. *J. Am. Chem. Soc.* **2004,** *126* (18), 5722-5729.
98. Piton, N.; Mu, Y.; Stock, G.; Prisner, T. F.; Schiemann, O.; Engels, J. W., Base-specific spin-labeling of RNA for structure determination. *Nucleic Acids Res.* **2007,** *35* (9), 3128-3143.
99. Krstić, I.; Frolow, O.; Sezer, D.; Endeward, B.; Weigand, J. E.; Suess, B.; Engels, J. W.; Prisner, T. F., PELDOR spectroscopy reveals preorganization of the neomycin-responsive riboswitch tertiary structure. *J. Am. Chem. Soc.* **2010,** *132* (5), 1454-1455.
100. Höbartner, C.; Sicoli, G.; Wachowius, F.; Gophane, D. B.; Sigurdsson, S. T., Synthesis and characterization of RNA containing a rigid and nonperturbing cytidine-derived spin label. *J. Org. Chem.* **2012,** *77* (17), 7749-7754.
101. Cekan, P.; Smith, A. L.; Barhate, N.; Robinson, B. H.; Sigurdsson, S. T., Rigid spin-labeled nucleoside Ç: A nonperturbing EPR probe of nucleic acid conformation. *Nucleic Acids Res.* **2008,** *36* (18), 5946-5954.
102. Schiemann, O.; Cekan, P.; Margraf, D.; Prisner, T. F.; Sigurdsson, S. T., Relative orientation of rigid nitroxides by PELDOR: Beyond distance measurements in nucleic acids. *Angew. Chem. Int. Ed.* **2009,** *48* (18), 3292-3295.
103. Smith, A. L.; Cekan, P.; Brewood, G. P.; Okonogi, T. M.; Alemayehu, S.; Hustedt, E. J.; Benight, A. S.; Sigurdsson, S. T.; Robinson, B. H., Conformational equilibria of bulged sites in duplex DNA studied by EPR spectroscopy. *J. Phys. Chem. B* **2009,** *113* (9), 2664-2675.
104. Marko, A.; Margraf, D.; Cekan, P.; Sigurdsson, S. T.; Schiemann, O.; Prisner, T. F., Analytical method to determine the orientation of rigid spin labels in DNA. *Phys. Rev. E* **2010,** *81* (2), 021911.
105. Grytz, C. M.; Kazemi, S.; Marko, A.; Cekan, P.; Güntert, P.; Sigurdsson, S. T.; Prisner, T. F., Determination of helix orientations in a flexible DNA by multi-frequency EPR spectroscopy. *Phys. Chem. Chem. Phys.* **2017,** *19* (44), 29801-29811.
106. Gophane, D. B.; Endeward, B.; Prisner, T. F.; Sigurdsson, S. T., Conformationally restricted isoindoline-derived spin labels in duplex DNA: Distances and rotational flexibility by pulsed electron–electron double resonance spectroscopy. *Chem. Eur. J.* **2014,** *20* (48), 15913-15919.
107. Gophane, D. B.; Endeward, B.; Prisner, T. F.; Sigurdsson, S. T., A semi-rigid isoindoline-derived nitroxide spin label for RNA. *Org. Biomol. Chem.* **2018,** *16* (5), 816-824.
108. Hatano, A.; Terado, N.; Kanno, Y.; Nakamura, T.; Kawai, G., Synthesis of a protected ribonucleoside phosphoramidite-linked spin label via an alkynyl chain at the 5′ position of uridine. *Synth. Commun.* **2019,** *49* (1), 136-145.
109. Chalmers, B. A.; Morris, J. C.; Fairfull-Smith, K. E.; Grainger, R. S.; Bottle, S. E., A novel protecting group methodology for syntheses using nitroxides. *Chem. Commun.* **2013,** *49* (88), 10382-10384.
110. Dane, E. L.; Corzilius, B.; Rizzato, E.; Stocker, P.; Maly, T.; Smith, A. A.; Griffin, R. G.; Ouari, O.; Tordo, P.; Swager, T. M., Rigid orthogonal bis-TEMPO biradicals with improved solubility for dynamic nuclear polarization. *J. Org. Chem.* **2012,** *77* (4), 1789-1797.

111. Seven, I.; Weinrich, T.; Gränz, M.; Grünewald, C.; Brüß, S.; Krstić, I.; Prisner, T. F.; Heckel, A.; Göbel, M. W., Photolabile Protecting Groups for Nitroxide Spin Labels. *Eur. J. Org. Chem.* **2014,** *2014* (19), 4037-4043.
112. Weinrich, T. J., E. A.; Scheffer, U. M.; Prisner, T. F.; Göbel, M. W., Phosphoramidite building blocks with protected nitroxides for the synthesis of spin-labeled DNA and RNA. *Beilstein J. Org. Chem.* **2018,** *14*, 1563–1569.
113. Weinrich, T.; Gränz, M.; Grünewald, C.; Prisner, T. F.; Göbel, M. W., Synthesis of a Cytidine Phosphoramidite with Protected Nitroxide Spin Label for EPR Experiments with RNA. *Eur. J. Org. Chem.* **2017,** *2017* (3), 491-496.
114. Weinrich, T.; Jaumann, E. A.; Scheffer, U.; Prisner, T. F.; Göbel, M. W., A cytidine phosphoramidite with protected nitroxide spin label: Synthesis of a full-length TAR RNA and investigation by in-line probing and EPR spectroscopy. *Chem. Eur. J.* **2018,** *24* (23), 6202-6207.
115. Sato, Y.; Hayashi, H.; Okazaki, M.; Aso, M.; Karasawa, S.; Ueki, S.; Suemune, H.; Koga, N., Water-proton relaxivities of DNA oligomers carrying TEMPO radicals. *Magn. Reson. Chem.* **2008,** *46* (11), 1055-1058.
116. Kurita, M.; Higuchi, Y.; Mirc, J.; Matsumoto, S.; Usui, K.; Suemune, H.; Aso, M., Synthesis and Electron Paramagnetic Resonance Studies of Oligodeoxynucleotides Containing 2-N-tert-Butylaminoxyl-2′-deoxyadenosines. *ChemBioChem* **2016,** *17* (24), 2346-2352.
117. Cekan, P.; Sigurdsson, S. T., Single base interrogation by a fluorescent nucleotide: each of the four DNA bases identified by fluorescence spectroscopy. *Chem. Commun.* **2008,** (29), 3393-3395.
118. Giassa, I.-C.; Rynes, J.; Fessl, T.; Foldynova-Trantirkova, S.; Trantirek, L., Advances in the cellular structural biology of nucleic acids. *FEBS Lett.* **2018,** *592* (12), 1997-2011.
119. Bonucci, A.; Ouari, O.; Guigliarelli, B.; Belle, V.; Mileo, E., In-cell EPR: Progress towards structural studies inside cells. *ChemBioChem* **2019**.
120. Luchinat, E.; Banci, L., In-cell NMR: A topical review. *IUCrJ* **2017,** *4* (2), 108-118.
121. Lippens, G.; Cahoreau, E.; Millard, P.; Charlier, C.; Lopez, J.; Hanoulle, X.; Portais, J. C., In-cell NMR: From metabolites to macromolecules. *Analyst* **2018,** *143* (3), 620-629.
122. Keyes, R. S.; Bobst, E. V.; Cao, Y. Y.; Bobst, A. M., Overall and internal dynamics of DNA as monitored by five-atom-tethered spin labels. *Biophys. J.* **1997,** *72* (1), 282-290.
123. Edwards, T. E.; Okonogi, T. M.; Robinson, B. H.; Sigurdsson, S. T., Site-Specific Incorporation of Nitroxide Spin-Labels into Internal Sites of the TAR RNA; Structure-Dependent Dynamics of RNA by EPR Spectroscopy. *J. Am. Chem. Soc.* **2001,** *123* (7), 1527-1528.
124. Miller, T. R.; Alley, S. C.; Reese, A. W.; Solomon, M. S.; McCallister, W. V.; Mailer, C.; Robinson, B. H.; Hopkins, P. B., A Probe for Sequence-Dependent Nucleic Acid Dynamics. *J. Am. Chem. Soc.* **1995,** *117* (36), 9377-9378.
125. Miller, T. R.; Hopkins, P. B., Toward the synthesis of a second-generation nitroxide spin probe for DNA dynamics studies. *Bioorg. Med. Chem. Lett.* **1994,** *4* (8), 981-986.
126. Okonogi, T. M.; Alley, S. C.; Reese, A. W.; Hopkins, P. B.; Robinson, B. H., Sequence-Dependent Dynamics of Duplex DNA: The Applicability of a Dinucleotide Model. *Biophys. J.* **2002,** *83* (6), 3446-3459.
127. Edwards, T. E.; Cekan, P.; Reginsson, G. W.; Shelke, S. A.; Ferré-D'Amaré, A. R.; Schiemann, O.; Sigurdsson, S. T., Crystal structure of a DNA containing the planar,

phenoxazine-derived bi-functional spectroscopic probe Ç. *Nucleic Acids Res.* **2011,** *39* (10), 4419-4426.
128. Marko, A.; Denysenkov, V.; Margraf, D.; Cekan, P.; Schiemann, O.; Sigurdsson, S. T.; Prisner, T. F., Conformational Flexibility of DNA. *J. Am. Chem. Soc.* **2011,** *133* (34), 13375-13379.
129. Hänsel, R.; Luh, L. M.; Corbeski, I.; Trantirek, L.; Dötsch, V., In-cell NMR and EPR spectroscopy of biomacromolecules. *Angew. Chem. Int. Ed.* **2014,** *53* (39), 10300-10314.
130. Freedberg, D. I.; Selenko, P., Live cell NMR. *Annu. Rev. Biochem.* **2014,** *43* (1), 171-192.
131. Narasimhan, S.; Scherpe, S.; Lucini Paioni, A.; van der Zwan, J.; Folkers, G. E.; Ovaa, H.; Baldus, M., DNP-supported solid-state NMR spectroscopy of proteins inside mammalian cells. *Angew. Chem. Int. Ed.* **2019,** *58* (37), 12969-12973.
132. Hänsel, R.; Foldynová-Trantírková, S.; Löhr, F.; Buck, J.; Bongartz, E.; Bamberg, E.; Schwalbe, H.; Dötsch, V.; Trantírek, L., Evaluation of Parameters Critical for Observing Nucleic Acids Inside Living Xenopus laevis Oocytes by In-Cell NMR Spectroscopy. *J. Am. Chem. Soc.* **2009,** *131* (43), 15761-15768.
133. Lim, K. W.; Amrane, S.; Bouaziz, S.; Xu, W.; Mu, Y.; Patel, D. J.; Luu, K. N.; Phan, A. T., Structure of the Human Telomere in K+ Solution: A Stable Basket-Type G-Quadruplex with Only Two G-Tetrad Layers. *J. Am. Chem. Soc.* **2009,** *131* (12), 4301-4309.
134. Padilla-Parra, S.; Tramier, M., FRET microscopy in the living cell: Different approaches, strengths and weaknesses. *BioEssays* **2012,** *34* (5), 369-376.
135. Raicu, V.; Singh, Deo R., FRET spectrometry: A new tool for the determination of protein quaternary structure in living cells. *Biophys. J.* **2013,** *105* (9), 1937-1945.
136. Fessl, T.; Adamec, F.; Polívka, T.; Foldynová-Trantírková, S.; Vácha, F.; Trantírek, L., Towards characterization of DNA structure under physiological conditions in vivo at the single-molecule level using single-pair FRET. *Nucleic Acids Res.* **2012,** *40* (16), e121-e121.
137. Azarkh, M.; Singh, V.; Okle, O.; Seemann, I. T.; Dietrich, D. R.; Hartig, J. S.; Drescher, M., Site-directed spin-labeling of nucleotides and the use of in-cell EPR to determine long-range distances in a biologically relevant environment. *Nat Protoc.* **2012,** *8*, 131-147.
138. Schmidt, M. J.; Fedoseev, A.; Summerer, D.; Drescher, M., Chapter eighteen - genetically encoded spin labels for in vitro and in-cell EPR studies of native proteins. In *Meth. Enzymol.*, Qin, P. Z.; Warncke, K., Eds. Academic Press: 2015; Vol. 563, pp 483-502.
139. Azarkh, M.; Okle, O.; Singh, V.; Seemann, I. T.; Hartig, J. S.; Dietrich, D. R.; Drescher, M., Long-range distance determination in a DNA model system inside Xenopus laevis oocytes by in-cell spin-label EPR. *ChemBioChem* **2011,** *12* (13), 1992-1995.
140. Krstić, I.; Hänsel, R.; Romainczyk, O.; Engels, J. W.; Dötsch, V.; Prisner, T. F., Long-range distance measurements on nucleic acids in cells by pulsed EPR spectroscopy. *Angew. Chem. Int. Ed.* **2011,** *50* (22), 5070-5074.
141. Joseph, B.; Sikora, A.; Cafiso, D. S., Ligand induced conformational changes of a membrane transporter in E. coli cells observed with DEER/PELDOR. *J. Am. Chem. Soc.* **2016,** *138* (6), 1844-1847.
142. Qi, M.; Groß, A.; Jeschke, G.; Godt, A.; Drescher, M., Gd(III)-PyMTA label is suitable for in-cell EPR. *J. Am. Chem. Soc.* **2014,** *136* (43), 15366-15378.

143. Yang, Y.; Yang, F.; Gong, Y.-J.; Chen, J.-L.; Goldfarb, D.; Su, X.-C., A reactive, rigid GdIII labeling tag for in-cell EPR distance measurements in proteins. *Angew. Chem. Int. Ed.* **2017,** *56* (11), 2914-2918.
144. Martorana, A.; Bellapadrona, G.; Feintuch, A.; Di Gregorio, E.; Aime, S.; Goldfarb, D., Probing protein conformation in cells by EPR distance measurements using Gd3+ spin labeling. *J. Am. Chem. Soc.* **2014,** *136* (38), 13458-13465.
145. Cattani, J.; Subramaniam, V.; Drescher, M., Room-temperature in-cell EPR spectroscopy: Alpha-synuclein disease variants remain intrinsically disordered in the cell. *Phys. Chem. Chem. Phys.* **2017,** *19* (28), 18147-18151.
146. Schmidt, M. J.; Fedoseev, A.; Summerer, D.; Drescher, M., Chapter Eighteen - Genetically Encoded Spin Labels for In Vitro and In-Cell EPR Studies of Native Proteins. In *Methods Enzymol.*, Qin, P. Z.; Warncke, K., Eds. Academic Press: 2015; Vol. 563, pp 483-502.
147. Robotta, M.; Gerding, H. R.; Vogel, A.; Hauser, K.; Schildknecht, S.; Karreman, C.; Leist, M.; Subramaniam, V.; Drescher, M., Alpha-synuclein binds to the inner membrane of mitochondria in an α-helical conformation. *ChemBioChem* **2014,** *15* (17), 2499-2502.
148. Karthikeyan, G.; Bonucci, A.; Casano, G.; Gerbaud, G.; Abel, S.; Thomé, V.; Kodjabachian, L.; Magalon, A.; Guigliarelli, B.; Belle, V.; Ouari, O.; Mileo, E., A bioresistant nitroxide spin label for in-cell EPR spectroscopy: In vitro and in oocytes protein structural dynamics studies. *Angew. Chem. Int. Ed.* **2018,** *130* (5), 1380-1384.
149. Saha, S.; Jagtap, A. P.; Sigurdsson, S. T., Site-directed spin labeling of 2′-amino groups in RNA with isoindoline nitroxides that are resistant to reduction. *Chem. Commun.* **2015,** *51* (66), 13142-13145.
150. Jagtap, A. P.; Krstic, I.; Kunjir, N. C.; Hänsel, R.; Prisner, T. F.; Sigurdsson, S. T., Sterically shielded spin labels for in-cell EPR spectroscopy: Analysis of stability in reducing environment. *Free Radical Res.* **2015,** *49* (1), 78-85.
151. Bobko, A. A.; Kirilyuk, I. A.; Grigor'ev, I. A.; Zweier, J. L.; Khramtsov, V. V., Reversible reduction of nitroxides to hydroxylamines: Roles for ascorbate and glutathione. *Free Radic. Biol. Med.* **2007,** *42* (3), 404-412.
152. Grytz, C. M.; Marko, A.; Cekan, P.; Sigurdsson, S. T.; Prisner, T. F., Flexibility and conformation of the cocaine aptamer studied by PELDOR. *Phys. Chem. Chem. Phys.* **2016,** *18* (4), 2993-3002.
153. Schnorr, K. A.; Gophane, D. B.; Helmling, C.; Cetiner, E.; Pasemann, K.; Fürtig, B.; Wacker, A.; Qureshi, N. S.; Gränz, M.; Barthelmes, D.; Jonker, H. R. A.; Stirnal, E.; Sigurdsson, S. T.; Schwalbe, H., Impact of spin label rigidity on extent and accuracy of distance information from PRE data. *J. Biomol. NMR* **2017,** *68* (1), 53-63.
154. Gophane, D. B.; Sigurdsson, S. T., Hydrogen-bonding controlled rigidity of an isoindoline-derived nitroxide spin label for nucleic acids. *Chem. Commun.* **2013,** *49* (10), 999-1001.
155. Haugland, M. M.; El-Sagheer, A. H.; Porter, R. J.; Peña, J.; Brown, T.; Anderson, E. A.; Lovett, J. E., 2′-Alkynylnucleotides: A sequence- and spin label-flexible strategy for EPR spectroscopy in DNA. *J. Am. Chem. Soc.* **2016,** *138* (29), 9069-9072.
156. Lin, K.-Y.; Jones, R. J.; Matteucci, M., Tricyclic 2'-deoxycytidine analogs: Syntheses and incorporation into oligodeoxynucleotides which have enhanced binding to complementary RNA. *J. Am. Chem. Soc.* **1995,** *117* (13), 3873-3874.
157. Volodarsky, L. B.; Reznikov, V. A.; Ovcharenko, V. I., *Synthetic chemistry of stable nitroxides*. Taylor & Francis: 1993.

158. Juliusson, H. Y.; Segler, A.-L. J.; Sigurdsson, S. T., Benzoyl-protected hydroxylamines for improved chemical synthesis of oligonucleotides containing nitroxide spin labels. *Eur. J. Org. Chem.* **2019,** *2019* (23), 3799-3805.
159. Sen, V. D.; Golubev, V. A., Kinetics and mechanism for acid-catalyzed disproportionation of 2,2,6,6-tetramethylpiperidine-1-oxyl. *J. Phys. Org. Chem.* **2009,** *22* (2), 138-143.
160. Engman, K. C.; Sandin, P.; Osborne, S.; Brown, T.; Billeter, M.; Lincoln, P.; Nordén, B.; Albinsson, B.; Wilhelmsson, L. M., DNA adopts normal B-form upon incorporation of highly fluorescent DNA base analogue tC: NMR structure and UV-Vis spectroscopy characterization. *Nucleic Acids Res.* **2004,** *32* (17), 5087-5095.
161. Sandin, P.; Stengel, G.; Ljungdahl, T.; Börjesson, K.; Macao, B.; Wilhelmsson, L. M., Highly efficient incorporation of the fluorescent nucleotide analogs tC and tCO by Klenow fragment. *Nucleic Acids Res.* **2009,** *37* (12), 3924-3933.
162. Gislason, K.; Sigurdsson, S. T., Synthesis of a 5′-6-Locked, 1,10-Phenanthroline-Containing Nucleoside and Its Incorporation into DNA. *Eur. J. Org. Chem.* **2010,** *2010* (24), 4713-4718.
163. Gislason, K.; Gophane, D. B.; Sigurdsson, S. T., Syntheses and photophysical properties of 5′–6-locked fluorescent nucleosides. *Org. Biomol. Chem.* **2013,** *11* (1), 149-157.
164. Gislason, K.; Sigurdsson, S. T., Rigid 5′-6-locked phenanthroline-derived nucleosides chelated to ruthenium and europium ions. *Bioorg. Med. Chem. Lett.* **2013,** *23* (1), 264-267.
165. Ge, P.; Kalman, T. I., Design and synthesis of 3,5-dialkylamino substituted 8H,10H-3(R),5(R),15b(S)-2,3,6,7-tetrahydro-1,5,3-dioxazepino[3,2-c]indolo[3,2-g]pteridine-7-ones. *Bioorg. Med. Chem. Lett.* **1997,** *7* (23), 3023-3026.
166. Ge, P.; Kalman, T. I., Structural assignment of 2,3,7,8-tetrahydro-5H,10H-[1,5,3]dioxazepino[3,2-c]indolo[3,2-g]pteridin-7-one, a New heterocyclic ring system. *Journal of Heterocyclic Chemistry* **1998,** *35* (1), 257-260.
167. S. Micallef, A.; C. Bott, R.; E. Bottle, S.; Smith, G.; M. White, J.; Matsuda, K.; Iwamura, H., Brominated isoindolines: Precursors to functionalised nitroxides. *J. Chem. Soc. Perkin Trans. 2* **1999,** (1), 65-72.
168. Fairfull-Smith, K. E.; Brackmann, F.; Bottle, S. E., The synthesis of novel isoindoline nitroxides bearing water-solubilising functionality. *Eur. J. Org. Chem.* **2009,** (12), 1902-1915.
169. Blinco, J. P.; Hodgson, J. L.; Morrow, B. J.; Walker, J. R.; Will, G. D.; Coote, M. L.; Bottle, S. E., Experimental and theoretical studies of the redox potentials of cyclic nitroxides. *J. Org. Chem.* **2008,** *73* (17), 6763-6771.
170. Snyder, C. D.; Rapoport, H., Oxidative cleavage of hydroquinone ethers with argentic oxide. *J. Am. Chem. Soc.* **1972,** *94* (1), 227-231.
171. Vickery, E. H.; Pahler, L. F.; Eisenbraun, E. J., Selective o-demethylation of catechol ethers. Comparison of boron tribromide and iodotrimethylsilane. *J. Org. Chem.* **1979,** *44* (24), 4444-4446.
172. Hirano, M.; Yakabe, S.; Chikamori, H.; H. Clark, J.; Morimoto, T., Oxidation by chemical manganese dioxide. Part 3.1 Oxidation of benzylic and allylic alcohols, hydroxyarenes and aminoarenes. *J. Chem. Res., Synop.* **1998,** (12), 770-771.
173. Hong, S.-J.; Piette, L. H., Electron spin resonance spin-label studies of intercalation of ethidium bromide and aromatic amine carcinogens in DNA. *Cancer Res.* **1976,** *36* (3), 1159-1171.

174. Ottaviani, M. F.; Ghatlia, N. D.; Bossmann, S. H.; Barton, J. K.; Duerr, H.; Turro, N. J., Nitroxide-labeled ruthenium(II)-polypyridyl complexes as EPR probes to study organized systems. 2. Combined photophysical and EPR investigations of B-DNA. *J. Am. Chem. Soc.* **1992,** *114* (23), 8946-8952.
175. Saha, S.; Hetzke, T.; Prisner, T. F.; Sigurdsson, S. T., Noncovalent spin-labeling of RNA: The aptamer approach. *Chem. Commun.* **2018,** *54* (83), 11749-11752.
176. Yoshimoto, K.; Nishizawa, S.; Minagawa, M.; Teramae, N., Use of abasic site-containing DNA strands for nucleobase recognition in water. *J. Am. Chem. Soc.* **2003,** *125* (30), 8982-8983.
177. Sato, Y.; Ichihashi, T.; Nishizawa, S.; Teramae, N., Strong and selective binding of amiloride to an abasic site in RNA duplexes: Thermodynamic characterization and microRNA detection. *Angew. Chem. Int. Ed.* **2012,** *51* (26), 6369-6372.
178. Sato, Y.; Toriyabe, Y.; Nishizawa, S.; Teramae, N., 2,4-Diamino-6,7-dimethylpteridine as a fluorescent ligand for binding and sensing an orphan cytosine in RNA duplexes. *Chem. Commun.* **2013,** *49* (85), 9983-9985.
179. Belmont, P.; Chapelle, C.; Demeunynck, M.; Michon, J.; Michon, P.; Lhomme, J., Introduction of a nitroxide group on position 2 of 9-phenoxyacridine: Easy access to spin labelled DNA-binding conjugates. *Bioorg. Med. Chem. Lett.* **1998,** *8* (6), 669-674.
180. Thomas, F.; Michon, J.; Lhomme, J., Interaction of a spin-labeled adenine−acridine conjugate with a DNA duplex containing an abasic site model. *Biochemistry* **1999,** *38* (6), 1930-1937.
181. Shelke, S. A.; Sigurdsson, S. T., Noncovalent and site-directed spin labeling of nucleic acids. *Angew. Chem. Int. Ed.* **2010,** *49* (43), 7984-7986.
182. Shelke, S. A.; Sigurdsson, S. T., Structural changes of an abasic site in duplex DNA affect noncovalent binding of the spin label ç. *Nucleic Acids Res.* **2011,** *40* (8), 3732-3740.
183. Shelke, S. A.; Sigurdsson, S. T., Effect of N3 Modifications on the Affinity of Spin Label ç for Abasic Sites in Duplex DNA. *ChemBioChem* **2012,** *13* (5), 684-690.
184. Reginsson, G. W.; Shelke, S. A.; Rouillon, C.; White, M. F.; Sigurdsson, S. T.; Schiemann, O., Protein-induced changes in DNA structure and dynamics observed with noncovalent site-directed spin labeling and PELDOR. *Nucleic Acids Res.* **2012,** *41* (1), e11-e11.
185. Kamble, N. R.; Gränz, M.; Prisner, T. F.; Sigurdsson, S. T., Noncovalent and site-directed spin labeling of duplex RNA. *Chem. Commun.* **2016,** *52* (100), 14442-14445.
186. Kamble, N. R.; Sigurdsson, S. T., Purine-derived nitroxides for noncovalent spin-labeling of abasic sites in duplex nucleic acids. *Chem. Eur. J.* **2018,** *24* (16), 4157-4164.
187. Heinz, M.; Erlenbach, N.; Stelzl, L. S.; Thierolf, G.; Kamble, N. R.; Sigurdsson, S. T H.; Prisner, T. F.; Hummer, G., High-resolution EPR distance measurements on RNA and DNA with the non-covalent $\acute{\rm G}$ spin label. *Nucleic Acids Research* **2019**.
188. Gago, F., Stacking interactions and intercalative DNA binding. *Methods* **1998,** *14* (3), 277-292.

Publications

I. Juliusson, H. Y., Segler, A. J. and Sigurdsson, S. T., Benzoyl-Protected Hydroxylamines for Improved Chemical Synthesis of Oligonucleotides Containing Nitroxide Spin Labels. *Eur. J. Org. Chem.*, **2019**, 3799-3805. doi:10.1002/ejoc.201900553

II. Juliusson, H. Y. and Sigurdsson, S. T., Reduction resistant and rigid nitroxide spin labels for DNA and RNA. *J. Org. Chem.*, **2019**, Just accepted.

III. Juliusson, H. Y. and Sigurdsson, S. T. (2020), Nitroxide-derived N-oxide phenazines for noncovalent spin-labeling of DNA. Manuscript submitted

Paper I

ChemPubSoc Europe

DOI: 10.1002/ejoc.201900553

EurJOC European Journal of Organic Chemistry

Full Paper

Nitroxide-Labeled Oligonucleotides | *Very Important Paper* |

Benzoyl-Protected Hydroxylamines for Improved Chemical Synthesis of Oligonucleotides Containing Nitroxide Spin Labels

Haraldur Y. Juliusson,[a][‡] Anna-Lena J. Segler,[a][‡] and Snorri Th. Sigurdsson*[a]

Abstract: Oligonucleotides containing nitroxide spin labels, used in biophysical studies of nucleic acids, are frequently prepared by chemical synthesis. However, during the synthesis of spin-labeled oligonucleotides, the nitroxides are partially reduced to the corresponding amines. Here we report that a benzoylated hydroxylamine can be used as a protected form of the nitroxide to avoid this reduction. The benzoyl group is stable through the oligonucleotide synthesis and is readily removed under standard oligonucleotide deprotection conditions, yielding a hydroxylamine that is oxidized in situ to the nitroxide. This method was used to incorporate the rigid spin labels **Ç** and **Çm** into DNA and RNA oligonucleotides, respectively, including a doubly labeled 36-nucleotide long DNAzyme. Enzymatic digestion of the spin-labeled oligonucleotides and subsequent HPLC analysis showed that the nitroxides were intact. This protecting group strategy facilitates the high-yielding synthesis of spin-labeled DNA and RNA oligonucleotides using the phosphoramidite method.

Introduction

Nucleic acids are essential for life as they contain the cellular blueprint in living organisms and are active participants in the cellular machinery, for example in regulation of gene expression.[1] Therefore, it is of great interest to determine their structure and dynamics in order to gain insights into their function. Several different techniques are used for such studies. X-ray crystallography can provide three-dimensional structures and precise arrangements of atoms in space, but growing a highly-diffractive single crystal can be a laborious and time-consuming task.[2] Moreover, the crystals of the biomolecules might not represent their biologically active conformation.[3] Nuclear magnetic resonance (NMR) spectroscopy provides high-resolution structural information under biologically relevant conditions as well as information on dynamics.[4] However, NMR has inherently low sensitivity and, therefore, a relatively large amount of sample is required and the measurements can be time-consuming.[5] Förster resonance energy transfer (FRET) is a technique that measures the distances between two or more chromophores.[6] FRET has been used extensively to study tertiary structures of nucleic acids and has enabled studies of single molecules.[7]

Electron paramagnetic resonance (EPR) spectroscopy is another method to study the structure and dynamics of nucleic acids. For structural studies, continuous wave (CW) EPR can be used to measure distances up to 25 Å.[8] Pulsed dipolar spectroscopy, such as pulsed electron-electron double resonance (PELDOR), also called double electron-electron resonance (DEER), relaxation induced dipolar modulation enhancement (RIDME), single frequency technique for refocusing dipolar couplings (SIFTER) and double quantum coherence (DQC) can be used to measure distances between 15–160 Å.[9] Information about dynamics of nucleic acids can be obtained directly from line-broadening of CW-EPR spectra[10] and from orientation studies using pulsed EPR.[11] In EPR spectroscopy, transitions between spin states of unpaired electrons in a magnetic field are measured. Since nucleic acids and most other biomolecules are diamagnetic, a paramagnetic center needs to be introduced. Paramagnetic metal ions have been used as spin labels for EPR[12] but more often organic radicals, such as nitroxides, are employed for spin labeling.[13]

Incorporation of spin labels at specific sites in nucleic acids is called site-directed spin-labeling (SDSL) and is performed either through covalent or noncovalent binding.[14] Covalent spin-labeling is either carried out post-synthetically or by using spin-labeled phosphoramidites as building blocks in chemical synthesis of nucleic acids.[14a,14b,14d] Post-synthetic labeling requires oligonucleotides that have reactive groups at specific sites for modification with the spin label after the oligonucleotide synthesis.[14a,14b,14d] An advantage of post-synthetic labeling is that the label is not exposed to the reagents used for oligonucleotide synthesis, but drawbacks include non-specific reactions with other functional groups present in nucleic acids and incomplete spin labeling. Also, the spin labels that are incorporated post-synthetically contain flexible tethers, that render distance measurements less accurate and relative orientation of labels cannot be determined.[15]

With the phosphoramidite method, it is possible to incorporate intricate labels with unique structural features, such as rigid labels, into nucleic acids.[16] Drawbacks of the phosphoramidite approach include the synthetic effort required to prepare spin-

[a] *Department of Chemistry, Science Institute, University of Iceland*
Dunhaga 3, 107 Reykjavik, Iceland
E-mail: snorrisi@hi.is
https://notendur.hi.is/snorrisi/
[‡] These authors contributed equally to this work
Supporting information and ORCID(s) from the author(s) for this article are available on the WWW under https://doi.org/10.1002/ejoc.201900553.

labeled phosphoramidites and exposure of the nitroxides to reagents used in the solid-phase synthesis, resulting in a partial[17] or even complete[18] reduction of the nitroxide to its corresponding amine. For oligonucleotides shorter than ca. 15-nucleotide (nt) long, the desired spin-labeled product can be readily separated from the reduced material by denaturing polyacrylamide gel electrophoresis (DPAGE). For longer oligonucleotides, on the other hand, the separation is usually a tedious and nontrivial task that often results in a mixture of spin-labeled and reduced material. Protecting the nitroxide with a group that is stable through the oligonucleotide synthesis would eliminate this drawback of spin-labeling nucleic acids by the phosphoramidite method.

Nitroxides have been protected as *O*-methyl hydroxylamines under reaction conditions that would otherwise reduce the nitroxide.[19] The methyl group can be removed by treatment with *meta*-chloroperbenzoic acid (*m*-CPBA), but this reagent can also oxidize nitrogen atoms in the heterocyclic nucleobases present in nucleic acids. The *tert*-butyldimethylsilyl (TBDMS) group has been used to protect the hydroxylamine of 2,2,6,6-tetramethylpiperidyl-1-oxyl (TEMPO) for the synthesis of a nitroxide-nitroxide biradical,[20] however, less than 50 % of the nitroxide was recovered after removal of the TBDMS groups. Photolabile protecting groups have been used to protect TEMPO during oligonucleotide synthesis, of both DNA and RNA; irradiation with light gave high yields of spin-labeled oligonucleotides.[21] Photoprotection of nitroxides is a useful method for photocaging, allowing a controlled release of the protecting group in functional nucleic acids.[22] However, additional synthetic effort is required to prepare and incorporate the photolabile protecting group and specialized equipment is needed to irradiate the oligomers with the right wavelength for deprotection. An ideal protecting group for routine preparation of spin-labeled oligonucleotides would be removed by using standard oligonucleotide deprotecting conditions, returning the radical without having to include an additional deprotection step. An acetyl group has been used to protect a TEMPO moiety attached to a deoxyuridine phosphoramidite during incorporation into DNA. After oligomer deprotection using standard conditions,[23] complete removal of the acetyl group required additional incubation with aqueous NaOH (0.5 M), conditions that are not compatible with RNA. During the course of this work, we also became aware of a report describing the incorporation of 2-*N*-*tert*-butylaminoxyl-2′-deoxyadenosine into DNA, utilizing acetylated hydroxylamine,[24] however, the structure of this nitroxide is very different from the nitroxides that are normally used for spin labeling.

Here we describe a protecting group strategy for chemical synthesis of nitroxide-labeled DNA and RNA that is based on protection of the corresponding hydroxylamine with a benzoyl group, which is compatible with the conditions of solid-phase synthesis of oligonucleotides. The benzoyl group is quantitatively removed under standard conditions used for oligonucleotide deprotection, yielding a hydroxylamine that oxidizes in situ to the corresponding nitroxide radical.[21a,25] This method was used to synthesize fully spin-labeled DNA and RNA oligonucleotides in high yields.

Results and Discussion

The main incentive for carrying out this work was to enable incorporation of rigid spin labels into long sequences (> 15 nt) by solid-phase synthesis, but such spin labels cannot be incorporated by post-synthetic labeling. Specifically, we were interested in incorporating the spin labels **Ç**[16] and **Çm**[26] (Figure 1) into DNA and RNA oligonucleotides, respectively. These spin labels are valuable probes of both structure and dynamics of nucleic acids.[16,26] An advantage of using these labels for developing a general nitroxide protecting group strategy is that reduction of the nitroxides yields the fluorescent amines **Çf**[16] and **Çmf**[27] (Figure 1), allowing for easy detection.

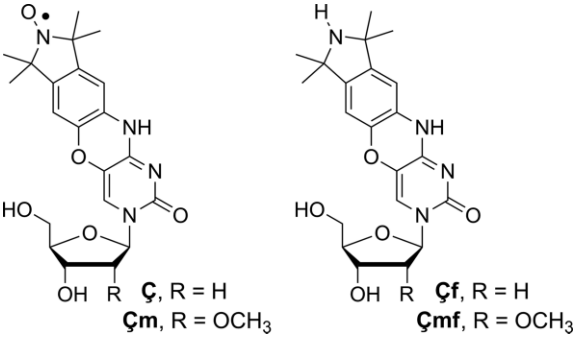

Figure 1. The rigid spin labels **Ç**[16] and **Çm**[26] and their corresponding amines **Çf**[16] and **Çmf**.[27]

The synthesis of **Ç-Bz** and **Çm-Bz** (Scheme 1) began by protecting the 5′- and 3′-hydroxyl groups of **Ç** and **Çm** with TBDMS. The resulting nitroxide radicals **1** and **2** were reduced with ascorbic acid to yield the corresponding hydroxylamines that were subsequently benzoylated, followed by removal of the TBDMS groups to give **Ç-Bz** and **Çm-Bz**. The benzoyl protecting group was shown to be stable under all reaction conditions used for oligonucleotide synthesis for more than five days, except when exposed to either 5-ethylthio tetrazole or 5-benzylthio tetrazole, present in the activation solutions, where slight removal of the benzoyl group was observed after 24 h (data not shown).

The benzoyl protecting group was readily removed within one and two hours under deprotecting conditions for RNA ($MeNH_2/NH_3$ in H_2O/EtOH) and DNA (satd. aq. NH_3), respectively. The 5′-hydroxyl groups of **Ç-Bz** and **Çm-Bz** (Scheme 1) were protected as 4,4′-dimethoxytrityl (DMT) ethers and subsequently phosphitylated to give phosphoramidites **3** and **4**, respectively, in good yields.

Phosphoramidite **4** was used to synthesize an 8-nt long, spin-labeled RNA oligomer (**I**, Table 1). This oligomer was chosen because short oligonucleotides that contain a reduced spin label can be separated by DPAGE from oligomers containing the nitroxide, thus allowing direct visualization of both products. An RNA of the same sequence was also synthesized with a phosphoramidite of the unprotected **Çm**[26] (**II**, Table 1) for comparison.

The phosphoramidite containing the protected spin label coupled well during the solid-phase synthesis as indicated by a strong orange color of the trityl cation that appears during re-

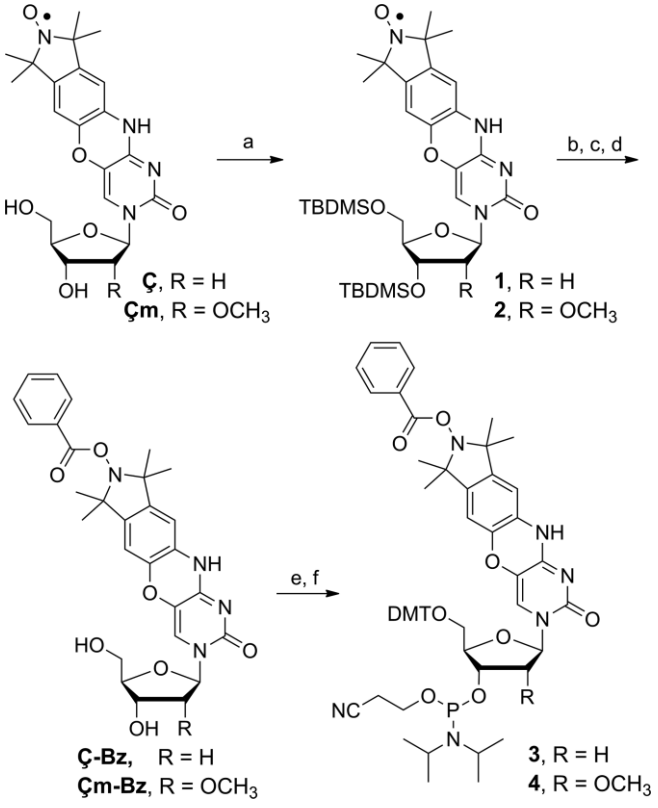

Scheme 1. Synthesis of **Ç-Bz** and **Çm-Bz** and their corresponding phosphoramidites. **a**. Imidazole, *tert*-butyldimethylsilyl chloride (TBDMSCl), DMF, pyridine. **b**. *L*-Ascorbic acid, 1,4-dioxane, H_2O. **c**. Benzoyl chloride (BzCl), Et_3N. **d**. *tert*-Butyl ammonium fluoride (TBAF), THF. **e**. 4,4′-Dimethoxytrityl chloride (DMTCl), 4-dimethylaminopyridine (DMAP), pyridine. **f**. 2-Cyanoethyl-*N*,*N*,*N*′,*N*′-tetraisopropylphosphorodiamidite, diisopropylammonium tetrazolide (DIPAT), CH_2Cl_2.

Table 1. Spin-labeled DNA and RNA oligonucleotides synthesized by solid-phase synthesis. Oligonucleotides **II*** and **VI*** were synthesized with the phosphoramidite of unprotected nitroxide spin-labels **Çm**[26] and **Ç**,[16] respectively. PHO is a phosphate.

No.	Sequence
I	5′-UGCAU**Çm**UU-3′
II*	5′-UGCAU**Çm**UU-3′
III	5′-AGA-UGC-GCG-**Çm**GC-GCG-ACU-GAC-3′
IV	5′-PHO-d(TGAGGTAGTAGGTTGTATA**Ç**T)-3′
V*	5′-PHO-d(TGAGGTAGTAGGTTGTATA**Ç**T)-3′
VI	5′-d(TGTAA**Ç**GCACTACCAGCGGCTGGAAATCT**Ç**TCTCGT)-3′

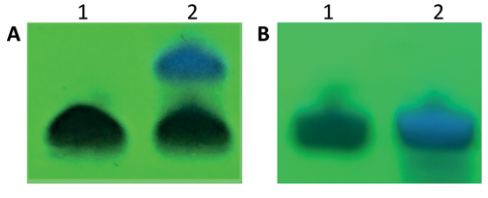

Figure 2. Analysis of spin-labeled oligonucleotides by DPAGE. **A**. Crude 8-mer RNA oligonucleotides **I** (lane 1) and **II** (lane 2) (5′-UGCAU**Çm**UU-3′), synthesized using **4** and the phosphoramidite of unprotected **Çm**,[26] respectively. **B**. Crude 21-mer DNA oligonucleotides **IV** (lane 1) and **V** (lane 2) [5′-d(PHO-TGAGGTAGTAGGTTGTATA**Ç**T)-3′], synthesized using **3** and the phosphoramidite of unprotected **Ç**,[16] respectively. PHO is a phosphate.

moval of the DMT group. Figure 2**A** shows a denaturing polyacrylamide gel of crude RNA **I** (lane 1) and RNA **II** (lane 2). No fluorescent band was detected for RNA **I** (Figure 2**A**, lane 1), synthesized with **Çm-Bz**. In contrast, RNA **II** (Figure 2**A**, lane 2), synthesized with the unprotected **Çm**, contained a strong fluorescent by-product, which indicated a partial reduction of the nitroxide to the corresponding **Çmf**.

For further analysis, crude RNAs **I** and **II** were digested with snake venom phosphodiesterase, nuclease P1 and calf spleen alkaline phosphatase, and the digest was analyzed by HPLC (Figure 3).[16] The HPLC chromatogram for RNA **I** (Figure 3**A**) contained five peaks, one for each natural nucleoside and a strongly retained nucleoside that was shown by co-injection to be **Çm**, while RNA **II** (Figure 3**B**) showed a peak for both **Çm** and **Çmf** along with the natural unmodified nucleosides.

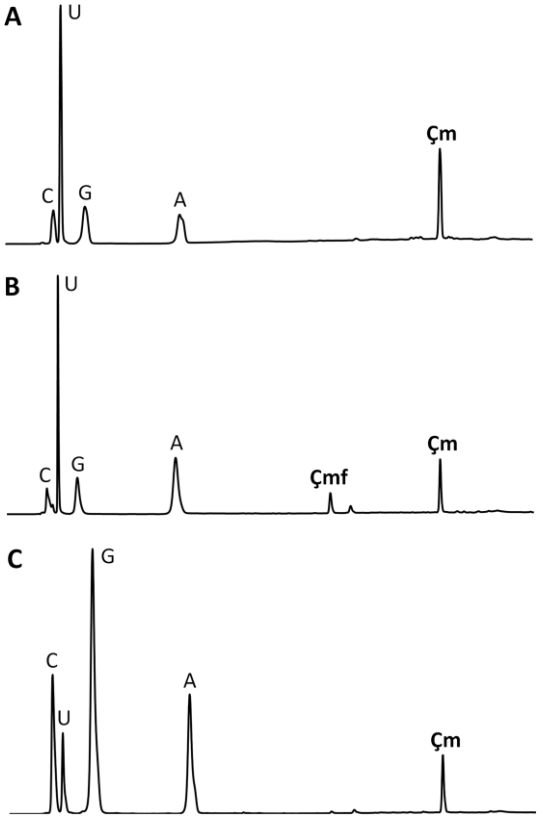

Figure 3. HPLC chromatograms of RNA oligonucleotides after enzymatic digestion with snake venom phosphodiesterase, nuclease P1, and alkaline phosphatase. **A**. Crude RNA **I** (5′-UGCAU**Çm**UU-3′) synthesized using **4**. **B**. Crude RNA **II** (5′-UGCAU**Çm**UU-3′) synthesized using the phosphoramidite of unprotected **Çm**.[26] **C**. RNA **III** (5′-AGAUGCGCG**Çm**GCGCGACUGAC-3′) synthesized using **4**.

Phosphoramidite **4** was also used to synthesize a 21-nt long RNA (**III**, Table 1), which was enzymatically digested and analyzed by HPLC (Figure 3**C**). In this case, a small peak (< 5 %) can be seen for **Çmf**, along with **Çm** and the natural nucleosides. These results show that the benzoyl protecting group on **Çm** was stable during the oligonucleotide synthesis and was completely removed during the deprotection, giving high yields of spin-labeled RNA.

In an analogous manner to the RNA synthesis, phosphoramidite **3** and a phosphoramidite of **Ç** that does not contain

the benzoyl protecting group were used to synthesize two 21-mer DNA oligonucleotides of the same sequence, (**IV** and **V**, Table 1). Here the spin-label was placed close to the 3′-end, which increases the exposure of the label to the chemicals used in each cycle of the oligonucleotide synthesis. Figure 2**B** shows DPAGE analysis of crude DNA **IV** (Figure 2**B**, lane 1) and crude DNA **V** (Figure 2**B**, lane 2). No fluorescent band was detected for DNA **IV** while DNA **V** showed a strong fluorescent band that overlapped with the band of the spin-labeled oligonucleotide.

These crude DNA samples were digested and analyzed by HPLC (Figure 4). While the digest of oligomer **IV** (Figure 4**A**) showed the natural nucleosides and **Ç**, the digest of oligomer **V** contained a very small peak for **Ç** along with some strongly retained impurities (Figure 4**B**). The quality of the synthesis of spin-labeled DNA was also reflected in the yields of purified material obtained from a 1 µmol synthesis, that gave 180 and 11 nmols of oligomers **VI** and **V**, respectively. Moreover, the small amount of oligo **V** obtained after repeated purifications gave a ca. 50:50 mixture of oligonucleotides containing **Ç** and **Çf**. To demonstrate the use of this method for the synthesis of a longer oligonucleotide, a 36-nt DNAzyme (**VI**, Table 1) containing **Ç** at two positions (6 and 31) was prepared. No fluorescent bands were detected upon purification of the oligonucleotide by DPAGE. Enzymatic digestion followed by HPLC analysis showed four peaks for the natural nucleosides and a peak for **Ç** (Figure 4**C**) in the ratios expected for a fully spin-labeled oligonucleotide.

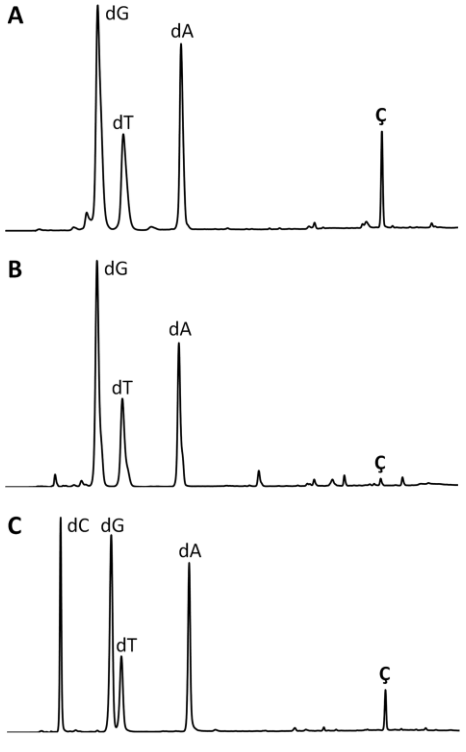

Figure 4. HPLC chromatograms of DNA oligonucleotides after enzymatic digestion with snake venom phosphodiesterase, nuclease P1, and alkaline phosphatase. **A**. Crude DNA **IV** [5′-d(PHO-TGAGGTAGTAGGTTGTATA**Ç**T)-3′] synthesized using **3**. **B**. Crude DNA **V** [5′-d(PHO-TGAGGTAGTAGGTTGTATA**Ç**T)-3′] synthesized using the phosphoramidite of unprotected **Ç**.[16] **C**. DNAzyme **VI** [5′-d(TGTAA**Ç**GCACTACCAGCGGCTGGAAATCT**Ç**TCTCGT)-3′] synthesized using **3**. PHO is a phosphate.

Conclusions

The nitroxide functional groups of **Ç** and **Çm** were protected by benzoylation of the corresponding hydroxylamines. The resulting **Ç-Bz** and **Çm-Bz** were converted into phosphoramidites and used for oligonucleotide synthesis of DNA and RNA of various lengths. The benzoyl protecting group was stable through the chemical synthesis of the oligonucleotides and was readily removed by standard oligonucleotide deprotection conditions to give nitroxide-labeled oligonucleotides; enzymatic digestion and HPLC analysis were used to quantify the spin label in the samples. These results show that this protecting group strategy for nitroxides can be used as a general method to prepare spin-labeled nucleic acids using the phosphoramidite approach.

Experimental Section

General Materials and Methods. All commercially available reagents were purchased from Sigma-Aldrich, Inc. or Acros Organics and used without further purification. 2′-Deoxyuridine and 2′-*O*-methyluridine were purchased from Rasayan Inc. USA. CH_2Cl_2, pyridine, and CH_3CN were dried with calcium hydride and freshly distilled before use. All moisture- and air-sensitive reactions were carried out in oven-dried glassware under an inert atmosphere of Ar. Thin-layer chromatography (TLC) was performed using glass plates pre-coated with silica gel (0.25 mm, F-25, Silicycle) and compounds were visualized under UV light and by *p*-anisaldehyde staining. Column chromatography was performed using 230–400 mesh silica gel (Silicycle). For acid-sensitive compounds the silica gel was basified by passing 3 % Et_3N in CH_2Cl_2 through the column before use. ^{1}H-, ^{13}C- and ^{31}P-NMR spectra were recorded with a Bruker Avance 400 MHz spectrometer. Commercial grade $CDCl_3$ was passed over basic alumina shortly before dissolving tritylated nucleosides for NMR analysis. Chemical shifts (δ) are reported in parts per million (ppm) relative to the partially deuterated NMR solvent $CDCl_3$ (7.26 ppm for ^{1}H NMR and 77.16 ppm for ^{13}C). ^{31}P-NMR chemical shifts are reported relative to 85 % H_3PO_4 as an external standard. All coupling constants were measured in Hertz (Hz). Nitroxide radicals show broadening and loss of NMR signals due to their paramagnetic nature and therefore, those NMR spectra are not shown. Mass spectrometric analyses of all organic compounds were performed on an ESI-HRMS (Bruker, MicrOTOF-Q) in a positive ion mode.

TBDMS-Ç (1). To a solution of **Ç**[16] (130 mg, 0.30 mmol) in DMF (3 mL) and pyridine (3 mL) were added imidazole (62 mg, 0.91 mmol) and TBDMSCl (137 mg, 0.91 mmol) and the resulting solution was stirred at 22 °C for 24 h. H_2O (50 mL) was added and the organic phase was extracted with EtOAc (3 × 10 mL). The combined organic phases were dried with Na_2SO_4 and concentrated in vacuo. The residue was purified by flash column chromatography using gradient elution ($MeOH/CH_2Cl_2$, 0:100 to 10:90), to yield **1** (160 mg, 95 %) as a yellow solid. HRMS (ESI): *m/z* calcd. for $C_{33}H_{53}N_4O_6Si_2 + Na^+$: 680.3401 $[M + Na]^+$, found 680.3396.

TBDMS-Ç-Bz (5). To a solution of **1** (53 mg, 0.08 mmol) in 1,4-dioxane (3.5 mL) was added *L*-ascorbic acid (72 mg, 0.41 mmol) in H_2O (1 mL) and the reaction mixture stirred at 40 °C for 30 min. H_2O (3.5 mL) and CH_2Cl_2 (5 mL) were added and the mixture was stirred for 5 min. The organic phase was separated and used directly in the next step by passing it through a plug of Na_2SO_4 under an inert atmosphere of Ar, into a solution of BzCl (46 µL, 0.41 mmol) and Et_3N (23 µL, 0.16 mmol) in CH_2Cl_2 (2 mL). The reaction was

stirred at 22 °C for 30 min, the solvent removed in vacuo and the residue purified by flash column chromatography using gradient elution ($MeOH/CH_2Cl_2$, 0:100 to 10:90), to yield **5** (55 mg, 95 %) as a yellow solid. ^1H NMR (400 MHz, $CDCl_3$): δ = 8.10–8.03 (m, 2H), 7.53 (d, J = 7.4 Hz, 1H), 7.40–7.44 (m, 3H), 7.19 (s, 1H), 6.34 (s, 1H), 6.22 (t, J = 6.1 Hz, 1H), 4.40–4.24 (m, 1H), 3.84 (dt, J = 8.6, 2.9 Hz, 2H), 3.76–3.66 (m, 1H), 2.36–2.22 (m, 1H), 2.26–2.32 (m, 1H), 2.06–1.90 (m, 1H), 1.42 (d, J = 10.1 Hz, 12H), 0.90 (s, 9H), 0.81 (s, 9H), 0.09 (d, J = 8.8 Hz, 6H), 0.00 ppm (s, 6H); ^{13}C NMR (101 MHz, $CDCl_3$): δ = 166.13, 160.85, 142.58, 140.14, 139.53, 133.08, 129.62, 128.54, 127.76, 121.42, 112.27, 108.11, 100.88, 87.59, 85.80, 71.24, 68.60, 67.27, 66.52, 62.49, 41.78, 26.06, 25.71, 18.49, 17.95, –4.55 –4.85, –5.46 ppm; HRMS (ESI): m/z calcd. for $C_{40}H_{58}N_4O_7Si_2 + Na^+$: 785.3742 $[M + Na]^+$, found 785.3736.

Ç-Bz. To a solution of **5** (118 mg, 0.16 mmol) in THF (3 mL) was added TBAF (0.5 mL, 0.50 mmol, 1.0 M in THF) at 0 °C and the reaction mixture was stirred at 0 °C for 8 h. The solvent was removed in vacuo and the residue purified by flash column chromatography using gradient elution ($MeOH/CH_2Cl_2$, 0:100 to 25:75), to yield **Ç-Bz** (67 mg, 81 %) as a yellow solid. ^1H NMR (400 MHz, $CDCl_3$): δ = 8.09 (d, J = 7.3 Hz, 2H), 7.70–7.62 (m, 2H), 7.55 (t, J = 7.7 Hz, 2H), 6.66 (s, 2H), 6.23 (t, J = 6.4 Hz, 1H), 4.39 (dt, J = 6.6, 3.5 Hz, 1H), 3.94 (m, J = 3.1 Hz, 1H), 3.81–3.73 (m, 2H), 2.34 (ddd, J = 13.5, 6.0, 3.7 Hz, 1H), 2.17 (dt, J = 13.4, 6.5 Hz, 1H), 1.47 ppm (s, 12H); ^{13}C NMR (101 MHz, $CDCl_3$): δ = 170.9, 146.8, 143.8, 143.0, 137.4, 133.1, 132.5, 112.7, 91.5, 90.1, 74.6, 72.4, 65.2, 62.1, 62.1, 44.3, 31.7, 27.4, 23.3, 16.5 ppm; HRMS (ESI): m/z calcd. for $C_{28}H_{30}N_4O_7 + Na^+$: 557.2012 $[M + Na]^+$, found 557.2007.

Ç-Bz-DMT (6). Ç-Bz (16 mg, 0.03 mmol), DMTCl (21 mg, 0.06 mmol) and DMAP (0.8 mg, 0.01 mmol) were added to a round-bottomed flask and dried in vacuo for 16 h. Pyridine (2 mL) was added and the solution stirred for 16 h, after which MeOH (0.50 mL) was added and the solvent removed in vacuo. The residue was purified by flash column chromatography using gradient elution ($MeOH/CH_2Cl_2$/Et_3N, 0:99:1 to 95:4:1), to yield **6** (20 mg, 95 %) as a yellow solid. ^1H NMR (400 MHz, $CDCl_3$): δ = 8.18–8.09 (m, 3H), 7.64–7.56 (m, 2H), 7.49 (d, J = 7.8 Hz, 4H), 7.40 (d, J = 8.2 Hz, 4H), 7.31 (t, J = 7.6 Hz, 2H), 7.20 (t, J = 7.3 Hz, 1H), 6.86 (dd, J = 8.7, 3.8 Hz, 4H), 6.52–6.46 (m, 1H), 6.43 (s, 1H), 6.25 (s, 1H), 4.70–4.56 (m, 1H), 4.15 (dd, J = 8.8, 5.2 Hz, 1H), 3.75 (d, J = 6.6 Hz, 6H), 3.41 (ddd, J = 26.5, 10.7, 3.2 Hz, 2H), 2.71 (d, J = 12.8 Hz, 1H), 2.37–2.21 (m, 1H), 1.48 ppm (d, J = 12.2 Hz, 12H); ^{13}C NMR (101 MHz, $CDCl_3$): δ = 166.21, 159.56, 154.79, 154.60, 148.34, 144.57, 142.44, 139.75, 139.32, 136.66, 133.17, 130.10, 130.05, 129.60, 129.38, 128.60, 128.15, 128.14, 128.05, 127.97, 126.91, 126.30, 122.05, 113.27, 108.58, 106.64, 86.88, 86.33, 86.26, 71.33, 68.65, 68.54, 63.40, 60.42, 55.21, 41.79, 39.06, 29.37, 28.87, 25.44, 21.07, 14.22 ppm; HRMS (ESI): m/z calcd. for $C_{49}H_{48}N_4O_9 + Na^+$: 859.3319 $[M + Na]^+$, found 859.3313.

Ç-Bz phosphoramidite (3). A solution of compound **6** (21 mg, 0.02 mmol) in CH_2Cl_2 (1 mL) was treated with diisopropyl ammonium tetrazolide (5 mg, 0.03 mmol) and 2-cyanoethyl *N*,*N*,*N*′,*N*′-tetraisopropylphosphane (11 µL, 0.03 mmol). The resulting solution was stirred at 22 °C for 2 h. CH_2Cl_2 (50 mL) was added and the solution washed with satd. aq. $NaHCO_3$ (3 × 50 mL) and brine (50 mL), dried with Na_2SO_4 and concentrated in vacuo. The residue was dissolved in a minimum amount of CH_2Cl_2 (few drops), followed by slow addition of *n*-hexane (40–50 mL) at 22 °C. The solvent was decanted from the precipitate and discarded. This procedure was repeated four times to give **3** (20 mg, 80 %) as a yellowish solid. ^1H NMR (400 MHz, $CDCl_3$): δ = 8.06–8.04 (m, 2H), 7.53 (s, 1H), 7.46–7.34 (m, 6H), 7.32–7.24 (m, 6H), 7.16 (dd, J = 7.4, 4.0 Hz, 1H), 6.79 (dq, J = 6.3, 2.2 Hz, 4H), 6.30–6.19 (m, 1H), 6.17 (d, J = 8.2 Hz, 1H), 4.58 (d, J = 14.0 Hz, 1H), 4.08 (t, J = 3.8 Hz, 1H), 3.69 (dd, J = 5.3, 2.1 Hz, 6H), 3.61–3.25 (m, 6H), 2.52 (q, J = 10.7, 8.4 Hz, 2H), 2.38 (t, J = 6.4 Hz, 1H), 2.22 (d, J = 11.4 Hz, 1H), 1.41 (t, J = 11.0 Hz, 12H), 1.13–0.97 (m, 12H) ppm; ^{13}C NMR (101 MHz, $CDCl_3$): δ = 158.61, 144.36, 139.29, 133.10, 130.18, 130.13, 130.10, 129.62, 129.47, 128.56, 128.26, 127.96, 126.99, 113.28, 113.25, 108.46, 86.88, 85.76, 77.22, 68.66, 68.59, 62.60, 58.36, 58.16, 55.24, 55.21, 43.38, 43.26, 43.20, 40.45, 31.59, 25.49, 24.65, 24.58, 24.51, 22.66, 20.25, 20.18, 14.12 ppm; ^{31}P NMR (162 MHz, $CDCl_3$): δ = 149.25, 148.63 ppm.

TBDMS-Çm (2). To a solution of **Çm**[26] (290 mg, 0.63 mmol) in DMF (6 mL) and pyridine (1.5 mL) were added TBDMSCl (286 mg, 1.89 mmol) and imidazole (129 mg, 1.89 mmol). The resulting solution was stirred at 22 °C for 16 h. H_2O (50 mL) and EtOAc (20 mL) were added, the organic phase separated and washed with satd. aq. $NaHCO_3$ (5 × 50 mL). The organic phase was dried with Na_2SO_4, concentrated in vacuo and purified by flash column chromatography using gradient elution ($MeOH/CH_2Cl_2$; 0:100 to 10:90), yielding **2** (299 mg, 81 %) as a yellow solid. HRMS (ESI): m/z calcd. for $C_{34}H_{55}N_4O_7Si_2 + Na^+$: 710.3501 $[M + Na]^+$, found 710.3500.

TBDMS-Çm-Bz (7). To a solution of **2** (235 mg, 0.34 mmol) in 1,4-dioxane (30 mL) was added *L*-ascorbic acid (301 mg, 1.71 mmol) in H_2O (5 mL). The reaction mixture was stirred at 40 °C for 1 h, after which CH_2Cl_2 (30 mL) and H_2O (30 mL) were added and the solution was stirred vigorously for 2 min. The organic phase was separated and filtered through a short pad of Na_2SO_4, in a dropping funnel under an inert atmosphere of Ar, into a solution of BzCl (198 µL, 0.34 mmol), Et_3N (953 µL, 6.83 mmol) in CH_2Cl_2 (10 mL). The solution was stirred at 22 °C for 2 h, washed with satd. aq. $NaHCO_3$ (3 × 100 mL), the organic phase dried with Na_2SO_4, concentrated in vacuo and the residue purified by flash column chromatography using gradient elution ($MeOH/CH_2Cl_2$; 0:100 to 10:90), to yield **7** (269 mg, quant.) as a yellow solid. ^1H NMR (400 MHz, $CDCl_3$): δ = 8.14 (s, 2H), 7.81 (s, 1H), 7.59 (t, J = 7.5 Hz, 1H), 7.49 (s, 1H), 7.51–7.44 (m, 2H), 6.41 (s, 1H), 5.88 (s, 1H), 4.22 (dt, J = 8.7, 4.3 Hz, 1H), 4.14–4.02 (m, 2H), 3.81 (dd, J = 11.9, 1.8 Hz, 1H), 3.68 (d, J = 4.6 Hz, 1H), 3.64 (s, 3H), 1.49 (s, 12H), 1.02 (s, 9H), 0.90 (s, 9H), 0.22 (dd, J = 7.5, 2.4 Hz, 6H), 0.09 ppm (dd, J = 5.9, 2.4 Hz, 6H); ^{13}C NMR (101 MHz, $CDCl_3$): δ = 171.21, 166.14, 160.84, 155.20, 153.56, 142.62, 140.04, 139.53, 133.19, 133.15, 130.29, 130.16, 129.63, 129.44, 129.03, 128.58, 128.29, 127.69, 126.27, 122.06, 111.93, 108.14, 88.08, 87.47, 84.14, 83.11, 68.71, 68.63, 68.61, 68.52, 68.03, 62.97, 61.64, 60.51, 57.98, 28.93, 26.37, 26.34, 25.82, 25.76, 25.49, 18.78, 18.73, 18.15, 18.10, –4.45, –4.50, –4.83, –5.11, –5.20, –5.29, –5.34 ppm; HRMS (ESI): m/z calcd. for $C_{41}H_{60}N_4O_8Si_2 + Na^+$: 815.3842 $[M + Na]^+$, found 815.3853.

Çm-Bz. To a solution of **7** (271 mg, 0.34 mmol) in THF (18 mL) was added TBAF (1.2 mL, 1.20 mmol, 1.0 M in THF) and the reaction stirred at 22 °C for 18 h. The reaction was concentrated in vacuo and the residue purified by flash column chromatography using gradient elution ($MeOH/CH_2Cl_2$; 0:100–10:90), to yield **Çm-Bz** (139 mg, 72 %) as a yellow solid. ^1H NMR (400 MHz, $CDCl_3$): δ = 8.11 (td, J = 7.3, 6.6, 1.4 Hz, 2H), 7.59 (td, J = 7.4, 3.6 Hz, 1H), 7.57–7.51 (m, 1H), 7.45 (dt, J = 18.4, 7.7 Hz, 2H), 6.45 (d, J = 18.7 Hz, 1H), 5.72–5.67 (m, 1H), 4.95 (s, 1H), 4.38 (t, J = 4.8 Hz, 1H), 4.31 (dt, J = 9.1, 4.8 Hz, 1H), 4.00 (d, J = 6.5 Hz, 2H), 3.89 (q, J = 5.4 Hz, 1H), 3.62 (d, J = 3.9 Hz, 3H), 1.51–1.24 ppm (m, 12H); ^{13}C NMR (101 MHz, $CDCl_3$): δ = 170.91, 166.35, 160.98, 154.87, 153.61, 142.50, 142.19, 141.16, 140.16, 139.44, 133.30, 130.12, 129.62, 129.23, 128.62, 128.36, 128.03, 127.93, 125.91, 125.39, 123.08, 111.54, 108.77, 100.90, 89.88, 84.49, 82.98, 77.39, 77.28, 77.08, 76.76, 68.61, 68.56, 68.11, 67.31, 67.26, 66.55, 63.66, 62.97, 60.69, 58.53, 53.46, 29.26, 28.77, 25.41, 24.99 ppm; HRMS (ESI): m/z calcd. for $C_{29}H_{32}N_4O_8 + Na^+$: 587.2112 $[M + Na]^+$, found 587.2096.

Çm-Bz-DMT (8). Toluene (3 × 5 mL) was evaporated from **Çm-Bz** (139 mg, 0.25 mmol), followed by sequential addition of pyridine (4 mL), DMTCl (834 mg, 2.46 mmol) and DMAP (6 mg, 0.05 mmol). The solution was stirred for 14 h, MeOH (400 µL) was added and the solvent removed in vacuo. The residue was purified by flash column chromatography using gradient elution ($MeOH/CH_2Cl_2/Et_3N$; 0:99:1 to 1:98:1), to yield **8** (87 mg, 41 %) as a yellow solid. ^1H NMR (400 MHz, $CDCl_3$): δ = 8.13 (d, J = 7.2 Hz), 7.72 (s, 1H), 7.60 (t, J = 7.7 Hz, 1H), 7.51–7.50 (m, 2H), 7.49–7.48 (m, 2H), 7.43–7.40 (m, 4H), 7.33–7.31 (m, 2H), 7.22–7.18 (m, 1H), 6.88 (s, 1H), 6.88–6.85 (m, 4H), 6.11 (s, 1H), 5.87 (s, 1H), 4.55–4.52 (m, 1H), 4.02 (d, J = 8.6 Hz, 1H), 3.93 (bs, 1H), 3.75 (s, 6H), 3.73 (s, 3H), 3.60–3.49 (m, 2H), 1.51 ppm (d, J = 25.2 Hz, 12H); ^{13}C NMR (101 MHz, $CDCl_3$): δ = 166.15, 158.57, 155.18, 153.79, 142.30, 139.88, 139.26, 135.57, 133.13, 130.09, 129.62, 129.47, 128.57, 128.23, 128.01, 127.84, 126.92, 125.98, 121.80, 113.36, 113.31, 111.78, 108.71, 87.87, 86.82, 83.77, 82.91, 68.70, 68.61, 68.19, 60.84, 58.56, 55.21, 45.82, 29.72, 25.47 ppm; HRMS (ESI): m/z calcd. for $C_{50}H_{50}N_4O_{10}$ + Na^+: 889.3419 $[M + Na]^+$, found 889.3395.

Çm-Bz phosphoramidite (4). A solution of **8** (20 mg, 0.02 mmol) in CH_2Cl_2 (1 mL) was treated with diisopropyl ammonium tetrazolide (6 mg, 0.04 mmol) and 2-cyanoethyl *N*,*N*,*N*′,*N*′-tetraisopropylphosphane (22 µL, 0.07 mmol). The reaction was stirred at 22 °C for 18 h. CH_2Cl_2 (15 mL) was added and the solution washed with satd. aq. $NaHCO_3$ (3 × 30 mL), dried with Na_2SO_4 and concentrated in vacuo. The residue was dissolved in Et_2O (2 mL) followed by slow addition of *n*-hexane (10 mL). The solvent was decanted from the precipitate and discarded. This procedure was repeated six times to yield **4** (18 mg, 71 %) as a yellow solid. ^1H NMR (400 MHz, $CDCl_3$): δ = 8.12 (dd, J = 8.3, 1.4 Hz, 4H), 7.64–7.57 (m, 3H), 7.53–7.44 (m, 10H), 7.44–7.34 (m, 11H), 7.31 (td, J = 7.8, 2.1 Hz, 6H), 7.22 (tt, J = 7.4, 1.9 Hz, 3H), 6.86 (ddt, J = 8.7, 5.9, 3.4 Hz, 10H), 6.14 (d, J = 15.5 Hz, 1H), 6.06 (d, J = 7.6 Hz, 1H), 5.97 (s, 1H), 4.29 (tt, J = 5.0, 2.6 Hz, 1H), 4.25–4.20 (m, 2H), 3.98 (q, J = 7.0, 6.4 Hz, 2H), 3.77–3.73 (m, 13H), 3.65 (dd, J = 4.0, 1.2 Hz, 6H), 2.46–2.38 (m, 2H), 1.55–1.38 (m, 28H), 1.26 (ddt, J = 5.7, 3.6, 2.2 Hz, 15H), 1.22–1.18 (m, 11H), 1.18–1.03 (m, 15H), 0.92–0.84 ppm (m, 8H); ^{13}C NMR (101 MHz, $CDCl_3$): δ = 165.92, 158.38, 155.03, 153.66, 142.02, 132.86, 130.10, 129.37, 128.32, 127.69, 126.77, 125.79, 121.65, 117.33, 113.00, 111.78, 108.29, 88.35, 86.49, 77.16, 68.45, 54.98, 43.16, 24.51, 20.10 ppm; ^{31}P NMR (162 MHz, $CDCl_3$): δ = 150.52, 150.08 ppm; HRMS (ESI): m/z calcd. for $C_{50}H_{60}N_4O_{10}$ + Na^+: 1089.4498 $[M + Na]^+$, found 1089.4498.

DNA and RNA Syntheses, Purification and Characterization. All commercial phosphoramidites, CPG columns, and solutions for oligonucleotide syntheses were purchased from ChemGenes Corp., USA. DNA and RNA solid-phase oligonucleotide syntheses were performed on an automated ASM800 DNA/RNA synthesizer (BIOSSET Ltd., Russia) using phosphoramidite chemistry. Unmodified and spin-labeled oligonucleotides were synthesized using a trityl-off protocol and phosphoramidites with standard protecting groups on 1 µmol scale (1000 Å CPG columns). Oxidation was performed with *tert*-butylhydroperoxide in toluene (1.0 M). Capping and detritylation were performed under standard conditions for DNA and RNA oligonucleotide synthesis.

The **Ç**-modified DNAs were synthesized using phosphoramidite **3**. Unmodified phosphoramidites were dissolved in CH_3CN (100 mM) and **3** was dissolved in 1,2-dichloroethane (100 mM). 5-Ethylthiotetrazole (250 mM) was used as a coupling agent and the coupling time was set to 1.5 min for unmodified phosphoramidites and to 5 min for the **Ç**-modified phosphoramidites. The DNAs were deprotected in satd. aqueous NH_3 at 55 °C for 8 h and dried in vacuo.

For the RNA synthesis, 2′*O*-TBDMS protected ribonucleoside phosphoramidites were used and dissolved in CH_3CN (100 mM). The **Çm**-modified RNAs were synthesized using phosphoramidite **4**, dissolved in 1,2-dichloroethane (100 mM). 5-Ethylthiotetrazole (250 mM) was used as a coupling agent for phosphoramidite **4**, 5-benzylthiotetrazole (250 mM) was used as a coupling agent for unmodified phosphoramidites and the coupling time was set to 7 min. The RNAs were deprotected and cleaved from the resin by adding a 1:1 solution (2 mL) of CH_3NH_2 (8 M in EtOH) and NH_3 (satd. in H_2O) and heating at 65 °C for 1 h. The solvent was removed in vacuo and the 2′*O*-TBDMS groups were removed by incubation in $Et_3N{\cdot}3HF$ (300 µL) in DMF (100 µL) at 55 °C for 1.5 h, followed by addition of deionized and sterilized water (100 µL). This mixture was transferred to a 50 mL Falcon tube and *n*-butanol (20 mL) was added and stored at –20 °C for 14 h, centrifuged and the solvent decanted from the RNA pellet.

All oligonucleotides were subsequently purified by 20 % DPAGE and extracted from the gel slices using the "crush and soak method" with Tris buffer (250 mM NaCl, 10 mM Tris, 1 mM Na_2EDTA, pH 7.5). The solutions were filtered through GD/X syringe filters (0.45 µm, 25 mm diameter, Whatman, USA) and were subsequently desalted using Sep-Pak cartridges (Waters, USA), following the instructions provided by the manufacturer. Dried oligonucleotides were dissolved in deionized and sterilized water (200 µL for each oligonucleotide). Concentrations of the oligonucleotides were determined by measuring absorbance at 260 nm using a Perkin Elmer Inc. Lambda 25 UV/Vis spectrometer and calculated by Beer's law. Mass spectrometric analyses of **Ç**- and **Çm**-labeled oligonucleotides were performed on an HRMS (ESI) (Bruker, MicrOTOF-Q) in negative ion mode.

Enzymatic Digestion of DNA and RNA and HPLC Analysis. To the oligonucleotide (4 nmol) in sterile water (8 µL) was added calf intestinal alkaline phosphatase (1 µL, 2 U), snake venom phosphodiesterase I (4 µL, 0.2 U), nuclease P1 from penicillium citrinum (5 µL, 1.5 U) and Tris buffer (2 µL, 500 mM Tris and 100 mM $MgCl_2$). The samples were incubated at 37 °C for 50 h. Enzymatically digested oligonucleotides were run on a Beckman Coulter Gold HPLC system using Beckman Coulter Ultrasphere C18 4.6 × 250 mm analytical column with UV detection at 254 nm. Solvent gradients for analytical RP-HPLC were run at 1.0 mL/min using following gradient program: solvent A, TEAA buffer (50 mM, pH 7.0); solvent B, CH_3CN; 0–4 min isocratic 4 % B, 4–14 min linear gradient 4–20 % B, 14–24 min linear gradient 20–50 % B, 24–29 min linear gradient 50–80 % B, for 29–30 min isocratic 80 % B, 30–35 min linear gradient 80–4 % B and 35–45 min isocratic 4 % B.

Acknowledgments

The authors acknowledge financial support by the Icelandic Research Fund (141062-051). The authors thank Dr S. Jonsdottir for assistance with collecting analytical data for structural characterization of new compounds and members of the Sigurdsson research group for helpful discussions.

Keywords: EPR spectroscopy · Nitroxides · Oligonucleotides · Site-directed spin labeling

[1] K. Chen, Boxuan S. Zhao, C. He, *Cell Chem. Biol.* **2016**, *23*, 74–85.
[2] A. Ducruix, R. Giegé, *Crystallization of Nucleic Acids and Proteins: A Practical Approach*, Oxford University Press, **1999**.
[3] D. R. Cooper, P. J. Porebski, M. Chruszcz, W. Minor, *Expert Opin. Drug Discovery* **2011**, *6*, 771–782.

[4] a) A. M. Spring-Connell, M. Evich, M. W. Germann, *Curr. Protoc. Nucleic Acid Chem.* **2018**, *72*, 7.28.21–27.28.39; b) L. G. Scott, M. Hennig, in *Bioinformatics: Data, Sequence Analysis and Evolution* (Ed.: J. M. Keith), Humana Press, Totowa, NJ, **2008**, pp. 29–61; c) M. Getz, X. Sun, A. Casiano-Negroni, Q. Zhang, H. M. Al-Hashimi, *Biopolymers* **2007**, *86*, 384–402.

[5] J. H. Lee, Y. Okuno, S. Cavagnero, *J. Magn. Reson.* **2014**, *241*, 18–31.

[6] S. Preus, L. M. Wilhelmsson, *ChemBioChem* **2012**, *13*, 1990–2001.

[7] M. F. Juette, D. S. Terry, M. R. Wasserman, Z. Zhou, R. B. Altman, Q. Zheng, S. C. Blanchard, *Curr. Opin. Chem. Biol.* **2014**, *20*, 103–111.

[8] a) N. K. Kim, A. Murali, V. J. DeRose, *Chem. Biol.* **2004**, *11*, 939–948; b) J. C. Macosko, M. S. Pio, I. Tinoco, Y. K. Shin, *RNA* **1999**, *5*, 1158–1166.

[9] a) G. W. Reginsson, O. Schiemann, *Biochem. Soc. Trans.* **2011**, *39*, 128; b) T. Schmidt, M. A. Wälti, J. L. Baber, E. J. Hustedt, G. M. Clore, *Angew. Chem. Int. Ed.* **2016**, *55*, 15905–15909; *Angew. Chem.* **2016**, *128*, 16137; c) P. Z. Qin, K. Warncke, *Electron Paramagnetic Resonance Investigations of Biological Systems by Using Spin Labels, Spin Probes, and Intrinsic Metal Ions*, Elsevier Science **2015**.

[10] M. Wanunu, Y. Tor, *Methods for Studying Nucleic Acid/Drug Interactions*, CRC Press, **2016**.

[11] a) B. Endeward, A. Marko, V. P. Denysenkov, S. T. Sigurdsson, T. F. Prisner, in *Methods in Enzymology, Vol. 564* (Eds.: P. Z. Qin, K. Warncke), Academic Press, **2015**, pp. 403–425; b) T. F. Prisner, A. Marko, S. T. Sigurdsson, *J. Magn. Reson.* **2015**, *252*, 187–198.

[12] a) A. Potapov, H. Yagi, T. Huber, S. Jergic, N. E. Dixon, G. Otting, D. Goldfarb, *J. Am. Chem. Soc.* **2010**, *132*, 9040–9048; b) Y. Yang, F. Yang, Y.-J. Gong, J.-L. Chen, D. Goldfarb, X.-C. Su, *Angew. Chem. Int. Ed.* **2017**, *56*, 2914–2918; *Angew. Chem.* **2017**, *129*, 2960.

[13] a) N. Kocherginsky, H. M. Swartz, *Nitroxide Spin Labels: Reactions in Biology and Chemistry*, Taylor & Francis, **1995**; b) M. Martinho, E. Fournier, N. Le Breton, E. Mileo, V. Belle, in *Electron Paramagnetic Resonance: Volume 26, Vol. 26*, The Royal Society of Chemistry, **2019**, pp. 66–88.

[14] a) G. Z. Sowa, P. Z. Qin, in *Progress in Nucleic Acid Research and Molecular Biology, Vol. 82* (Ed.: P. M. Conn), Academic Press, **2008**, pp. 147–197; b) M. M. Haugland, J. E. Lovett, E. A. Anderson, *Chem. Soc. Rev.* **2018**, *47*, 668–680; c) N. R. Kamble, S. T. Sigurdsson, *Chem. Eur. J.* **2018**, *24*, 4157–4164; d) S. A. Shelke, S. T. Sigurdsson, *Eur. J. Org. Chem.* **2012**, *2012*, 2291; e) S. Saha, T. Hetzke, T. F. Prisner, S. T. Sigurdsson, *Chem. Commun.* **2018**, *54*, 11749–11752.

[15] a) K. Nakatani, Y. Tor, *Modified Nucleic Acids*, Springer International Publishing, **2016**; b) I. Tkach, S. Pornsuwan, C. Höbartner, F. Wachowius, S. T. Sigurdsson, T. Y. Baranova, U. Diederichsen, G. Sicoli, M. Bennati, *Phys. Chem. Chem. Phys.* **2013**, *15*, 3433–3437; c) P. E. Spindler, P. Schöps, W. Kallies, S. J. Glaser, T. F. Prisner, *J. Magn. Reson.* **2017**, *280*, 30–45.

[16] N. Barhate, P. Cekan, A. P. Massey, S. T. Sigurdsson, *Angew. Chem. Int. Ed.* **2007**, *46*, 2655–2658; *Angew. Chem.* **2007**, *119*, 2709.

[17] a) N. Piton, Y. Mu, G. Stock, T. F. Prisner, O. Schiemann, J. W. Engels, *Nucleic Acids Res.* **2007**, *35*, 3128–3143; b) P. Cekan, A. L. Smith, N. Barhate, B. H. Robinson, S. T. Sigurdsson, *Nucleic Acids Res.* **2008**, *36*, 5946–5954.

[18] A. Hatano, N. Terado, Y. Kanno, T. Nakamura, G. Kawai, *Synth. Commun.* **2019**, *49*, 136–145.

[19] B. A. Chalmers, J. C. Morris, K. E. Fairfull-Smith, R. S. Grainger, S. E. Bottle, *Chem. Commun.* **2013**, *49*, 10382–10384.

[20] E. L. Dane, B. Corzilius, E. Rizzato, P. Stocker, T. Maly, A. A. Smith, R. G. Griffin, O. Ouari, P. Tordo, T. M. Swager, *J. Org. Chem.* **2012**, *77*, 1789–1797.

[21] a) I. Seven, T. Weinrich, M. Gränz, C. Grünewald, S. Brüß, I. Krstić, T. F. Prisner, A. Heckel, M. W. Göbel, *Eur. J. Org. Chem.* **2014**, *2014*, 4037–4043; b) T. Weinrich, E. A. Jaumann, U. Scheffer, T. F. Prisner, M. W. Göbel, *Chem. Eur. J.* **2018**, *24*, 6202–6207.

[22] a) C. Brieke, F. Rohrbach, A. Gottschalk, G. Mayer, A. Heckel, *Angew. Chem. Int. Ed.* **2012**, *51*, 8446–8476; *Angew. Chem.* **2012**, *124*, 8572; b) S. Keyhani, T. Goldau, A. Blümler, A. Heckel, H. Schwalbe, *Angew. Chem. Int. Ed.* **2018**, *57*, 12017–12021; *Angew. Chem.* **2018**, *130*, 12193.

[23] Y. Sato, H. Hayashi, M. Okazaki, M. Aso, S. Karasawa, S. Ueki, H. Suemune, N. Koga, *Magn. Reson. Chem.* **2008**, *46*, 1055–1058.

[24] M. Kurita, Y. Higuchi, J. W. Mirc, S. Matsumoto, K. Usui, H. Suemune, M. Aso, *ChemBioChem* **2016**, *17*, 2346–2352.

[25] a) J. F. W. Keana, G. S. Heo, G. T. Gaughan, *J. Org. Chem.* **1985**, *50*, 2346–2351; b) D. R. Alessi, J. E. T. Corrie, J. Feeney, I. P. Trayer, D. R. Trentham, *J. Chem. Soc., Perkin Trans. 1* **1991**, 2243–2247; c) É. G. Rozantsev, V. A. Golubev, *Zzv. Akad. Nauk SSSR, Ser. Khim.* **1966**, 000–000; d) V. D. Sholle, V. A. Golubev, É. G. Rozantsev, *Bull. Acad. Sci. USSR Div. Chem. Sci. (Engl. Transl.)* **1972**, *21*, 1163–1165; e) K. E. Fairfull-Smith, F. Brackmann, S. E. Bottle, *Eur. J. Org. Chem.* **2009**, *2009*, 1902–1915; f) K. Hideg, J. Csekö, H. O. Hankovszky, P. Sohár, *Can. J. Chem.* **1986**, *64*, 1482–1490.

[26] C. Höbartner, G. Sicoli, F. Wachowius, D. B. Gophane, S. T. Sigurdsson, *J. Org. Chem.* **2012**, *77*, 7749–7754.

[27] H. Gustmann, A.-L. J. Segler, D. B. Gophane, A. J. Reuss, C. Grünewald, M. Braun, J. E. Weigand, S. T. Sigurdsson, J. Wachtveitl, *Nucleic Acids Res.* **2019**, *47*, 15–28.

Received: April 10, 2019

Supporting Information

Benzoyl-Protected Hydroxylamines for Improved Chemical Synthesis of Oligonucleotides Containing Nitroxide Spin Labels

Haraldur Y. Juliusson, Anna-Lena J. Segler, and Snorri Th. Sigurdsson*

ejoc201900553-sup-0001-SupMat.pdf

Table of contents

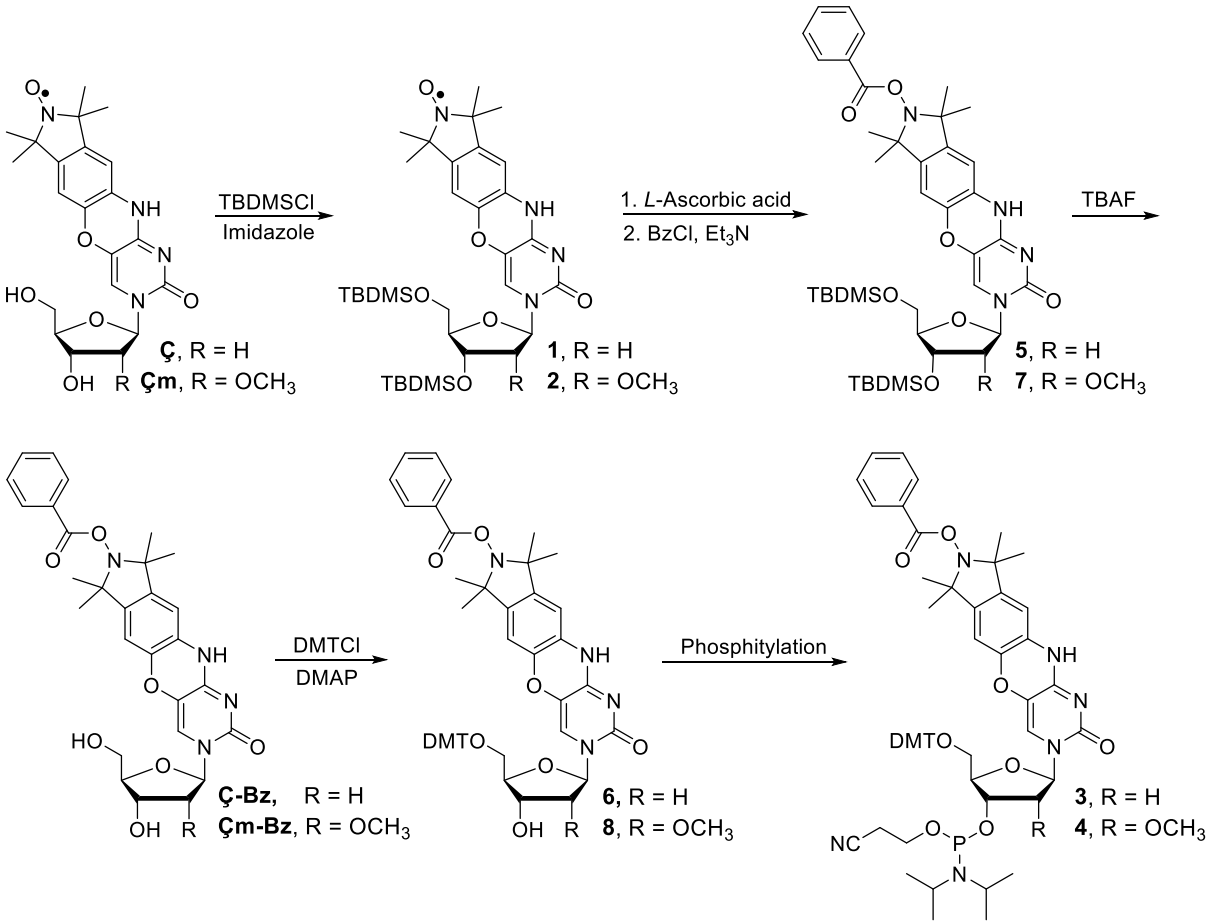

Scheme S1. Synthesis of phosphoramidites **3** and **4.**

MS analyses of oligonucleotides. The incorporation of **Ç** and **Çm** into oligonucleotides was confirmed by HRMS (ESI) analysis. The calculated and observed monoisotopic masses of spin-labeled oligonucleotides are listed in **Table S1**.

Table S1. Monoisotopic masses of spin-labeled oligonucleotides. Oligonucleotides II* and VI* were synthesized with the phosphoramidite of unprotected nitroxide spin-labels **Çm** and **Ç**, respectively. PHO is a phosphate.

Name	Sequence	(calculated)	(found)
I	5‘-UGCAU**Çm**UU-3‘	2662.4	2662.3
II*	5‘-UGCAU**Çm**UU-3‘	2662.4	2662.7
III	5‘-AGA-UGC-GCG-**Çm**GC-GCG-ACU-GAC-3‘	6953.0	6952.5
IV*	5‘-d(PHO-TGAGGTAGTAGGTTGTATA**Ç**T)-3	6809.2	6807.7
V	5‘-d(PHO-TGAGGTAGTAGGTTGTATA**Ç**T)-3	6809.2	6808.0
VI	5‘-d(TGTAA**Ç**GCACTACCAGCGGCTGGAAATCT**Ç**TCTCGT)-3‘	11400.4	11400.1

^{1}H and ^{13}C NMR spectra

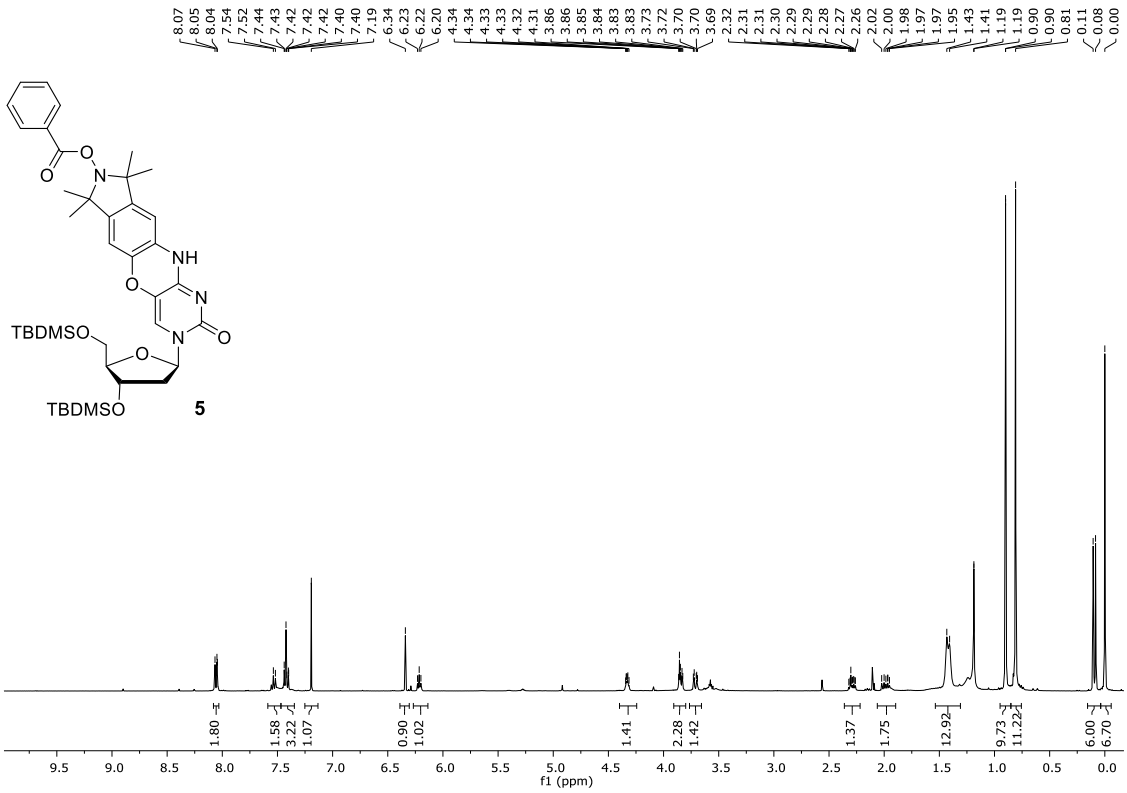

Figure S1. ^{1}H NMR of **5**.

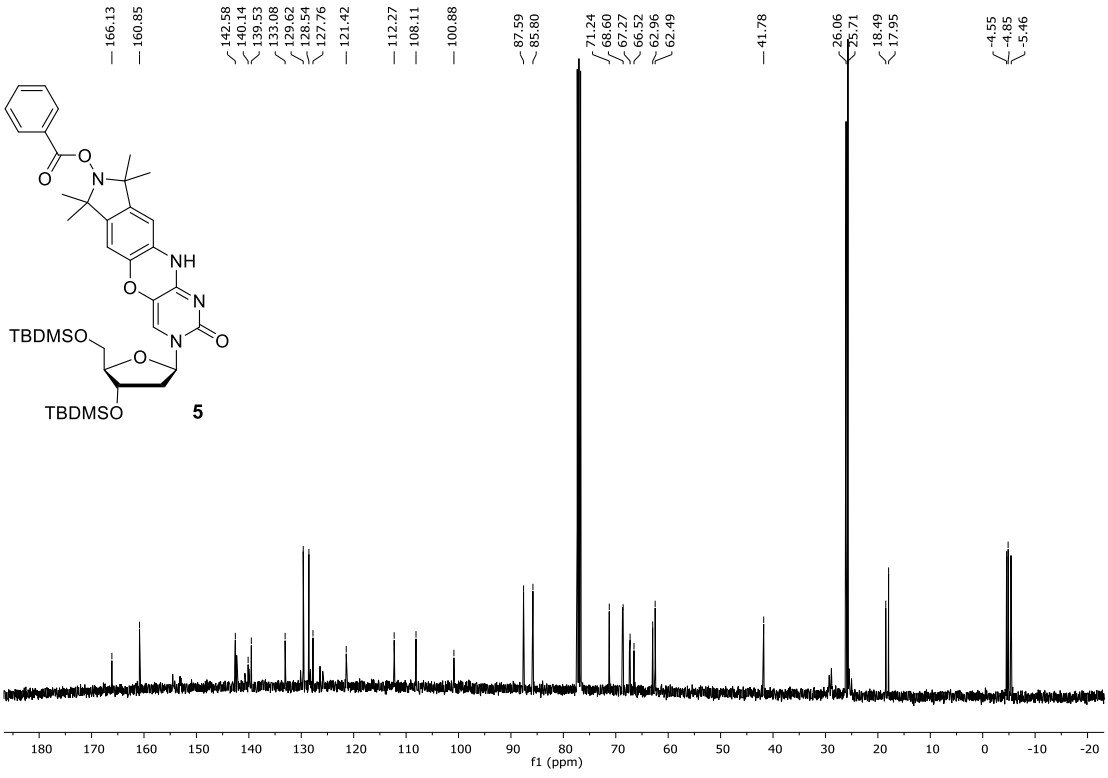

Figure S2. ^{13}C NMR of **5**.

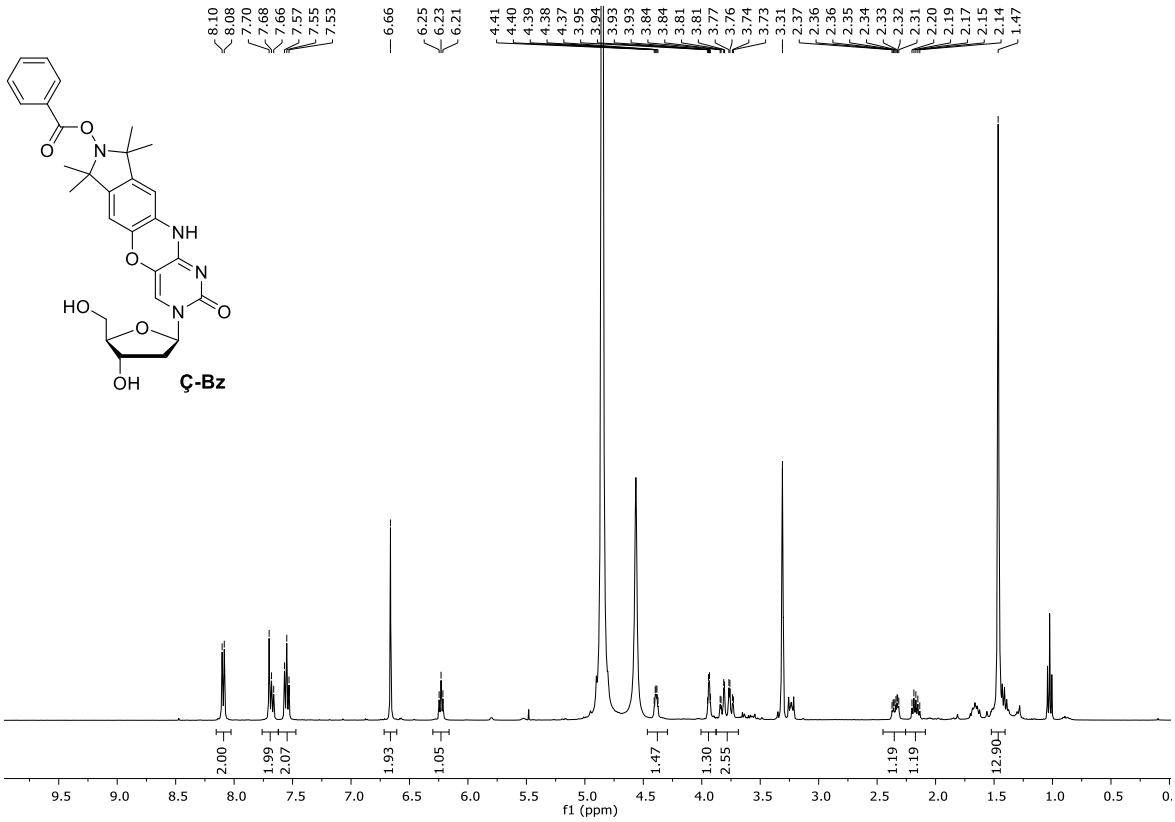

Figure S3. ^{1}H NMR of **Ç-Bz**.

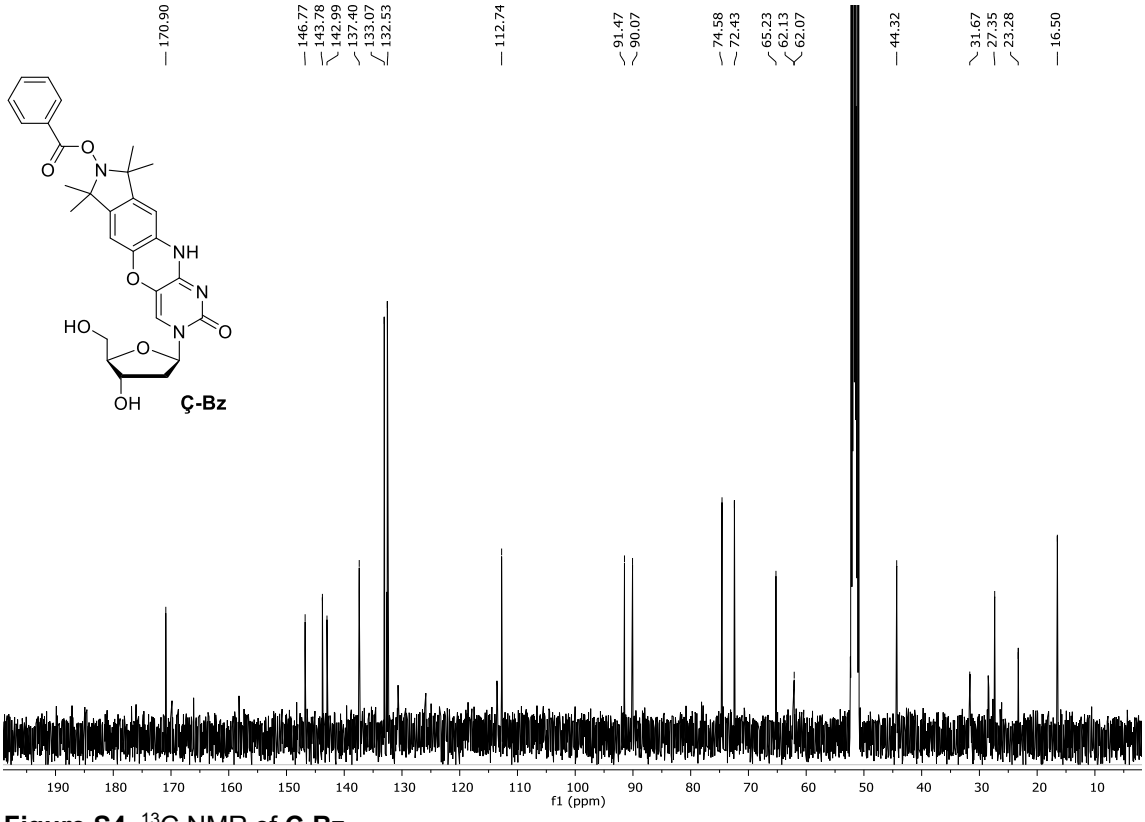

Figure S4. ^{13}C NMR of **Ç-Bz**.

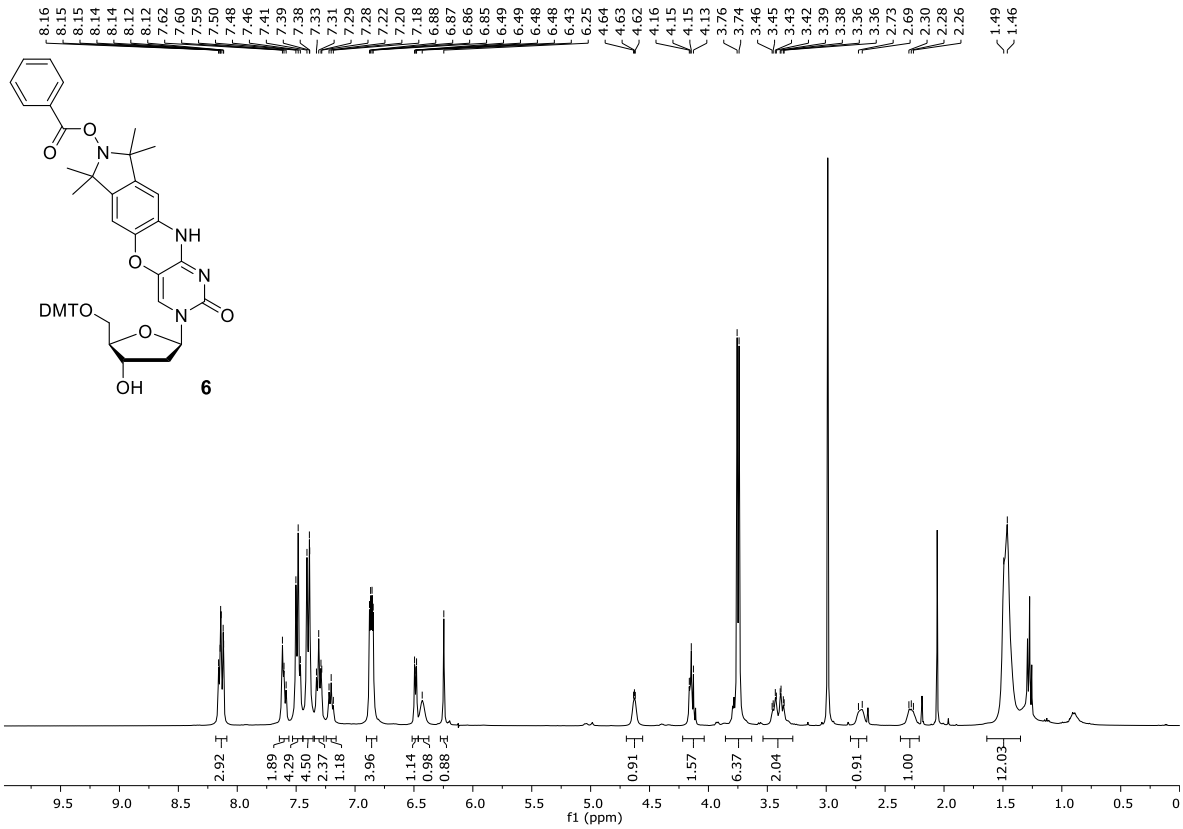

Figure S5. ^{1}H NMR of tritylated nucleoside **6**.

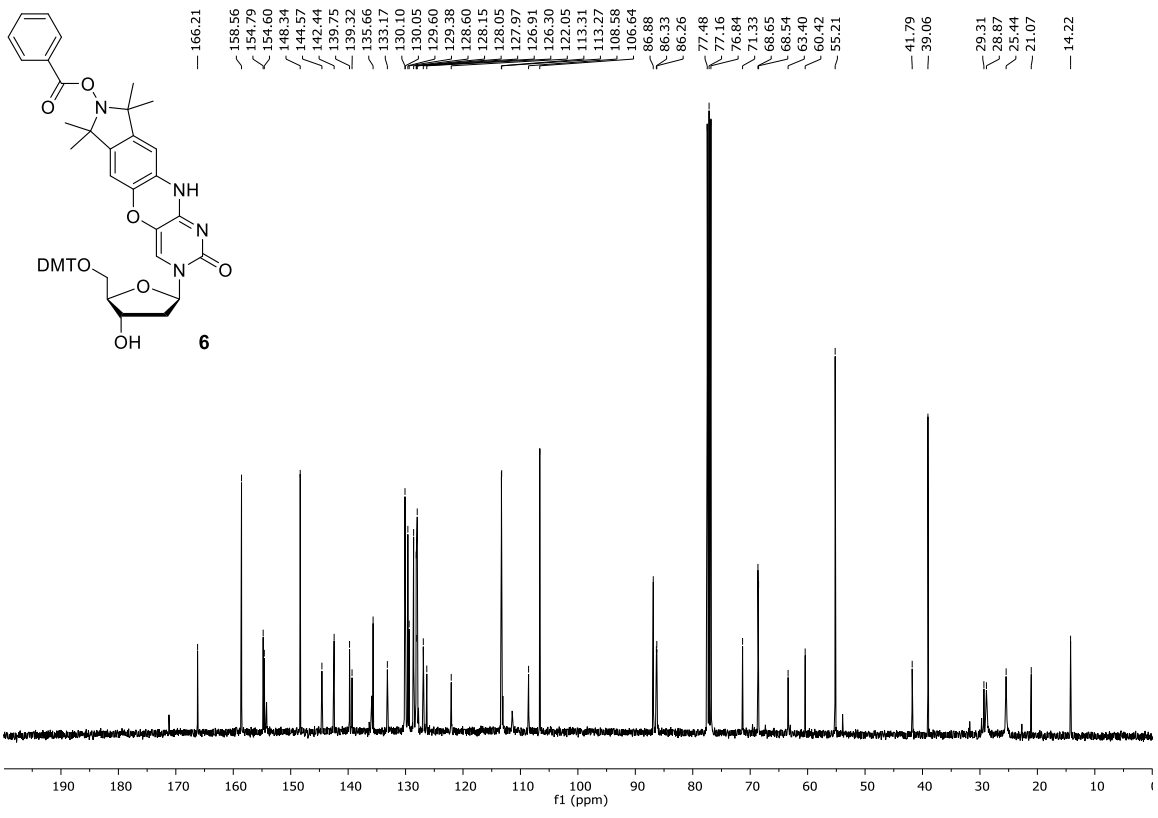

Figure S6. ^{13}C NMR of tritylated nucleoside **6**.

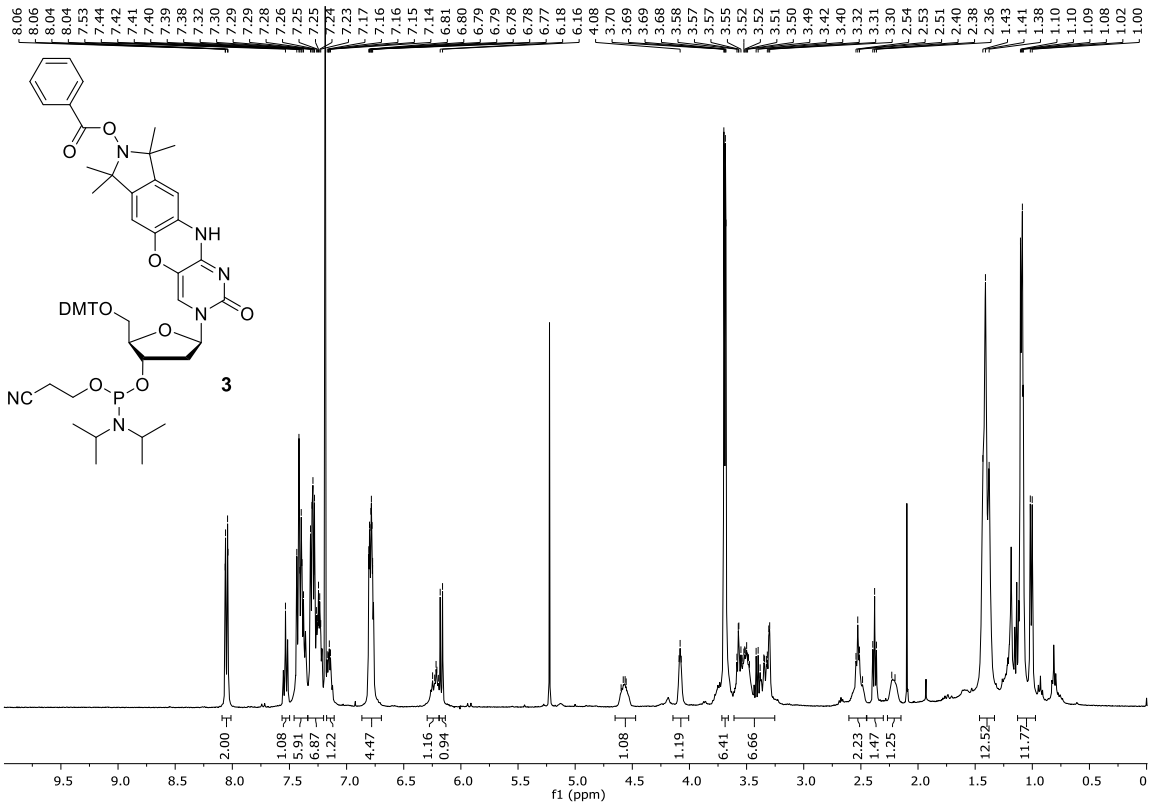

Figure S7. ^{1}H NMR of phosphoramidite **3**.

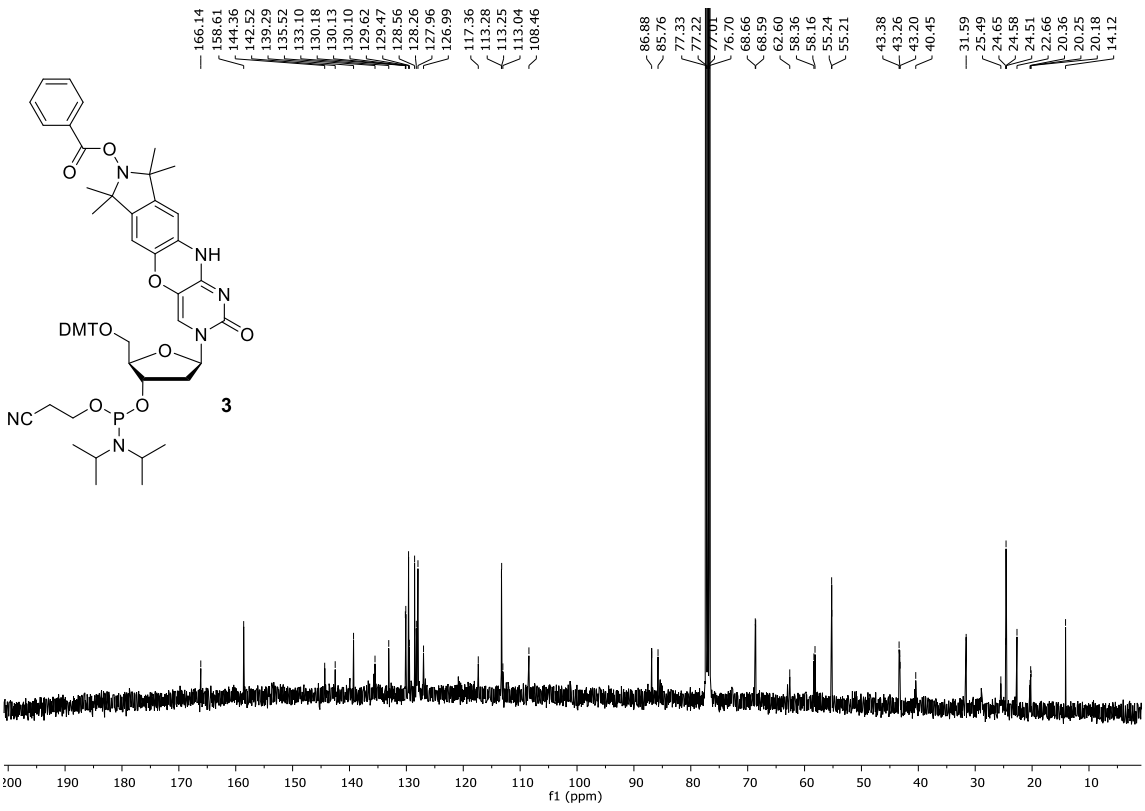

Figure S8. ^{13}C NMR of phosphoramidite **3**.

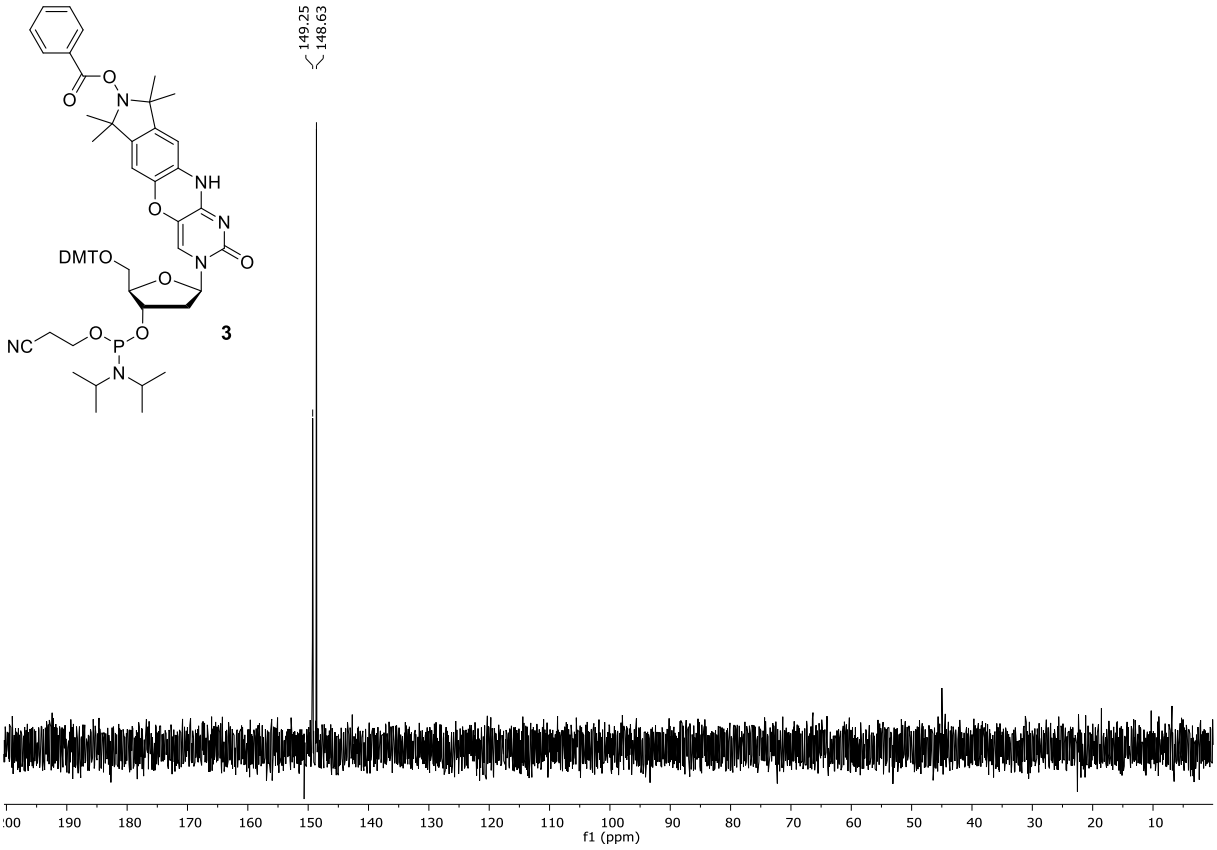

Figure S9. ^{31}P NMR of phosphoramidite **3**.

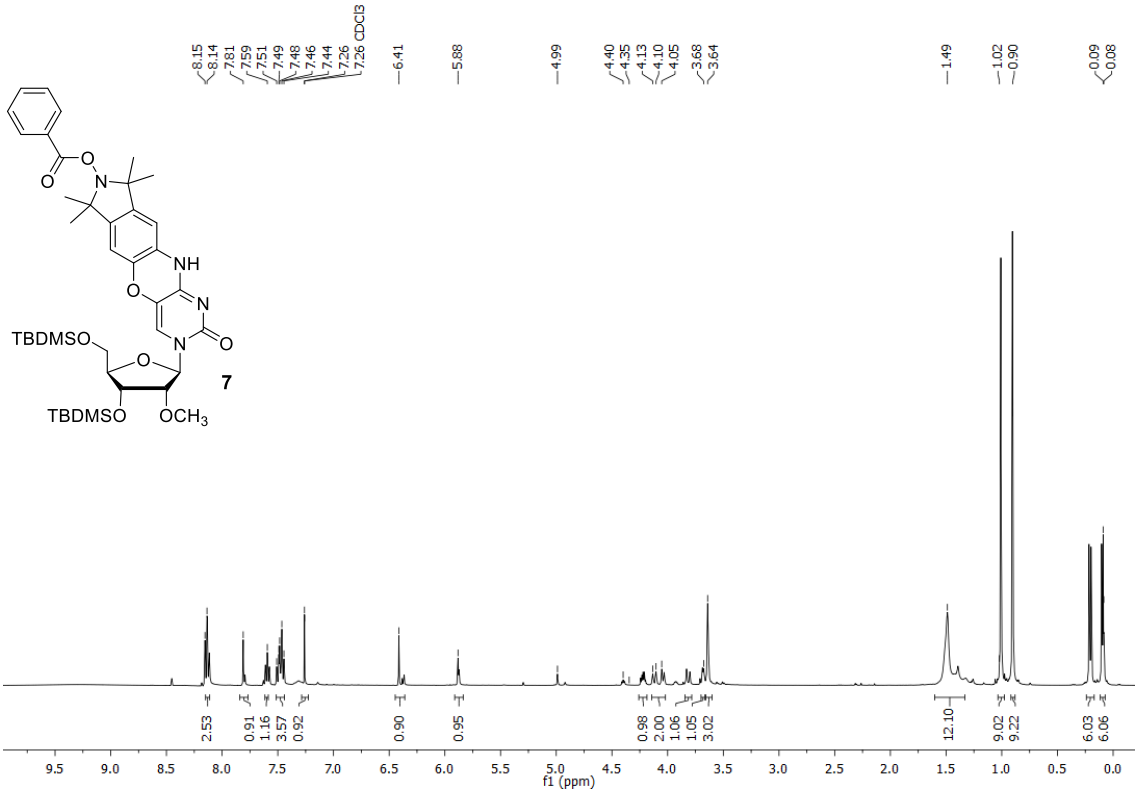

Figure S10. ^{1}H NMR of **7**.

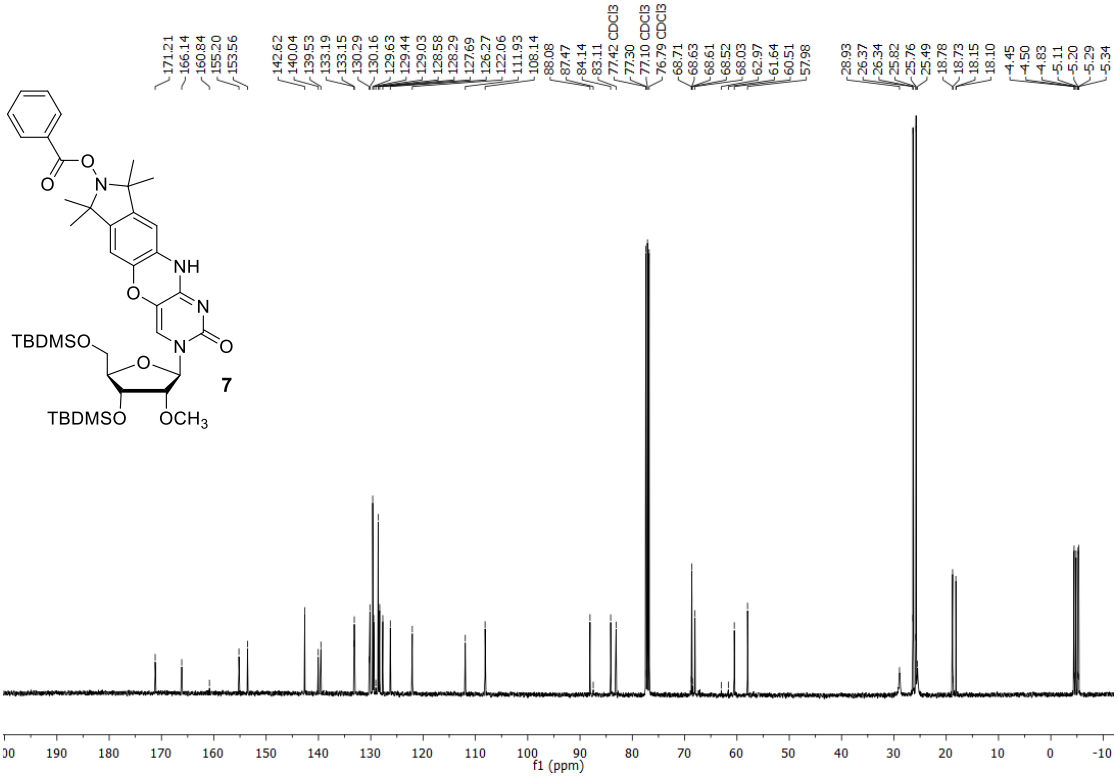

Figure S11. ^{13}C NMR of **7**.

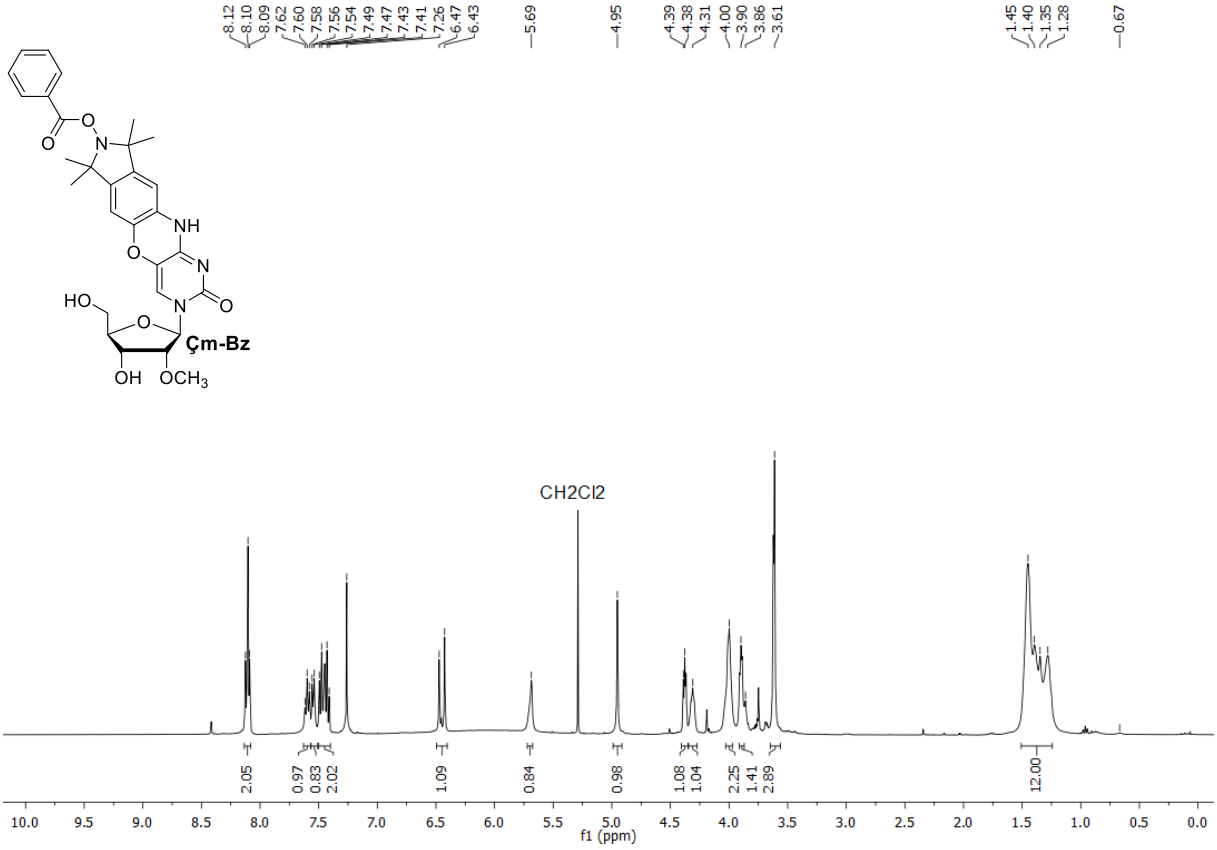

Figure S12. ^{1}H NMR of **Çm-Bz.**

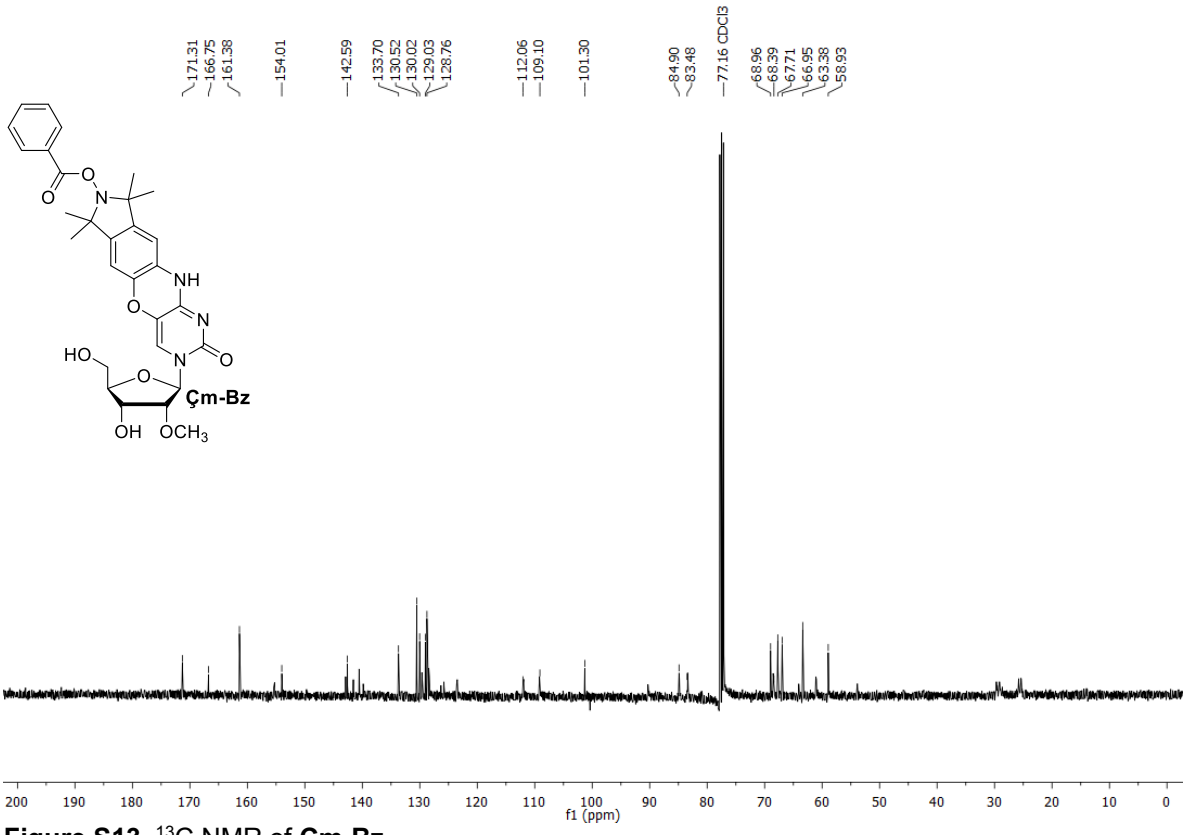

Figure S13. ^{13}C NMR of **Çm-Bz**.

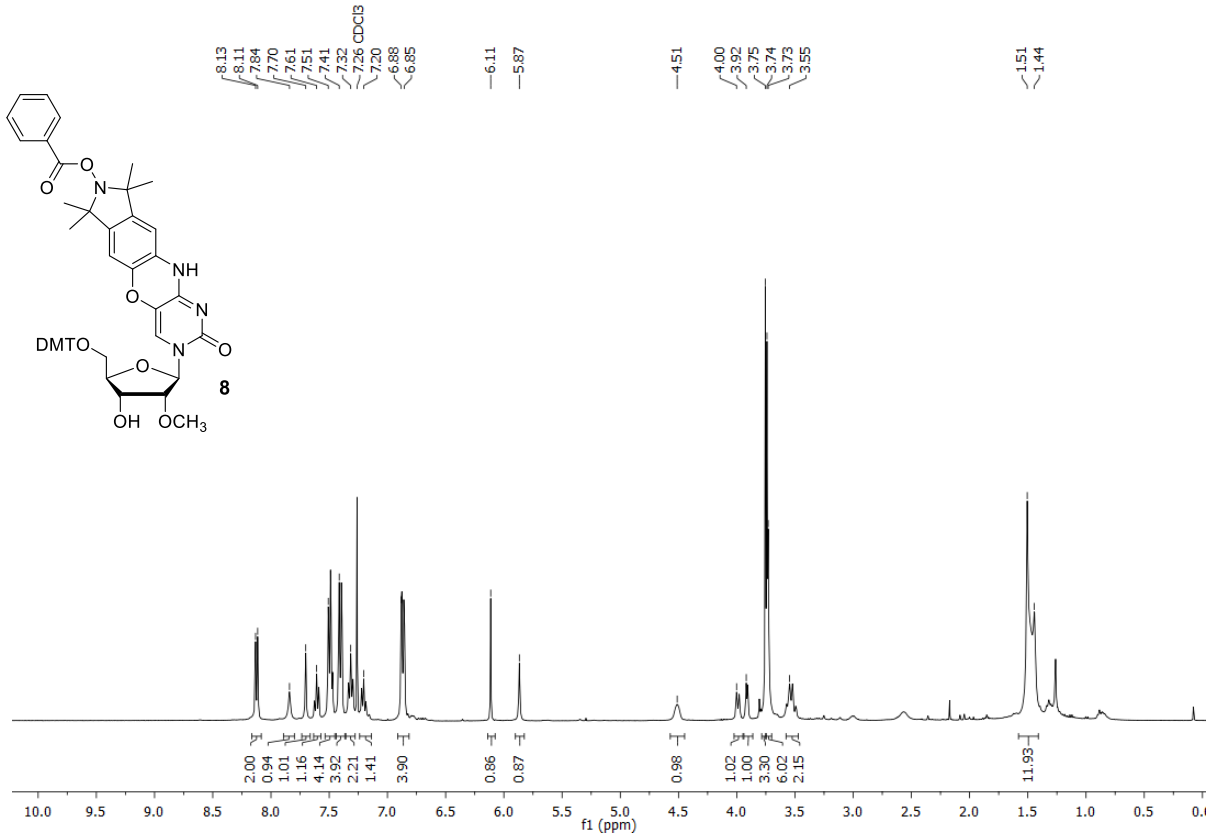

Figure S14. ^{1}H NMR of tritylated nucleoside **8**.

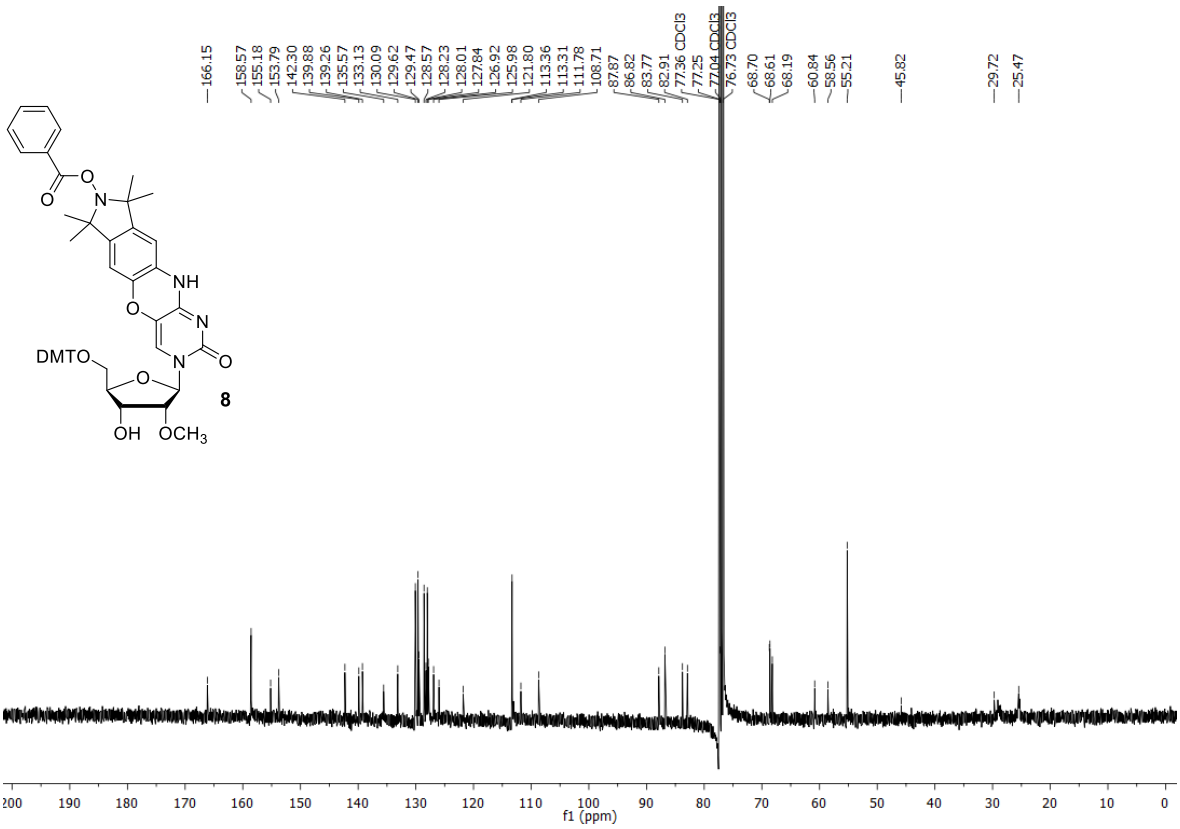

Figure S15. ^{13}C NMR of tritylated nucleoside **8**.

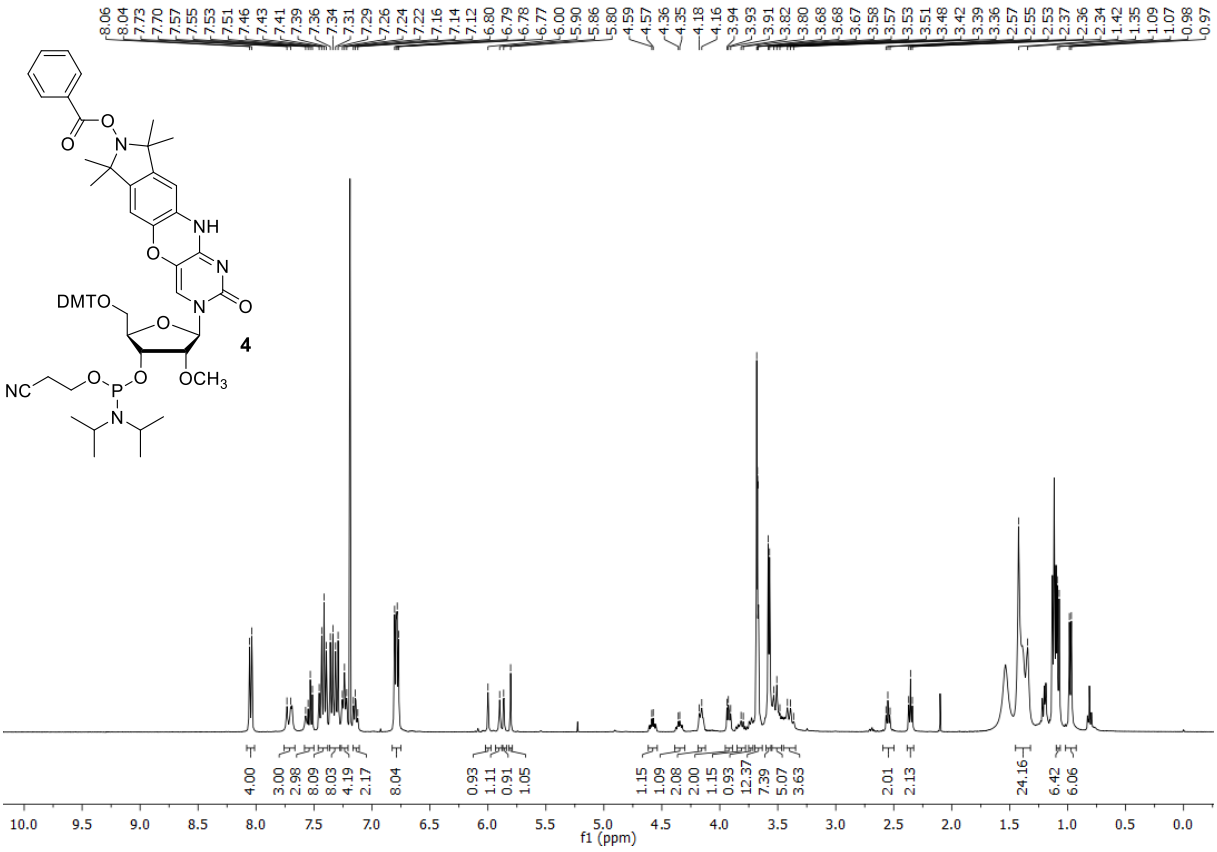

Figure S16. ^{1}H NMR of phosphoramidite **4**.

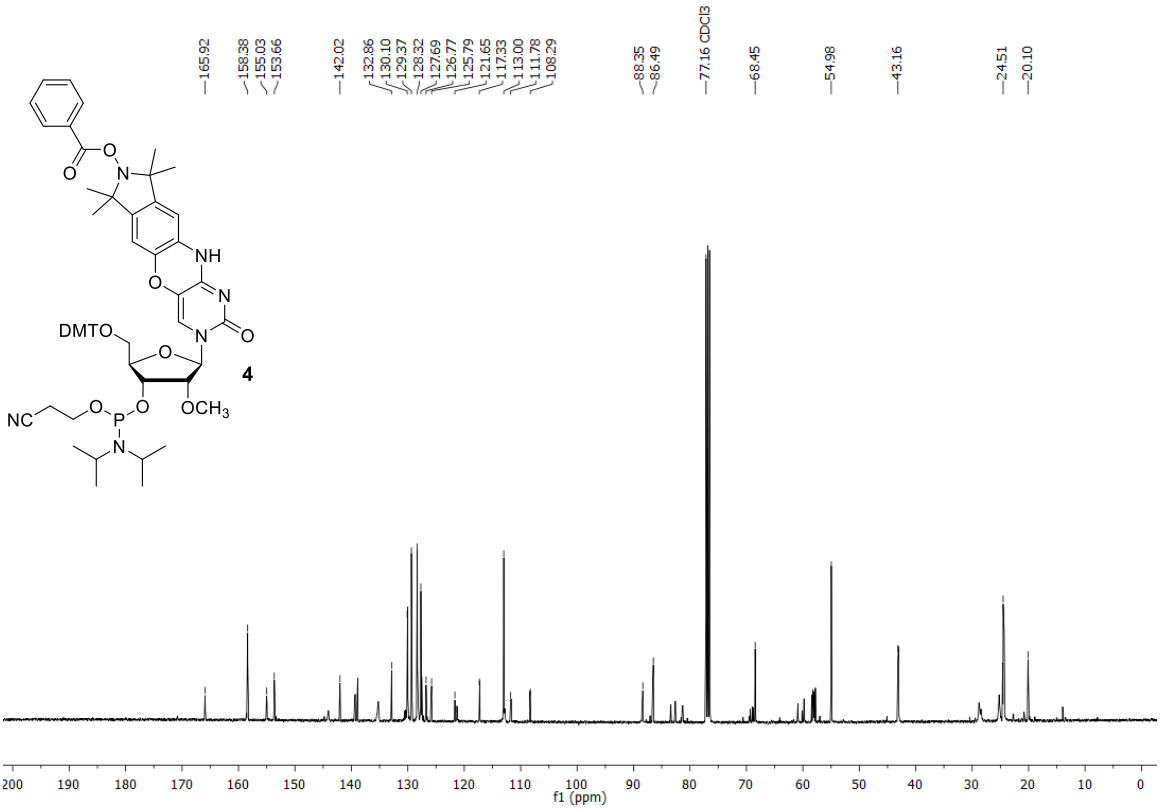

Figure S17. ^{13}C NMR of phosphoramidite **4**.

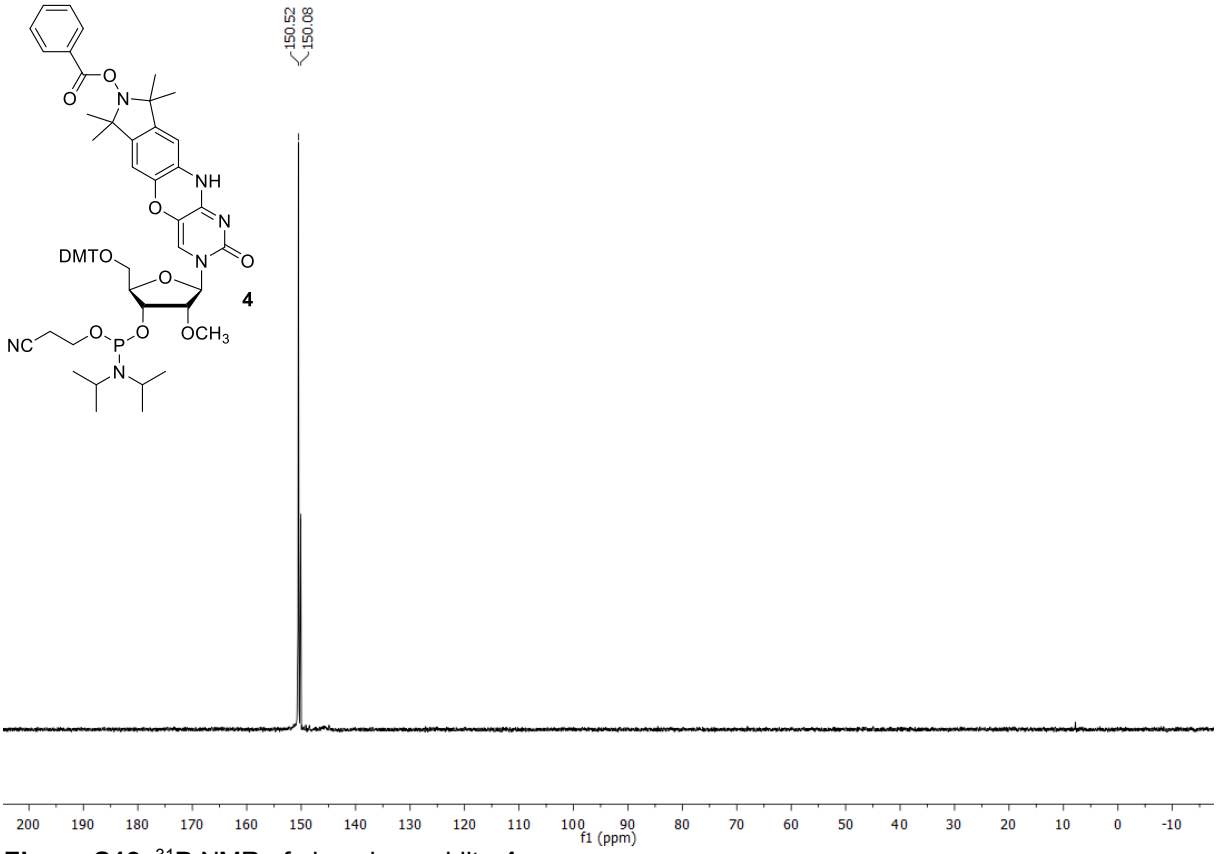

Figure S18. ^{31}P NMR of phosphoramidite **4**.

Mass spectra measured by HRMS (ESI)

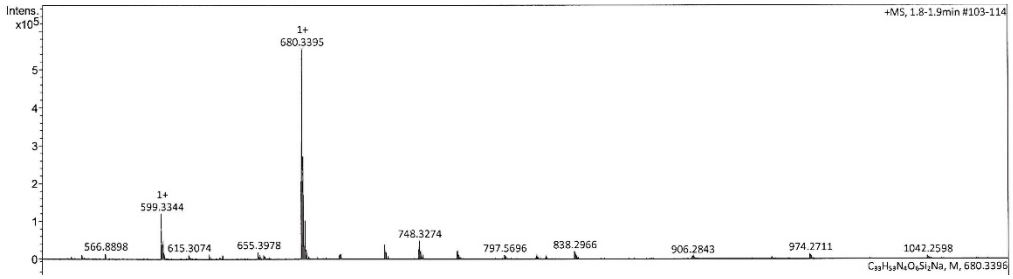

Figure S19. Mass spectrum of **1**.

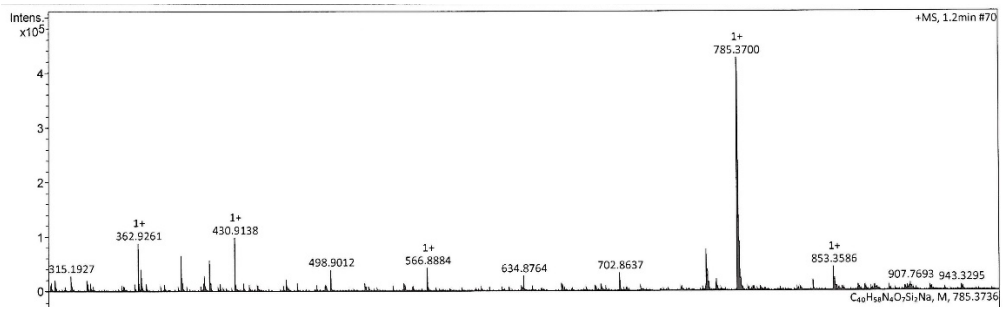

Figure S20. Mass spectrum of **5**.

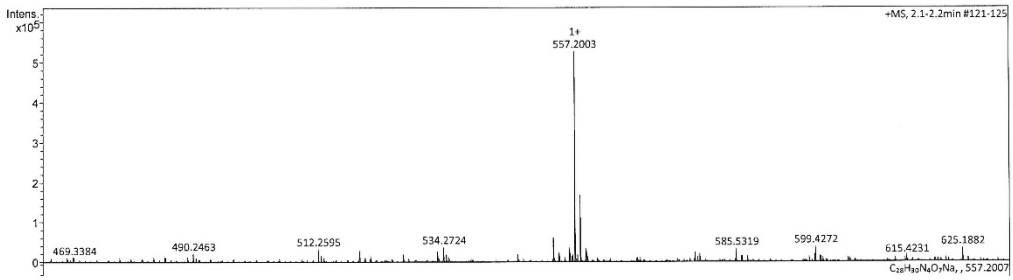

Figure S21. Mass spectrum of **Ç-Bz**.

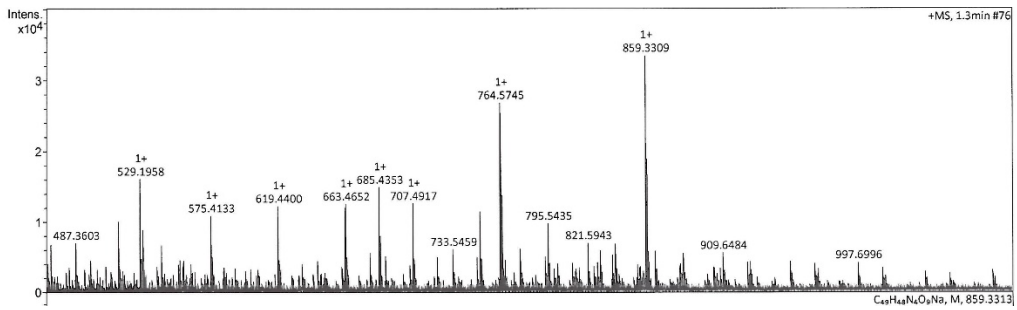

Figure S22. Mass spectrum of **6**.

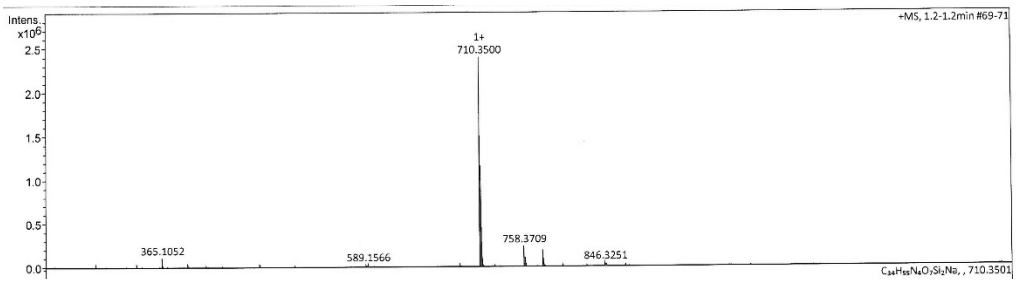

Figure S23. Mass spectrum of **2**.

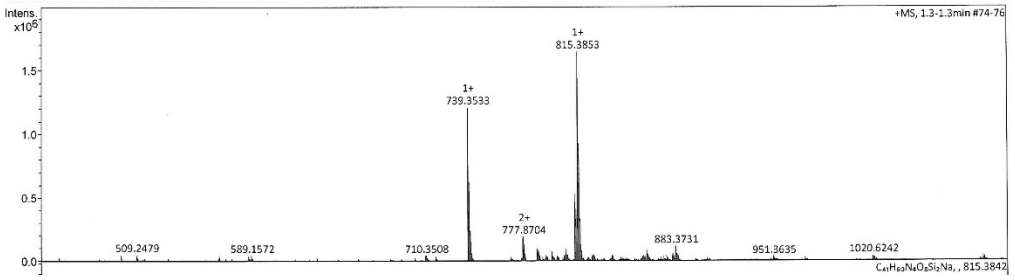

Figure S24. Mass spectrum of **7**.

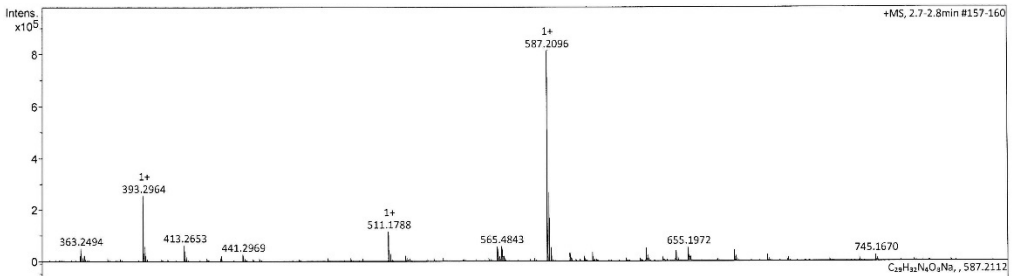

Figure S25. Mass spectrum of **Çm-Bz**.

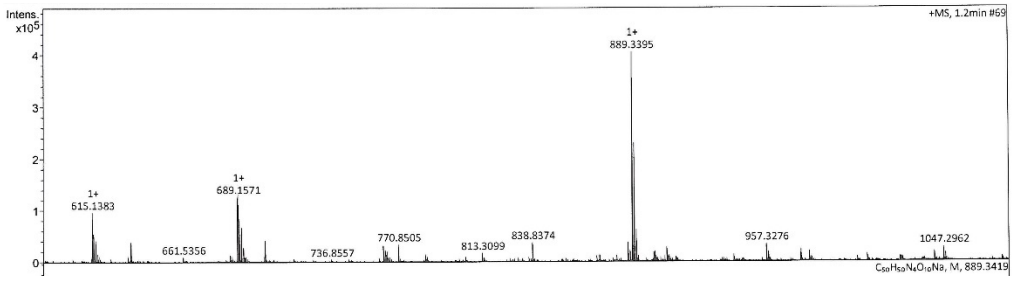

Figure S26. Mass spectrum of **8**.

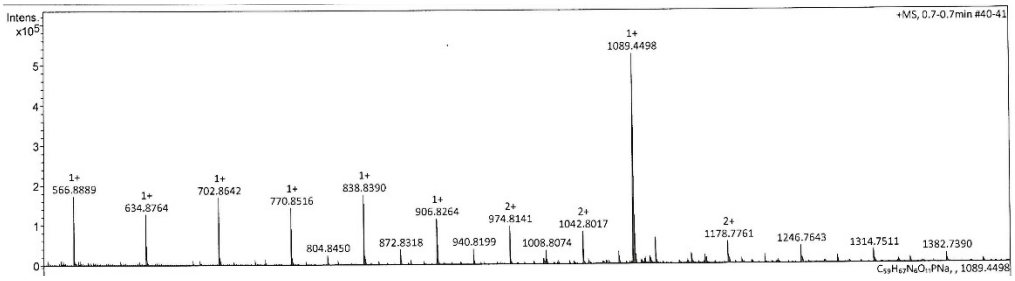

Figure S27. Mass spectrum of **4**.

CW-EPR measurements and spin counting. CW-EPR spectra were recorded on a MiniScope MS200 spectrometer using 100 kHz modulation frequency, 1.0 G modulation amplitude, and 2.0 mW microwave power. The samples were placed in a quartz capillary (BLAUBRANDintraMARK) prior to EPR measurements. Samples of spin-labeled oligonucleotides for EPR measurements were prepared by dissolving spin-labeled, single-stranded DNA or RNA (2.0 nmol) in phosphate buffer (10 mM phosphate, 100 mM NaCl, 0.1 mM Na_2EDTA, pH 7.0; 10 µL, oligonucleotide final conc. 200 µM). The EPR spectra of spin-labeled oligonucleotides I-VI are shown in **Figure S28**.

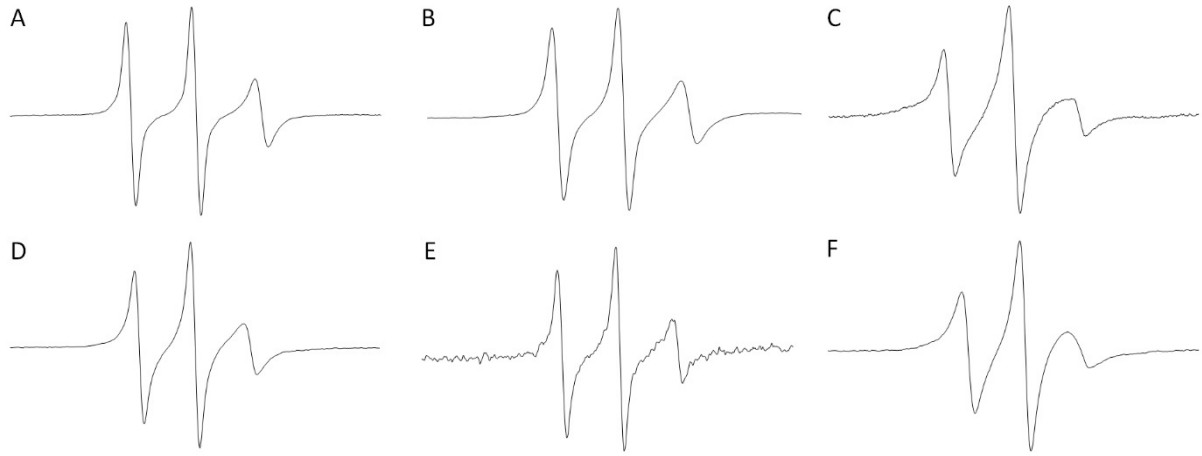

Figure S28. EPR spectra of oligonucleotides. **A**. Crude RNA **I** (5'-UGCAU**Çm**UU-3') synthesized using **4**. **B**. Crude RNA **II** (5'-UGCAU**Çm**UU-3') synthesized using the phosphoramidite of unprotected **Çm**. **C**. RNA **III** (5'-AGAUGCGCG**Çm**GCGCGACUGAC-3') synthesized using **4**. **D**. Crude DNA **IV** (5'-d(PHO-TGAGGTAGTAGGTTGTATA**Ç**T)-3') synthesized using **3**. **E**. Crude DNA **V** (5'-d(PHO-TGAGGTAGTAGGTTGTATA**Ç**T)-3') synthesized using the phosphoramidite of unprotected **Ç**. **F**. DNAzyme **VI** (5'-d(TGTAA**Ç**GCACTACCAGCGGCTGGAAATCTÇTCTCGT)-3') synthesized using **3**. PHO is a phosphate.

The amount of spin labels in each oligonucleotide was determined by spin counting. A stock solution of 4-hydroxy-TEMPO (1.0 M) was prepared in phosphate buffer (10 mM phosphate, 100 mM NaCl, 0.1 mM Na_2EDTA, pH 7.0). The stock solution was diluted into samples of different concentrations (0-0.5 mM) and each sample was measured by EPR spectroscopy. The area under the peaks of each sample, obtained by double integration, was plotted against its concentration to yield a standard curve, used to determine the spin-labeling efficiency with an error margin of 5-10% (**Table S2**).

Table S2. Spin labeling efficiency of oligonucleotides. Oligonucleotides II* and V* were synthesized with the phosphoramidite of unprotected nitroxide spin-labels **Çm** and **Ç**, respectively. PHO is a phosphate.

Name	Sequence	Efficiency (%)
I	5‘-UGCAU**Çm**UU-3‘	96
II*	5‘-UGCAU**Çm**UU-3‘	49
III	5‘-AGA-UGC-GCG-**Çm**GC-GCG-ACU-GAC-3‘	93
IV	5‘-d(PHO-TGAGGTAGTAGGTTGTATA**Ç**T)-3	96
V*	5‘-d(PHO-TGAGGTAGTAGGTTGTATA**Ç**T)-3	5
VI	5‘-d(TGTAA**Ç**GCACTACCAGCGGCTGGAAATCT**Ç**TCTCGT)-3‘	99

Paper II

Reduction resistant and rigid nitroxide spin labels for DNA and RNA

Haraldur Y. Juliusson and Snorri Th. Sigurdsson*

University of Iceland, Department of Chemistry, Science Institute, Dunhaga 3, 107 Reykjavik, Iceland.

**E-mail: snorrisi@hi.is*

Keywords

In-cell EPR spectroscopy, sterically-shielded nitroxides, oligonucleotides, reduction resistant nitroxides, rigid spin labels

For Table of Contents Only / Abstract Graphics

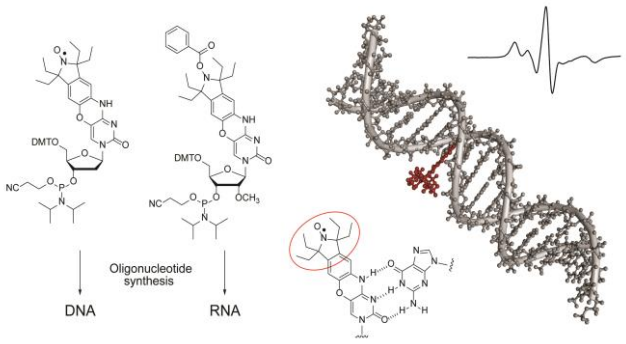

Abstract

Electron paramagnetic resonance (EPR) spectroscopy, coupled with site-directed spin labeling (SDSL), is a useful method for studying conformational changes of biomolecules in cells. In order to employ *in-cell* EPR using nitroxide-based spin labels, the structure of the nitroxides must confer reduction resistance in order to withstand the reductive environment within cells. Here we report the synthesis of two new spin labels, **EÇ** and **EÇm**, both of which possess the rigidity and the reduction resistance needed for extracting detailed structural information by EPR spectroscopy. **EÇ** and **EÇm** were incorporated into DNA and RNA, respectively, by oligonucleotide synthesis. Both labels were shown to be non-perturbing of duplex structure. Partial reduction of **EÇm** during RNA synthesis was circumvented by protection of the nitroxide as a benzoylated hydroxylamine.

Introduction

Nucleic acids are central to molecular biology and partake in essential biological processes,[1] including storage, expression and transmission of genetic information,[2] as well as catalysis of chemical reactions[3, 4] and regulation of genetic expression.[5-7] Understanding their biological functions relies on structural knowledge. Biomolecules have been intensively studied *in vitro* by a number of biochemical and biophysical methods, such as X-ray crystallography,[8] nuclear magnetic resonance (NMR) spectroscopy,[9, 10] Förster resonance energy transfer (FRET)[11, 12] and electron paramagnetic resonance (EPR) spectroscopy.[13-16] Although biomolecules have been extensively studied *in vitro*, the question remains whether the structure and dynamics of biomolecules are different in cells, since the intracellular environment may be impossible to reproduce *in vitro*, in particular factors such as viscosity, molecular crowding, interactions with other macromolecules, and concentration of ions.[17]

Increased effort is being directed towards exploring biomolecules within cells, in particular using spectroscopic methods, such as NMR, FRET and EPR.[17-20] *In-cell* NMR has been used to study the structure and dynamics of nucleic acids in several cell types, along with membranes and disordered proteins.[17, 19-23] *In-cell* NMR has mostly been used to monitor enzymatic or "nonspecific" interactions,[21] and requires isotopic labeling of molecules to overcome cellular background signals. *In-cell* FRET has been used to study inter- and intra-molecular interactions through distance measurements between two fluorescent tags.[24, 25] EPR spectroscopy has also been used to measure distances within biomolecules in cells and recent studies have highlighted its advantages.[18, 26, 27] EPR requires small amounts of material, has virtually no background signals, is not limited by molecular size, and structural information can be readily obtained through distance measurements by dipolar EPR-experiments, such as pulsed electron-electron double resonance (PELDOR/DEER).[26, 28-30]

There are examples of paramagnetic biomolecules, such as metalloproteins[31] and proteins that contain paramagnetic cofactors.[32] However, the majority of biomolecules are diamagnetic and, therefore, a paramagnetic center (spin label) must be introduced in order to carry out EPR

studies. For *in-cell* EPR, three types of spin labels have been used. Gd(III) complexes have been used for distance measurements in proteins (**Figure 1A**),[33-35] for example ubiquitin that contained two 4PS-PyMTA-Gd(III) labels. Trityl radicals (**Figure 1B**) have also been used for distance measurements in cells, specifically between a trityl-labeled cytochrome P450 and a native metal cofactor.[36] Nitroxides have also been used for *in-cell* EPR,[18, 26, 28-30, 37-39] but limitation of most nitroxides is that they are rapidly reduced in the reducing environment encountered within cells.[37, 40, 41] However, sterically-shielded nitroxides, in particular tetraethyl-derived nitroxides, are resistant towards reduction.[41] For example, a tetraethyl-derived pyrrolidine nitroxide has been used to spin label a chaperone protein for *in-cell* EPR (**Figure 1C**). Only minimal reduction of the radical was observed and enabled the EPR study of structural features of the chaperone protein through determination of inter-spin distances.[42] A tetraethyl-derived isoindoline spin label has recently been used for post-synthetic labeling of 2'-amino groups of RNA (**Figure 1D**) and shown to be stable in the presence of ascorbic acid.[43] Preliminary *in-cell* EPR measurements with this label have revealed structural changes in duplex RNAs (unpublished data). However, the semi-flexible nature of the linker attaching the spin label to the RNA limited the structural information that could be obtained.

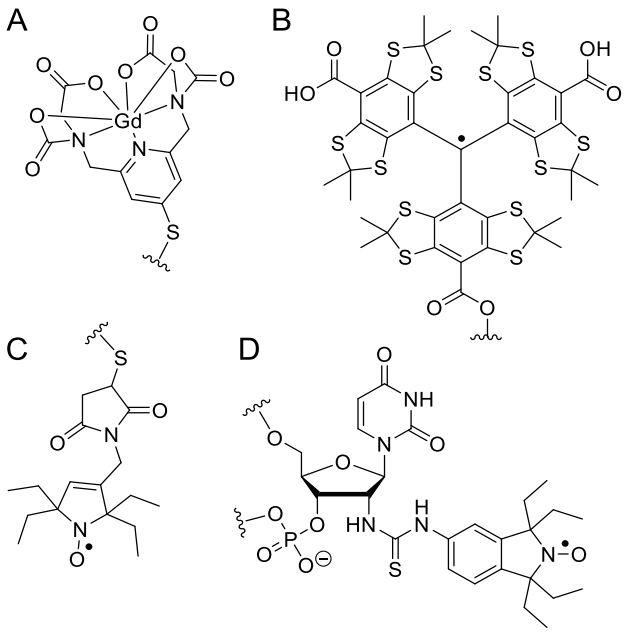

Figure 1. Different spin labels used for in-cell EPR measurements. **A.** 4PS-PyMTA-Gd(III) linked to a protein.[44] **B.** A trityl-based spin label linked to a protein.[36] **C.** M-TETPO linked to a protein.[42] **D.** A tetra-ethyl derived spin label conjugated to a 2'-amino labeled uridine through a thiourea linkage.[43]

The rigid spin labels **Ç**[45] and **Çm**[46] (**Figure 2**) have been shown to provide more detailed information on structural changes and dynamics in nucleic acids[47] than flexible and semi-flexible labels. Here we describe the synthesis and characterization of the corresponding tetraethyl nitroxide spin labels **EÇ** and **EÇm** (**Figure 2**). These spin labels combine two characteristics necessary for obtaining detailed structural information about nucleic acids in cells by EPR spectroscopy, namely rigidity and reduction resistance.

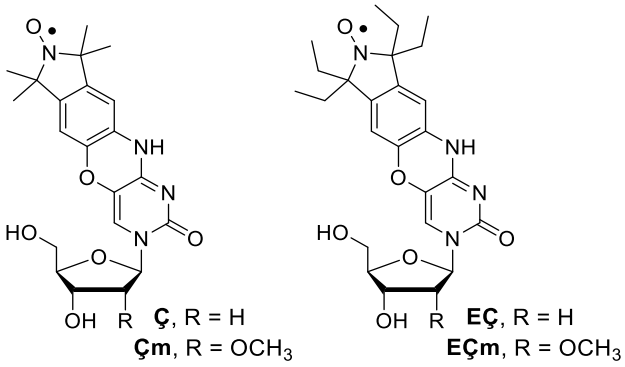

Figure 2. The rigid spin labels **Ç**[45] and **Çm**[46] and their corresponding tetraethyl derivatives **EÇ** and **EÇm**.

Results and discussion

Synthesis of EÇ and EÇm and their stability towards reduction

The synthesis of **EÇ** and **EÇm** started with the preparation of ethylisoindoline derivative **4** (**Scheme 1**). Compound **1**[48] was aminated[49] to afford amino-nitro derivative **2**. Hydrolysis of **2** yielded **3** and hydrogenation of the nitro group gave ethylisoindoline-derived aminophenol **4**. To incorporate the ethylisoindoline moiety into nucleosides, the dihalogenated nucleosides **5**[45] and **6**[46] were coupled with **4** in the presence of Et_3N to provide intermediates **7** and **8**, respectively, followed by ring-closure[45, 46, 50] to afford phenoxazine derivatives **EÇf** and **EÇmf**. Direct oxidation of **EÇf** and **EÇmf** using either hydrogen peroxide and Na_2WO_4[45] or *m*-chloroperoxybenzoic acid (*m*-CPBA)[51] under a variety of conditions resulted in very low yields of the desired product along with multiple other products. However, oxidation of TBDMS-protected **EÇf** and **EÇfm** with *m*-CPBA in the presence of NaN_3[49] afforded **9** and **10** in excellent yields. The TBDMS groups were subsequently removed with TBAF to yield nucleosides **EÇ** and **EÇm**.

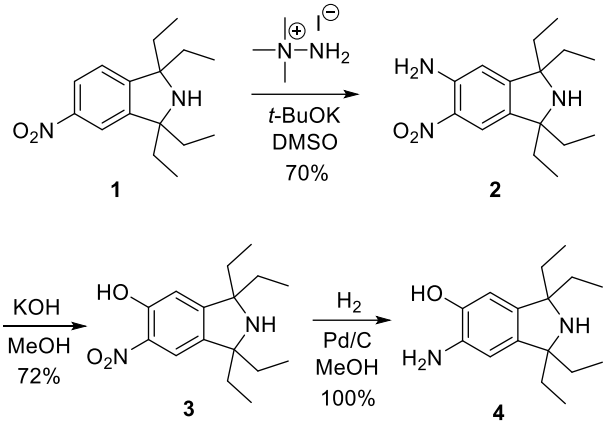

Scheme 1. Synthesis of tetraethylisoindoline **4**.

The resistance of **EÇm** towards reduction in presence of ascorbic acid, frequently used to evaluate the stability of nitroxides,[41] was investigated and compared to its tetramethyl derivative **Çm**.[46] The normalized EPR signal intensity was plotted as a function of time and showed that the tetramethyl derived **Çm** was almost fully reduced within 1 h, while ca. 90% of the **EÇm** nucleoside was still intact after 16 h (**Figure S29**).

The 5'-hydroxyl groups of **EÇ** and **EÇm** were protected as 4,4'-dimethoxytrityl (DMT) ethers and subsequent 3'-phosphitylation yielded phosphoramidites **11** and **12** (**Scheme 2**), used for incorporation of **EÇ** and **EÇm** into DNA and RNA oligonucleotides by solid phase synthesis, respectively. While working with DMT-protected **EÇ**, **EÇm** and phosphoramidites **11** and **12**, we discovered that the DMT groups were unusually labile. Even dissolving these compounds in polar and/or protic solvents, such as CH_3CN or MeOH, lead to rapid loss of the DMT group. The use of nonpolar or chlorinated solvents such as CH_2Cl_2 or 1,2-dichloroethane circumvented this decomposition.

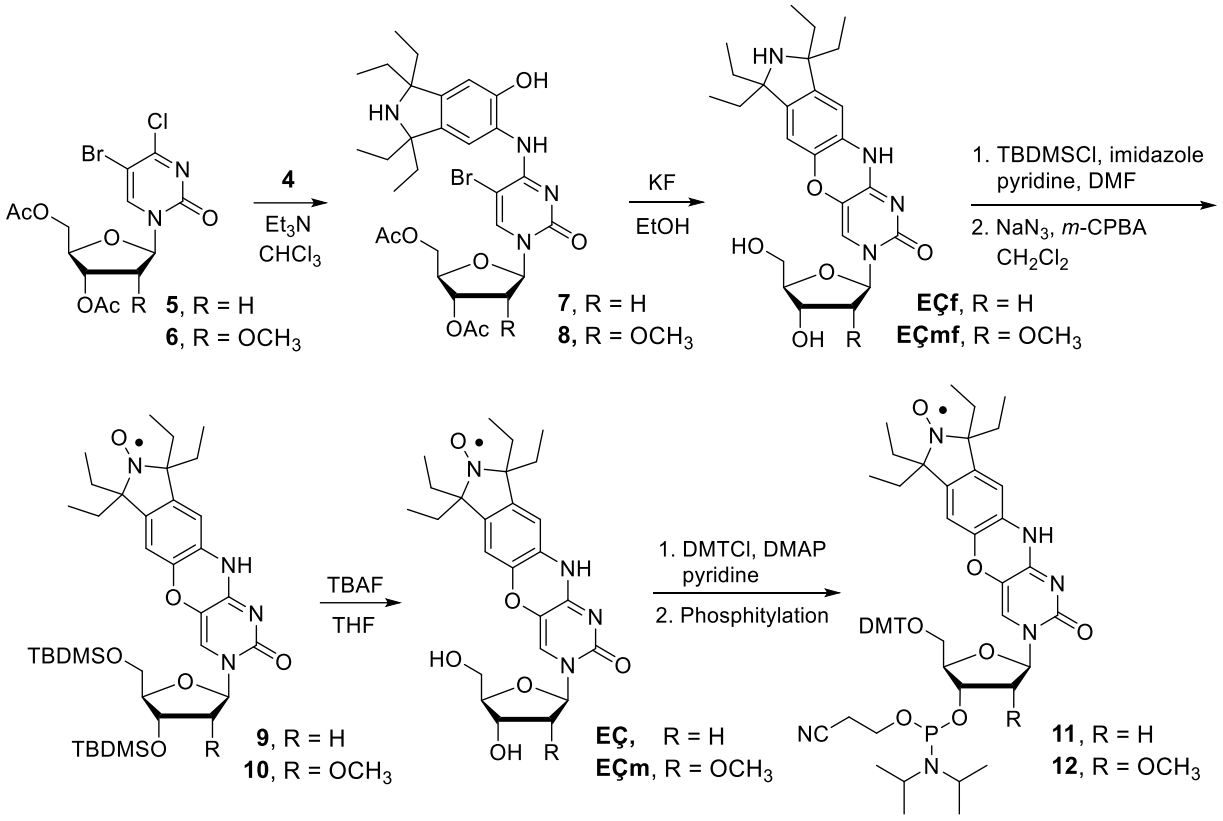

Scheme 2. Synthesis of spin-labeled nucleosides **EÇ** and **EÇm** and their corresponding phosphoramidites. Yields were as follows: **EÇf** (56%, over 2 steps), **EÇmf** (60%, over 2 steps), **9** (83% over 2 steps), **10** (81%, over 2 steps), **EÇ** (91%), **EÇm** (94%), **11** (77%, over 2 steps) and **12** (63%, over 2 steps).

Syntheses of spin-labeled DNA oligonucleotides

Phosphoramidite **11** was used for the synthesis of seven different oligodeoxynucleotides containing **EÇ** by automated solid-phase synthesis (**Table S1**). The DNAs varied in length and position of the spin-label. The spin-labeled phosphoramidite **11** coupled well during the solid-phase synthesis, as indicated by a strong orange color of the trityl cation that appears during removal of the DMT group. Analysis of the crude oligodeoxynucleotides by denaturing polyacrylamide gel electrophoresis (DPAGE) did not reveal any failure bands that would have resulted for partial coupling of **11**. The **EÇ**-modified oligomers migrated slightly slower than the

unmodified strands of the same sequence by DPAGE, consistent with incorporation of the spin label, which was confirmed by mass spectrometry (**Table S1**).

The DNA oligomers were enzymatically digested and the digests were analyzed by high performance liquid chromatography (HPLC) (**Figure S30**).[52, 53] The HPLC chromatograms for digests of DNAs **I-VII** each showed five peaks, one for each natural nucleoside and a strongly retained nucleoside that was shown by co-injection[45] to be **EÇ**. Chromatograms for the longer oligonucleotides (**III**, **IV**, **VI** and **VII**) also contained an additional small peak around 20.5 minutes that was shown by co-injection to be **EÇf**. It is well known that nitroxide radicals get partially,[53] or even fully,[54] reduced during oligonucleotide synthesis using the phosphoramidite approach. Although the tetraethyl groups on **EÇ** render the nitroxide significantly more resistant to reduction by common reducing agents, they do not provide full protection against reduction (through disproportionation)[55] by the acids used for oligonucleotide synthesis, dichloroacetic acid and ethylthiotetrazole. The amounts of **EÇf** and **EÇ** was quantified, showing that ca. 6-18% of the spin-labels had been reduced. These results were further confirmed with spin-counting of DNAs **I**-**VII** by EPR spectroscopy giving 81-100% spin labeling (**Table S1**). It should be noted that more extensive reduction was observed in oligodeoxynucleotides of similar length that were synthesized using the phosphoramidite of the tetramethyl derived **Ç**.[53]

A molecular model of a **EÇ** within a B-form DNA duplex (**Figure 3A**) shows that the spin label is well accommodated in the major groove of the duplex. To determine experimentally whether the **EÇ** spin-label caused a structural perturbation of the B-DNA, circular dichroism (CD) spectra were recorded (**Figure S32**), along with collecting thermal denaturation data (**Table 1, Figure S33**). The CD spectra of the modified and unmodified DNA duplexes were almost identical, all possessing negative and positive molar ellipticities at ca. 250 and 280 nm, respectively, characteristic of a right-handed B-DNA. In general, the thermal denaturation experiments showed that the spin labels did not result in a significant decrease in the melting temperature, with ΔT_Ms ranging from -0.8 to -2.8 °C. Increased stability was actually observed for duplexes **B** and **I**. The increase of the T_M for duplex **B** of +5.6 °C and decrease for duplex

D of -1.5 °C, is nearly identical to what has been observed for **Ç** in the same location of the same sequence (ΔT_M +5.7 °C and ΔT_M -1.1 °C, respectively).[52]

Table 1. Sequences of spin-labeled DNA and RNA duplexes and their thermal denaturation analysis.

	DNA and RNA sequences	T_M (°C)	ΔT_M
A	5'-d(CGCGAATTCGCG)-3' 3'-d(GCGCTTAAGCGC)-5'	58.2	
B	5'-d(CGCG AATT**EÇ**GCG)-3' 3'-d(GCG**EÇ**TTAAG CGC)-5'	63.8	+5.6
C	5'-d(GACCTCGCATCGTG)-3' 3'-d(CTGGAGCGTAGCAC)-5'	60.8	
D	5'-d(GACCTCG**EÇ**ATCGTG)-3' 3'-d(CTGGAGCG TAGCAC)-5'	59.3	-1.5
E	5'-d(AGTGGACGCTTGGGGTGTA)-3' 3'-d(CACCTGCGAACCCCACATA)-5'	66.6	
F	5'-d(AGTGGA**EÇ**GCTTGGG GTGTA)-3' 3'-d(CACCT GCGAACCC**EÇ**ACATA)-5'	63.8	-2.8
G	5'-d(AGTGGA**EÇ**GCTTGG GGTGTA)-3' 3'-d(CACCT GCGAACC**EÇ**CACATA)-5'	65.0	-1.6
H	5'-d(AGTGGA**EÇ**GCTTG GGGTGTA)-3' 3'-d(CACCT GCGAAC**EÇ**CCACATA)-5'	65.8	-0.8
I	5'-d(AGTGGA**EÇ**GCTT GGGGTGTA)-3' 3'-d(CACCT GCGAA**EÇ**CCCACATA)-5'	67.4	+0.8
J	5'-AGUGGACGCUUGUGGGGUGUA -3' 3'- CACCUGCGAACACCCCACAUA-5'	77.0	
K	5'-AGUGGA**EÇm**GCUUGUGGGG UGUA -3' 3'- CACCUG CGAACACCC**EÇm**ACAUA-5'	74.0	-3.0
L	5'-AGUGGA**EÇm**GCUUGUGGG GUGUA -3' 3'- CACCUG CGAACACC**EÇm**CACAUA-5'	76.0	-1.1
M	5'-AGUGGA**EÇm**GCUUGUGG GGUGUA -3' 3'- CACCUG CGAACAC**EÇm**CCACAUA-5'	75.6	-1.4
N	5'-AGUGGA**EÇm**GCUUGUG GGGUGUA -3' 3'- CACCUG CGAACA**EÇm**CCCACAUA-5'	74.6	-2.4

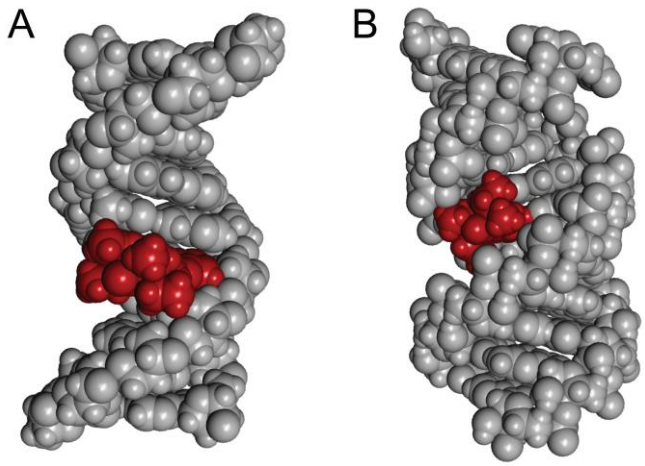

Figure 3. Space-filling models of **EÇ**- and **EÇm**-labeled oligonucleotide duplexes. A. B-form DNA duplex with **EÇ** projected into the major groove. B. A-form RNA duplex containing **EÇm**. The oligonucleotide constituents are shown in grey and the spin-labeled nucleotides in red.

All oligonucleotides were characterized by continuous-wave (CW) EPR spectroscopy (**Figure S34**), which also confirmed duplex formation. **Figure 4** shows a comparison of the CW-EPR spectra of **EÇ**, the **EÇ**-labeled 19-mer DNA single strand **III** and the corresponding 19-mer DNA duplex **F**. The nucleoside showed three sharp lines (**Figure 4A**) that broadened after incorporation into the 19-mer oligoribonucleotide 5'-d(AGTGGA**EÇ**GCTTGGGGTGTA)-3' (**Figure 4B**). Upon annealing to its complementary strand 5'-d(ATACA**EÇ**CCCAAGCGTCCAC)-3', the CW-EPR spectrum broadened further, showing a splitting of the high- and low-field components (**Figure 4C**), characteristic for the formation of a spin labeled duplex containing a rigid spin label.[45, 46]

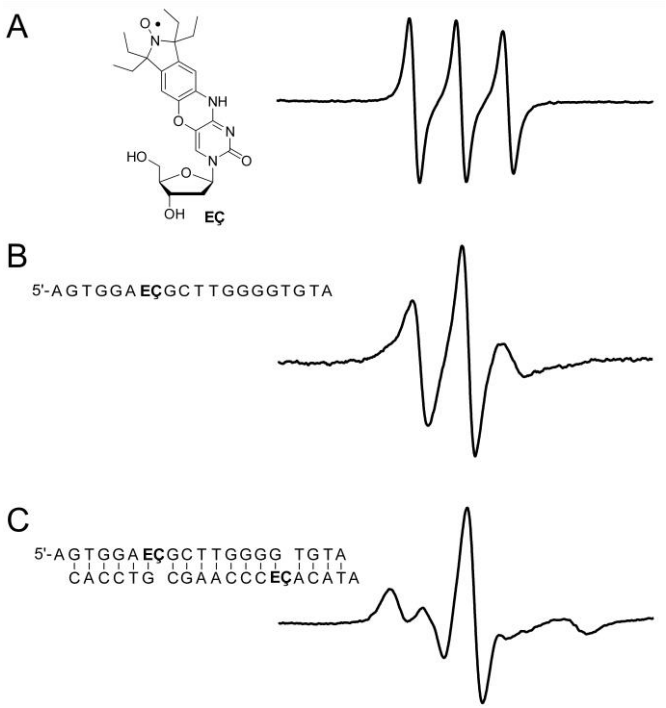

Figure 4. A. EPR spectum of **EÇ**. B. EPR spectrum of a **EÇ**-labeled 19-mer DNA single strand 5'-d(AGTGGA**EÇ**GCTTGGGGTGTA)-3'. C. EPR spectrum of a **EÇ**-labeled duplex 5'-d(AGTGGA**EÇ**GCTTGGGGTGTA)-3'·5'-d(ATACA**EÇ**CCCAAGCGTCCAC)-3'. EPR spectra were recorded at 20 °C in a phosphate buffer (2 nmol of DNA; 10 mM phosphate, 100 mM NaCl, 0.1 mM Na_2EDTA, pH 7.0).

Syntheses of spin-labeled RNA oligonucleotides

In a manner analogous to the synthesis of **EÇ**-modified DNA, phosphoramidite **12** was used to synthesize five 21-nucleotide long **EÇm**-labeled RNAs (**Table S1**). HPLC chromatograms of enzymatic digests of RNAs **XII**-**XVI** (**Figure S31A**-**E**) showed five peaks, one for each natural nucleoside and one for **EÇm**. An additional peak or two were observed in digests of five oligonucleotides, one corresponding to inosine (from partial enzymatic hydrolysis of A by an adenosine deaminase-contamination in phosphodiesterase I)[56] (**Figure S31B, C, D** and **E**) and the other corresponding to **EÇmf** (**Figure S31A, B** and **D**). The reduction of **EÇm** to **EÇmf** was determined from the chromatograms to be 30-49% and further confirmed by spin-counting using EPR spectroscopy (**Table S1**, **XII**, **XIII** and **XV**). The more extensive reduction of **EÇm** compared to reduction of **EÇ** during DNA synthesis can be explained by longer exposure of

the spin label to oligonucleotide reagents during RNA synthesis. Recent reports of protecting nitroxides prior to the oligonucleotide synthesis of RNA have shown to be effective to circumvent their reduction;[53, 57] we chose to employ benzoyl protection of the corresponding hydroxylamine of **EÇm**.[53]

Synthesis of Bz-EÇm and its corresponding phosphoramidite

The synthesis of **Bz-EÇm** (**Scheme 3**) began with reduction of the TBDMS-protected nitroxide **10** to yield the corresponding hydroxylamine, which was subsequently benzoylated to give **13**. Heating **10** at 60 °C for 24 h with 20 equivalents of ascorbic acid was required for reducing this structurally hindered nitroxide. Subsequent removal of the TBDMS groups of **13** gave **Bz-EÇm**. The benzoyl protecting-group was shown to be stable under all conditions used for oligonucleotide synthesis for more than a week (data not shown) and was efficiently removed in 2.5 h using conventional deprotecting conditions for RNA (1:1, 40% $MeNH_2$:40% NH_3 in H_2O), returning **EÇm** in quantitative yields. The 5'-hydroxyl group of **Bz-EÇm** (**Scheme 3**) was protected as 4,4'-dimethoxytrityl (DMT) ether and subsequently phosphitylated to give phosphoramidite **14** in good yields.

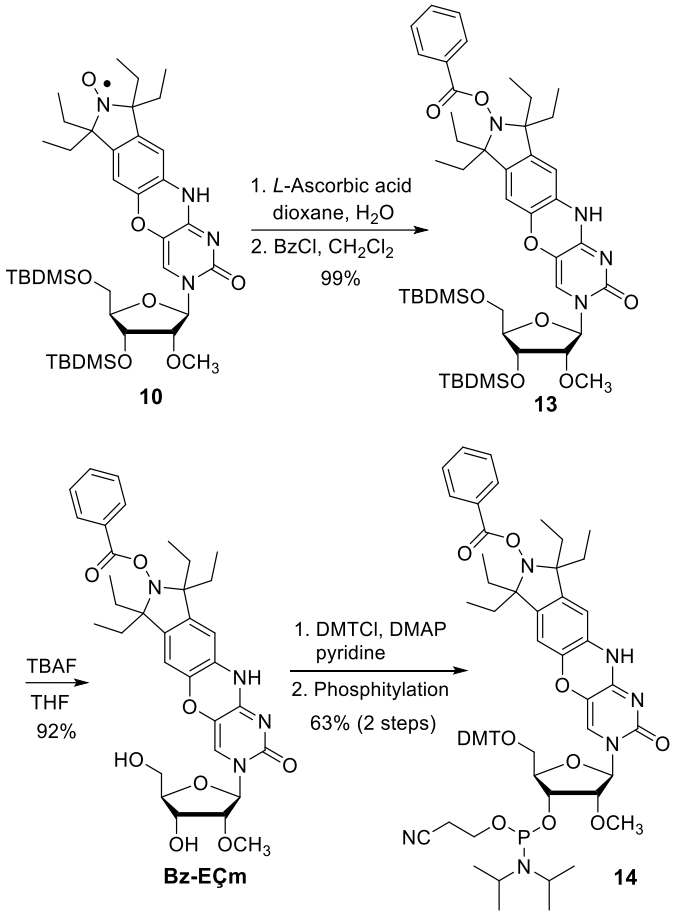

Scheme 3. Synthesis of **Bz-EÇm** and its corresponding phosphoramidite.

Syntheses of spin-labeled RNA oligonucleotides using phosphoramidite 14

Phosphoramidite **14** was used to repeat the synthesis of oligonucleotides **XII**, **XIII** and **XV** (**Table S1**). As before, the protected spin label coupled well during the solid-phase synthesis. Spin counting by EPR spectroscopy showed 96-99% spin labeling, indicating that little or no reduction of the spin label had occurred during the synthesis (**Table S1**, **XVII**, **XVIII** and **XIX**). This was further confirmed by HPLC analysis of the enzymatic digests of RNAs **XVII**, **XVIII** and **XIX** (**Figure S31F**, **G** and **H**), that showed complete absence of **EÇmf**. The HPLC analyses also showed that the benzoyl protecting group had been completely removed during the RNA deprotection. The stabilities of the spin-labeled duplexes **V**, **XIV** and the **Ç**-labeled DNA 5′-PHO-d(TGAGGTAGTAGGTTGTATA**Ç**T-3′ were tested in the presence of ascorbic acid, like before with the nucleosides. **Figure. 5** shows the EPR signal as a function of time. There was

a striking difference in the stability of the tetraethyl derived spin-labeled oligonucleotides as compared to spin labels: the **Ç**-labeled DNA was fully reduced within 20 min while the tetraethyl labeled DNA(**EÇ**) and RNA(**EÇm**) were almost completely intact after 12 h

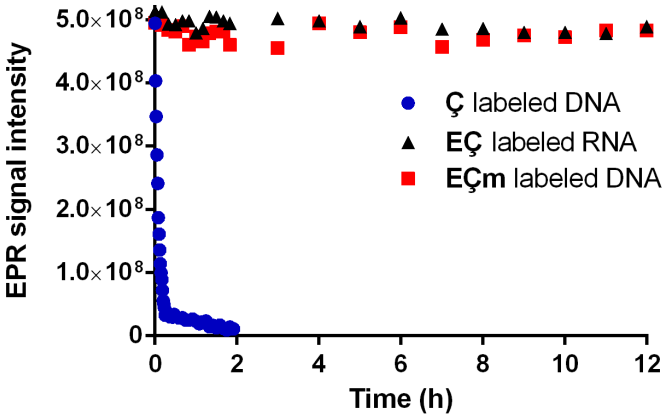

Figure 5. Stabilities of **EÇ**-labeled DNA single strand **V** (square), **EÇm**-labeled RNA single-strand **XIV** (triangle) and the **Ç**-labeled DNA 5′-PHO-d(TGAGGTAGTAGGTTGTATA**Ç**T-3′ (circle) towards reduction (5 mM ascorbic acid, 10 mM phosphate, 100 mM NaCl, 0.1 mM Na2EDTA, pH 7.0), PHO is a phosphate.

A model of **EÇm** within an A-form RNA duplex (**Figure 3B**) shows that the spin label fits tightly into the major groove of the duplex. CD spectra of the RNA duplexes (unmodified and modified) showed negative and positive molar ellipticities at ca. 210 nm and 263 nm, respectively, as expected for A-form RNA (**Figure S32**). Thermal denaturing experiments showed only minor destabilization of the duplexes by **EÇm,** with the ΔT_Ms ranging from -1.1 to -3.0 °C. Since each duplex contains two labels, the change in T_m caused by **EÇm** was less than -2.0 °C per modification, relative to the unmodified RNA, which is a similar result to that obtained with **Çm** modified RNA duplexes of similar length.[46] All these RNA duplexes have one strand in common (**Table S1**, **XVII**) which is complimentary to all the other strands (**Table S1**, **XVIII**, **XIV**, **XIX** and **XVI**). Thus, the only difference between the spin-labeled duplexes is the position of **EÇm** in the complementary strand. Therefore, the minor differences in the melting temperatures are likely due to flanking-sequence dependence, as has been observed with both phenoxazine-derived spin labels[46, 52] and fluorophores[58, 59] in DNA.

Conclusions

The tetraethyl-derived rigid spin labels **EÇ** and **EÇm** were synthesized and incorporated into DNA and RNA, respectively. The spin-labeled oligonucleotides were analyzed by UV-vis, CD and EPR spectroscopy as well as enzymatic digestion followed by HPLC analysis. Together this data verified incorporation of the spin labels and showed them to be non-perturbating of duplex structures. A minor reduction of the **EÇ** spin label was observed during the automated synthesis of **EÇ**-labeled DNA, but substantial reduction of **EÇm** took place during the synthesis of **EÇm**-labeled RNA. This reduction was circumvented by using a benzoyl protecting group for the hydroxylamine prepared from **EÇm**.[53] The new tetraethyl-derived rigid labels **EÇ** and **EÇm** showed dramatically increased resistance towards reduction by ascorbic acid, when compared to its tetramethyl derivatives **Ç**[45] and **Çm**,[46] which will enable the investigation of structure and dynamics of DNA and RNA by *in-cell* EPR spectroscopy.

Experimental section

General materials, instruments and methods. All commercially available reagents were purchased from Sigma-Aldrich co GMBH. or Acros Organics and used without further purification, except diisopropylammonium tetrazolide and 2-cyanoethyl *N*,*N*,*N'*,*N'*-tetraisopropylphosphorodiamidite, which were purchased from ChemGenes Corp., USA. All commercial phosphoramidites, CPG columns and solutions for oligonucleotide syntheses were also purchased from ChemGenes Corp., USA. 2'-Deoxyuridine and 2'-O-methyluridine were purchased from Rasayan Inc. USA. CH_2Cl_2, pyridine and CH_3CN were dried over calcium hydride and freshly distilled before use. All moisture- and air-sensitive reactions were carried out in oven-dried glassware under an inert atmosphere of Ar. Thin-layer chromatography (TLC) was performed using glass plates pre-coated with silica gel (0.25 mm, F-25, Silicycle) and compounds were visualized under UV light and by *p*-anisaldehyde staining. Column chromatography was performed using 230–400 mesh silica gel (Silicycle). ^{1}H-, ^{13}C- and ^{31}P-NMR spectra were recorded with a Bruker Avance 400 MHz spectrometer. Commercial grade $CDCl_3$ was passed over basic alumina shortly before dissolving tritylated nucleosides for NMR analysis. Chemical shifts are reported in parts per million (ppm) relative to the partially deuterated NMR solvents $CDCl_3$ (7.26 ppm for ^{1}H NMR and 77.16 ppm for ^{13}C), CD_3OD (3.35, 4.78 ppm for ^{1}H NMR and 49.3 ppm for ^{13}C), and DMSO-d_6 (2.49 ppm for ^{1}H NMR and 39.7 ppm for ^{13}C). ^{31}P-NMR chemical shifts are reported relative to 85% H_3PO_4 (at 0.0 ppm) as an external standard. All coupling constants are reported in Hertz (Hz). Nitroxide radicals show broadening and loss of NMR signals due to their paramagnetic nature and, therefore, those NMR spectra are not shown. Mass spectrometric analyses of all organic compounds were performed on an ESI-HRMS (Bruker, MicrOTOF-Q) in positive ion mode. DNA and RNA solid-phase oligonucleotide syntheses were performed on an automated ASM800 DNA/RNA synthesizer (BIOSSET Ltd., Russia) using phosphoramidite chemistry. Unmodified and spin-labeled oligonucleotides were synthesized using a trityl-off protocol and phosphoramidites with standard protecting groups on 1 μmol scale (1000 Å CPG columns). Oxidation was performed

with *tert*-butylhydroperoxide (1.0 M) in toluene. Capping and detritylation were performed using standard conditions for DNA and RNA synthesis. Concentrations of the oligonucleotides were determined by measuring UV absorbance at 260 nm using a Perkin Elmer Inc. Lambda 25 UV/Vis spectrometer and calculated by Beer′s law. Mass spectrometric analyses of **EÇ**- and **EÇm**-labeled oligonucleotides were performed on an ESI-HRMS (Bruker, MicrOTOF-Q) in negative ion mode. HPLC analysis of enzymatic digests were performed on a Beckman Coulter Gold HPLC system using Beckman Coulter Ultrasphere C18 4.6 x 250 mm analytical column with UV detection at 254 nm. Solvent gradients for analytical RP-HPLC were run at 1.0 mL/min using the following gradient program: solvent A, TEAA buffer (50 mM, pH 7.0); solvent B, CH_3CN; 0-4 min isocratic 4% B, 4-14 min linear gradient 4-20% B, 14-24 min linear gradient 20-50% B, 24-29 min linear gradient 50-80% B, 29-30 min isocratic 80%, 30-35 min linear gradient 80-4% B and 35-45 min isocratic 4% B. CD spectra of the duplexes were recorded in a Jasco J-810 spectropolarimeter. Cuvettes with 1 mm path length were used and the CD data were recorded from 350 nm to 200 nm at 25 °C. Prior to analysis by CD, thermal denaturation and EPR, an appropriate quantity of each DNA or RNA stock solutions was dried on a Thermo Scientific ISS 110 SpeedVac and dissolved in phosphate buffer (10 mM phosphate, 100 mM NaCl, 0.1 mM Na_2EDTA, pH 7.0). DNA and RNA duplexes were formed by annealing in an MJ Research PTC 200 Thermal Cycler using the following protocol: 90 °C for 2 min, 60 °C for 5 min, 50 °C for 5 min, 40 °C for 5 min and 22 °C for 15 min. CW-EPR spectra were recorded on a MiniScope MS200 spectrometer using 100 kHz modulation frequency, 1.0 G modulation amplitude, and 2.0 mW microwave power. The samples were placed in a quartz capillary (BLAUBRAND intraMARK) prior to EPR measurements.

1,1,3,3-Tetraethyl-6-nitroisoindolin-5-amine (2). To a solution of *N,N,N*-trimethylhydrazine iodide (1.83 g, 99.9 mmol) in DMSO (15 mL) was added *t*-BuOK (1.12 g, 99.9 mmol) and the solution stirred at 22 °C for 30 min. Compound **1** (1.00 g, 45.4 mmol) was added and the solution stirred further for 14 h. The reaction mixture was poured into ice-cold water (50 mL), followed by extraction with CH_2Cl_2 (3 x 50 mL), the combined organic phases dried over

Na_2SO_4, filtered and concentrated *in vacuo*. The crude product was purified by flash-column chromatography using a gradient elution (100:0 to 90:10, CH_2Cl_2:MeOH), to give compound **2** (0.750 g, 70%) as an orange solid. ^{1}H NMR (400 MHz, d_6-DMSO) δ = 7.62 (s, 1H), 7.29 (s, 2H), 6.73 (s, 1H), 1.56 (qdd, *J* = 13.8, 7.3, 4.2 Hz, 8H), 0.80 (q, *J* = 7.6 Hz, 12H) ppm. ^{13}C{^{1}H} NMR (101 MHz, d_6-DMSO) δ = 157.0, 146.0, 136.2, 130.0, 118.1, 111.5, 67.3, 66.5, 40.1, 39.9, 39.7, 39.5, 39.3, 39.0, 38.8, 33.3, 33.0, 8.8, 8.7, 8.6 ppm. HRMS (ESI-TOF) m/z: $[M + H]^+$ Calcd for $C_{16}H_{26}N_3O_2^+$: 292.2020; found 292.2017.

1,1,3,3-Tetraethyl-6-nitroisoindolin-5-ol (3). To a solution of potassium hydroxide (13.1 g, 0.234 mmol) in 10% H_2O/MeOH (80 mL) was added 1,1,3,3-tetraethyl-6-nitroisoindolin-5-amine (**2**) (2.75 g, 11.7 mmol) and the reaction mixture heated in a closed vial at 140 ºC for 24 h. The reaction mixture was poured onto ice and extracted with EtOAc (3 x 100 mL), the combined organic phases were dried over Na_2SO_4 and the solvent was removed *in vacuo*. The residue was purified by flash-column chromatography, using a gradient elution (100:0 to 90:10, CH_2Cl_2:MeOH), to give compound **3** (2.01 g, 72%) as a bright yellow solid. ^{1}H NMR (400 MHz, $CDCl_3$) δ = 10.69 (s, 1H), 7.77 (s, 1H), 6.82 (s, 1H), 1.76 – 1.59 (m, 8H), 0.89 (t, *J* = 7.5 Hz, 12H) ppm. ^{13}C{^{1}H} NMR (101 MHz, $CDCl_3$) δ = 155.1, 133.0, 118.5, 113.1, 33.62, 33.43, 29.7, 8.78, 8.73 ppm. HRMS (ESI-TOF) m/z: $[M + H]^+$ Calcd for $C_{16}H_{25}N_2O_3^+$: 293.1860; found 293.1878.

6-Amino-1,1,3,3-tetraethylisoindolin-5-ol (4). A solution of compound **3** (400 mg, 2.54 mmol) in MeOH (30 mL) containing 10% Pd/C (40.0 mg) was stirred in the dark under an atmosphere of H_2 (1 atm) for 2 h. The reaction mixture was filtered through a pad of celite and the filtrate was concentrated *in vacuo* to yield crude product **4** (348 mg), which was directly used for the next step without further purification. ^{1}H NMR (400 MHz, $CDCl_3$) δ =6.48 (s, 2H), 1.83 – 1.49 (m, 8H), 1.07 – 0.59 (m, 12H). HRMS (ESI-TOF) m/z: $[M + H]^+$ Calcd for $C_{16}H_{27}N_2O^+$: 263.2118; found 263.2111.

((2R,3S,5R)-3-acetoxy-5-(5-bromo-4-chloro-2-oxopyrimidin-1(2H)-yl)tetrahydrofuran-2-yl)methyl acetate (5). A solution of 5-Bromo-3',5'-diacetyl-2'-deoxyuridine (0.80 g, 2.05 mmol)

and PPh_3 (1.34 g, 5.13mmol), in a mixture of CH_2Cl_2 and CCl_4 (10 + 10 mL), was refluxed for 40 min. The solvent was removed in vacuo, and the residue was purified by silica gel flash column chromatography using a gradient elution (EtOAc/CH_2Cl_2; 5:95 to 15:85) to yield compound **5** as a white solid (0.63 g, 75% yield). ^{1}H NMR (400 MHz, $CDCl_3$) δ = 8.20 (s, 1H), 6.04 (t, *J* = 6.4 Hz, 1H), 5.12 (dt, *J* = 6.3, 2.9 Hz, 1H), 4.38 – 4.20 (m, 3H), 2.73 (ddd, *J* = 14.5, 6.0, 3.0 Hz, 1H), 2.14 (dt, *J* = 14.3, 6.7 Hz, 1H), 2.03 (s, 3H), 2.00 (s, 3H).^{13}C{^{1}H} NMR (101 MHz, $CDCl_3$) δ 170.2, 170.0, 165.5, 151.4, 144.0, 100.0, 97.1, 88.1, 83.5, 77.6, 77.3, 76.9, 73.4, 63.2, 60.3, 53.6, 38.9, 21.0, 20.8, 14.1. HRMS (ESI-TOF) m/z: [M + Na]$^+$ Calcd for $C_{13}H_{14}BrClN_2O_3Na^+$ 430.9616; Found 430.9628.

5-Bromo-3',5'-diacetyl-*N*-4-(2-hydroxytetraethylisoindolinyl)-2'-deoxycytidine (7). To a solution of compound **4** (262 mg, 0.706 mmol) and compound **5** (346 mg, 0.847 mmol) in $CHCl_3$ (10 mL) was added Et_3N (180 µL, 1.29 mmol) and the solution stirred at 22 °C for 16 h. The solvent was removed *in vacuo*, and the crude product was used in the next reaction without purification. ^{1}H NMR (400 MHz, $CDCl_3$) δ = 7.97 (s, 1H), 7.84 (s, 1H), 7.39 (s, 1H), 6.80 (s, 1H), 6.31 – 6.20 (m, 1H), 5.21 (dt, *J* = 5.9, 2.5 Hz, 1H), 4.38 (d, *J* = 3.3 Hz, 2H), 4.32 (d, *J* = 3.0 Hz, 1H), 2.71 (ddd, *J* = 14.2, 5.6, 2.4 Hz, 1H), 2.15 (s, 3H), 2.10 (s, 3H), 1.85 – 1.67 (m, 8H), 0.87 (q, *J* = 7.4 Hz, 13H). ^{13}C{^{1}H} NMR (101 MHz, $CDCl_3$) δ = 170.4, 170.2, 157.0, 153.4, 148.7, 140.4, 125.5, 116.1, 88.6, 86.9, 82.9, 77.2, 73.9, 63.7, 50.8, 39.0, 32.9, 32.7, 31.9, 29.7, 29.4, 22.7, 20.9, 20.9, 14.1, 8.8, 8.7 ppm. HRMS (ESI-TOF) m/z: [M + H]$^+$ Calcd for $C_{29}H_{40}BrN_4O_7^+$: 635.2075; found 635.2063.

7,7,9,9-tetraethyl-3-((2R,4S,5R)-4-hydroxy-5-(hydroxymethyl)tetrahydrofuran-2-yl)-7,8,9,11-tetrahydropyrimido[4',5':5,6][1,4]oxazino[2,3-f]isoindol-2(3H)-one (EÇf). To a solution of compound **7** (449 mg, 0.706 mmol) in abs. EtOH (50 mL) was added KF (1.0 g, 17.0 mmol) and the mixture was refluxed for 42 h. The reaction mixture was cooled to room temperature and the salts were filtered from the solution. The filtrate was concentrated *in vacuo* and the residue purified by flash-column chromatography, using a gradient elution (100:0 to 75:25, CH_2Cl_2:MeOH), to yield **EÇf** (187 mg, 56%) as a pale yellow solid. ^{1}H NMR (400 MHz,

CD_3OD) δ = 7.67 (s, 1H), 6.67 (s, 1H), 6.44 (s, 1H), 6.21 (t, *J* = 6.5 Hz, 1H), 4.37 (dt, *J* = 6.6, 3.7 Hz, 1H), 3.91 (q, *J* = 3.0 Hz, 1H), 3.86 – 3.65 (m, 2H), 2.31 (ddd, *J* = 13.3, 5.8, 3.6 Hz, 1H), 2.13 (dt, *J* = 13.4, 6.6 Hz, 1H), 1.61 (qd, *J* = 14.0, 11.6, 7.3 Hz, 8H), 0.81 (dd, *J* = 8.8, 4.8 Hz, 12H) ppm. $^{13}C\{^1H\}$ NMR (101 MHz, CD_3OD) δ = 156.4, 155.9, 144.2, 143.5, 143.3, 129.9, 127.0, 123.5, 112.0, 110.8, 89.1, 87.6, 72.2, 70.2, 70.1, 62.8, 42.0, 34.4, 34.3, 9.4, 9.3 ppm. HRMS (ESI-TOF) m/z: $[M + H]^+$ Calcd for $C_{25}H_{35}N_4O_5^+$: 471.2602; found 471.2603.

3-((2R,4S,5R)-4-((tert-butyldimethylsilyl)oxy)-5-(((tert-butyldimethylsilyl)oxy)methyl)tetrahydrofuran-2-yl)-7,7,9,9-tetraethyl-7,8,9,11-tetrahydropyrimido[4',5':5,6][1,4]oxazino[2,3-f]isoindol-2(3H)-one (TBDMS-EÇf). A solution of **EÇf** (2.30 g, 4.89 mmol), TBDMSCl (2.21 g, 14.7 mmol) and imidazole (0.992 g, 14.7 mmol) in a mixture of pyridine and DMF (1:1, 20 mL) was stirred at 22 °C for 24 h. The reaction mixture was poured onto ice and extracted with EtOAc (3 x 100 mL), the combined organic phases were dried over Na_2SO_4 and the solvent removed was *in vacuo*. The residue was purified by flash-column chromatography, using a gradient elution (100:0 to 90:10, CH_2Cl_2:MeOH), to yield **TBDMS-EÇf** (3.38 g, 99%) as a pale yellow solid. ^1H NMR (400 MHz, $CDCl_3$) δ = 7.45 (s, 2H), 6.33 (s, 1H), 6.25 (t, *J* = 6.1 Hz, 1H), 4.42 – 4.35 (m, 1H), 3.96 – 3.83 (m, 2H), 3.83 – 3.71 (m, 1H), 2.33 (ddd, *J* = 13.2, 6.2, 4.3 Hz, 1H), 2.08 – 1.95 (m, 2H), 1.67 (s, 8H), 0.96 (s, 9H), 0.89 (s, 21H), 0.15 (d, *J* = 8.4 Hz, 6H), 0.09 – 0.04 (m, 9H) ppm. $^{13}C\{^1H\}$ NMR (101 MHz, $CDCl_3$) δ = 154.7, 153.8, 128.1, 108.9, 87.7, 85.9, 77.4, 71.4, 62.7, 41.9, 33.7, 29.8, 26.2, 26.0, 25.9, 22.8, 18.6, 18.1, 8.9, 1.2, -4.5, -4.7, -5.3, -5.3 ppm. HRMS (ESI-TOF) m/z: $[M + H]^+$ Calcd for $C_{37}H_{63}N_4O_5Si_2^+$: 699.4332; found 699.4280.

3-((2R,4S,5R)-4-((tert-butyldimethylsilyl)oxy)-5-(((tert-butyldimethylsilyl)oxy)methyl)tetrahydrofuran-2-yl)-7,7,9,9-tetraethyl-8-oxyl-7,8,9,11-tetrahydropyrimido[4',5':5,6][1,4]oxazino[2,3-f]isoindol-2(3H)-one (9). To a solution of **TBDMS-EÇf** (400 mg, 0.572 mmol) in CH_2Cl_2 (10 mL) was added NaN_3 (198 mg, 1.14 mmol) and the solution stirred for 15 min at 22 °C. *m*-CPBA (74.9 mg, 1.14 mmol) was added and the solution stirred for 4 h. The reaction mixture was concentrated *in vacuo* and the crude product

purified by flash-column chromatography, using a gradient elution (100:0 to 83:17, CH_2Cl_2:MeOH), to yield **9** (339 mg, 83%) as a bright yellow solid. HRMS (ESI-TOF) m/z: [M + Na]$^+$ Calcd for $C_{37}H_{61}N_4O_6Si_2Na^{\bullet+}$: 736.4022; found 736.3997.

7,7,9,9-tetraethyl-8-oxidanyl-3-((2R,4S,5R)-4-hydroxy-5-(hydroxymethyl)tetrahydrofuran-2-yl)-7,8,9,11-tetrahydropyrimido[4',5':5,6][1,4]oxazino[2,3-f]isoindol-2(3H)-one (EÇ). To a solution of **9** (500 mg, 0.700 mmol) in anhydrous THF (3 mL) was added TBAF (2.03 mL, 7.00 mmol) and the solution stirred at 22 °C for 12 h. The solvent was removed *in vacuo* and the residue purified by flash-column chromatography, using a gradient elution (100:0 to 75:25, CH_2Cl_2:MeOH), to yield **EÇ** (310 mg, 91%) as a yellow solid. HRMS (ESI-TOF) m/z: [M + Na]$^+$ Calcd for $C_{25}H_{33}N_4O_6Na^{\bullet+}$: 508.2298; found 508.2292

3-((2R,4S,5R)-5-((bis(4-methoxyphenyl)(phenyl)methoxy)methyl)-4-hydroxytetrahydrofuran-2-yl)-7,7,9,9-tetraethyl-8-oxidanyl-7,8,9,11-tetrahydropyrimido[4',5':5,6][1,4]oxazino[2,3-f]isoindol-2(3H)-one (DMT-EÇ). Residual MeOH was co-evaporated with toluene (3 x 5 mL) from **EÇ** (477 mg, 0.982 mmol), followed by sequential addition of pyridine (10 mL), DMTrCl (433 mg, 1.28 mmol) and DMAP (27.0 mg, 0.197 mmol). The solution was stirred at 22°C for 6 h, MeOH (400 µL) was added and the solvent removed *in vacuo*. The residue was purified by flash-column chromatography, using a gradient elution (1:99:0 to 1:95.5:3.5, Et_3N:CH_2Cl_2:MeOH), to yield **DMT- EÇ** (735 mg, 95%) as a yellow solid. HRMS (ESI-TOF) m/z: [M + Na]$^+$ Calcd for $C_{46}H_{51}N_4O_8Na^{\bullet+}$: 810.3601; found 810.3599

(2R,3S,5R)-2-((bis(4-methoxyphenyl)(phenyl)methoxy)methyl)-5-(7,7,9,9-tetraethyl-8-oxidanyl-2-oxo-7,8,9,11-tetrahydropyrimido[4',5':5,6][1,4]oxazino[2,3-f]isoindol-3(2H)-yl)tetrahydrofuran-3-yl (2-cyanoethyl) diisopropylphosphoramidite (11). To a solution of **DMT- EÇ** (100 mg, 0.127 mmol) in CH_2Cl_2 (5 mL) were added diisopropylammonium tetrazolide (171 mg, 1.52 mmol) and 2-cyanoethyl *N*,*N*,*N'*,*N'*-tetraisopropylphosphorodiamidite (52 µL, 0.17 mmol). The resulting solution was stirred at 22 °C for 2 h. CH_2Cl_2 (50 mL) was

added and the organic phase washed sequentially with satd. aq. $NaHCO_3$ (3 × 50 mL) and brine (50 mL), dried over Na_2SO_4 and concentrated *in vacuo*. The residue was dissolved in a minimum amount of CH_2Cl_2 (few drops), followed by a slow addition of *n*-hexane (40-50 mL) at 22 °C. The solvent was decanted from the precipitate and discarded. This procedure was repeated four times to give **11** (100 mg, 80%) as a yellowish solid. ^{31}P NMR (162 MHz, $CDCl_3$): δ = 150.27, 149.35 ppm. HRMS (ESI-TOF) m/z: $[M + Na]^+$ Calcd for $C_{55}H_{68}N_6O_9Na^{\bullet+}$: 1010.4678; found 1010.4578,

5-Bromo-3',5'-diacetyl-*N*-4-(2-hydroxytetraethylisoindolinyl)-2'-methoxycytidine (8). To a solution of compound **4** (592 mg, 2.03 mmol) and **6** (1021 mg, 2.32 mmol) in $CHCl_3$ (10 mL) was added Et_3N (180 µL, 1.29 mmol) and the solution stirred at 22 °C for 16 h. The solvent was removed *in vacuo*, and the crude product was used in the next reaction without purification. ^1H NMR (400 MHz, $CDCl_3$) δ = 8.30 (s, 1H), 7.98 (s, 1H), 7.82 (s, 1H), 7.57 (s, 1H), 6.91 (s, 1H), 5.90 – 5.79 (m, 1H), 4.73 (dd, *J* = 9.3, 5.0 Hz, 1H), 4.47 – 4.29 (m, 3H), 4.05 – 3.97 (m, 1H), 3.51 (s, 1H), 2.17 (s, 3H), 2.14 (s, 3H), 1.80 – 1.50 (m, 8H), 0.84 (dtd, *J* = 10.3, 7.4, 3.8 Hz, 12H).$^{13}C\{^1H\}$ NMR (101 MHz, $CDCl_3$) δ = 170.2, 170.1, 170.04, 169.97, 166.0, 157.6, 153.5, 153.1, 146.1, 145.6, 143.9, 142.5, 140.3, 127.5, 119.1, 116.3, 100.0, 89.8, 89.5, 88.4, 87.5, 81.7, 81.7, 78.8, 78.4, 77.5, 77.4, 77.2, 76.9, 68.9, 68.7, 68.6, 68.4, 61.4, 61.1, 59.0, 58.9, 53.5, 33.7, 33.5, 29.6, 21.09, 21.07, 20.51, 20.49, 8.9. HRMS (ESI-TOF) m/z: $[M + H]^+$ Calcd for $C_{30}H_{42}BrN_4O_8^+$: 665.2181; found 665.2165.

7,7,9,9-tetraethyl-3-((2R,3R,4R,5R)-4-hydroxy-5-(hydroxymethyl)-3-methoxytetrahydrofuran-2-yl)-7,8,9,11-tetrahydropyrimido[4',5':5,6][1,4]oxazino[2,3-f]isoindol-2(3H)-one (EÇmf). To a solution of compound **8** (1.35 g, 2.03 mmol) in abs. EtOH (200 mL) was added KF (1.18 g, 20.2 mmol) and the mixture was refluxed for 42 h. The mixture was cooled to room temperature and the salts were removed by filtration. The filtrate was concentrated *in vacuo* and the residue purified by flash-column chromatography, using a gradient elution (100:0 to 75:25, CH_2Cl_2:MeOH), to yield **EÇmf** (567 mg, 60%) as a pale yellow solid. ^1H NMR (400 MHz, CD_3OD) δ = 7.91 (s, 1H), 6.82 – 6.74 (m, 1H), 6.72 (s, 1H), 5.88 (d,

J = 2.6 Hz, 1H), 4.23 (dd, *J* = 7.1, 5.1 Hz, 1H), 4.02 – 3.87 (m, 2H), 3.85 – 3.73 (m, 2H), 3.57 (s, 3H), 2.02 – 1.96 (m, 8H), 1.00 (td, *J* = 7.3, 4.7 Hz, 12H) ppm. $^{13}C\{^{1}H\}$ NMR (101 MHz, CD_3OD) δ 156.1, 155.7, 144.9, 138.7, 138.0, 129.6, 129.3, 123.9, 112.4, 111.6, 89.7, 85.6, 85.5, 75.4, 69.4, 61.2, 59.0, 49.7, 49.6, 49.5, 49.4, 49.3, 49.2, 49.1, 48.9, 48.7, 48.5, 48.0, 31.9, 9.3, 8.78, 8.77 ppm. HRMS (ESI-TOF) m/z: $[M + H]^+$ Calcd for $C_{26}H_{37}N_4O_6^+$: 501.2708; found 501.2706.

3-((2R,3R,4R,5R)-4-((tert-butyldimethylsilyl)oxy)-5-(((tert-butyldimethylsilyl)oxy)methyl)-3-methoxytetrahydrofuran-2-yl)-7,7,9,9-tetraethyl-7,8,9,11-tetrahydropyrimido[4',5':5,6][1,4]oxazino[2,3-f]isoindol-2(3H)-one (TBDMS-EÇmf). A solution of **EÇmf** (416 mg, 0.832 mmol), TBDMSCl (376 mg, 2.50 mmol) and imidazole (170 mg, 2.50 mmol) in a mixture of pyridine and DMF (1:1, 10 mL) was stirred at 22 °C for 24 h. The reaction mixture was poured onto ice and extracted with EtOAc (3 x 100 mL), the combined organic phases were dried over Na_2SO_4 and the solvent was removed *in vacuo*. The residue was purified by flash-column chromatography, using a gradient elution (100:0 to 90:10, CH_2Cl_2:MeOH), to yield **TBDMS-EÇmf** (600 mg, 99%) as a pale yellow solid. HRMS (ESI-TOF) m/z: $[M + H]^+$ Calcd for $C_{38}H_{65}N_4O_6Si_2^+$: 729.4437 $[M+H]^+$; found 729.4436.

3-((2R,3R,4R,5R)-4-((tert-butyldimethylsilyl)oxy)-5-(((tert-butyldimethylsilyl)oxy)methyl)-3-methoxytetrahydrofuran-2-yl)-7,7,9,9-tetraethyl-8-oxyl-7,8,9,11-tetrahydropyrimido[4',5':5,6][1,4]oxazino[2,3-f]isoindol-2(3H)-one (10). To a solution of **TBDMS-EÇmf** (153 mg, 0.249 mmol) in CH_2Cl_2 (10 mL) was added NaN_3 (65 mg, 1.0 mmol) and the solution stirred at 22 °C for 15 min. *m*-CPBA (86 mg, 0.5 mmol) was added, the solution stirred for 30 h, the solvent removed *in vacuo* and the crude product purified by flash-column chromatography, using a gradient elution (100:0 to 83:17, CH_2Cl_2:MeOH), to yield **10** (150 mg, 81%) as a bright yellow solid. HRMS (ESI-TOF) m/z: $[M + Na]^+$ Calcd for $C_{38}H_{63}N_4O_7Si_2Na^{\bullet+}$: 766.4127; found 766.4069.

7,7,9,9-tetraethyl-8-oxyl-3-((2R,3R,4R,5R)-4-hydroxy-5-(hydroxymethyl)-3-methoxytetrahydrofuran-2-yl)-7,8,9,11-tetrahydropyrimido[4',5':5,6][1,4]oxazino[2,3-

f]isoindol-2(3H)-one (EÇm). To a solution of **EÇm** (377 mg, 0.507 mmol) in THF (3 mL) was added TBAF (1.50 ml, 5.07 mmol) and the reaction mixture was stirred at 22 °C for 12 h. The solvent was removed *in vacuo* and the residue purified by flash-column chromatography, using a gradient elution (100:0 to 90:10, CH_2Cl_2:MeOH), to yield **EÇm** (249 mg, 94%) as a yellow solid. HRMS (ESI-TOF) m/z: $[M + Na]^+$ Calcd for $C_{26}H_{35}N_4O_7Na^{\bullet+}$: 538.2403; found 538.2399.

3-((2R,3R,4R,5R)-5-((bis(4-methoxyphenyl)(phenyl)methoxy)methyl)-4-hydroxy-3-methoxytetrahydrofuran-2-yl)-7,7,9,9-tetraethyl-8-oxidanyl-7,8,9,11-tetrahydropyrimido[4',5':5,6][1,4]oxazino[2,3-f]isoindol-2(3H)-one (EÇm-DMT). Residual MeOH was co-evaporated with toluene (3 x 5 mL) from **EÇm** (400 mg, 0.776 mmol), followed by sequential addition of pyridine (4 mL), DMTCl (315 mg, 0.930 mmol) and DMAP (18.6 mg, 0.155 mmol). The solution was stirred at 22°C for 14 h, MeOH (400 µL) was added and the solvent removed *in vacuo*. The residue was purified by flash-column chromatography, using a gradient elution (99:1:0 to 98:1:1, CH_2Cl_2:Et_3N:MeOH), to yield **EÇm-DMT** (514 mg, 81%) as a yellow solid. HRMS (ESI-TOF) m/z: $[M + Na]^+$ Calcd for $C_{47}H_{53}N_4O_9Na^{\bullet+}$: 840.3705; found 840.3646.

(2R,3R,4R,5R)-2-((bis(4-methoxyphenyl)(phenyl)methoxy)methyl)-4-methoxy-5-(7,7,9,9-tetraethyl-8-oxidanyl-2-oxo-7,8,9,11-tetrahydropyrimido[4',5':5,6][1,4]oxazino[2,3-f]isoindol-3(2H)-yl)tetrahydrofuran-3-yl (2-cyanoethyl) diisopropylphosphoramidite (12). A solution of **EÇm-DMT** (225 mg, 0.275 mmol) in CH_2Cl_2 (1 mL) was treated with diisopropylammonium tetrazolide (70.6 mg, 0.413 mmol) and 2-cyanoethyl *N,N,N´,N´*-tetraisopropylphosphorodiamidite (262 µL, 0.825 mmol). The solution was stirred at 22 °C for 18 h. CH_2Cl_2 (25 mL) was added and the organic phase washed sequentially with satd. aq. $NaHCO_3$ (3 × 30 mL) and brine (50 mL), dried with Na_2SO_4 and concentrated *in vacuo*. The residue was dissolved in a minimum amount of CH_2Cl_2 (few drops), followed by a slow addition of *n*-hexane (40-50 mL) at 22 °C. The solvent was decanted from the precipitate and discarded. This procedure was repeated six times to yield **12** (199 mg, 71%) as a yellow solid. ^{31}P NMR (162 MHz, $CDCl_3$): δ = 151.03, 150.16 ppm.

3-((2R,3R,4R,5R)-4-((tert-butyldimethylsilyl)oxy)-5-(((tert-butyldimethylsilyl)oxy)methyl)-3-methoxytetrahydrofuran-2-yl)-7,7,9,9-tetraethyl-2-oxo-2,7,9,11-tetrahydropyrimido[4',5':5,6][1,4]oxazino[2,3-f]isoindol-8(3H)-yl benzoate (13). To a solution of **10** (227 mg, 0.305 mmol) in 1,4-dioxane (30 mL) was added *L*-ascorbic acid (537 mg, 3.05 mmol) in H_2O (5 mL). The solution was stirred at 60 °C for 24 h, after which CH_2Cl_2 (30 mL) and H_2O (30 mL) were added and the mixture stirred vigorously for 2 min. The organic phase was filtered through a short column of Na_2SO_4 into a solution of BzCl (198 µL, 1.53 mmol) and Et_3N (220 µL, 1.53 mmol) in CH_2Cl_2 (10 mL). The solution was stirred at 22 °C for 2 h, washed with satd. aq. $NaHCO_3$ (3 x 100 mL), the organic phase dried over Na_2SO_4 and concentrated *in vacuo*. The residue purified by flash-column chromatography, using a gradient elution (100:0 to 90:10, CH_2Cl_2:MeOH), to yield **13** (259 mg, quant.) as a yellow solid. ^{1}H NMR (400 MHz, $CDCl_3$) δ = 8.18 – 8.12 (m, 1H), 8.12 – 8.05 (m, 2H), 7.84 (s, 1H), 7.62 – 7.53 (m, 2H), 7.53 – 7.42 (m, 3H), 6.39 (s, 1H), 5.88 (d, *J* = 9.6 Hz, 1H), 4.29 – 4.20 (m, 1H), 4.13 (dd, *J* = 12.1, 2.0 Hz, 1H), 4.05 (d, *J* = 8.9 Hz, 1H), 3.82 (dd, *J* = 11.9, 1.6 Hz, 1H), 3.65 (s, 4H), 2.23 – 1.56 (m, 8H), 0.96 (d, *J* = 39.9 Hz, 30H), 0.21 (d, *J* = 7.0 Hz, 6H), 0.10 (d, *J* = 5.2 Hz, 6H) ppm. ^{13}C{^{1}H} NMR (101 MHz, $CDCl_3$) δ = 165.9, 155.3, 153.4, 142.0, 137.7, 137.4, 133.3, 133.0, 130.2, 129.6, 128.5, 128.3, 127.6, 125.6, 122.0, 113.3, 110.1, 87.9, 84.1, 83.1, 74.4, 74.2, 68.0, 60.5, 57.9, 30.2, 29.2, 26.3, 25.8, 18.7, 18.1, 9.5, 8.7, -4.5, -4.9, -5.2, -5.4 ppm. HRMS (ESI-TOF) m/z: $[M + Na]^+$ Calcd for $C_{45}H_{68}N_4O_8Si_2Na^+$: 871.4473; found 871.4468

7,7,9,9-tetraethyl-3-((2R,3R,4R,5R)-4-hydroxy-5-(hydroxymethyl)-3-methoxytetrahydrofuran-2-yl)-2-oxo-2,7,9,11-tetrahydropyrimido[4',5':5,6][1,4]oxazino[2,3-f]isoindol-8(3H)-yl benzoate (Bz-EÇm). To a solution of compound **13** (250 mg, 0.294 mmol) in THF (10 mL) was added TBAF (0.863 mL, 2.95 mmol, 1.0 M in THF) and the reaction was stirred at 22 °C for 12 h. The solvent was removed *in vacuo* and the residue purified by flash-column chromatography, using a gradient elution (100:0 to 90:10, CH_2Cl_2:MeOH), to yield **Bz-EÇm** (168 mg, 92%) as a yellow solid. ^{1}H NMR (400 MHz, $CDCl_3$) δ = 8.33 – 8.25 (m, 3H), 7.91 – 7.84 (m, 1H), 7.75 (t, *J* = 7.7 Hz, 2H),

6.83 (d, *J* = 19.3 Hz, 2H), 6.18 (d, *J* = 2.3 Hz, 1H), 4.51 (dd, *J* = 7.2, 5.0 Hz, 1H), 4.34 – 4.18 (m, 2H), 4.07 (dd, *J* = 12.3, 2.3 Hz, 2H), 3.86 (s, 3H), 2.42 – 1.82 (m, 9H), 1.31 – 1.00 (m, 14H) ppm. $^{13}C\{^{1}H\}$ NMR (101 MHz, $CDCl_3$) δ = 166.1, 153.2, 141.9, 138.6, 137.0, 133.0, 129.1, 128.8, 128.3, 128.1, 124.2, 123.0, 111.6, 110.8, 88.1, 84.1, 83.8, 77.4, 74.0, 73.9, 67.5, 59.5, 57.8, 48.7, 48.5, 48.3, 48.1, 47.9, 47.7, 47.5, 29.9, 29.2, 28.7, 8.7, 7.9 ppm. HRMS (ESI-TOF) m/z: $[M + Na]^+$ Calcd for $C_{33}H_{40}N_4O_8Na^+$: 643.2738; found 643.2746

3-((2R,3R,4R,5R)-5-((bis(4-methoxyphenyl)(phenyl)methoxy)methyl)-4-hydroxy-3-methoxytetrahydrofuran-2-yl)-7,7,9,9-tetraethyl-2-oxo-2,7,9,11-tetrahydropyrimido[4',5':5,6][1,4]oxazino[2,3-f]isoindol-8(3H)-yl benzoate (Bz-EÇm-DMT). Residual MeOH was co-evaporated with toluene (3 x 5 mL) from **Bz-EÇm** (118 mg, 0.192 mmol), followed by sequential addition of pyridine (4 mL), DMTCl (192 mg, 0.572 mmol) and DMAP (12.0 mg, 0.0952 mmol). The solution was stirred at 22°C for 14 h, MeOH (400 µL) was added and the solvent removed *in vacuo*. The residue was purified by flash-column chromatography, using a gradient elution (99:1:0 to 98:1:1, CH_2Cl_2:Et_3N:MeOH), to yield **Bz-EÇm-DMT** (151 mg, 86%) as a yellow solid. ^{1}H NMR (400 MHz, $CDCl_3$) δ = 8.02 – 7.96 (m, 2H), 7.57 – 7.46 (m, 2H), 7.46 – 7.35 (m, 5H), 7.35 – 7.27 (m, 5H), 7.27 – 7.16 (m, 3H), 7.10 (t, *J* = 7.3 Hz, 2H), 6.82 – 6.73 (m, 5H), 6.08 (d, *J* = 18.3 Hz, 1H), 5.82 (s, 1H), 4.35 (s, 1H), 4.01 – 3.88 (m, 1H), 3.76 (d, *J* = 5.3 Hz, 1H), 3.67 (s, 7H), 3.62 (s, 3H), 3.45 (s, 3H), 1.98 – 1.58 (m, 9H), 0.95 – 0.78 (m, 13H) ppm. $^{13}C\{^{1}H\}$ NMR (101 MHz, $CDCl_3$) δ = 166.0, 158.6, 158.5, 155.2, 153.8, 145.1, 141.7, 137.2, 135.3, 133.0, 130.4, 130.1, 129.6, 129.5, 128.5, 127.95, 127.92, 126.7, 125.3, 121.4, 113.3, 113.2, 110.3, 87.8, 86.7, 83.8, 82.7, 74.3, 74.2, 68.5, 58.4, 55.2, 46.0, 30.2, 29.7, 29.2, 9.4, 9.1, 8.7 ppm. HRMS (ESI-TOF) m/z: $[M + Na]^+$ Calcd for $C_{54}H_{58}N_4O_{10}Na^+$: 945.4045; found 945.4012

3-((2R,3R,4R,5R)-5-((bis(4-methoxyphenyl)(phenyl)methoxy)methyl)-4-(((2-cyanoethoxy)(diisopropylamino)phosphaneyl)oxy)-3-methoxytetrahydrofuran-2-yl)-7,7,9,9-tetraethyl-2-oxo-2,7,9,11-tetrahydropyrimido[4',5':5,6][1,4]oxazino[2,3-f]isoindol-8(3H)-yl benzoate (14). A solution of **Bz-EÇm-DMT** (150 mg, 0.163 mmol) in

CH_2Cl_2 (3 mL) was treated with diisopropylammonium tetrazolide (41.8 mg, 0.244 mmol) and 2-cyanoethyl *N,N,N´,N´*-tetraisopropylphosphorodiamidite (155 µL, 0.488 mmol). The solution was stirred at 22 °C for 18 h. CH_2Cl_2 (25 mL) was added and the organic phase washed sequentially with satd. aq. $NaHCO_3$ (3 × 30 mL) and brine (50 mL), dried over Na_2SO_4 and concentrated *in vacuo*. The residue was dissolved in a minimum amount of CH_2Cl_2 (few drops), followed by a slow addition of *n*-hexane (40-50 mL) at 22 °C. The solvent was decanted from the precipitate and discarded. This procedure was repeated six times to yield **14** (130 mg, 71%) as a yellow solid. ^{1}H NMR (400 MHz, $CDCl_3$) δ = 8.12 – 8.03 (m, 4H), 7.68 (d, *J* = 19.9 Hz, 2H), 7.62 – 7.54 (m, 3H), 7.54 – 7.44 (m, 9H), 7.44 – 7.34 (m, 9H), 7.30 (td, *J* = 7.8, 2.4 Hz, 5H), 7.20 (t, *J* = 7.3 Hz, 2H), 6.86 (dtd, *J* = 8.8, 6.7, 6.2, 3.4 Hz, 8H), 6.23 – 5.87 (m, 4H), 4.57 (d, *J* = 15.0 Hz, 1H), 4.34 (d, *J* = 12.8 Hz, 1H), 4.24 (d, *J* = 7.8 Hz, 2H), 3.90 (ddd, *J* = 19.9, 10.0, 5.4 Hz, 3H), 3.81 (d, *J* = 2.2 Hz, 1H), 3.77 (d, *J* = 2.3 Hz, 12H), 3.63 (d, *J* = 2.6 Hz, 8H), 3.61 – 3.53 (m, 5H), 3.52 – 3.41 (m, 4H), 2.63 (t, *J* = 6.1 Hz, 2H), 2.42 (t, *J* = 6.4 Hz, 2H), 2.16 – 1.50 (m, 23H), 1.17 (dd, *J* = 15.1, 6.8 Hz, 19H), 1.04 (d, *J* = 6.7 Hz, 7H) ppm. ^{13}C{^{1}H} NMR (101 MHz, $CDCl_3$) δ = 158.7, 158.6, 133.0, 130.5, 130.3, 129.6, 128.5, 128.1, 127.9, 113.2, 110.3, 77.2, 74.3, 74.2, 58.0, 55.3, 55.2, 43.4, 43.2, 31.6, 24.7, 24.7, 24.6, 24.5, 22.7, 20.3, 14.1, 9.4, 8.7 ppm. ^{31}P NMR (162 MHz, $CDCl_3$) δ = 150.84, 150.02. HRMS (ESI-TOF) m/z: $[M + Na]^+$ Calcd for $C_{63}H_{75}N_6O_{11}PNa^+$: 1145.5129; found 1145.5098.

DNA and RNA synthesis and purification. Unmodified phosphoramidites (2'-deoxy for DNA and 2'O-TBDMS protected for RNA) were dissolved in CH_3CN (0.1 M) and phosphoramidites **11**, **12** and **14** were dissolved in 1,2-dichloroethane (0.1 M). 5-Ethylthiotetrazole (0.25 M in CH_3CN) was used as a coupling agent for DNA and 5-benzylthiotetrazole (0.25 M in CH_3CN) for RNA. The coupling time was set to 1.5 min for unmodified phosphoramidites of DNA, 5 min for the **EÇ**-modified phosphoramidite **11** and 7 min for both unmodified phosphoramidites of RNA and **EÇm**-modified phosphoramidites **12** and **14**. After completion of the DNA synthesis, the DNAs were cleaved from the resin and deprotected in a sat. aq. NH_3 solution at 55 °C for 8 h, after which the solvent was removed *in vacuo*. After completion of the RNA synthesis, the

RNAs synthesized using phosphoramidite **12** were deprotected and cleaved from the resin in a 1:1 solution (2 mL) of CH_3NH_2 (8 M in EtOH) and NH_3 (33% w/w in H_2O) at 65 °C for 1 h, while the oligonucleotides synthesized using phosphoramidite **14** were deprotected and cleaved from the resin in a 1:1 solution (2 mL) of CH_3NH_2 (40% in H_2O) and NH_3 (40% w/w in H_2O) at 65 °C for 2.5 h. The solvent was removed *in vacuo* and the 2'O-TBDMS groups were removed by incubation in a solution of $Et_3N{\cdot}3HF$ (300 µL) in DMF (100 µL) at 55 °C for 1.5 h, followed by addition of deionized and sterilized water (100 µL). This solution was transferred to a 50 mL Falcon tube, *n*-butanol (20 mL) was added and the mixture stored at −20 °C for 14 h, centrifuged at 4°C and the solvent decanted from the RNA pellet.

All oligonucleotides were subsequently purified by 20% DPAGE and extracted from the gel slices using the "crush and soak method" with Tris buffer (250 mM NaCl, 10 mM Tris, 1 mM Na_2EDTA, pH 7.5). The solutions were filtered through GD/X syringe filters (0.45 µm, 25 mm diameter, Whatman, USA) and subsequently desalted using Sep-Pak cartridges (Waters, USA), following the instructions provided by the manufacturer. Dried oligonucleotides were dissolved in deionized and sterilized water (200 µL for each oligonucleotide).

Enzymatic digestion of DNA and RNA and HPLC analysis. To the oligonucleotide (4 nmol) in sterile water (8 µL) was added calf intestinal alkaline phosphatase (1 µL, 2 U), snake venom phosphodiesterase I (4 µL, 0.2 U), nuclease P1 from penicillium citrinum (5 µL, 1.5 U) and Tris buffer (2 µL, 0.5 M Tris and 0.1 M $MgCl_2$). The samples were incubated at 37 °C for 50 h, after which they were analyzed by HPLC chromatography (**Figure S30** and **Figure S31**).

CD measurements. To determine if **EÇ** and **EÇm** labels had any effect on the DNA and RNA duplex conformation, circular dichroism (CD) spectra of all unmodified duplexes and their spin-labeled counterparts were recorded. DNA and RNA duplexes were prepared by dissolving complimentary single-stranded oligonucleotides (2.5 nmol) of each in a phosphate buffer (100 µL; 10 mM phosphate, 100 mM NaCl, 0.1 mM Na_2EDTA, pH 7.0) and annealed. The annealed samples were diluted to 200 µL with the same buffer (**Figure S32**).

Thermal denaturing experiments. To determine if **EÇ** or **EÇm** affected the stability of the DNA or RNA duplexes, the thermal denaturation curves of unmodified and spin-labeled oligomers were determined. Both DNA and RNA samples were prepared by dissolving 4.0 nmol of each strand in a phosphate buffer (100 µL; 10 mM phosphate, 100 mM NaCl, 0.1 mM Na_2EDTA, pH 7.0), annealed, diluted to 1.0 mL with the phosphate buffer (pH 7.0) and degassed with Ar. The samples were heated up from 22 °C to 90 °C (1.0 °C/min) and the absorbance at 260 nm was recorded at 1.0 °C intervals (**Table 1**, **Figure S33**).

CW-EPR measurements and spin counting. Samples of spin-labeled oligonucleotides for EPR measurements were prepared by dissolving spin-labeled, single stranded DNA or RNA (2.0 nmol) in phosphate buffer (10 µL; 10 mM phosphate, 100 mM NaCl, 0.1 mM Na_2EDTA, pH 7.0, oligonucleotide final conc. 200 µM) (**Figure S34**). The amount of spin labels in each oligonucleotide was determined by spin counting. A stock solution of 4-hydroxy-TEMPO (1.0 M) was prepared in phosphate buffer (10 mM phosphate, 100 mM NaCl, 0.1 mM Na_2EDTA, pH 7.0). The stock solution was diluted into samples of different concentrations (0-0.5 mM) and each sample was measured by EPR spectroscopy. The area under the peaks of each spectrum, obtained by double integration, was plotted against its concentration to yield a standard curve, used to determine the spin-labeling efficiency with an error margin of 5-10% (**Table S1**).

Supporting information availability statement

The Supporting Information is available free of charge on the ACS Publications website at https:// pubs.acs.org.

Table with spin-labeled oligonucleotides and their analysis by MS and EPR spectroscopy, ^{1}H-, ^{13}C- and ^{31}P-NMR spectra, stability of **EÇ** and **EÇm** in ascorbic acid, HPLC analyses of enzymatic digestions, CD spectra of oligonucleotide duplexes, thermal denaturing experiments of spin-labeled oligonucleotides and CW-EPR spectra of spin labeled oligonucleotides.

Acknowledgements

The authors acknowledge financial support by the Icelandic Research Fund (173727-051). The authors thank Dr S. Jonsdottir for assistance with collecting analytical data for structural characterization of new compounds and members of the Sigurdsson research group for helpful discussions.

References

1. Blackburn, G. M.; Egli, M.; Gait, M. J.; Loakes, D.; Williams, D. M.; Flavell, A.; Allen, S.; Fisher, J., *Nucleic acids in chemistry and biology*. RSC Pub.: 2006.
2. Alberts, B.; Wilson, J. H.; Johnson, A.; Hunt, T.; Lewis, J.; Roberts, K.; Raff, M.; Walter, P., *Molecular biology of the cell*. Garland Science: 2008.
3. Steitz, T. A., A structural understanding of the dynamic ribosome machine. *Nat. Rev. Mol. Cell Biol.* **2008,** *9* (3), 242-253.
4. Fedor, M. J.; Williamson, J. R., The catalytic diversity of RNAs. *Nat. Rev. Mol. Cell Biol.* **2005,** *6* (5), 399-412.
5. Kumar, A., Garg, S. and Garg, N., Regulation of gene expression. In *Rev. Cell Biol. Mol. Med.*, R. A. Meyers (Ed.). 2014; pp 1-59.
6. Meister, G.; Tuschl, T., Mechanisms of gene silencing by double-stranded RNA. *Nature* **2004,** *431* (7006), 343-349.
7. Uludag, H.; Ubeda, A.; Ansari, A., At the intersection of biomaterials and gene therapy: Progress in non-viral delivery of nucleic acids. *Front Bioeng Biotechnol* **2019,** *7* (131).
8. Shi, Y., A glimpse of structural biology through X-ray crystallography. *Cell* **2014,** *159* (5), 995-1014.
9. Sugiki, T.; Kobayashi, N.; Fujiwara, T., Modern technologies of solution nuclear magnetic resonance spectroscopy for three-dimensional structure determination of proteins open avenues for life scientists. *Comput. Struct. Biotechnol. J.* **2017,** *15*, 328-339.
10. Dračínský, M.; Hodgkinson, P., Solid-state NMR studies of nucleic acid components. *RSC Adv.* **2015,** *5* (16), 12300-12310.
11. Sasmal, D. K.; Pulido, L. E.; Kasal, S.; Huang, J., Single-molecule fluorescence resonance energy transfer in molecular biology. *Nanoscale* **2016,** *8* (48), 19928-19944.
12. Dimura, M.; Peulen, T. O.; Hanke, C. A.; Prakash, A.; Gohlke, H.; Seidel, C. A. M., Quantitative FRET studies and integrative modeling unravel the structure and dynamics of biomolecular systems. *Curr. Opin. Chem. Biol.* **2016,** *40*, 163-185.
13. Jeschke, G., The contribution of modern EPR to structural biology. *Emerg. Top. Life. Sci.* **2018,** *2* (1), 9-18.
14. Gränz, M.; Erlenbach, N.; Spindler, P.; Gophane, D. B.; Stelzl, L. S.; Sigurdsson, S. T.; Prisner, T. F., Dynamics of nucleic acids at room temperature revealed by pulsed EPR spectroscopy. *Angew. Chem. Int. Ed.* **2018,** *57* (33), 10540-10543.
15. Timmel, C. R.; Harmer, J. R., *Structural information from spin-labels and intrinsic paramagnetic centres in the biosciences*. Springer Berlin Heidelberg: 2014.
16. Haugland, M. M.; Lovett, J. E.; Anderson, E. A., Advances in the synthesis of nitroxide radicals for use in biomolecule spin labelling. *Chem. Soc. Rev.* **2018,** *47* (3), 668-680.
17. Giassa, I.-C.; Rynes, J.; Fessl, T.; Foldynova-Trantirkova, S.; Trantirek, L., Advances in the cellular structural biology of nucleic acids. *FEBS Lett.* **2018,** *592* (12), 1997-2011.
18. Bonucci, A.; Ouari, O.; Guigliarelli, B.; Belle, V.; Mileo, E., In-cell EPR: Progress towards structural studies inside cells. *ChemBioChem* **2019**, doi:10.1002/cbic.201900291.
19. Luchinat, E.; Banci, L., In-cell NMR: A topical review. *IUCrJ* **2017,** *4* (2), 108-118.
20. Lippens, G.; Cahoreau, E.; Millard, P.; Charlier, C.; Lopez, J.; Hanoulle, X.; Portais, J. C., In-cell NMR: From metabolites to macromolecules. *Analyst* **2018,** *143* (3), 620-629.
21. Hänsel, R.; Luh, L. M.; Corbeski, I.; Trantirek, L.; Dötsch, V., In-cell NMR and EPR spectroscopy of biomacromolecules. *Angew. Chem. Int. Ed.* **2014,** *53* (39), 10300-10314.
22. Freedberg, D. I.; Selenko, P., Live cell NMR. *Annu. Rev. Biochem.* **2014,** *43* (1), 171-192.
23. Narasimhan, S.; Scherpe, S.; Lucini Paioni, A.; van der Zwan, J.; Folkers, G. E.; Ovaa, H.; Baldus, M., DNP-supported solid-state NMR spectroscopy of proteins inside mammalian cells. *Angew. Chem. Int. Ed.* **2019,** *58* (37), 12969-12973.

24. Padilla-Parra, S.; Tramier, M., FRET microscopy in the living cell: Different approaches, strengths and weaknesses. *BioEssays* **2012,** *34* (5), 369-376.
25. Raicu, V.; Singh, Deo R., FRET spectrometry: A new tool for the determination of protein quaternary structure in living cells. *Biophys. J.* **2013,** *105* (9), 1937-1945.
26. Azarkh, M.; Singh, V.; Okle, O.; Seemann, I. T.; Dietrich, D. R.; Hartig, J. S.; Drescher, M., Site-directed spin-labeling of nucleotides and the use of in-cell EPR to determine long-range distances in a biologically relevant environment. *Nat Protoc.* **2012,** *8*, 131-147.
27. Schmidt, M. J.; Fedoseev, A.; Summerer, D.; Drescher, M., Chapter eighteen - genetically encoded spin labels for in vitro and in-cell EPR studies of native proteins. In *Meth. Enzymol.*, Qin, P. Z.; Warncke, K., Eds. Academic Press: 2015; Vol. 563, pp 483-502.
28. Azarkh, M.; Okle, O.; Singh, V.; Seemann, I. T.; Hartig, J. S.; Dietrich, D. R.; Drescher, M., Long-range distance determination in a DNA model system inside Xenopus laevis oocytes by in-cell spin-label EPR. *ChemBioChem* **2011,** *12* (13), 1992-1995.
29. Krstić, I.; Hänsel, R.; Romainczyk, O.; Engels, J. W.; Dötsch, V.; Prisner, T. F., Long-range distance measurements on nucleic acids in cells by pulsed EPR spectroscopy. *Angew. Chem. Int. Ed.* **2011,** *50* (22), 5070-5074.
30. Joseph, B.; Sikora, A.; Cafiso, D. S., Ligand induced conformational changes of a membrane transporter in E. coli cells observed with DEER/PELDOR. *J. Am. Chem. Soc.* **2016,** *138* (6), 1844-1847.
31. Lu, Y.; Yeung, N.; Sieracki, N.; Marshall, N. M., Design of functional metalloproteins. *Nature* **2009,** *460* (7257), 855-862.
32. Denysenkov, V. P.; Prisner, T. F.; Stubbe, J.; Bennati, M., High-field pulsed electron–electron double resonance spectroscopy to determine the orientation of the tyrosyl radicals in ribonucleotide reductase. *PNAS* **2006,** *103* (36), 13386.
33. Qi, M.; Groß, A.; Jeschke, G.; Godt, A.; Drescher, M., Gd(III)-PyMTA label is suitable for in-cell EPR. *J. Am. Chem. Soc.* **2014,** *136* (43), 15366-15378.
34. Yang, Y.; Yang, F.; Gong, Y.-J.; Chen, J.-L.; Goldfarb, D.; Su, X.-C., A reactive, rigid GdIII labeling tag for in-cell EPR distance measurements in proteins. *Angew. Chem. Int. Ed.* **2017,** *56* (11), 2914-2918.
35. Martorana, A.; Bellapadrona, G.; Feintuch, A.; Di Gregorio, E.; Aime, S.; Goldfarb, D., Probing protein conformation in cells by EPR distance measurements using Gd3+ spin labeling. *J. Am. Chem. Soc.* **2014,** *136* (38), 13458-13465.
36. Jassoy, J. J.; Berndhäuser, A.; Duthie, F.; Kühn, S. P.; Hagelueken, G.; Schiemann, O., Versatile Trityl Spin Labels for Nanometer Distance Measurements on Biomolecules In Vitro and within Cells. *Angew. Che. Int. Ed.* **2017,** *56* (1), 177-181.
37. Cattani, J.; Subramaniam, V.; Drescher, M., Room-temperature in-cell EPR spectroscopy: Alpha-synuclein disease variants remain intrinsically disordered in the cell. *Phys. Chem. Chem. Phys.* **2017,** *19* (28), 18147-18151.
38. Schmidt, M. J.; Fedoseev, A.; Summerer, D.; Drescher, M., Chapter Eighteen - Genetically Encoded Spin Labels for In Vitro and In-Cell EPR Studies of Native Proteins. In *Methods Enzymol.*, Qin, P. Z.; Warncke, K., Eds. Academic Press: 2015; Vol. 563, pp 483-502.
39. Robotta, M.; Gerding, H. R.; Vogel, A.; Hauser, K.; Schildknecht, S.; Karreman, C.; Leist, M.; Subramaniam, V.; Drescher, M., Alpha-synuclein binds to the inner membrane of mitochondria in an α-helical conformation. *ChemBioChem* **2014,** *15* (17), 2499-2502.
40. Bobko, A. A.; Kirilyuk, I. A.; Grigor'ev, I. A.; Zweier, J. L.; Khramtsov, V. V., Reversible reduction of nitroxides to hydroxylamines: Roles for ascorbate and glutathione. *Free Radic. Biol. Med.* **2007,** *42* (3), 404-412.
41. Jagtap, A. P.; Krstic, I.; Kunjir, N. C.; Hänsel, R.; Prisner, T. F.; Sigurdsson, S. T., Sterically shielded spin labels for in-cell EPR spectroscopy: Analysis of stability in reducing environment. *Free Radical Res.* **2015,** *49* (1), 78-85.
42. Karthikeyan, G.; Bonucci, A.; Casano, G.; Gerbaud, G.; Abel, S.; Thomé, V.; Kodjabachian, L.; Magalon, A.; Guigliarelli, B.; Belle, V.; Ouari, O.; Mileo, E., A bioresistant nitroxide spin

label for in-cell EPR spectroscopy: In vitro and in oocytes protein structural dynamics studies. *Angew. Chem. Int. Ed.* **2018,** *130* (5), 1380-1384.
43. Saha, S.; Jagtap, A. P.; Sigurdsson, S. T., Site-directed spin labeling of 2'-amino groups in RNA with isoindoline nitroxides that are resistant to reduction. *Chem. Commun.* **2015,** *51* (66), 13142-13145.
44. Yang, Y.; Yang, F.; Li, X.-Y.; Su, X.-C.; Goldfarb, D., In-cell EPR distance measurements on ubiquitin labeled with a rigid PyMTA-Gd(III) tag. *J. Phys. Chem. B* **2019,** *123* (5), 1050-1059.
45. Barhate, N.; Cekan, P.; Massey, A. P.; Sigurdsson, S. T., A nucleoside that contains a rigid nitroxide spin label: A fluorophore in disguise. *Angew. Chem. Int. Ed.* **2007,** *46* (15), 2655-2658.
46. Höbartner, C.; Sicoli, G.; Wachowius, F.; Gophane, D. B.; Sigurdsson, S. T., Synthesis and characterization of RNA containing a rigid and nonperturbing cytidine-derived spin label. *J. Org. Chem.* **2012,** *77* (17), 7749-7754.
47. Grytz, C. M.; Kazemi, S.; Marko, A.; Cekan, P.; Güntert, P.; Sigurdsson, S. T.; Prisner, T. F., Determination of helix orientations in a flexible DNA by multi-frequency EPR spectroscopy. *Phys. Chem. Chem. Phys.* **2017,** *19* (44), 29801-29811.
48. Haugland, M. M.; El-Sagheer, A. H.; Porter, R. J.; Peña, J.; Brown, T.; Anderson, E. A.; Lovett, J. E., 2'-Alkynylnucleotides: A sequence- and spin label-flexible strategy for EPR spectroscopy in DNA. *J. Am. Chem. Soc.* **2016,** *138* (29), 9069-9072.
49. Gophane, D. B.; Sigurdsson, S. T., Hydrogen-bonding controlled rigidity of an isoindoline-derived nitroxide spin label for nucleic acids. *Chem. Commun.* **2013,** *49* (10), 999-1001.
50. Lin, K.-Y.; Jones, R. J.; Matteucci, M., Tricyclic 2'-deoxycytidine analogs: Syntheses and incorporation into oligodeoxynucleotides which have enhanced binding to complementary RNA. *J. Am. Chem. Soc.* **1995,** *117* (13), 3873-3874.
51. Volodarsky, L. B.; Reznikov, V. A.; Ovcharenko, V. I., *Synthetic chemistry of stable nitroxides*. Taylor & Francis: 1993.
52. Cekan, P.; Smith, A. L.; Barhate, N.; Robinson, B. H.; Sigurdsson, S. T., Rigid spin-labeled nucleoside Ç: A nonperturbing EPR probe of nucleic acid conformation. *Nucleic Acids Res.* **2008,** *36* (18), 5946-5954.
53. Juliusson, H. Y.; Segler, A.-L. J.; Sigurdsson, S. T., Benzoyl-protected hydroxylamines for improved chemical synthesis of oligonucleotides containing nitroxide spin labels. *Eur. J. Org. Chem.* **2019,** *2019* (23), 3799-3805.
54. Hatano, A.; Terado, N.; Kanno, Y.; Nakamura, T.; Kawai, G., Synthesis of a protected ribonucleoside phosphoramidite-linked spin label via an alkynyl chain at the 5' position of uridine. *Synth. Commun.* **2019,** *49* (1), 136-145.
55. Sen, V. D.; Golubev, V. A., Kinetics and mechanism for acid-catalyzed disproportionation of 2,2,6,6-tetramethylpiperidine-1-oxyl. *J. Phys. Org. Chem.* **2009,** *22* (2), 138-143.
56. Cekan, P.; Sigurdsson, S. T., Single base interrogation by a fluorescent nucleotide: each of the four DNA bases identified by fluorescence spectroscopy. *Chem. Commun.* **2008,** (29), 3393-3395.
57. Weinrich, T.; Gränz, M.; Grünewald, C.; Prisner, T. F.; Göbel, M. W., Synthesis of a Cytidine Phosphoramidite with Protected Nitroxide Spin Label for EPR Experiments with RNA. *Eur. J. Org. Chem.* **2017,** *2017* (3), 491-496.
58. Engman, K. C.; Sandin, P.; Osborne, S.; Brown, T.; Billeter, M.; Lincoln, P.; Nordén, B.; Albinsson, B.; Wilhelmsson, L. M., DNA adopts normal B-form upon incorporation of highly fluorescent DNA base analogue tC: NMR structure and UV-Vis spectroscopy characterization. *Nucleic Acids Res.* **2004,** *32* (17), 5087-5095.
59. Sandin, P.; Stengel, G.; Ljungdahl, T.; Börjesson, K.; Macao, B.; Wilhelmsson, L. M., Highly efficient incorporation of the fluorescent nucleotide analogs tC and tCO by Klenow fragment. *Nucleic Acids Res.* **2009,** *37* (12), 3924-3933.

Reduction resistant and rigid nitroxide spin labels for DNA and RNA

Haraldur Yngvi Juliusson and Snorri Th. Sigurdsson*

University of Iceland, Department of Chemistry, Science Institute, Dunhaga 3, 107 Reykjavik, Iceland.

**E-mail: snorrisi@hi.is*

Table of contents

Spin-labeled oligonucleotides and their analysis by MS and EPR spectroscopy. The spin-labeled oligonucleotides prepared are listed in **Table S1**. The incorporation of **EÇ** and **EÇm** into oligonucleotides was confirmed by HRMS (ESI) analysis. The calculated and observed monoisotopic masses of spin-labeled oligonucleotides are listed in **Table S1**. The amount of spin labels in each oligonucleotide was determined by spin counting using EPR spectroscopy[1] (**Table S1**, far right column).

Table S1. Monoisotopic masses and spin-labeling efficiency of spin-labeled oligonucleotides. Oligonucleotides **XVII**, **XVIII** and **XIX** were synthesized with the protected phosphoramidite **14**.

No.	Sequence	Calculated Mass	Measured Mass	Radical content (%)
I	5'-d(CGCGAATT**EÇ**GCG)-3'	3904.8	3901.2	99
II	5'-d(GACCTCG**EÇ**ATCGTG)-3'	4497.9	4494.2	96
III	5'-d(AGTGGA**EÇ**GCTTGGGGTGTA)-3'	6198.1	6192.6	82
IV	5'-d(ATACA**EÇ**CCCAAGCGTCCAC)-3'	5944.9	5939.7	81
V	5'-d(ATACAC**EÇ**CCAAGCGTCCAC)-3'	5944.9	5939.7	100
VI	5'-d(ATACACC**EÇ**CAAGCGTCCAC)-3'	5944.9	5939.7	82
VII	5'-d(ATACACCC**EÇ**AAGCGTCCAC)-3'	5944.9	5939.7	94
XVI	5'-d(CACGATGCGAGGTC)-3'	4288.8	4285.1	
VIII	5'-d(CGCGAATTCGCG)-3'	3646.4	3643.1	
IX	5'-d(GACCTCGCATCGTG)-3'	4239.8	4236.1	
X	5'-d(AGTGGACGCTTGGGGTGTA)-3'	5939.9	5934.6	
XI	5'-d(ATACACCCCAAGCGTCCAC)-3'	5686.7	5682.0	
XII	5'-AGUGGA**EÇm**GCUUGUGGGGUGUA-3'	7097.1	7056.5	52
XIII	5'-AUACA**EÇm**CCCACAAGCGUCCAC-3'	6869.1	6863.6	71
XIV	5'-AUACAC**EÇm**CCACAAGCGUCCAC-3'	6869.1	6863.6	98
XV	5'-AUACACC**EÇm**CACAAGCGUCCAC-3'	6869.1	6860.6	64
XVI	5'-AUACACCC**EÇm**ACAAGCGUCCAC-3'	6869.1	6863.6	94
XVII	5'-AGUGGA**EÇm**GCUUGUGGGGUGUA-3'	7097.1	7096.5	99
XVIII	5'-AUACA**EÇm**CCCACAAGCGUCCAC-3'	6869.1	6863.6	100
XIX	5'-AUACACC**EÇm**CACAAGCGUCCAC-3'	6869.1	6863.6	98
XX	5'-AGUGGACGCUUGUGGGGUGUA-3'	6825.1	6819.4	
XXI	5'-AUACACCCCACAAGCGUCCAC-3'	6597.09	6591.5	

^{1}H-, ^{13}C- and ^{31}P-NMR spectra

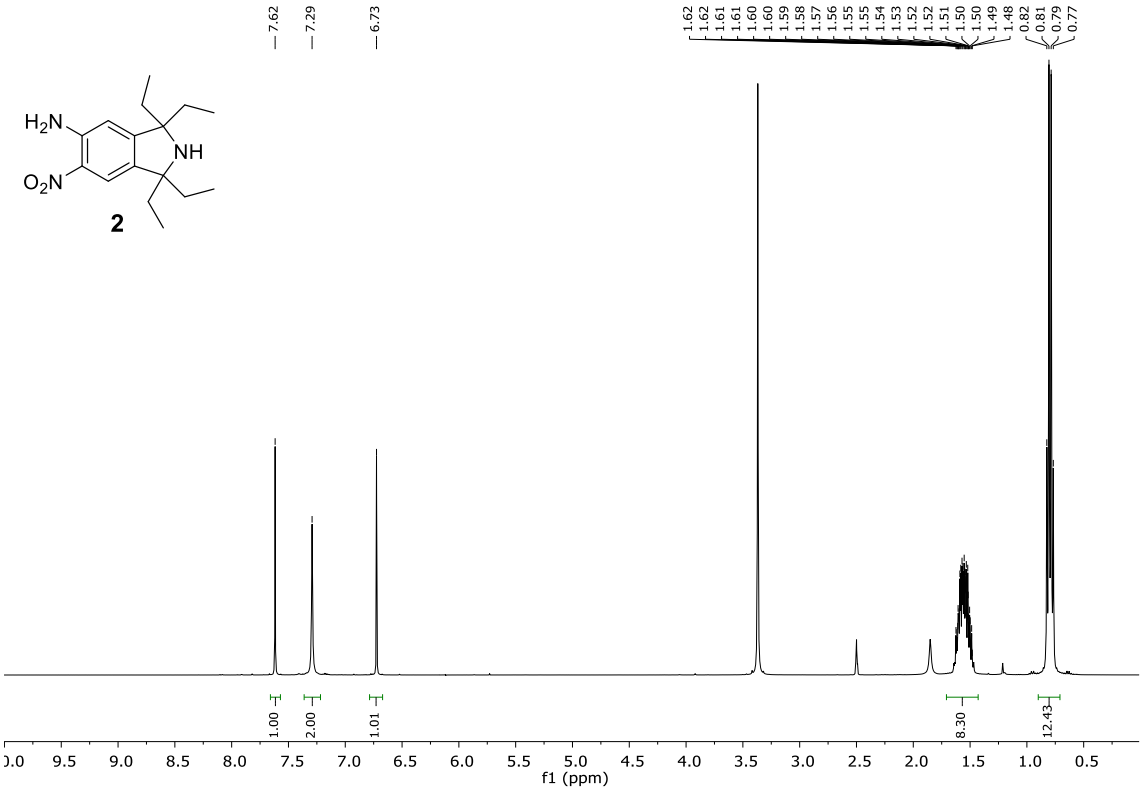

Figure S1. ^{1}H-NMR spectrum of **2**.

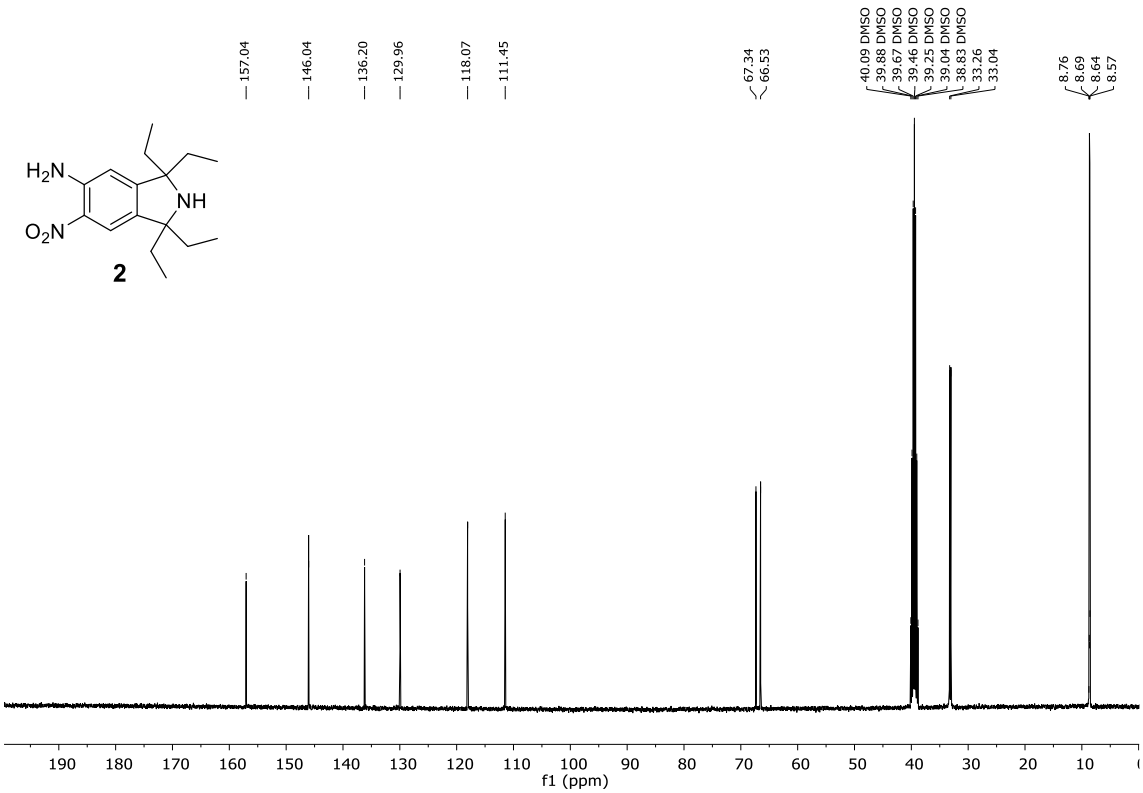

Figure S2. ^{13}C-NMR spectrum of **2**.

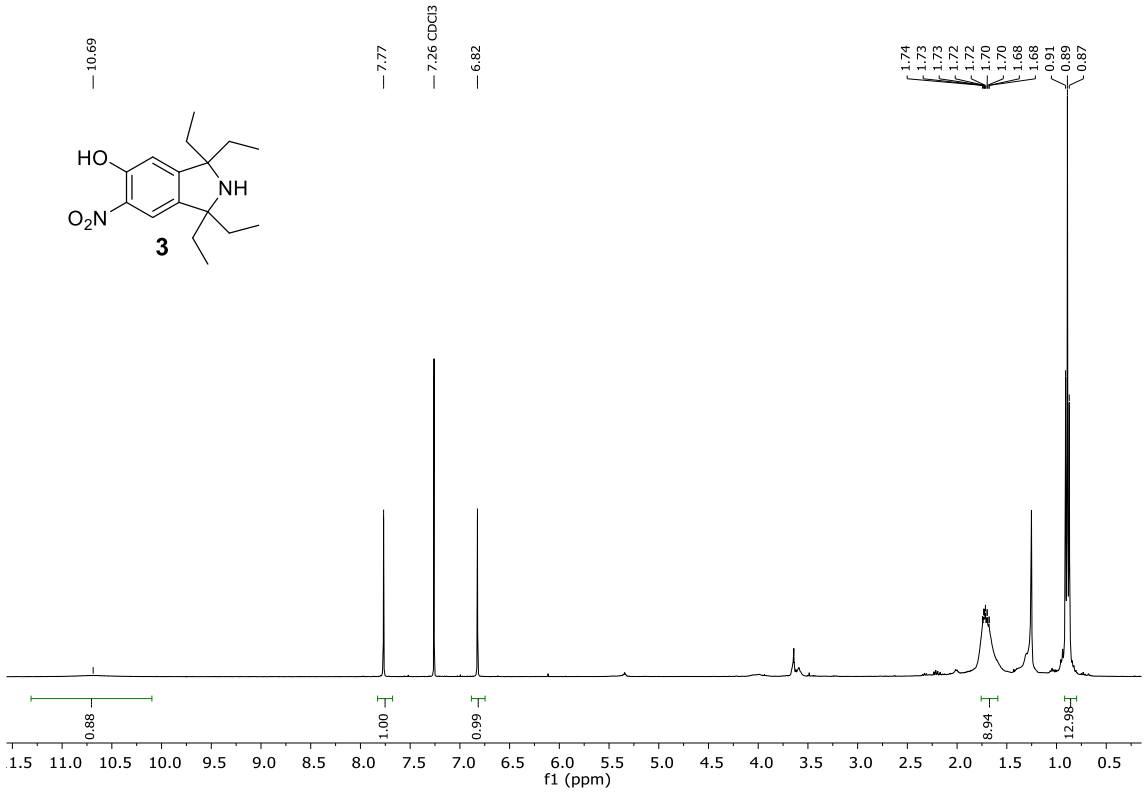

Figure S3. ^{1}H-NMR spectrum of **3**.

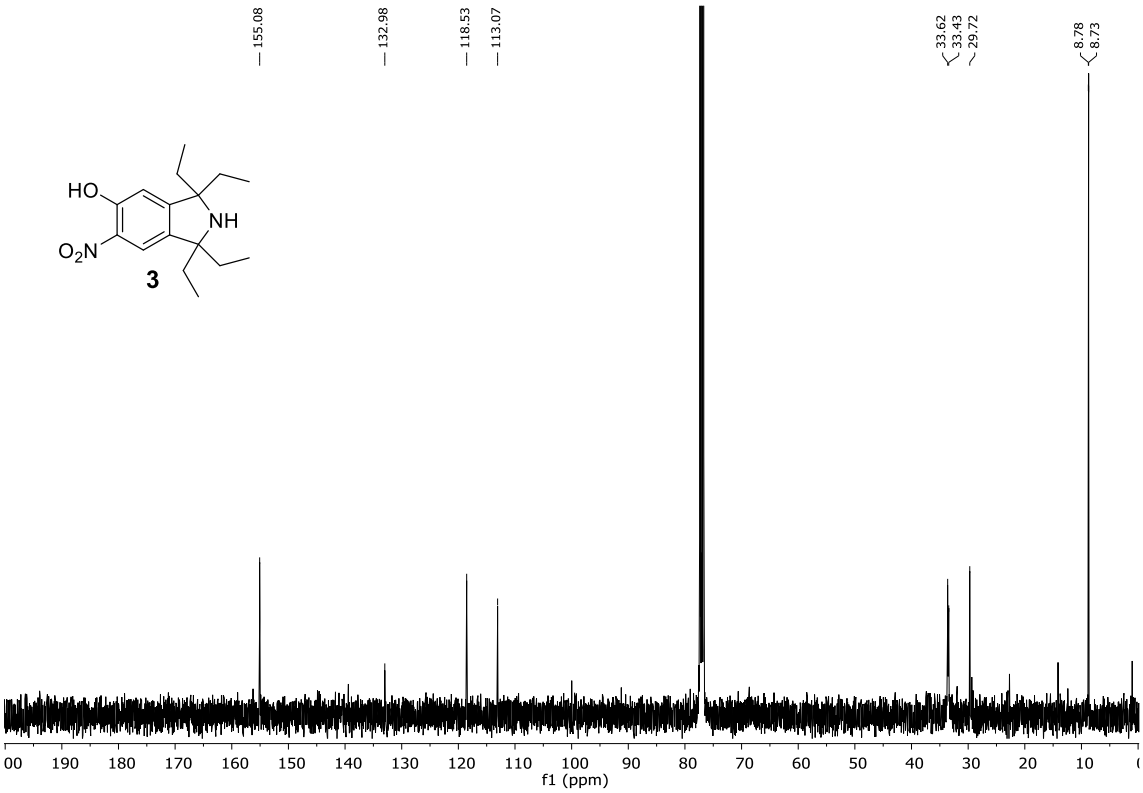

Figure S4. ^{13}C-NMR spectrum of **3**.

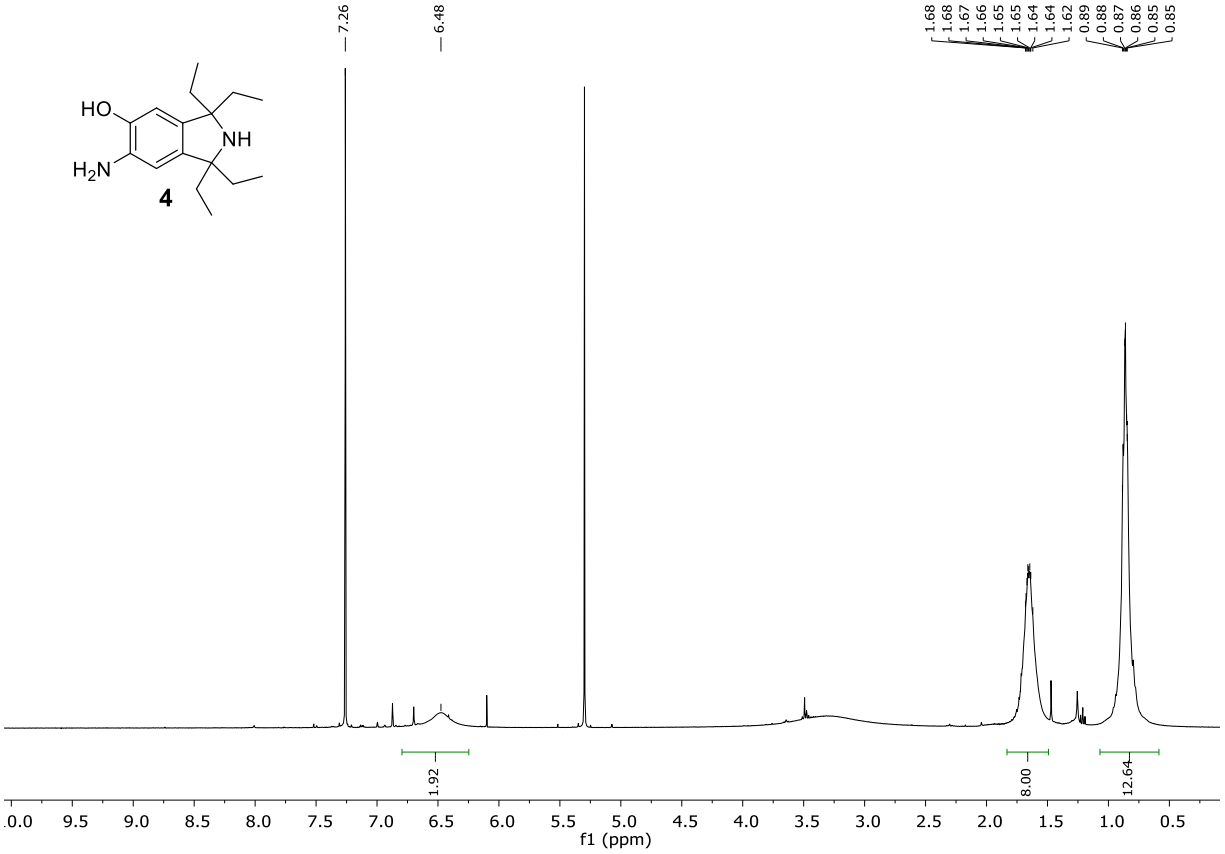

Figure S5. ^{1}H-NMR spectrum of **4**.

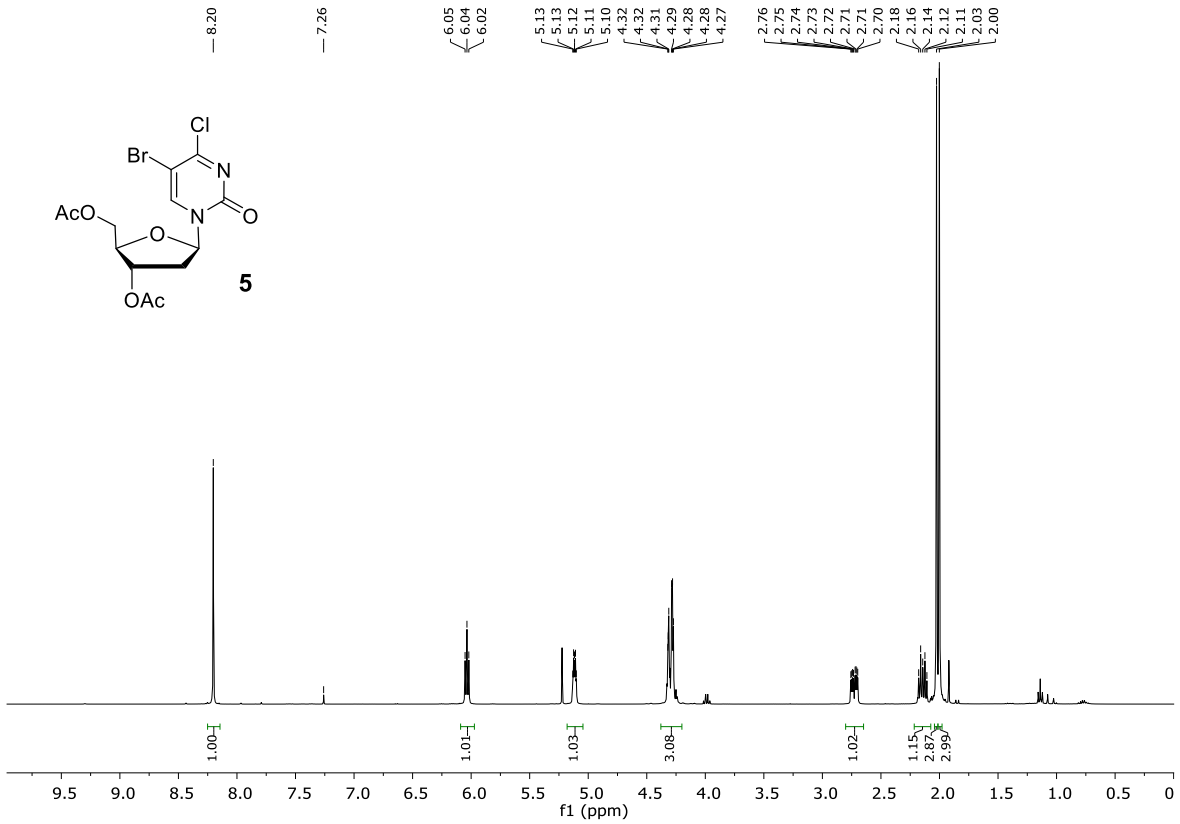

Figure S6. ^{1}H-NMR spectrum of **5**.

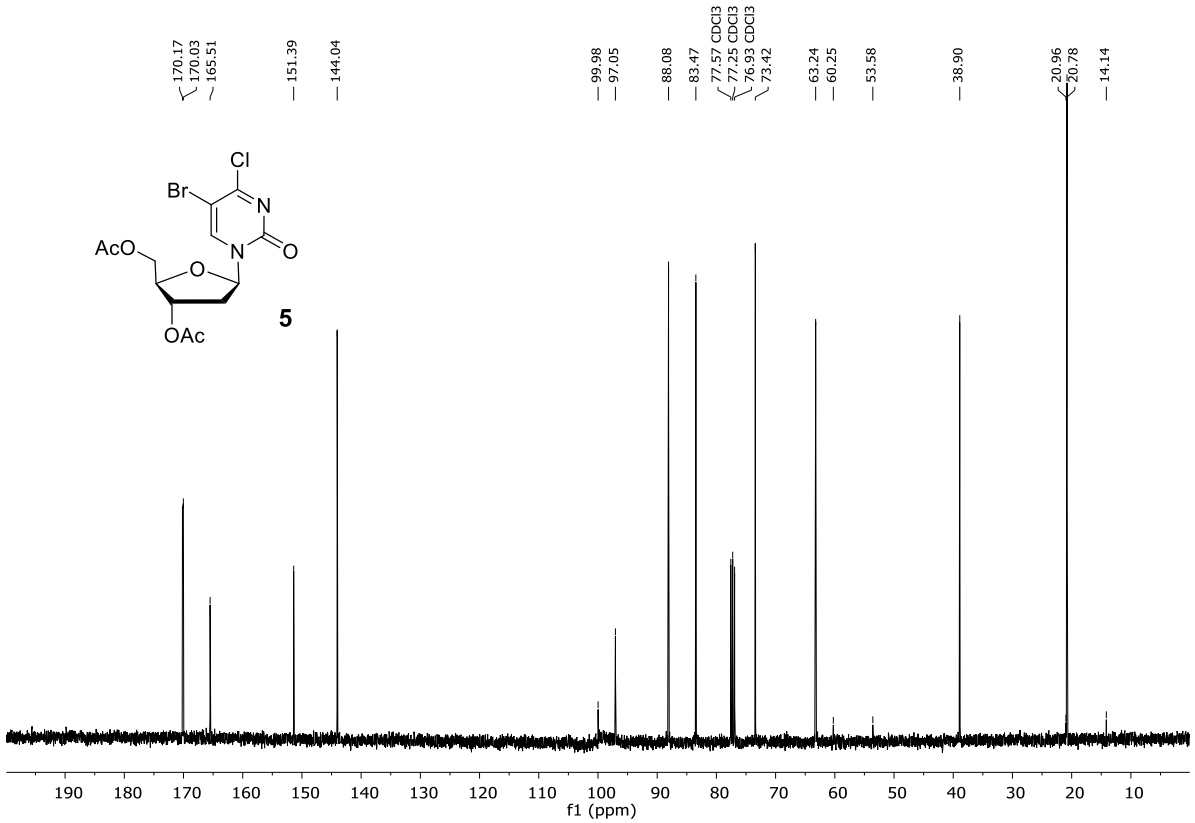

Figure S7. ^{13}C-NMR spectrum of **5**.

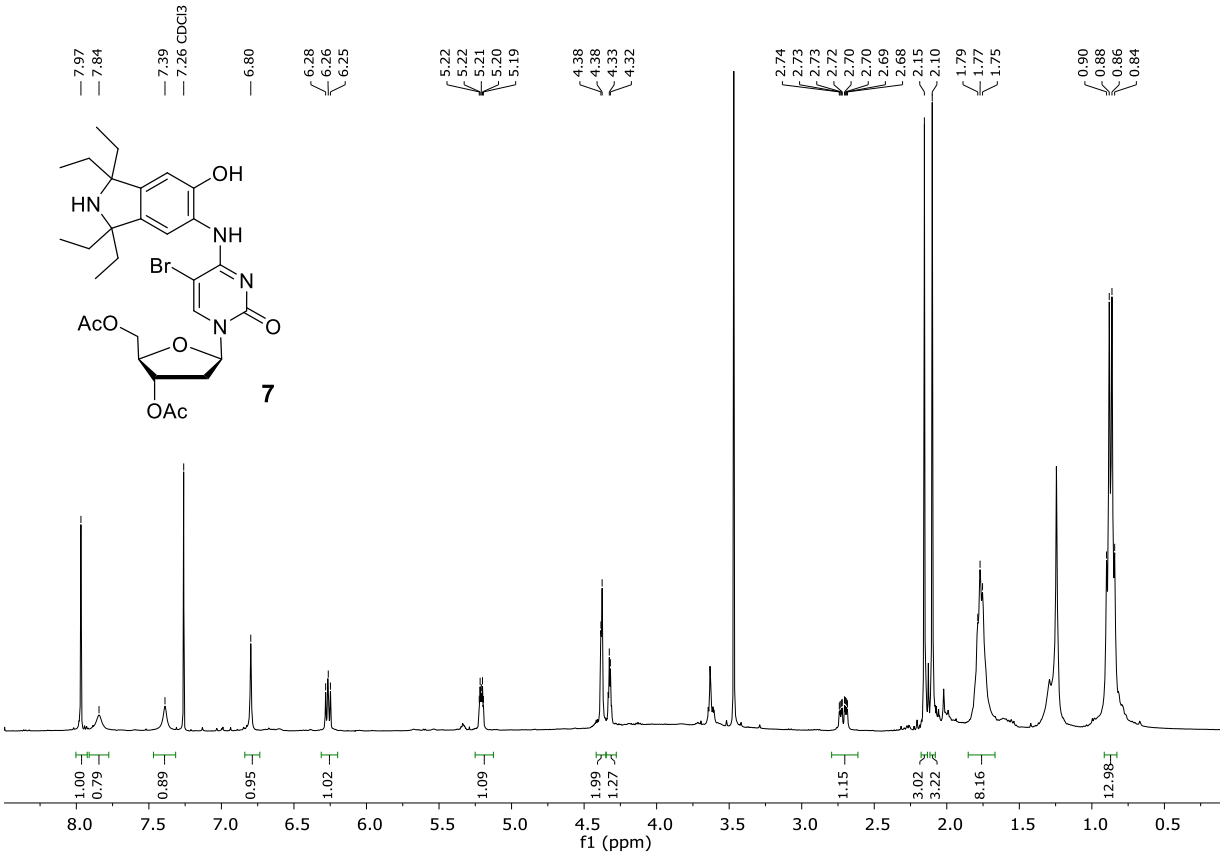

Figure S8. ^{1}H-NMR spectrum of **7**.

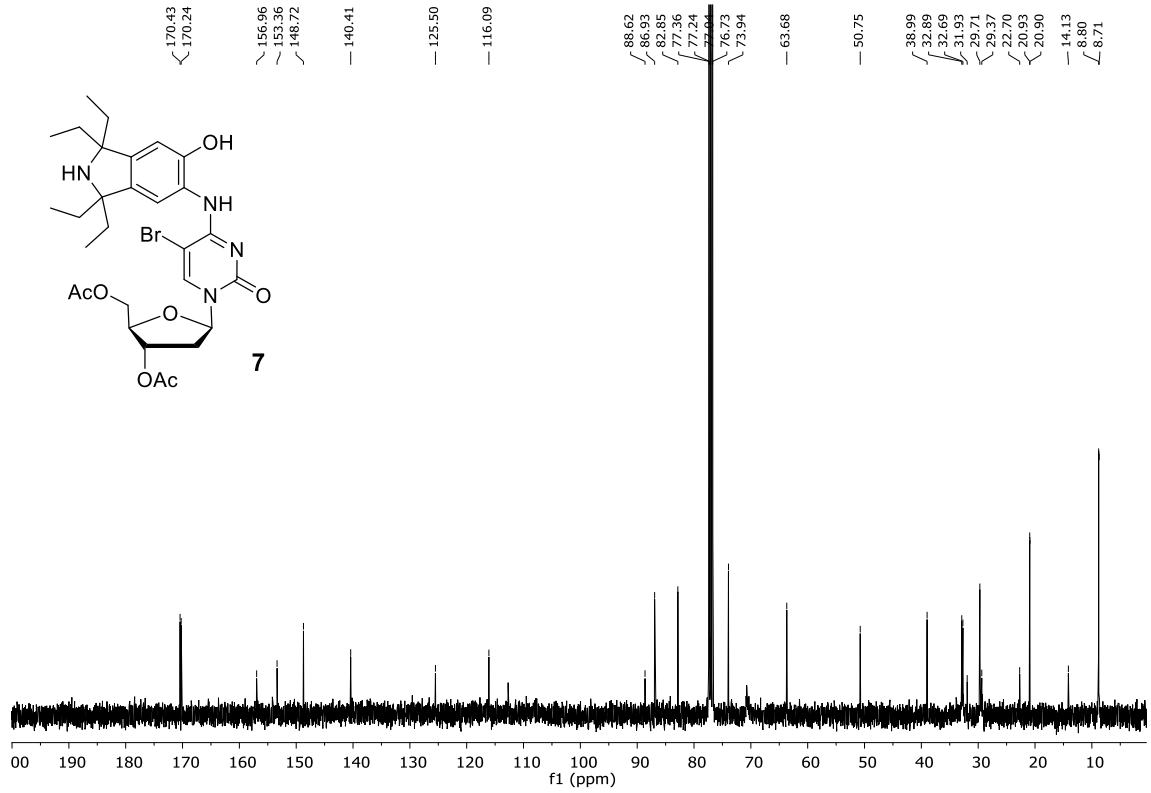

Figure S9. ^{13}C-NMR spectrum of **7**.

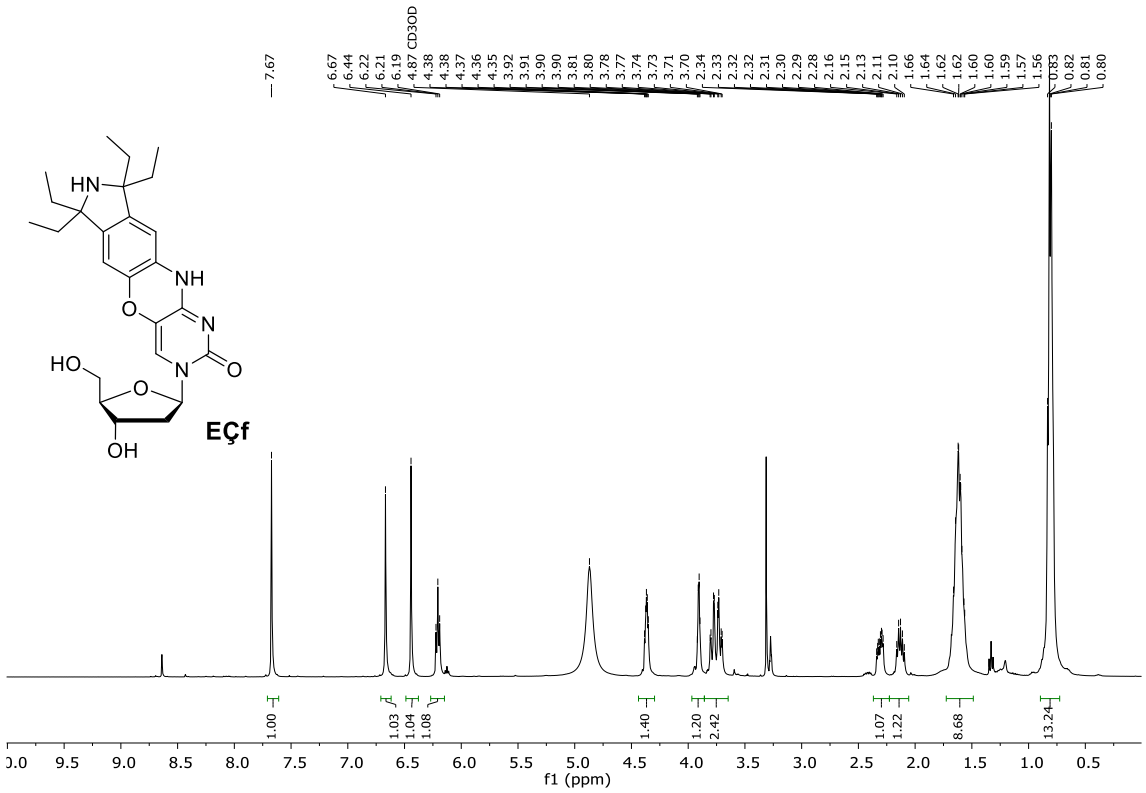

Figure S10. 1H-NMR spectrum of **EÇf**.

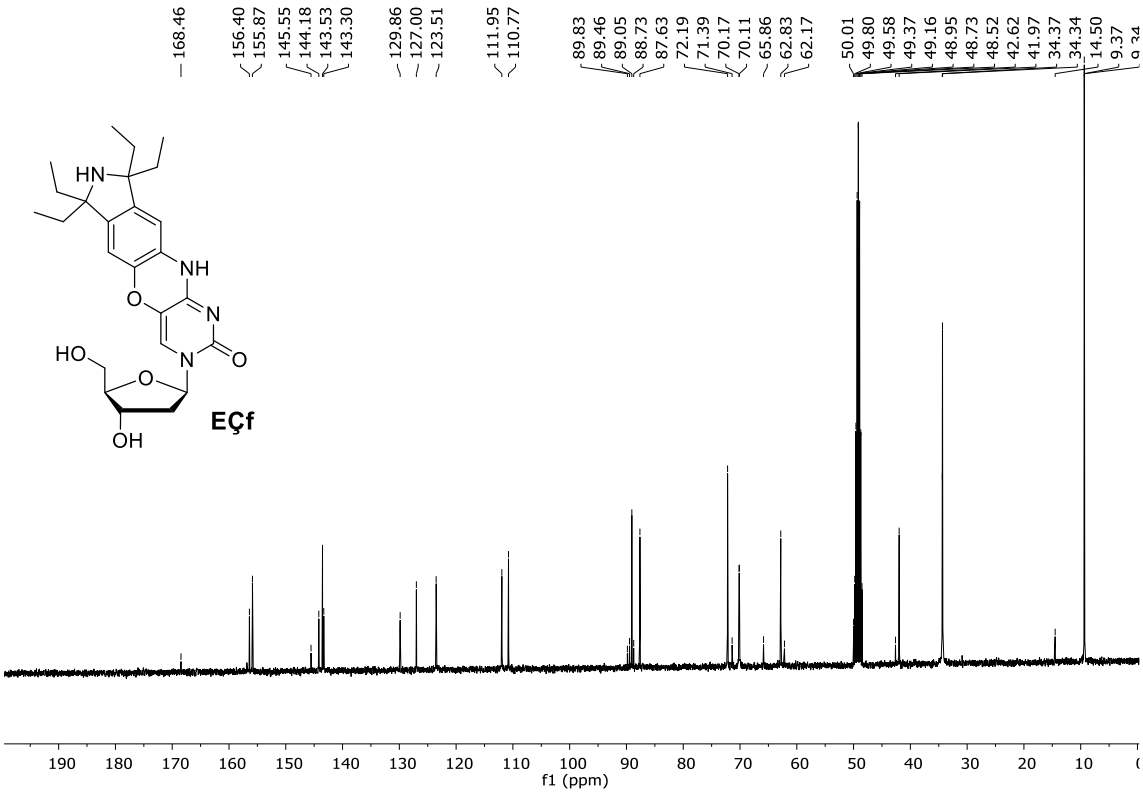

Figure S11. ^{13}C-NMR spectrum of **EÇf**.

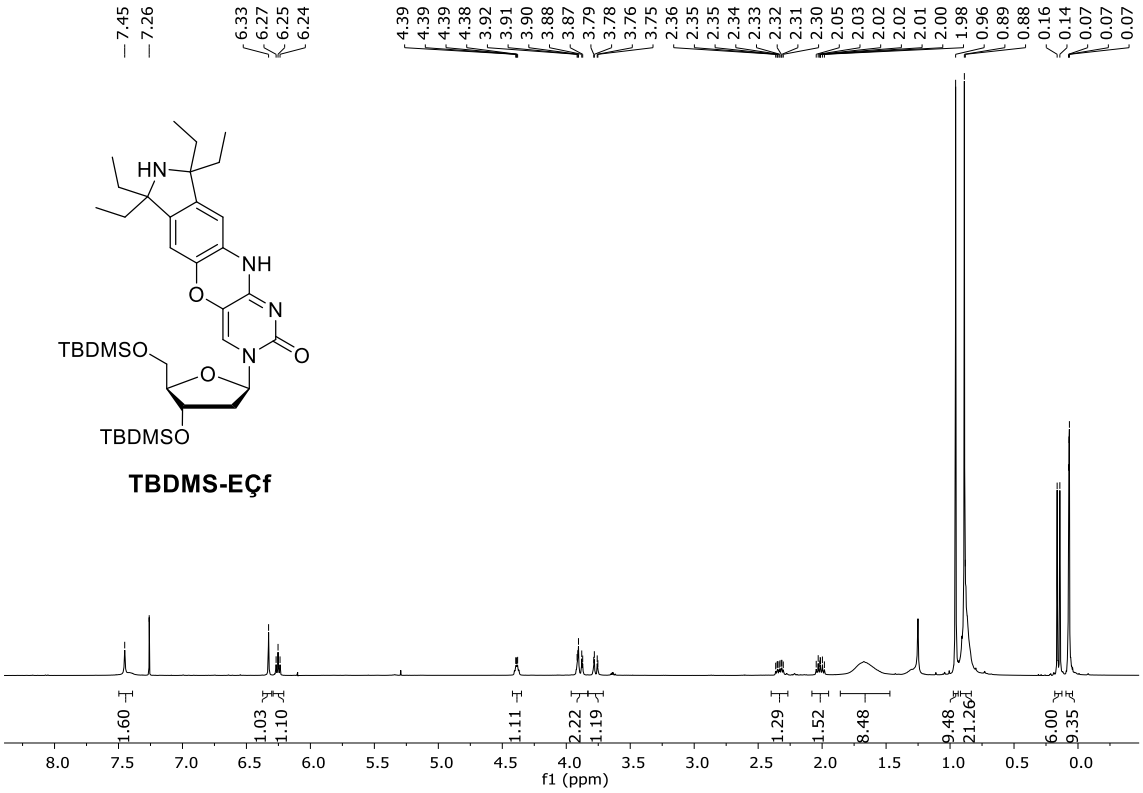

Figure S12. ^{1}H-NMR spectrum of **TBDMS-EÇf**.

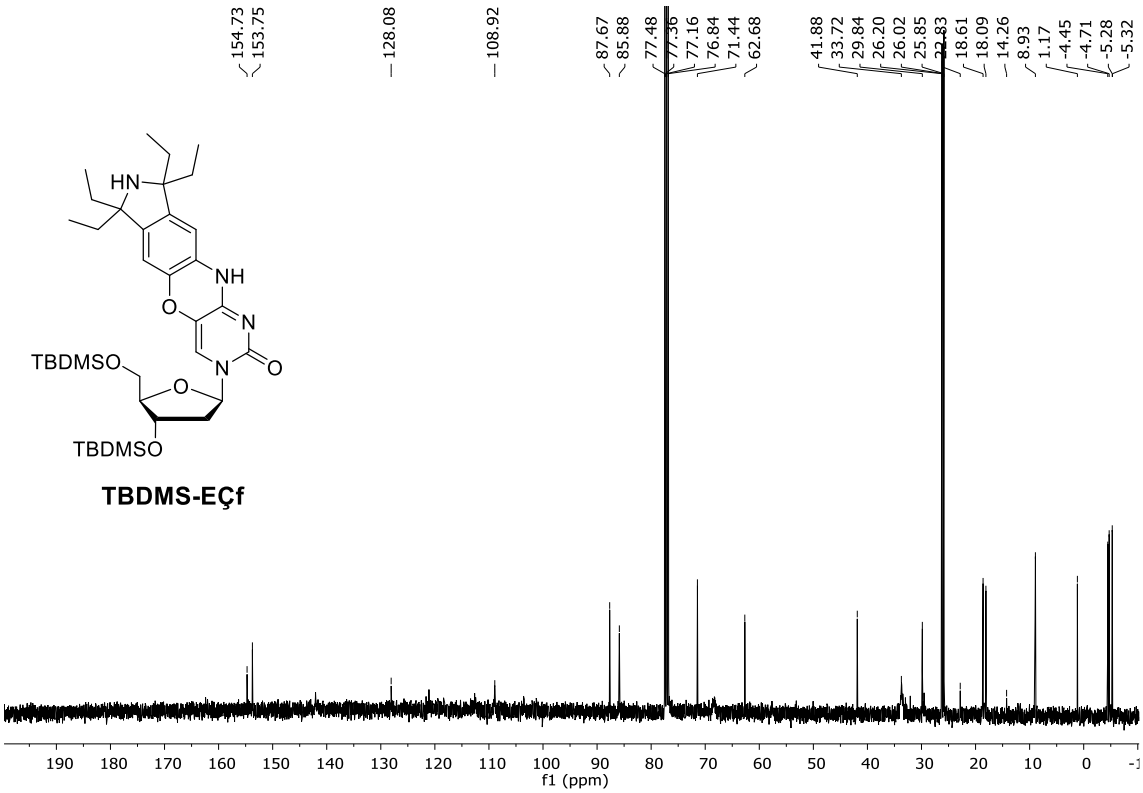

Figure S13. ^{13}C-NMR spectrum of **TBDMS-EÇf**.

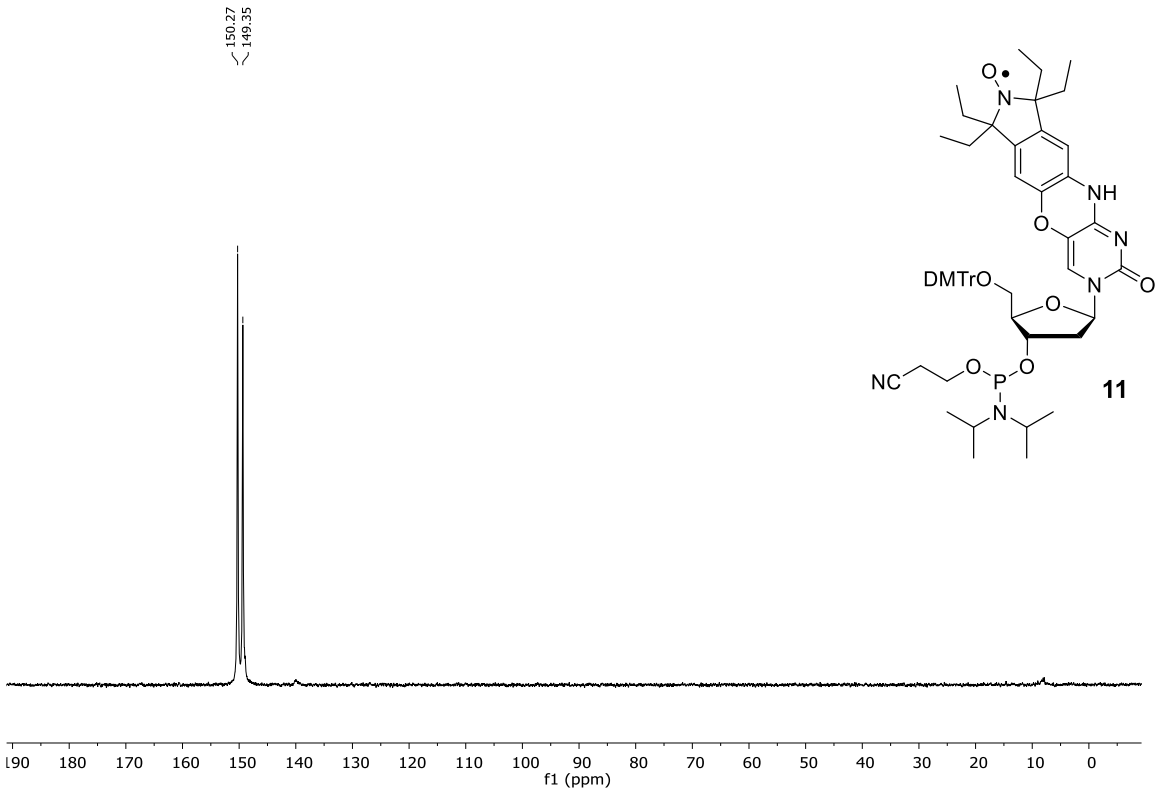

Figure S14. ^{31}P-NMR spectrum of phosphoramidite **11**.

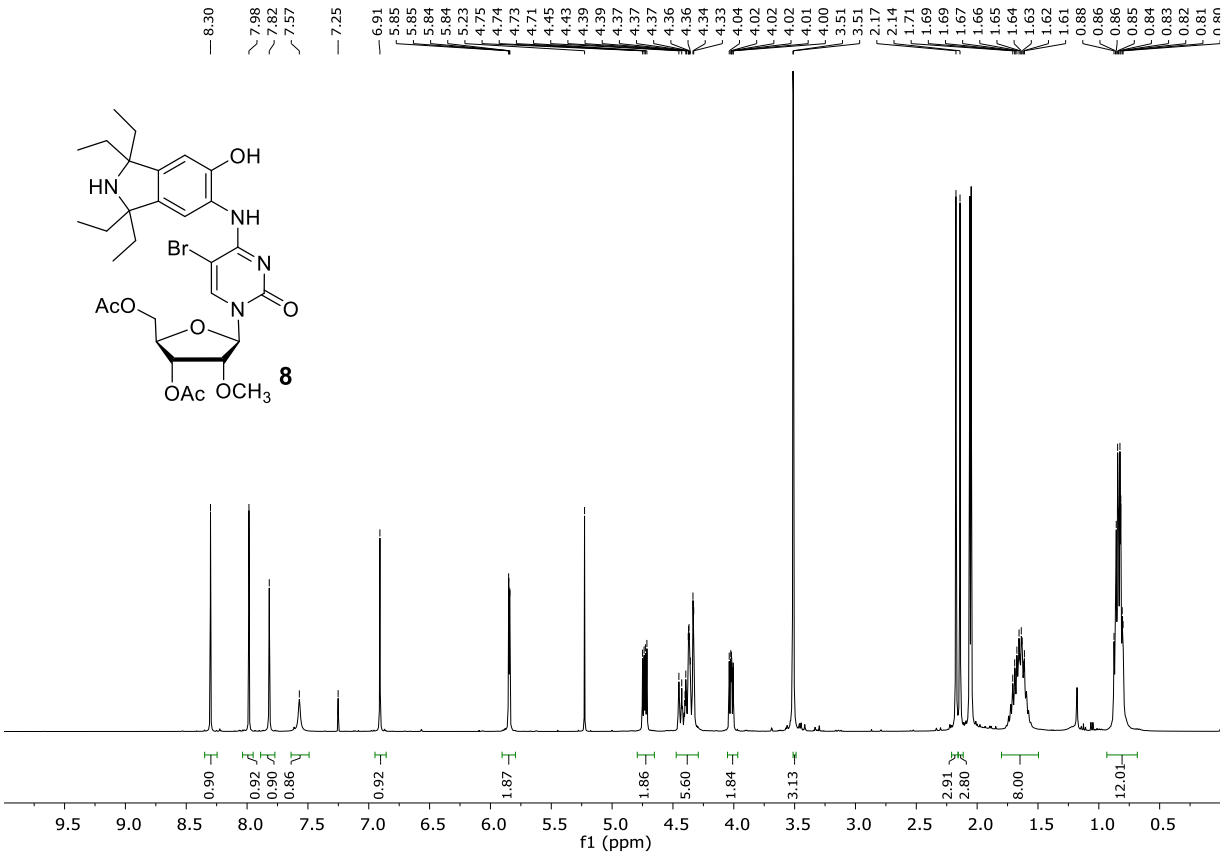

Figure S15. ^{1}H-NMR spectrum of **8**.

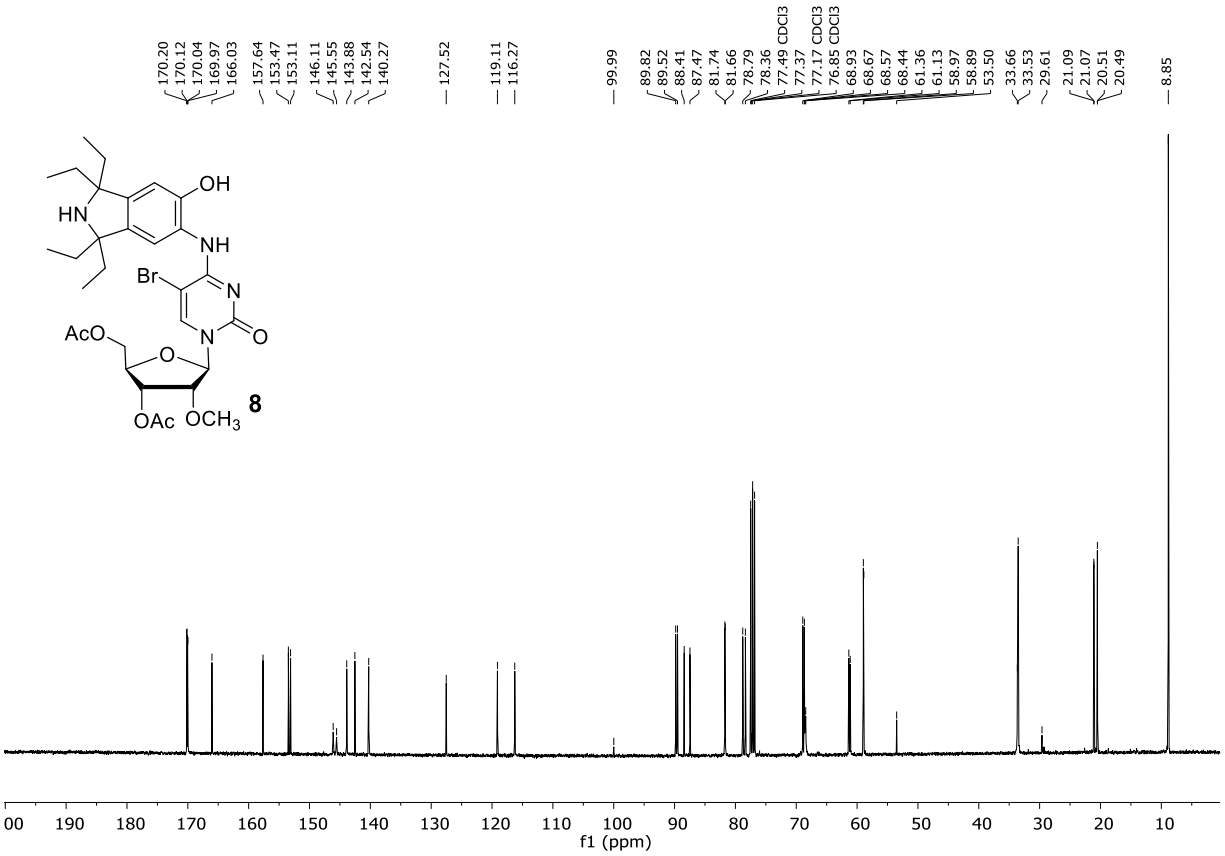

Figure S16. ^{13}C-NMR spectrum of **8**.

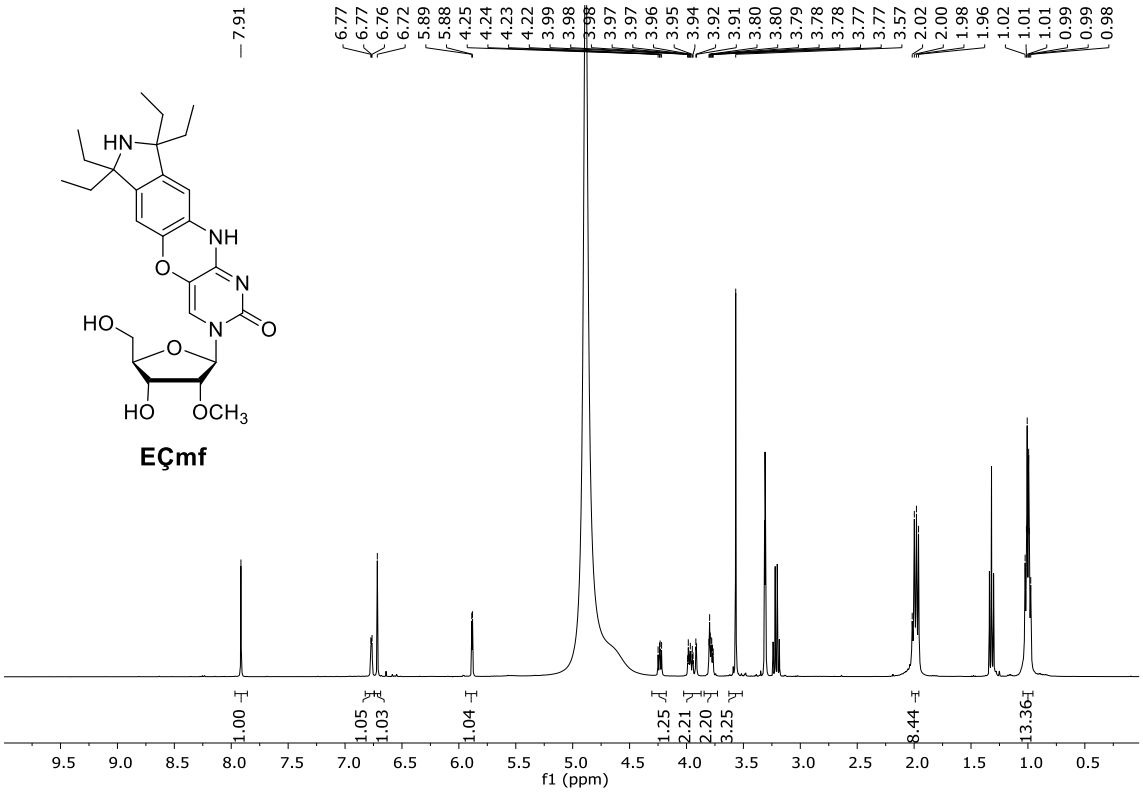

Figure S17. ^{1}H-NMR spectrum of **EÇmf**.

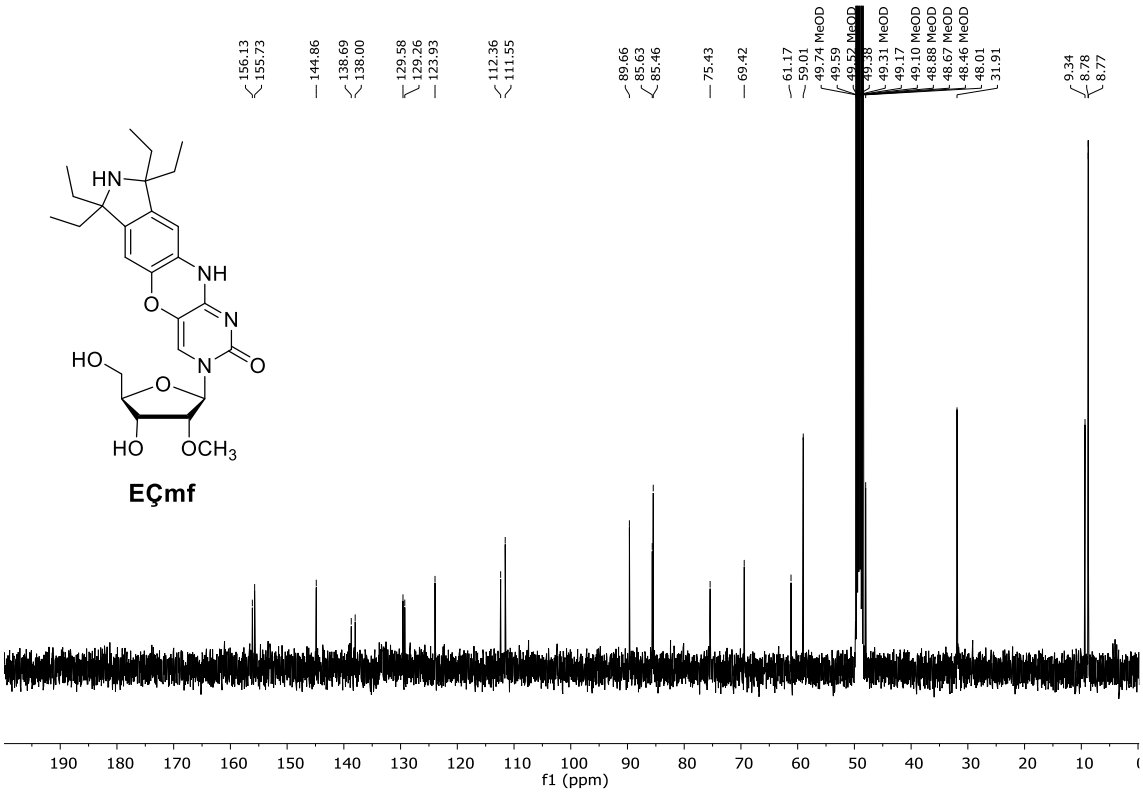

Figure S18. ^{13}C-NMR spectrum of **EÇmf**.

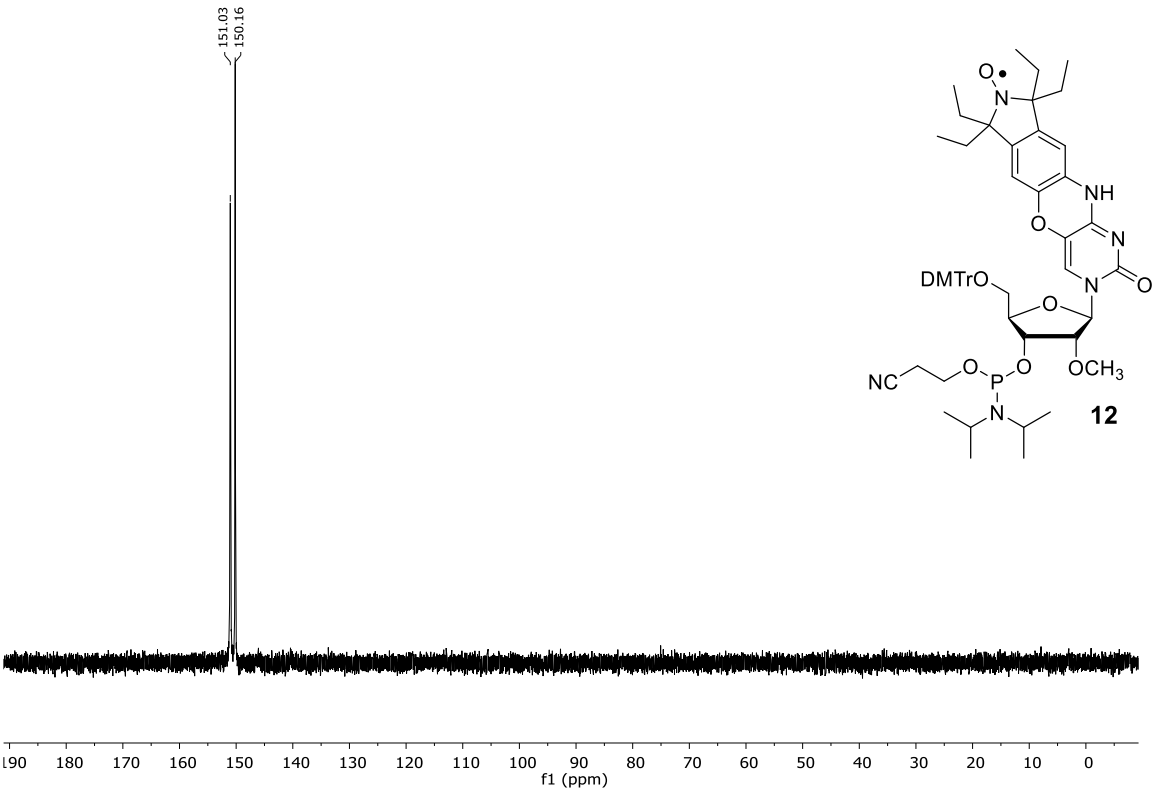

Figure S19. ^{31}P-NMR spectrum of phosphoramidite **12**.

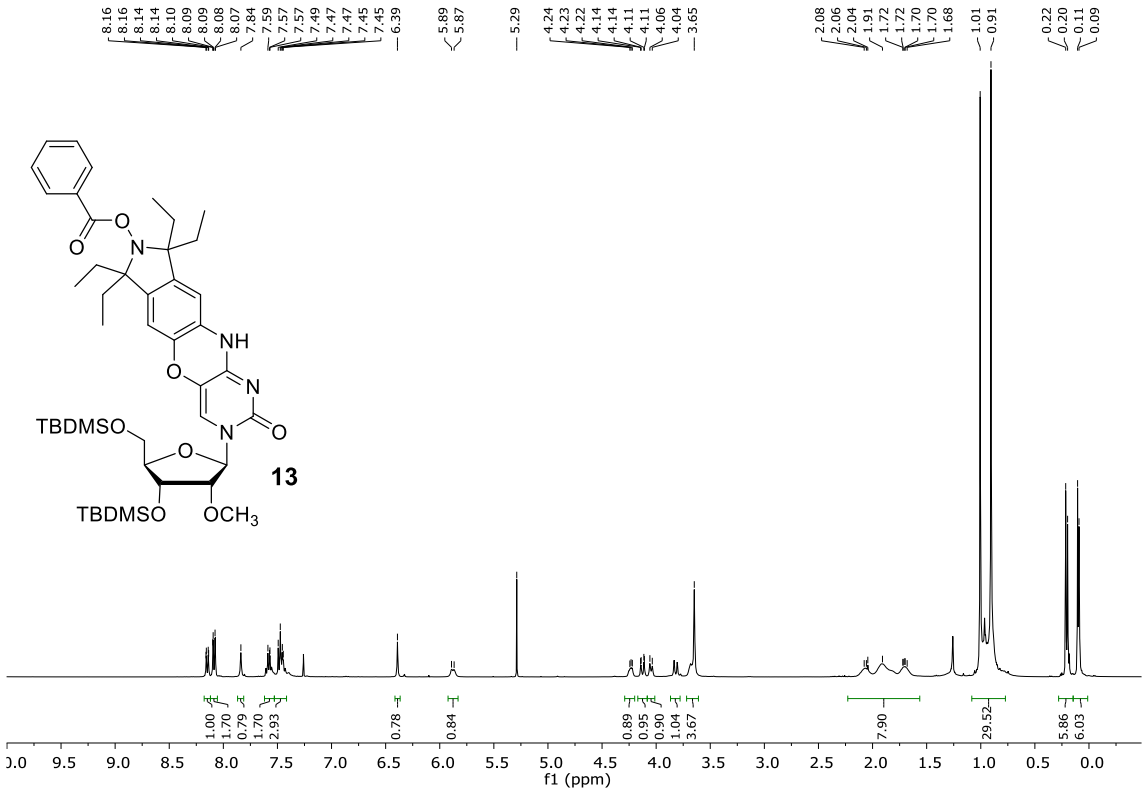

Figure S20. ^{1}H-NMR spectrum of **13**.

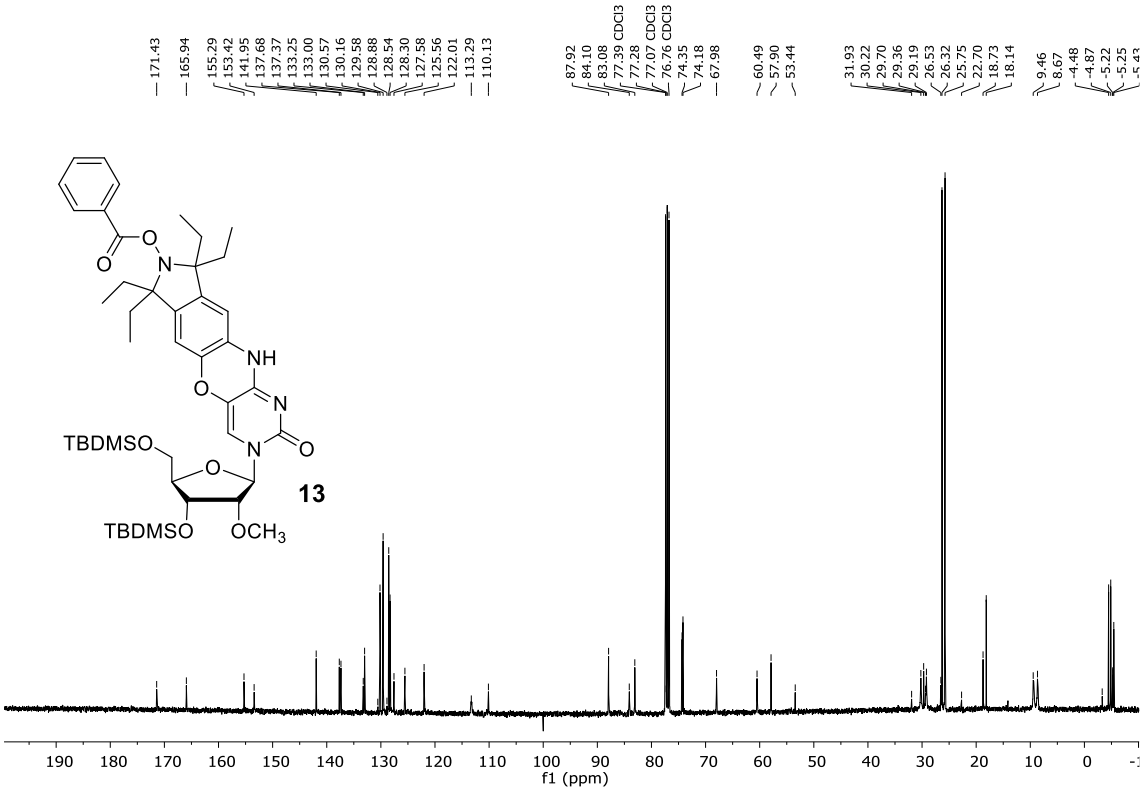

Figure S21. ^{13}C-NMR spectrum of **13**.

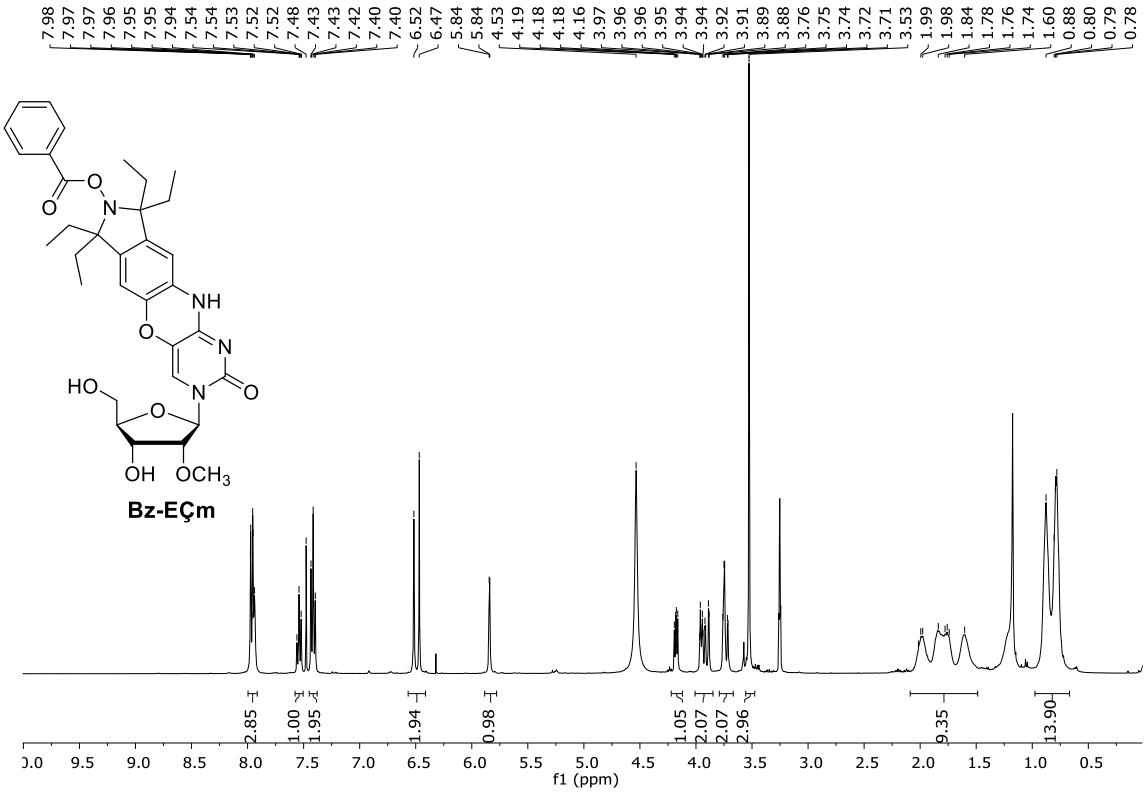

Figure S22. ^{1}H-NMR spectrum of **Bz-EÇm**.

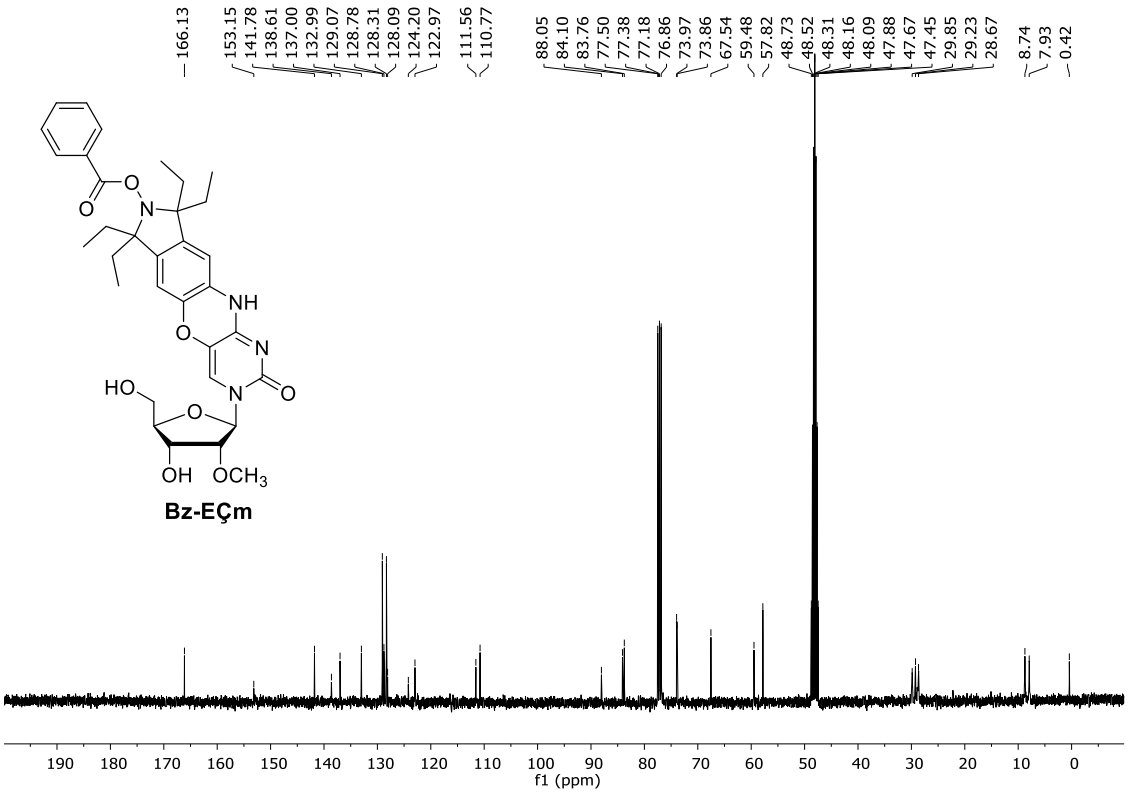

Figure S23. ^{13}C-NMR spectrum of **Bz-EÇm**.

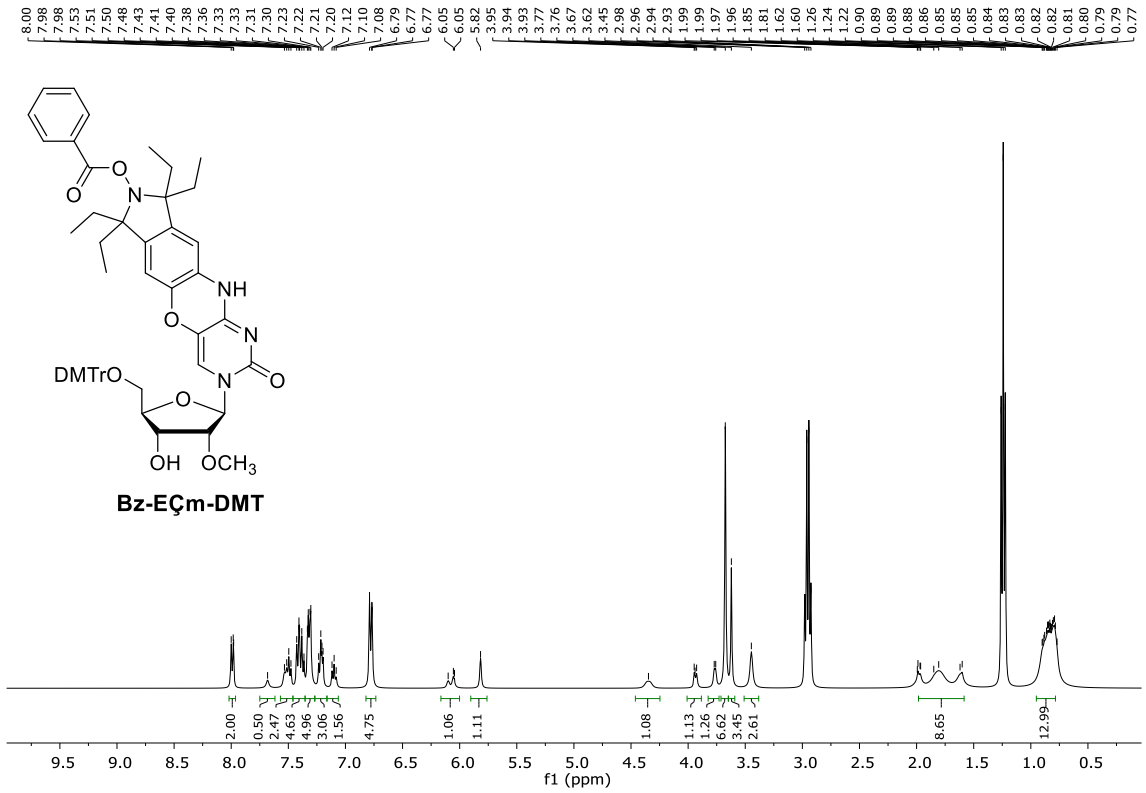

Figure S24. ^{1}H-NMR spectrum of **Bz-EÇm-DMT**.

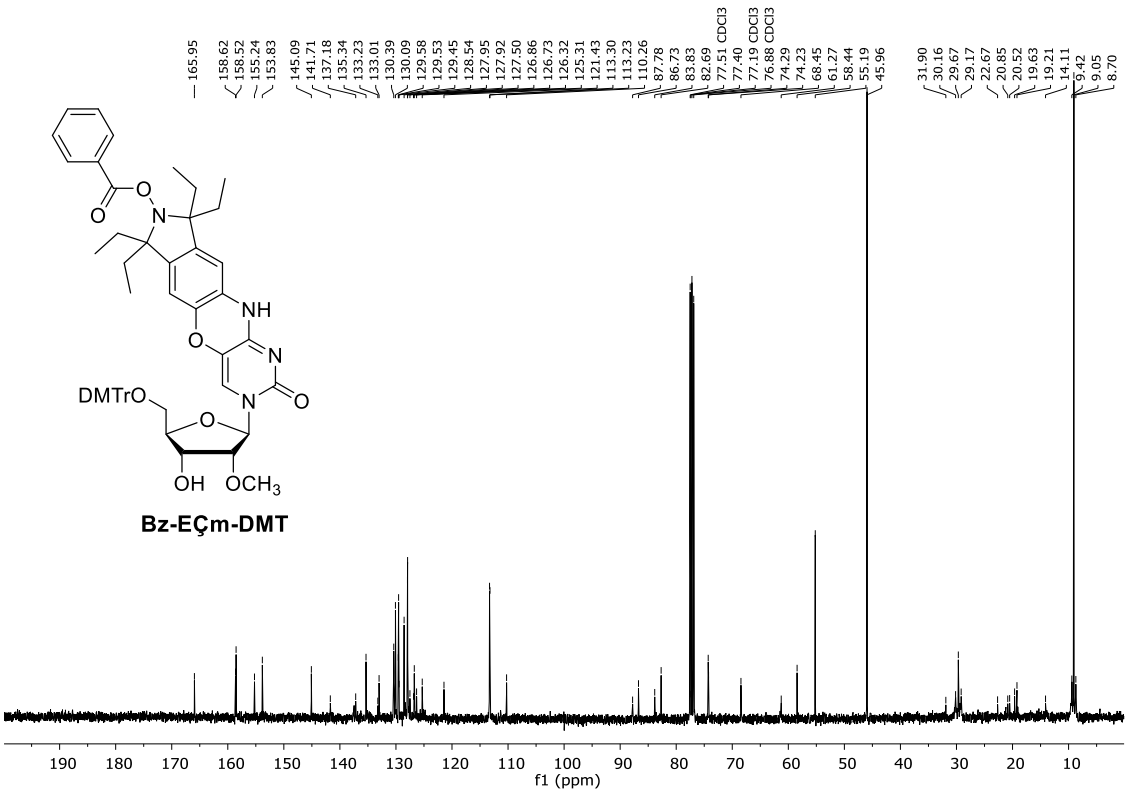

Figure S25. ^{13}C-NMR spectrum of **Bz-EÇm-DMT**.

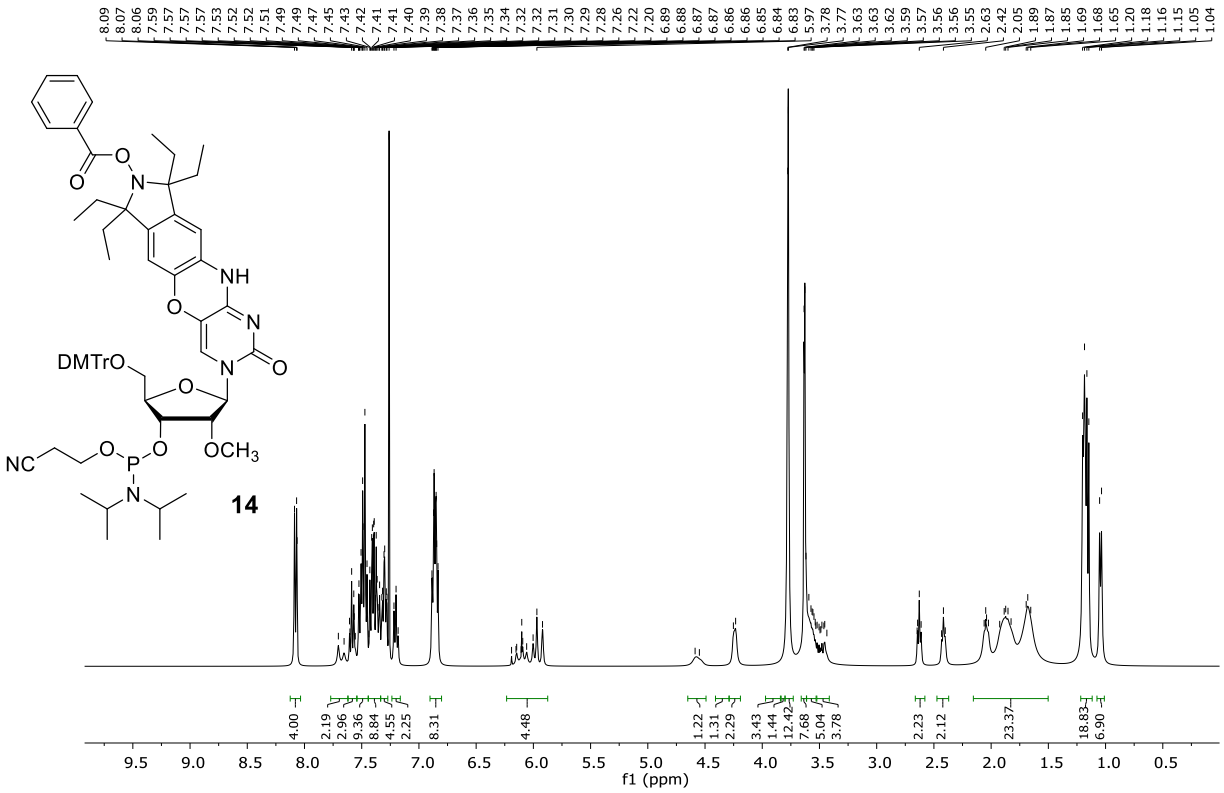

Figure S26. ^{1}H-NMR spectrum of **14**.

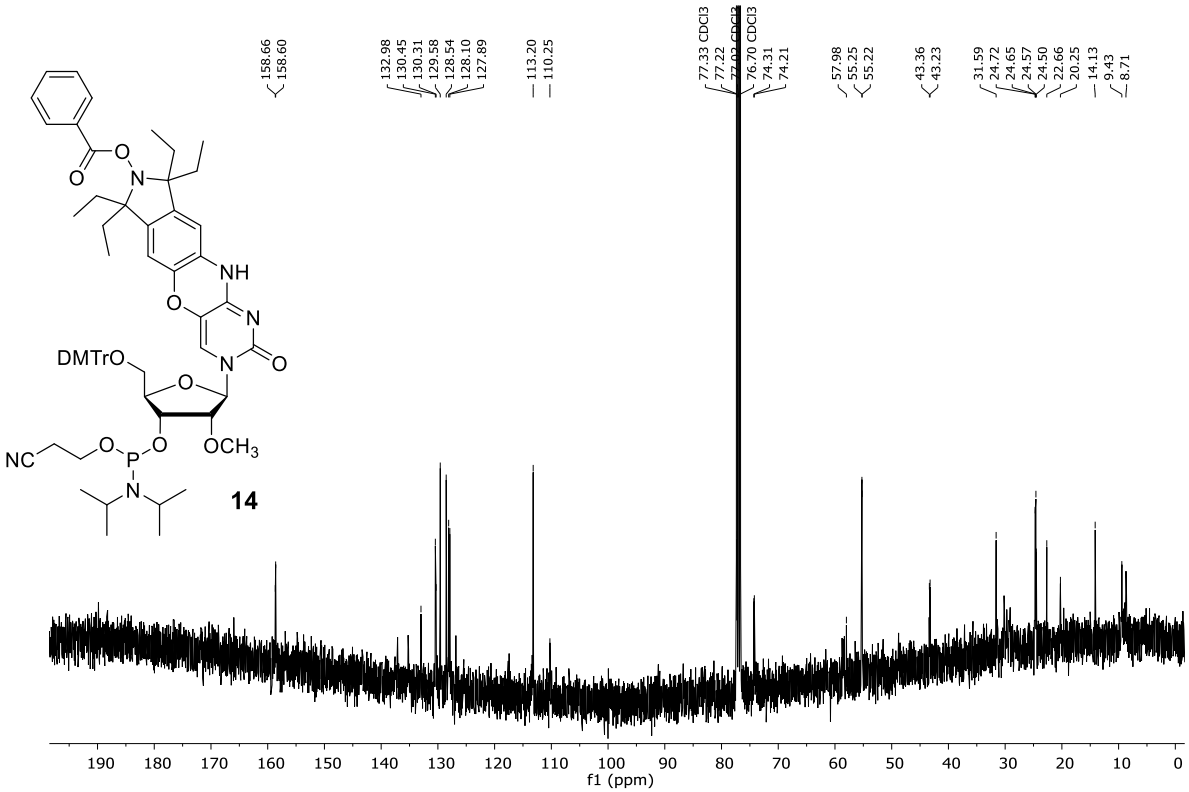

Figure S27. ^{13}C-NMR spectrum of **14**.

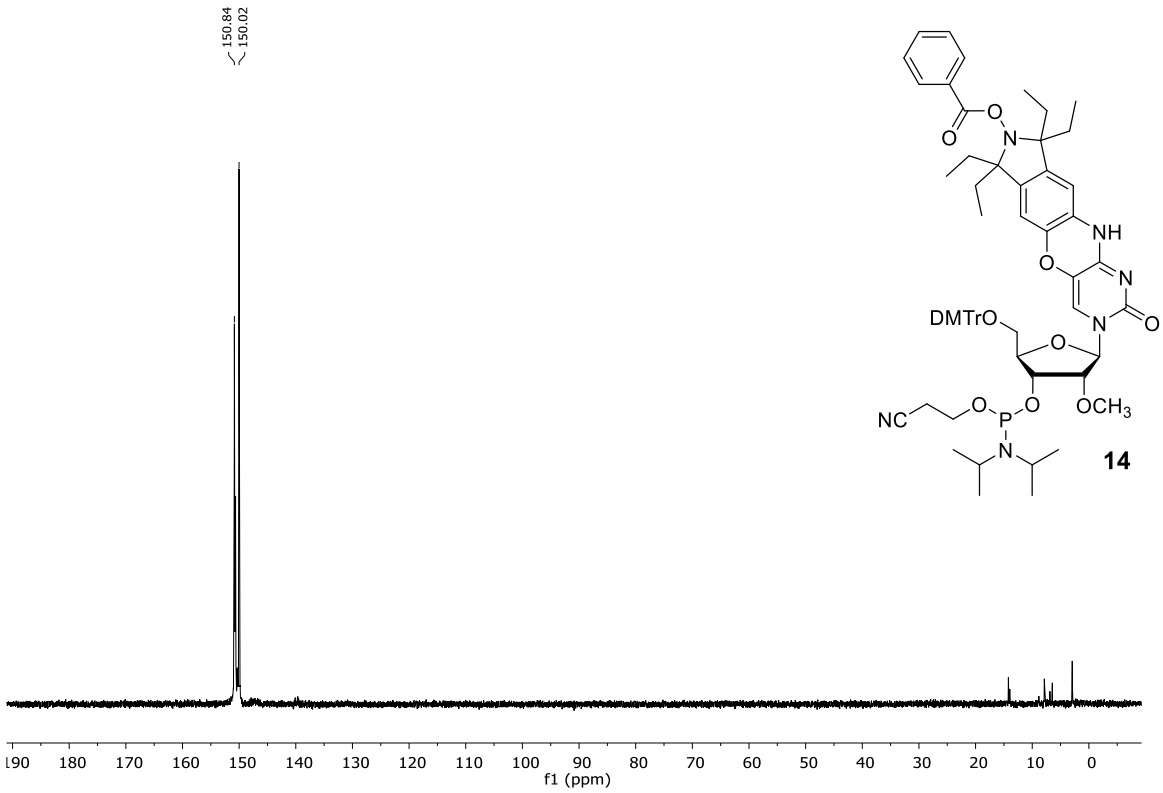

Figure S28. ^{31}P-NMR spectrum of phosphoramidite **14**.

Stability of EÇ and EÇm in ascorbic acid

The stability of **EÇ**, **EÇm**, **EÇ**-labeled DNA, and **EÇm**-labeled RNA in the presence of ascorbate was determined in the following manner. Each sample was dissolved in a solution of ascorbic acid (200 µM nitroxide, 5 mM ascorbic acid, 10 mM phosphate, 100 mM NaCl, 0.1 mM Na_2EDTA, pH 7.0, 10 µL) by immediate vortexing, followed by a brief centrifugation, placement in an EPR tube that was sealed in both ends and placed in the spectrometer. The first measurement was immediately performed, and subsequent measurements performed at set time-intervals. The parameters on the EPR spectrometer were as follows: B0: 337.0 mT; range: 12 mT; sweep time: 30 s; smooth: 0.1 s; NOPs: 4096; number of passes: 1. The temperature was set to 22 °C throughout the measurement. The EPR signal decay was subsequently plotted as a function of time (**Figures 5** and **S29**).

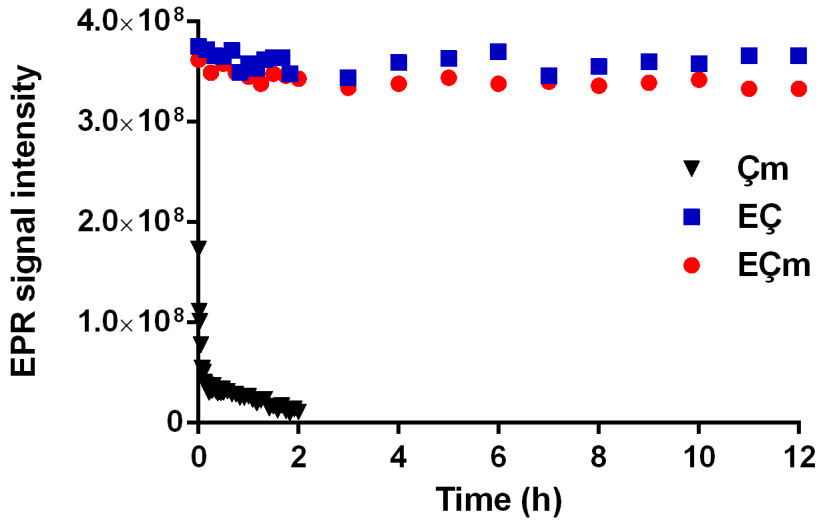

Figure S29. Stability of **EÇ, EÇm** and **Çm** in ascorbic acid (200 µM conc. of radical and 5 mM ascorbic acid in PDB buffer pH: 7.0). The EPR signal intensity is plotted as a function of time**.**

HPLC analyses of enzymatic digestion

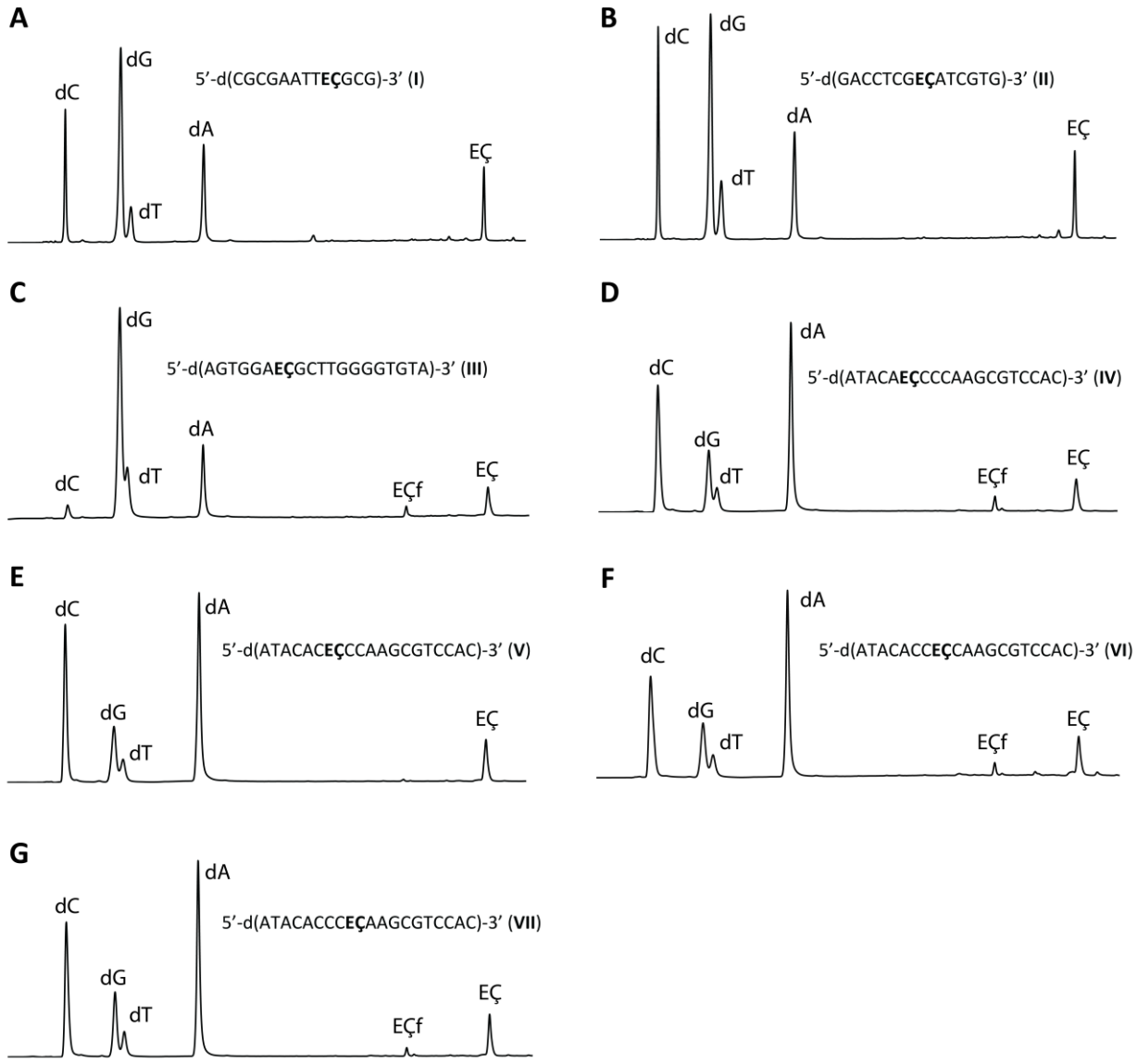

Figure S30. HPLC chromatograms of DNA oligonucleotides after enzymatic digestion with snake venom phosphodiesterase, nuclease P1, and alkaline phosphatase.[1-2]

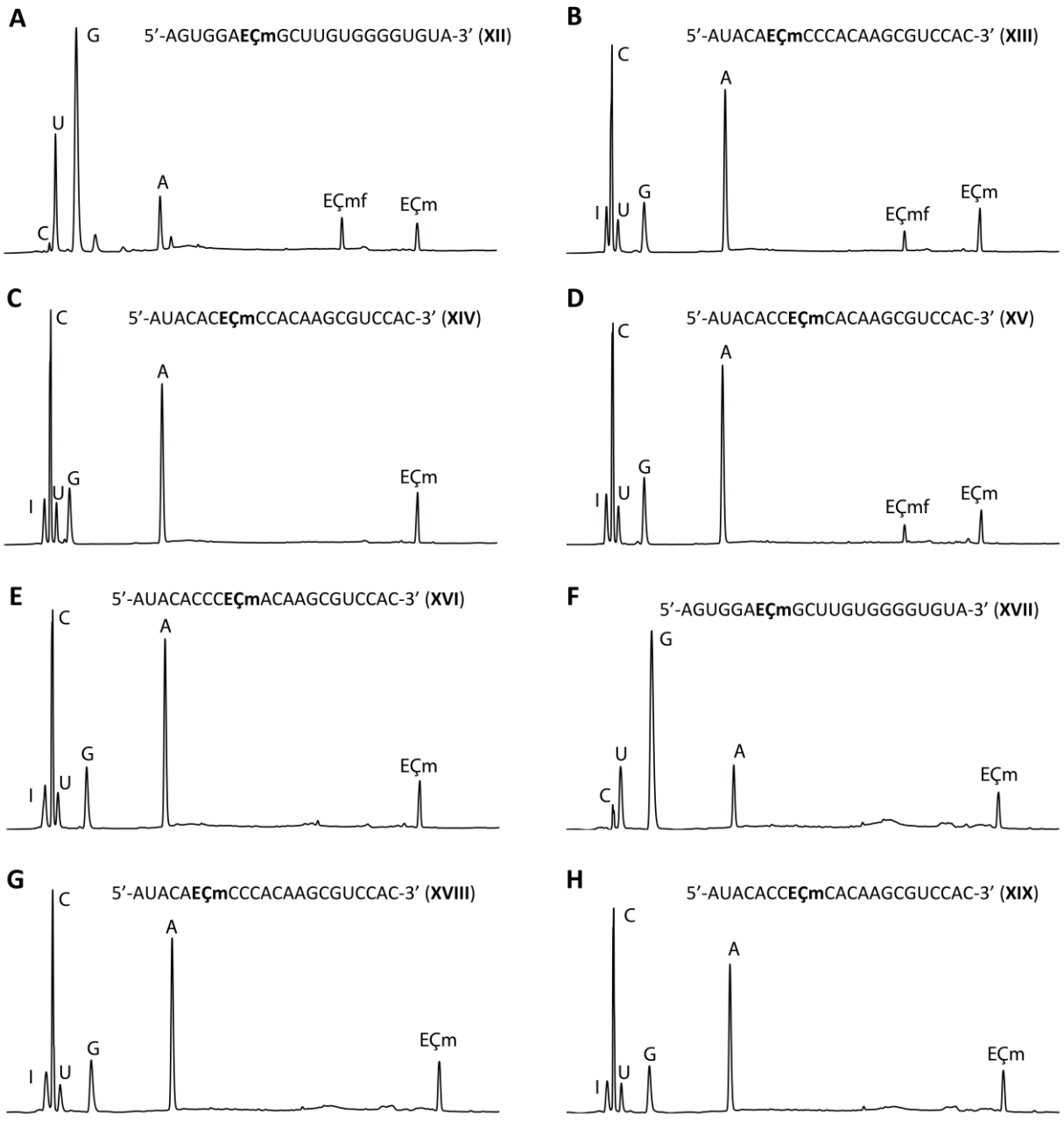

Figure S31. HPLC chromatograms of RNA oligonucleotides after enzymatic digestion with snake venom phosphodiesterase, nuclease P1, and alkalinephosphatase.

CD spectra of oligonucleotide duplexes

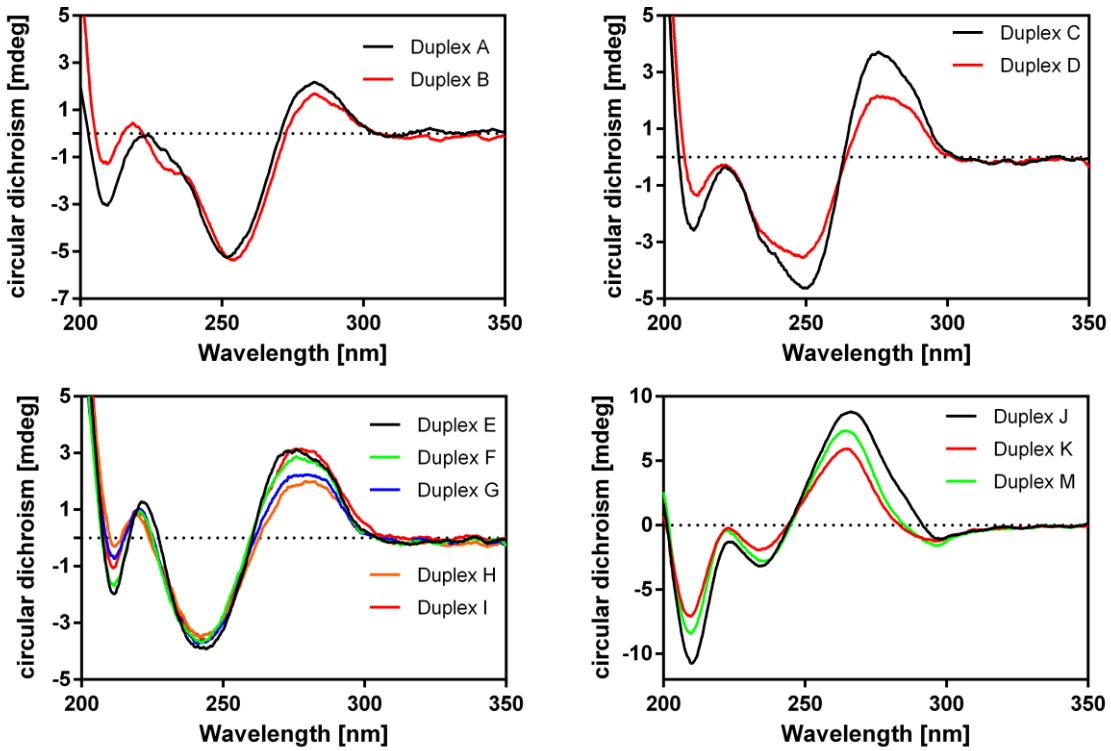

Figure S32. CD spectra of unmodified DNA and RNA duplexes along with their **EÇ** and **EÇm** labeled counterparts.

Thermal denaturing experiments of spin-labeled oligonucleotides

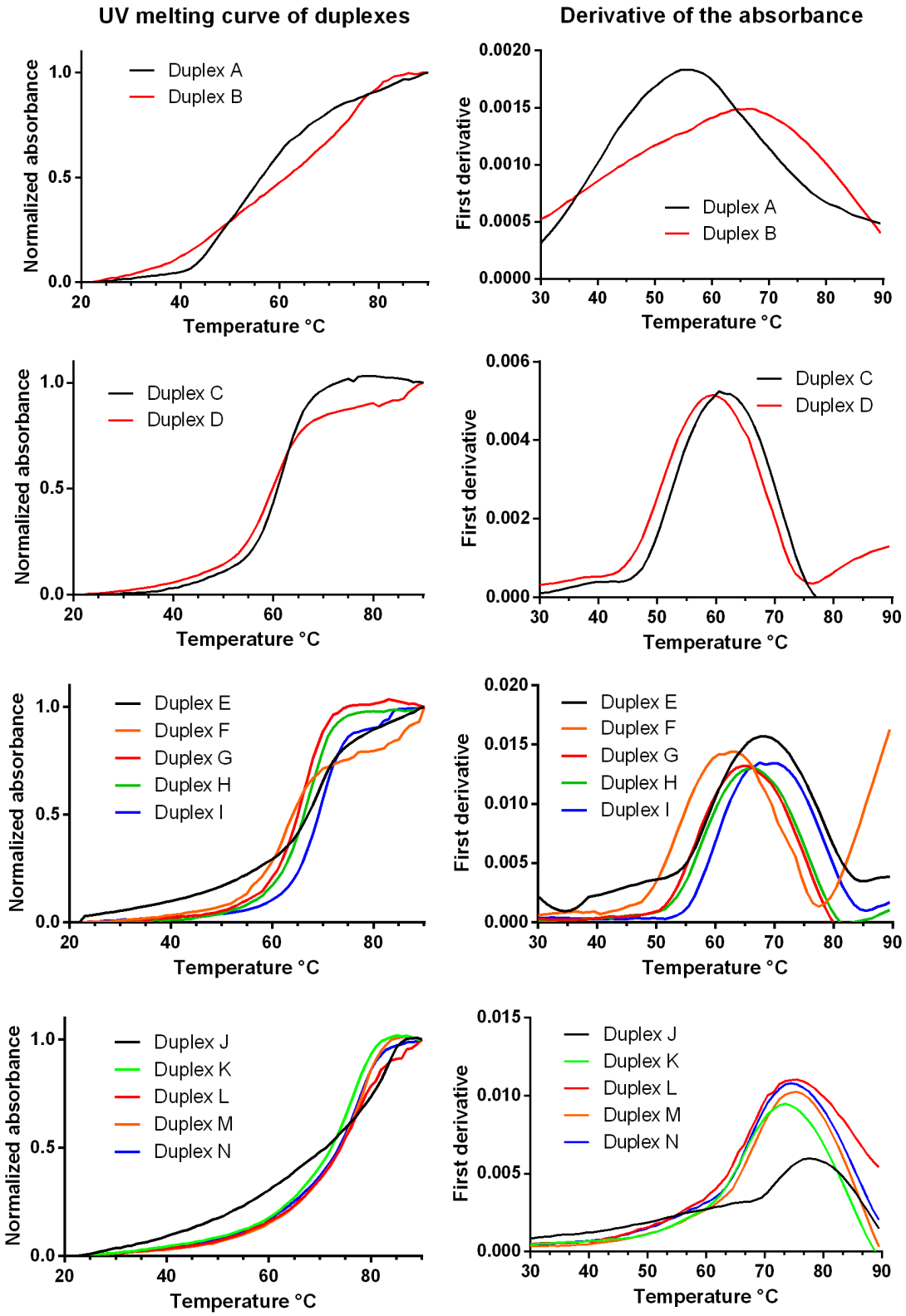

Figure S33. Thermal denaturing analysis of duplexes.

CW-EPR spectra of spin labeled oligonucleotides

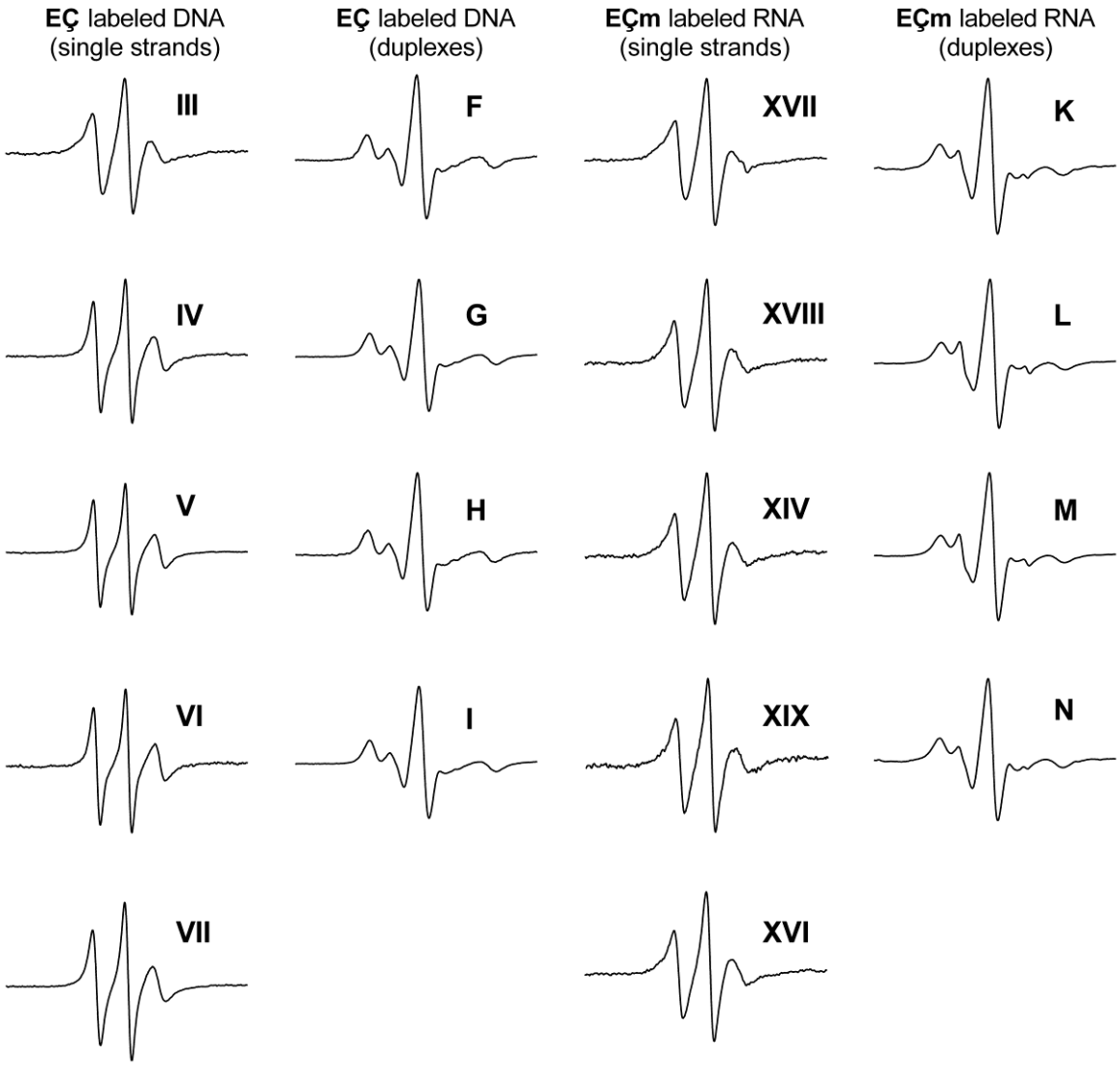

Figure S34. EPR spectra of spin-labeled oligonucleotides.

References

[1] H. Y. Juliusson, A.-L. J. Segler, S. T. Sigurdsson, *Eur. J. Org. Chem.* **2019**, *2019*, 3799-3805.
[2] P. Cekan, A. L. Smith, N. Barhate, B. H. Robinson, S. T. Sigurdsson, *Nucleic Acids Res.* **2008**, *36*, 5946-5954.

Paper III

Nitroxide-derived *N*-oxide phenazines for noncovalent spin-labeling of DNA

Haraldur Y. Juliusson[a] and Snorri Th. Sigurdsson*[a]

Abstract: Two *o*-benzoquinone derivatives of isoindoline were synthesized for use as building blocks for incorporation of isoindoline nitroxides into different compounds and materials. These *o*-quinones were condensed with a number of *o*-phenylenediamines to form isoindoline-phenazines in high yields. Subsequent oxidation gave phenazine-di-*N*-oxide isoindoline nitroxides that were evaluated for noncovalent and site-directed spin-labeling of duplex DNA and RNA that contained abasic sites. While no specific binding was observed for RNA, the unsubstituted phenazine-*N,N*-dioxide tetramethyl isoindoline nitroxide showed high binding affinity and specificity towards abasic sites in duplex DNA that contained cytosine as the orphan base.

Introduction

The field of radical chemistry has advanced considerably since the isolation and characterization of Fremy's salt (**1**) (**Figure 1**), an inorganic compound containing a nitroxide, described in 1845.[1] Over the years, the diversity of organic nitroxide radicals, a.k.a. aminoxyl radicals, has steadily increased. Of note is the synthesis of 2,2,6,6-tetramethyl-4-piperidone-1-oxyl (4-oxo-TEMPO) (**2**) (**Figure 1**), described by Lebedev *et al*. in 1959.[2] The subsequent discovery of Rozantsev and Neiman that nitroxides can be involved in various organic reactions without affecting the aminoxyl group,[3] opened the door for the synthesis of numerous structurally diverse radicals.[4] Stable nitroxide radicals have been utilized in a variety of applications, such as antioxidants,[5] free radical scavengers,[6] stabilizers in the materials industry,[7] catalytic oxidizers[8] and site-directed spin labels.[9]

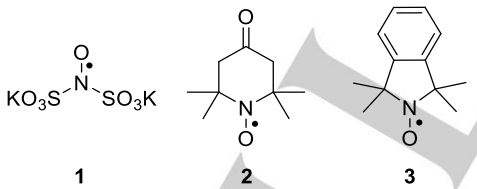

1 2 3

Figure 1. Structures of common aminoxyl radicals: Fremy's salt (**1**), 2,2,6,6-tetramethyl-4-piperidone-1-oxyl (4-oxo-TEMPO) (**2**) and an isoindoline nitroxide (**3**).

Isoindoline-based nitroxides (**3**) (**Figure 1**) have been the subject of much attention, because the fusion of the nitroxide-containing ring to the aromatic ring provides rigidity and renders them resistant to ring opening reactions, which is a significant decomposition pathway for pyrrolidine and piperidine nitroxides.[10] Isoindoline-nitroxides also have narrower electron paramagnetic resonance (EPR) line widths,[11] and the aromatic ring, which can undergo a variety of substitution reactions, can be used to build more complex structures for a wide range of applications.

Nitroxides have been used extensively as spin labels to study the structure and dynamics of biomolecules,[9] in particular nucleic acids and proteins. The term site-directed spin-labeling (SDSL) refers to the process of incorporation of a spin label at specific sites on diamagnetic biopolymers. For nucleic acid spin-labeling, there are three main approaches, namely the phosphoramidite approach, post-synthetic labeling and noncovalent labeling. The first two methods rely on covalent attachment of the spin labels that usually require time-consuming and non-trivial synthetic transformations. On the other hand, noncovalent spin-labeling utilizes binding through van der Waals interactions, hydrogen bonding and π-stacking. There are reports of spin-labeled intercalators and groove binders that bind to nucleic acids noncovalently, but most of them lack the sequence specificity that is usually required for EPR studies.[12] Noncovalent site-directed spin-labeling of the malachite green (MG) RNA aptamer has recently been reported, which utilized a spin-labeled derivative of tetramethylrosamine (TMR), and is the first example of site-specific spin labeling of a completely unmodified RNA.[13] Abasic sites in duplex nucleic acids have also been used as binding sites for noncovalent binding of small molecules. For example, fluorescent compounds that bind to abasic sites have been used for the detection of single nucleotide polymorphisms (SNPs).[14] An adenine acridine-derived spin-label has been used as an intercalator for noncovalent spin-labeling of a DNA duplex containing an abasic site.[15] The spin label **ç**, a cytosine-based spin label, bound specifically to abasic sites in duplex DNA opposite guanine (G).[16] The semi-flexible G-spin (**Ġ**), a guanine-based spin label, was found to bind to abasic sites in duplex RNA opposite cytosine (C) with high affinity.[17] In spite of these advances, there is still demand for new methods for making different functionalized nitroxide radicals that might possess improved qualities for noncovalent spin-labeling, and other applications.

Phenazines are an interesting class of compounds as they are redox-active and can therefore accept and donate electrons.[18] They are present in several natural products that are produced by Gram-positive and Gram-negative bacteria or by archaeal *Methanosarcina* species.[19] Phenazines display various interesting biologically-relevant functions[20] such as DNA-intercalation,[20-21] inhibition of topoisomerases,[22] production of reactive oxygen species (ROS)[23] and radical scavenging.[24] Oxidized phenazines, phenazine-di-*N*-oxides (**4**) (**Figure 2**), have also been reported to be good intercalators into duplex DNA.[25] The synthesis of substituted phenazines presents a challenge since most of the synthetic methods that have been reported are low yielding and can tolerate a limited number of functional groups.[20] Early approaches of synthesizing

[a] H. Y. Juliusson, Prof. Dr. S. Th. Sigurdsson
Department of Chemistry
Science Institute, University of Iceland
Dunhaga 3, 107 Reykjavik, Iceland.
E-mail: snorrisi@hi.is
Supporting information for this article is given via a link at the end of the document

phenazines, such as the Wohl-Aue procedure[26] (1901) and the Bamberger-Ham reaction[27] (1911) were performed under harsh conditions, were low yielding and formed a significant number of byproducts. In the mid-1960s, Haddadin and coworkers reported the Beirut reaction[28] which addressed some of the limitations of phenazine substituents met in earlier procedures. The synthesis of phenazines through Pd-catalyzed coupling was reported in late 2000[29] and further improved in 2013 by Laha *et al*.[30] The condensation of *o*-phenylenediamines with *o*-benzoquinones, generated *in situ* from the corresponding catechols, has also been an important route that directly gives phenazines in moderate to high yields.[20,31]

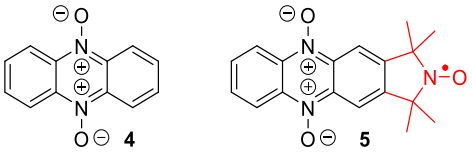

Figure 2. A structure of phenazine-di-*N*-oxide (**4**) and an isoindoline nitroxide-derived phenazine-di-*N*-oxide (**5**).

Here we describe the synthesis of *o*-benzoquinone derivatives of isoindoline that were condensed with a number of commercially available *o*-phenylenediamines to form isoindoline-phenazine skeletons. Oxidation of the isoindoline-phenazine moieties gave isoindoline-phenazine-*N,N*-dioxide nitroxide radicals, such as **5** (**Figure 2**), that were evaluated for noncovalent spin-labeling of nucleic acids. Compound **5** showed extensive binding affinity and specificity towards abasic sites in DNA.

Results and Discussion

The main incentive of this study was to prepare an isoindoline skeleton that would enable easy synthesis of structurally diverse nitroxide radicals, in particular by condensation with *o*-phenylenediamines to create isoindoline-phenazine structures. We designed *o*-benzoquinone derivatives of both tetramethyl (**6**) and tetraethyl (**7**) isoindoline, as tetraethyl isoindoline nitroxides are more resistant to reduction,[32] for condensation with *o*-phenylenediamines.

Synthesis of o-quinone isoindolines 6 and 7

The synthesis of **6** and **7** (**Scheme 1**) started with substitution of the bromines on tetramethylisoindoline **8**[33] and tetraethylisoindoline **9**[34] with methoxide to yield compounds **10**[35] and **11**, respectively. Initial attempts to prepare *o*-quinone derivatives **6** and **7** from **10** and **11**, respectively, by AgO and nitric acid-assisted oxidation[36] gave **6** and **7** only in very low yields. Therefore, dihydroxyl derivatives **12** and **13** were first prepared by demethylation of **10** and **11**, respectively. Reactions of **10** and **11** with boron tribromide or iodotrimethylsilane, commonly used for demethylation of methyl ethers,[37] under a variety of conditions led to complex mixtures of products, which at best resulted in very low yields of **12** and **13**. However, demethylation with iodotrimethylsilane, followed by a water-free workup and precipitation gave **12** and **13** in excellent yields. *O*-quinones **6** and **7** were subsequently obtained in excellent yields by oxidation of **12** and **13** with MnO_2 in the presence of air.[38]

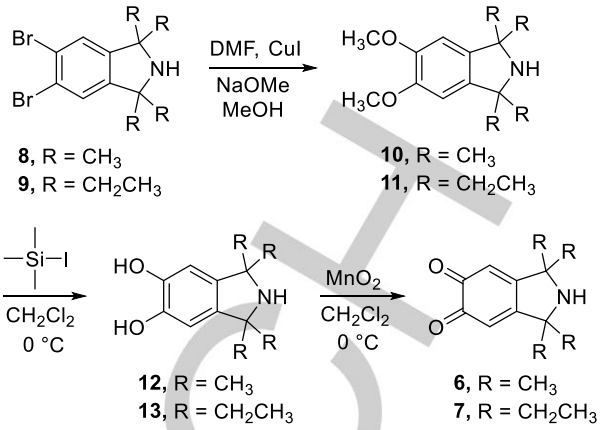

Scheme 1. Synthesis of *o*-quinone isoindolines **6** and **7**. Yields were as follows: **10** (95%), **11** (62%), **12** (91%), **13** (77%), **6** (88%), **7** (93%).

Condensation of 6 and 7 with o-phenylenediamines to give phenazines

Several different conditions were evaluated for condensation of **6** with *o*-phenylenediamine **14** (**Table 1**) to obtain **15**. Most of the solvents that were evaluated resulted in moderate to excellent yields. Acetic acid (**Table 1**, entry 3) and EtOH (70% in H_2O) (**Table 1**, entry 5) proved to be the best conditions. Using catalytic amount of a base led only to rapid decomposition of the diketones (**Table 1**, entry 6-8). In contrast, acetic acid was very effective as a catalyst. The optimal conditions proved to be 70% EtOH (aq.) with catalytic amount of acetic acid (**Table 1**, entry 11).

Table 1. Evaluation of reaction conditions for the synthesis of phenazine **15** from *o*-quinone **6**.

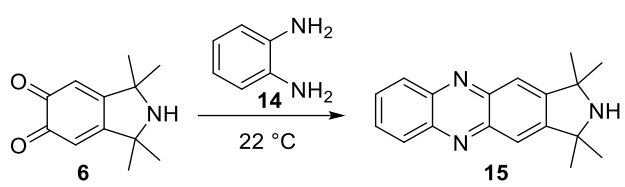

No.	Solvent	Catalyst	Time	Yield (%)
1	EtOH	-	40 min	90
2	CH2Cl2	-	60 min	70
3	AcOH	-	<1 min	95
4	CH3CN	-	50 min	83
5	70% EtOH	-	30 min	94
6	70% EtOH	KOH	<5 min	0
7	EtOH	Pyridine	10 min	<1%
8	EtOH	Et3N	10 min	<5%
9	CH3CN	AcOH	10 min	95
10	CH2Cl2	AcOH	10 min	95
11	70% EtOH	AcOH	<1 min	99
12	EtOH	AcOH	5 min	95

A number of commercially available *o*-phenylenediamines with different functional groups were condensed with *o*-benzoquinones **6** and **7** to both investigate the scope of the condensation reaction and to create a small library of compounds for noncovalent spin-labeling (**Table 2**). All the selected *o*-phenylenediamines condensed readily with the diketones to give the desired products in near quantitative yields (>93%) (**Table 2**, entry 1-6), except for **24** (**Table 2**, entry 7) which did not give the desired product using any of the reaction conditions listed in **Table 1**. We postulate that the low solubility of **24** was the cause; low rate of condensation led to decomposition of *o*-quinones **6** and **7**, both of which had limited stability in solution at room temperature (complete decomposition in 1-2 h). Compound **24** was soluble in DMSO but did not yield any condensed products upon incubation with **6** (in the presence or absence of a catalytic amount of acetic acid).

Table 2. Condensation of **6** and **7** with different derivatives of *o*-diamines.

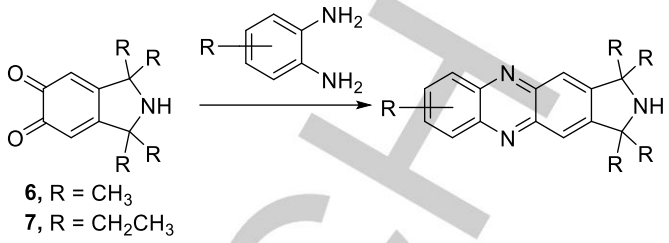

6, R = CH_3
7, R = CH_2CH_3

Diamine	*O*-quinone	Product	Yield (%)
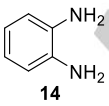 **14**	**6**	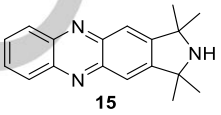 **15**	99
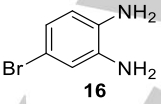 **16**	**6**	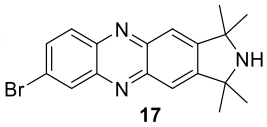 **17**	95
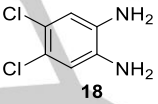 **18**	**6**	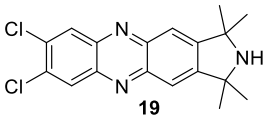 **19**	95
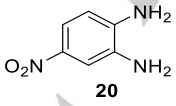 **20**	**6**	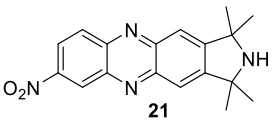 **21**	93
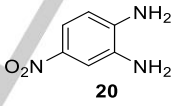 **20**	**7**	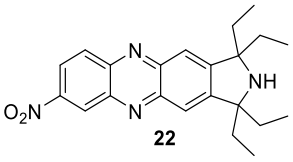 **22**	90
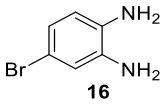 **16**	**7**	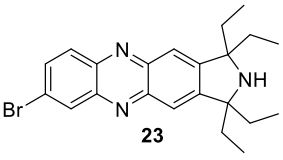 **23**	96
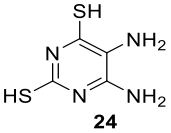 **24**	**6**	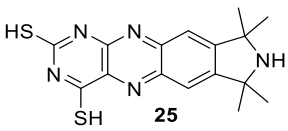 **25**	0

Phenazine-N-oxide derived nitroxides

While oxidizing the phenazines with *m*-CPBA, it became apparent that the level of oxidation could be controlled by the number of equivalents of the oxidizing agent used in the reaction. When **15** was treated with one equivalent of *m*-CPBA, only nitroxide **26** was obtained (**Scheme 2**). The mono-*N*-oxide aminoxyl radical **27** was obtained with 2.2 eq. of the oxidizing agent and 5.5 eq. gave the di-*N*-oxide radical **5** (**Scheme 2**), all in very good to excellent yields.

For evaluating the isoindoline nitroxide-derived phenazines as noncovalent spin labels for duplex DNA and RNA containing abasic sites, the di-*N*-oxides were prepared, since **26** and **27** had limited or no solubility in water. Oxidation of compounds **15**, **17**, **19**, **21** and **23** gave the desired phenazine di-*N*-oxide radicals **5** and **28**-**31** in very good yields (**Table 3**).

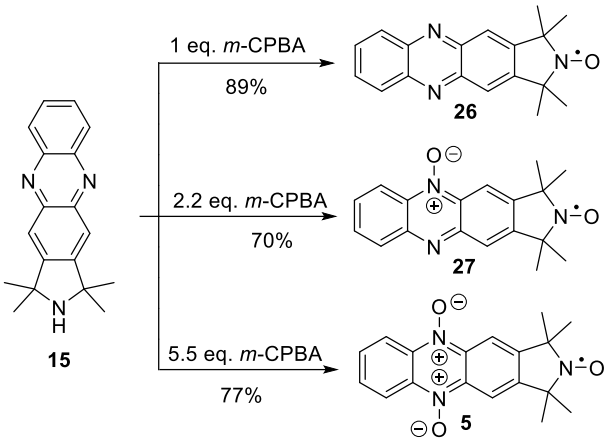

Scheme 2. Reaction of phenazine **15** with different amounts of oxidizing agent.

Since NMR spectra of the paramagnetic phenazine di-*N*-oxide nitroxides give limited information due to peak-broadening and even loss of NMR signals, UV-vis spectroscopy was used for spectroscopic characterization of the di-*N*-oxides (**Figure S30**), in addition to HRMS. Absorption peaks at 250 and 370 nm for the phenazine derivatives were red-shifted to 290 and 490 nm upon oxidation to the di-*N*-oxide radicals. The phenazine di-*N*-oxide skeleton rendered the radicals water soluble to some extent, with the exception of the tetraethyl derivative **31**, which made it possible to evaluate almost all as spin labels.

Spin-labeling of abasic sites in duplex oligonucleotides

Binding of **5**, **28**, **29** and **30** to abasic sites in DNA duplexes was evaluated by EPR spectroscopy.[16] Each spin label was incubated with a 14-mer duplex DNA containing an abasic site with either G, T, A or C as the orphan base at -30 °C (**Figure 3**). The EPR spectrum of each spin label in the absence of DNA (**Figure 3**, top row) showed comparatively narrow lines, consistent with fast tumbling of the radical in solution. In contrast, an EPR spectrum of a spin label bound to a DNA duplex is wider due to a longer rotational correlation time,[16] as observed for spin label **5**, which showed high binding affinity and specificity towards abasic sites opposite to C (**Figure 3**, spectrum in upper box). Nitroxide **5** also showed nearly full binding (ca. 90%) opposite to A (**Figure 3**, spectrum in lower box), but a moderate to low binding opposite to T, represented by the mixture of slow- and fast-moving components in its EPR spectrum. No binding of **5** was observed to abasic sites opposite to G nor to an unmodified duplex. Spin label **28** and **29** showed limited binding to abasic sites while **30** showed extensive binding to abasic sites opposite to all the nucleobases (C, A, G and T). However, substantial binding of **30** was also observed to the unmodified duplex to an extent of ca. 85% (**Figure 3**, bottom row to the right). The extensive nonspecific binding of **30** is most likely due to a large dipole moment, because of the nitro group, which facilitates intercalation.[39]

Table 3. Oxidation of isoindoline-phenazines to the corresponding isoindoline-phenazine di-N-oxide nitroxide radicals.

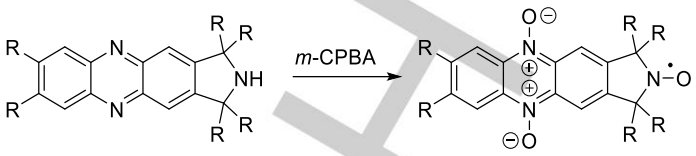

Starting compound	Product	Yield (%)
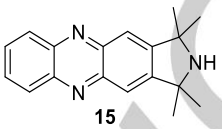 **15**	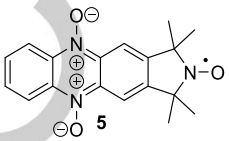 **5**	77
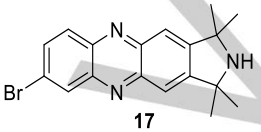 **17**	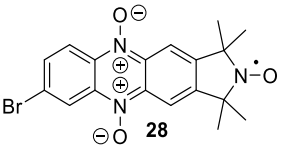 **28**	72
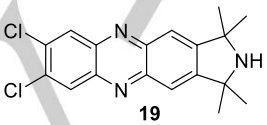 **19**	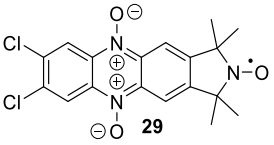 **29**	70
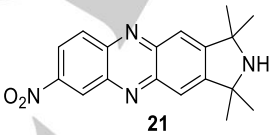 **21**	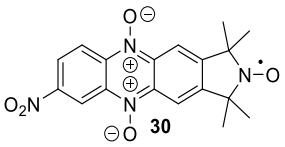 **30**	78
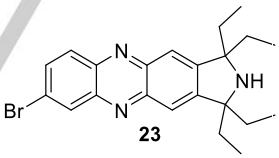 **23**	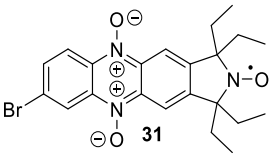 **31**	75

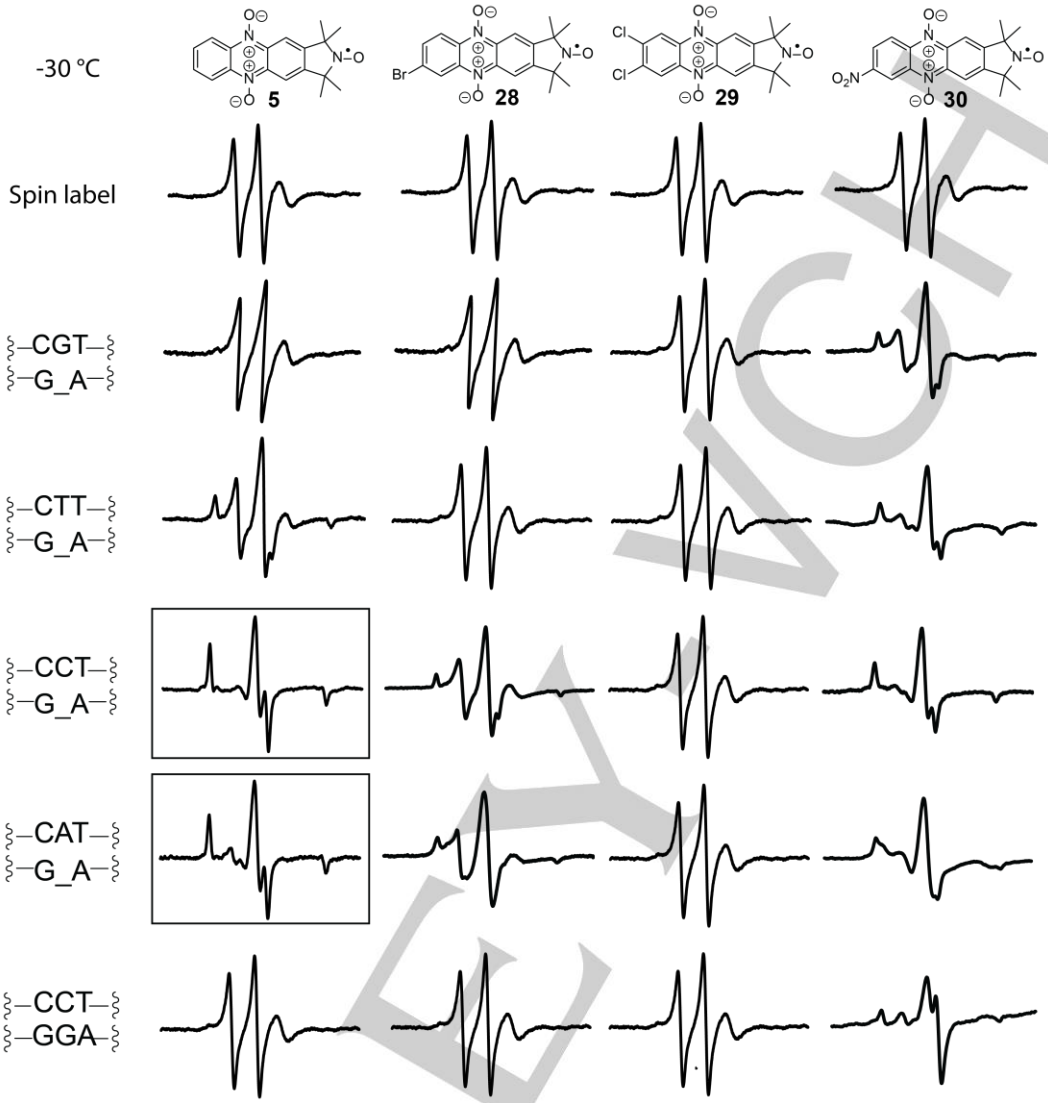

Figure 3. Noncovalent spin labeling of abasic sites in DNA duplexes evaluated by EPR spectroscopy at -30 °C. EPR spectra of the labels without DNA (top row) and in the presence of unmodified DNA (bottom row) is shown for comparison. The central four rows show the spin labels in the presence of DNA duplexes containing an abasic site (denoted by "_") opposite to the orphan bases G, T, A and C. Only a part of the DNA construct is shown to the left; the complete sequence is 5'-d(GACCTCG_ATCGTG)-3'·5'-d(CACGATXCGAGGTC)-3', where X represents the orphan base. EPR spectra of the spin-labels (100 μM) in the presence of DNA duplexes (200 μM) were recorded in phosphate buffer (10 mM $NaHPO_4$, 100 mM NaCl, 0.1 mM Na_2EDTA, pH 7.0) containing 30% ethylene glycol and 2% DMSO at -30 °C.

As spin label **5** exhibited full binding to abasic sites opposite to C and almost full binding opposite to A, the temperature dependence was investigated to obtain information about the relative affinity of the spin label to the abasic sites in question (**Figure 4**). Significant binding was already observed for the abasic site opposite to C at 0 °C, while close to no binding was seen for A, and almost full binding was observed at -20 °C (>95%). Little to no binding was observed at +10 °C and no binding was seen at +20 °C (data not shown). Comparison with the binding affinity of the previously reported noncovalent spin labels **Ǵ** (K_d = 6.02 x 10^{-6} M at 0 °C)[17b] and **ç** (K_d = 1.36 x 10^{-4} M at 0 °C)[16] to abasic sites in DNA opposite to C, shows that spin label **5** possesses higher affinity (K_d = 1.4 x 10^{-6} M at 0 °C). Spin label **5** did not show any binding to 14-mer duplex RNA containing an abasic site opposite to G, U, A or C at -30 °C (**Figure S31**), demonstrating its selectivity for DNA. In contrast, **Ǵ** shows extensive binding to abasic sites in RNA opposite C, even at +20 °C.

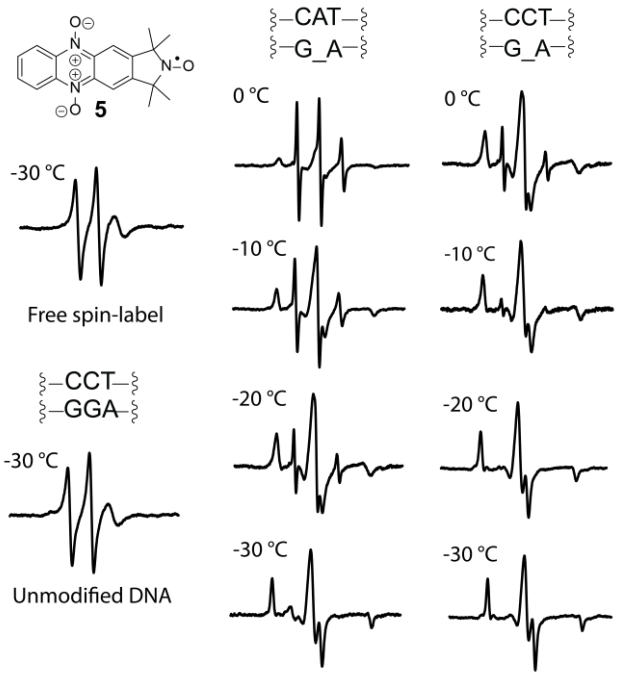

Figure 4. Evaluation of temperature-dependent noncovalent spin-labeling of spin label **5** to abasic sites in DNA duplexes opposite to A (middle column) and C (right column), by EPR spectroscopy. The EPR spectra of **5** alone and in the presence of an unmodified DNA at -30 °C are shown to the left. The EPR measurements were performed under the same conditions as listed in figure legend to **Figure 3**.

Conclusion

We have demonstrated the synthesis of *o*-benzoquinone derivatives for both tetramethyl- and tetraethyl-isoindoline that were readily condensed with a number of commercially available *o*-phenylenediamines in near quantitative yields. Oxidation of the isoindoline-phenazines gave phenazine di-*N*-oxide nitroxide radicals that were evaluated as noncovalent spin labels for DNA and RNA containing abasic sites. Spin label **5** showed high binding affinity and specificity towards abasic sites opposite to C in DNA and is therefore a promising spin label for future EPR studies of DNAs. Moreover, the *o*-benzoquinone isoindoline derivatives **6** and **7** give access to various diversely substituted phenazine structures carrying the isoindoline moiety and thereby facilitate the incorporation of paramagnetic centers into other functional systems.

Experimental Section

General materials and methods. All commercially available reagents were purchased from Sigma-Aldrich co gmph or Acros Organics and used without further purification. CH_2Cl_2 was dried over calcium hydride and freshly distilled before use. All moisture- and air-sensitive reactions were carried out in oven-dried glassware under an inert atmosphere of Ar. Thin-layer chromatography (TLC) was performed using glass plates pre-coated with silica gel (0.25 mm, F-25, Silicycle) and compounds were visualized under UV light and by *p*-anisaldehyde staining. Column chromatography was performed using 230–400 mesh silica gel (Silicycle). ^{1}H- and ^{13}C-NMR spectra were recorded with a Bruker Avance 400 MHz spectrometer. Chemical shifts are reported in parts per million (ppm) relative to the partially deuterated NMR solvents $CDCl_3$ (7.26 ppm for ^{1}H NMR and 77.16 ppm for ^{13}C) and CD_3OD (3.35, 4.78 ppm for ^{1}H NMR and 49.3 ppm for ^{13}C). All coupling constants were measured in Hertz (Hz). Nitroxide radicals show broadening and loss of NMR signals due to their paramagnetic nature and therefore, those NMR spectra are not shown. Mass spectrometric analyses of all organic compounds were performed on an HRMS (ESI) (Bruker, MicrOTOF-Q) in positive ion mode.

DNA and RNA synthesis and purifications. All commercial phosphoramidites, CPG columns, 5-ethylthiotetrazole and acetonitrile for oligomer synthesis were purchased from ChemGenes Corp., USA. All other required reagents and solvents were purchased from Sigma-Aldrich Co gmbh. Unmodified oligonucleotides and those containing abasic sites were synthesized on an automated ASM800 DNA synthesizer (Biosset, Russia) using a trityl-off protocol and commercially available phosphoramidites with standard protecting groups on a 1.0 µmole scale (1000 Å CPG columns). The DNA oligomers were deprotected in satd. NH_3 at 55 °C for 8 h and dried *in vacuo*. The RNA oligomers were deprotected in a 1:1 solution (2 mL) of CH_3NH_2 (8 M in EtOH) and NH_3 (33% w/w in H_2O) at 65 °C for 45 min. The solvent was removed *in vacuo* and the TBDMS-protecting groups were removed by incubation in NEt_3:3HF (600 µL) for 90 min at 55 °C in DMF (200 µL), followed by addition of water (200 µL). This solution was transferred to a 50 mL Falcon tube, *n*-butanol (20 mL) was added and the mixture stored at −20 °C for 14 h, centrifuged at 4 °C and the solvent decanted from the RNA pellet. The oligonucleotides were purified by 20% denaturing polyacrylamide gel electrophoresis. The oligonucleotides were visualized by UV light and the bands were excised from the gel, crushed and extracted from the gel matrix with a Tris buffer (250 mM NaCl, 10 mM Tris, 1 mM Na_2EDTA, pH 7.5). The extracts were filtered through 0.45 µm, 25 mm diameter GD/X syringe filters (Whatman, USA) and desalted using Sep-Pak cartridges (Waters, USA), according to the manufacturer's instructions. After removing the solvent *in vacuo*, the oligomers were dissolved in deionized and sterilized water (200 µL). Oligonucleotides were quantified using Beer's law and measurements of absorbance at 260 nm, using extinction coefficients determined by using the WinLab oligonucleotide calculator (V2.85.04, PerkinElmer).

EPR measurements. Solutions for CW-EPR experiments were prepared by mixing aliquots of stock solutions of a single-stranded oligomer containing an abasic site, its complementary strand and the spin label in question (1:1.2:0.5). The solvent was evaporated *in vacuo* and the resulting residue was dissolved in phosphate buffer (10 µL; 10 mM $NaHPO_4$, 100 mM NaCl, 0.1 mM Na_2EDTA, pH 7.0) and annealed as followed: 90 °C for 2 min, 60 °C for 5 min, 50 °C for 5 min, 22 °C for 15 min and dried using a SpeedVac. The residue was dissolved in an aqueous 30% ethylene glycol solution (10 µL) containing 2% DMSO and placed in a 50 µL quartz capillary (BLAUBRAND intraMARK) (final concentration of nucleic acid duplex 200 µM). The EPR spectra were recorded using 100-200 scans on a MiniScope MS200 (Magnettech Germany) spectrometer (100 kHz modulation frequency, 1.0 G modulation amplitude and 2.0 mW microwave power). A magnettech temperature controller M01 (± 0.5 °C) was used as temperature regulator.

5,6-Dimethoxy-1,1,3,3-tetramethylisoindoline (10). A solution of **8** (350 mg, 1.05 mmol) in DMF (1.5 mL) was added to a stirred solution of NaOMe in MeOH (5 M, 2 mL). Copper iodide (60 mg, 0.3 mmol) was added and the mixture heated at 145 °C for 29 h. The reaction mixture was cooled to room temperature, poured onto ice and extracted with Et_2O (3 x 30 mL). The combined organic phases were washed with H_2O (2 x 30 mL) and brine (3 x 30 mL), dried over Na_2SO_4 and concentrated *in vacuo* to yield **10** (160 mg, 95%) as a brown-orange solid, which was directly used for the next step without further purification. ^{1}H-NMR (400 MHz, $CDCl_3$): δ = 6.62 (s, 2H), 3.90 (s, 6H), 1.45 (s, 12H). ^{13}C-NMR (101 MHz, $CDCl_3$): δ = 148.9, 140.3, 104.5, 62.8, 56.5, 32.0. HRMS (ESI) *m/z* $[M+H]^+$ calcd for $C_{14}H_{22}NO_2^+$: 236.1645; found 236.1632.

1,1,3,3-Tetramethylisoindoline-5,6-diol (12). A solution of **10** (100 mg, 0.425 mmol) in CH_2Cl_2 (5 mL) was treated with iodotrimethylsilane (0.2 mL, 1.40 mmol) at 0 °C and the reaction mixture was stirred at 22 °C for 72 h. MeOH (10 mL) was added and the solution was stirred for 1 h and concentrated *in vacuo* to yield a black oily residue that subsequently solidified. The black residue was dissolved in a minimum amount of MeOH (1 mL) followed by a slow addition of CH_2Cl_2 (20 mL) to yield a gray precipitate. The solid was filtered and washed with cold CH_2Cl_2 to yield **12** (80 mg, 91%) as a white solid. ^{1}H-NMR (400 MHz, CD_3OD): δ = 6.72 (s, 2H), 1.67 (s, 12H). ^{13}C-NMR (101 MHz, CD_3OD) δ = 148.7, 131.0, 109.3, 77.1, 25.5. HRMS (ESI) *m/z* $[M+H]^+$ calcd for $C_{12}H_{18}NO_2^+$: 208.1332; found 208.1336.

1,1,3,3-Tetramethylisoindoline-5,6-dione (6). A solution of **12** (25 mg, 0.12 mmol) in MeOH (0.5 mL) was added to a stirred solution of MnO_2 (1.0 g) in CH_2Cl_2 (20 mL) and the resulting mixture stirred at 22 °C for 3 h. The reaction mixture was filtered through a Büchner funnel, MnO_2 was recovered, the filtrate was concentrated *in vacuo* and the residue purified by flash-column chromatography, using a gradient elution (CH_2Cl_2/MeOH, 100:0 to 90:10), to yield **6** (22 mg, 88 %) as a dark brown solid. ^{1}H-NMR (400 MHz, $CDCl_3$): δ = 6.17 (s, 2H), 1.44 (s, 12H). ^{13}C-NMR (101 MHz, $CDCl_3$): δ = 178.7, 167.3, 120.8, 70.6, 60.6, 31.6, 30.6, 29.7, 27.5. HRMS (ESI) *m/z* $[M+H]^+$ calcd for $C_{12}H_{16}NO_2^+$: 206.1176; found 206.1172.

1,1,3,3-Tetraethyl-5,6-dimethoxyisoindoline (11). A solution of **9** (350 mg, 0.90 mmol) in anhydrous DMF (1.5 mL) was added to a stirred solution of NaOMe in MeOH (5 M, 2 mL). Copper iodide (60 mg, 0.3 mmol) was added and the mixture was heated at 145 °C for 29 h. The reaction mixture was cooled to room temperature, poured onto ice and extracted with Et_2O (3 x 30 mL). The combined organic phases were washed with H_2O (2 x 30 mL) and brine (3 x 30 mL), dried over Na_2SO_4 and concentrated *in vacuo* to yield **11** (160 mg, 62%) as a brown-orange solid, which was directly used for the next step without further purification. ^{1}H-NMR (400 MHz, $CDCl_3$) δ = 6.56 (s, 2H), 3.87 (s, 6H), 1.75 – 1.57 (m, 8H), 0.88 (t, *J* = 7.5 Hz, 12H).

1,1,3,3-Tetraethylisoindoline-5,6-diol (13). A solution of **11** (160 mg, 0.552 mmol) in CH_2Cl_2 (5 mL) was treated with iodotrimethylsilane (0.26 mL, 1.82 mmol) at 0 °C and the solution was stirred at 22 °C for 72 h. MeOH (10 mL) was added and the solution stirred for 1 h and concentrated *in vacuo* to yield a black oily residue that subsequently solidified. The black residue was dissolved in minimum amount of MeOH (1 mL) followed by a slow addition of CH_2Cl_2 (20 mL) to yield a gray precipitate. The solid was filtered and washed with cold CH_2Cl_2 to yield **13** (112 mg, 77%) as a white solid. ^{1}H-NMR (400 MHz, CD_3OD): δ = 6.64 (s, 2H), 2.04 (q, *J* = 7.4 Hz, 8H), 1.03 (t, *J* = 7.4 Hz, 12H). ^{13}C-NMR (101 MHz, CD_3OD): δ = 147.9, 132.2, 110.7, 76.8, 31.7, 8.7. HRMS (ESI) *m/z* $[M+H]^+$ calcd for $C_{16}H_{26}NO_2^+$: 264.1958; found 264.1948.

1,1,3,3-Tetraethylisoindoline-5,6-dione (7). A solution of **13** (27 mg, 0.10 mmol) in MeOH (0.5 mL) was added to a stirred solution of MnO_2 (1000 mg) in CH_2Cl_2 (20 mL) and the resulting mixture stirred for 3 h at room temperature. The reaction mixture was filtered through a Büchner funnel, MnO_2 was recovered, the filtrate was concentrated *in vacuo* and the residue purified by flash-column chromatography (CH_2Cl_2 100%), to yield **7** (25 mg, 93 %) as a dark brown solid. ^{1}H-NMR (400 MHz, $CDCl_3$): δ = 6.10 (s, 2H), 1.65 (qd, *J* = 14.1, 7.3 Hz, 8H), 0.93 (t, *J* = 7.4 Hz, 12H). ^{13}C-NMR (101 MHz, $CDCl_3$): δ = 178.8, 166.4, 121.6, 66.5, 32.9, 8.5. HRMS (ESI) *m/z* $[M+H]^+$ calcd for $C_{16}H_{24}NO_2^+$: 262.1802; found 262.1801.

Isoindoline phenazine 15. To a solution of 70% EtOH in H_2O (4 mL) containing 1 drop of AcOH was added **6** (98.4 mg, 0.48 mmol) and **14** (73.5 mg, 0.48 mmol) and the solution was stirred at 22 °C for 30 min. The solvent was removed *in vacuo* and the residue purified by flash-column chromatography, using a gradient elution (CH_2Cl_2/MeOH, 100:0 to 90:10), to yield **15** (131.8 mg, 99 %) as a yellowish solid. ^{1}H-NMR (400 MHz, $CDCl_3$): δ = 8.11 (dd, *J* = 6.7, 3.4 Hz, 2H), 7.85 (s, 2H), 7.69 (dd, *J* = 6.7, 3.4 Hz, 2H), 1.53 (s, 13H). ^{13}C-NMR (101 MHz, $CDCl_3$) δ = 154.95, 142.95, 130.03, 129.43, 120.76, 103.38, 62.29, 32.11. HRMS (ESI) *m/z* $[M+H]^+$ calcd for $C_{18}H_{20}N_3^+$: 278.1652; found 278.1633.

Bromo isoindoline phenazine 17. To a solution of 70% EtOH in H_2O (2.5 mL) containing 1 drop of AcOH was added **6** (16.4 mg, 0.079 mmol) and **16** (14.9 mg, 0.079 mmol) and the solution was stirred at 22 °C for 30 min. The solvent was removed *in vacuo* and the residue purified by flash-column chromatography, using a gradient elution (CH_2Cl_2/MeOH, 100:0 to 90:10), to yield **17** (26.7 mg, 95 %) as a brownish-yellow solid. ^{1}H-NMR (400 MHz, $CDCl_3$): δ = 8.41 (d, *J* = 2.0 Hz, 1H), 8.07 (d, *J* = 9.2 Hz, 1H), 7.92 (s, 2H), 7.85 (dd, *J* = 9.2, 2.1 Hz, 1H), 1.67 – 1.59 (m, 13H). ^{13}C-NMR (101 MHz, $CDCl_3$): δ = 155.9, 155.5, 143.8, 143.5, 143.2, 141.6, 133.8, 131.5, 130.7, 124.5, 121.0, 120.9, 62.5, 32.1, 29.7. HRMS (ESI) *m/z* $[M+H]^+$ calcd for $C_{18}H_{19}BrN_3^+$: 356.0757; found 356.0757.

Dichloro isoindoline phenazine 19. To a solution of 70% EtOH in H_2O (2.5 mL) containing 1 drop of AcOH was added **6** (12.0 mg, 0.058 mmol) and **18** (10.3 mg, 0.058 mmol) and the solution was stirred at 22 °C for 30 min. The solvent was removed *in vacuo* and the residue purified by flash-column chromatography, using a gradient elution (CH_2Cl_2/MeOH, 100:0 to 90:10), to yield **19** (19.1 mg, 95 %) as a brownish yellow solid. ^{1}H-NMR (400 MHz, $CDCl_3$) δ = 8.35 (s, 2H), 7.91 (s, 2H), 1.65 (s, 12H). ^{13}C-NMR (101 MHz, $CDCl_3$): δ = 144.0, 141.6, 129.8, 121.1, 117.6, 77.5, 77.2, 76.8, 62.7, 32.1, 29.8. HRMS (ESI) *m/z* $[M+H]^+$ calcd for $C_{18}H_{18}Cl_2N_3^+$: 346.0872; found 346.0862.

Nitro isoindoline phenazine 21. To a solution of 70% EtOH in H_2O (4 mL) containing 1 drop of AcOH was added **6** (24.4 mg, 0.12 mmol) and **20** (18.2 mg, 0.12 mmol) and the solution was stirred at 22 °C for 30 min. The solvent was removed *in vacuo* and the residue purified by flash-column chromatography, using a gradient elution (CH_2Cl_2/MeOH, 100:0 to 90:10), to yield **21** (35.7 mg, 93 %) as a bright yellow solid. ^{1}H-NMR (400 MHz, $CDCl_3$): δ = 9.16 (d, *J* = 2.2 Hz, 1H), 8.54 (dd, *J* = 9.5, 2.5 Hz, 1H), 8.36 (d, *J* = 9.5 Hz, 1H), 7.99 (d, *J* = 6.1 Hz, 2H), 1.69 (d, *J* = 2.0 Hz, 12H). ^{13}C-NMR (101 MHz, $CDCl_3$): δ = 147.9, 144.9, 144.3, 141.2, 131.4, 126.6, 123.0, 121.3, 121.2, 62.8, 32.0, 29.8. HRMS (ESI) *m/z* $[M+H]^+$ calcd for $C_{18}H_{19}N_4O^{2+}$: 323.1503; found 323.1501.

Ethylnitro isoindoline phenazine 22. To a solution of 70% EtOH in H_2O (2.5 mL) containing 1 drop of AcOH was added **7** (50 mg, 0.191 mmol) and **20** (29.3 mg, 0.191 mmol) and the solution was stirred at 22 °C for 30 min. The solvent was removed *in vacuo* and the residue purified by flash-column chromatography, using a gradient elution (CH_2Cl_2/MeOH, 100:0 to 95:5), to yield **22** (65.2 mg, 90 %) as a brownish yellow solid. ^{1}H-NMR (400 MHz, $CDCl_3$) δ 9.17 (d, *J* = 2.4 Hz, 1H), 8.53 (d, *J* = 2.5 Hz, 1H), 8.35 (d, *J* = 9.5 Hz, 1H), 7.93 (d, *J* = 5.4 Hz, 2H), 1.97 – 1.79 (m, 8H), 0.98 (td, *J* = 7.4, 1.5 Hz, 12H). ^{13}C-NMR (101 MHz, $CDCl_3$) δ = 155.9, 154.9, 146.8, 143.8, 143.7, 143.2, 140.0, 130.3, 125.5, 121.8, 120.9, 120.7, 67.2, 67.1, 33.0, 28.7, 7.9, 0.0. HRMS (ESI) *m/z* $[M+H]^+$ calcd for $C_{22}H_{27}N_4O_2^+$: 379.2129; found 379.2126.

Ethylbromo isoindoline phenazine 23. To a solution of 70% EtOH in H_2O (2.5 mL) containing 1 drop of AcOH was added **7** (12.6 mg, 0.048 mmol) and **16** (8.9 mg, 0.048 mmol) and the solution was stirred at 22 °C for 30 min. The solvent was removed *in vacuo* and the residue purified by flash-column chromatography, using a gradient elution (CH_2Cl_2/ MeOH, 100:0 to 95:5), to yield **23** (19 mg, 96 %) as a brownish-yellow solid. ^{1}H-NMR (400 MHz, $CDCl_3$): δ = 8.41 (d, *J* = 2.1 Hz, 1H), 8.07 (d, *J* = 9.2 Hz, 1H), 7.87 (s, 2H), 7.85 (dd, *J* = 9.2, 2.1 Hz, 1H), 1.95 – 1.77 (m, 9H), 0.97 (t, *J* = 7.4 Hz, 13H). ^{13}C-NMR (101 MHz, $CDCl_3$) δ = 142.6, 142.4, 142.1, 140.5, 132.7, 130.4, 129.7, 123.2, 120.7, 120.6, 67.0, 33.0, 7.7, 0.0. HRMS (ESI) *m/z* $[M+H]^+$ calcd for $C_{22}H_{27}BrN_3^+$: 412.1383; found 412.1383.

Isoindoline phenazine radical 26. To a solution of **15** (10 mg, 0.036 mmol) in CH_2Cl_2 (2 mL), was added *m*-chloroperoxybenzoic acid (6.2 mg, 0.036 mmol) and the resulting solution stirred at 22 °C for 12 h in a

closed reaction vial. The solution was poured onto ice, extracted with CH_2Cl_2 (3 x 10 mL), dried over Na_2SO_4 and concentrated *in vacuo*. The crude product was purified by preparative TLC (CH_2Cl_2/MeOH; 95:5) to yield **26** (9.4 mg, 89% yield) as a yellow solid. HRMS (ESI) *m/z* $[M+Na]^+$ calcd for $C_{18}H_{18}N_3O^+$: 315.1348; found 315.1308.

Dioxidized isoindoline phenazine 27. To a solution of **15** (10 mg, 0.036 mmol) in CH_2Cl_2 (2 mL), was added *m*-chloroperoxybenzoic acid (13.6 mg, 0.079 mmol) and the resulting solution stirred at 22 °C for 12 h in a closed reaction vial. The solution was poured onto ice, extracted with CH_2Cl_2 (3 x 10 mL), dried over Na_2SO_4 and concentrated *in vacuo*. The crude product was purified by preparative TLC (CH_2Cl_2/MeOH; 95:5) to yield **27** (7.8 mg, 70% yield) as an orange-red solid. HRMS (ESI) *m/z* $[M+Na]^+$ calcd for $C_{18}H_{18}N_3O_2^+$: 331.1297; found 331.1286.

Trioxidized isoindoline phenazine 5. To a solution of **15** (10 mg, 0.036 mmol) in CH_2Cl_2 (2 mL), was added *m*-chloroperoxybenzoic acid (34.2 mg, 0.198 mmol) and the resulting solution stirred at 22 °C for 12 h in a closed reaction vial. The solution was poured onto ice, extracted with CH_2Cl_2 (3 x 10 mL), dried over Na_2SO_4 and concentrated *in vacuo*. The crude product was purified by preparative TLC (CH_2Cl_2/MeOH; 95:5) to yield **5** (9 mg, 77% yield) as a bright red solid. HRMS (ESI) *m/z* $[M+Na]^+$ calcd for $C_{18}H_{18}N_3O_3^+$: 347.1240; found 347.1215.

Trioxidized bromo isoindoline phenazine 28. To a solution of **17** (10 mg, 0.028 mmol) in CH_2Cl_2 (2 mL), was added *m*-chloroperoxybenzoic acid (26.6 mg, 0.154 mmol) and the resulting solution stirred at 22 °C for 12 h in a closed reaction vial. The solution was poured onto ice, extracted with CH_2Cl_2 (3 x 10 mL), dried over Na_2SO_4 and concentrated *in vacuo*. The crude product was purified by preparative TLC (CH_2Cl_2/MeOH; 95:5) to yield **28** (8.1 mg, 72% yield) as a deep brown-red solid. HRMS (ESI) *m/z* $[M+Na]^+$ calcd for $C_{18}H_{17}N_3O_3Br^+$: 425.0345; found 425.0360.

Trioxidized dichloro isoindoline phenazine 29. To a solution of **19** (10 mg, 0.029 mmol) in CH_2Cl_2 (2 mL), was added *m*-chloroperoxybenzoic acid (26.6 mg, 0.154 mmol) and the resulting solution stirred at 22 °C for 12 h in a closed reaction vial. The solution was poured onto ice, extracted with CH_2Cl_2 (3 x 10 mL), dried over Na_2SO_4 and concentrated *in vacuo*. The crude product was purified by preparative TLC (CH_2Cl_2/MeOH; 95:5) to yield **29** (7.9 mg, 70% yield) as a brownish solid. HRMS (ESI) *m/z* $[M+H]^+$ calcd for $C_{18}H_{17}N_3O_3Cl_2^+$: 393.0641; found 393.0556.

Trioxidized nitro isoindoline phenazine 30. To a solution of **21** (10 mg, 0.031 mmol) in CH_2Cl_2 (2 mL), was added m-chloroperoxybenzoic acid (29.4 mg, 0.171 mmol) and the resulting solution stirred at 22°C for 12 h in a closed reaction vial. The solution was poured onto ice, extracted with CH_2Cl_2 (3 x 10 mL), dried over Na_2SO_4 and concentrated *in vacuo*. The crude product was purified by preparative TLC (CH_2Cl_2/MeOH; 95:5) to yield **30** (8.9 mg, 78% yield) as a bright red solid.

Acknowledgements

The authors acknowledge financial support by the Icelandic Research Fund (173727-051). The authors thank Dr S. Jonsdottir for assistance with collecting analytical data for structural characterization of new compounds, Dr. Thomas Halbritter for critically reading this manuscript and the members of the Sigurdsson research group for helpful discussions.

Keywords: aminoxyl radicals • EPR spectroscopy • noncovalent spin labels • phenazines • oligonucleotides;

[1] T. Série, in *Annales de chimie et de physique, Vol. 15*, **1845**.

[2] O. L. Lebedev, M. I. Khidekel, G. A. Razuvaev, *Dokl. Akad. Nauk SSSR* **1961**, *140*, 1327–1329.

[3] M. B. Neiman, E. G. Rozantsev, Y. G. Mamedova, *Nature* **1962**, *196*, 472-474.

[4] a) E. G. Rozantsev, *Free nitroxyl radicals*, Plenum Press, **1970**; b) L. B. Volodarsky, V. A. Reznikov, V. I. Ovcharenko, *Synthetic chemistry of stable nitroxides*, CRC Press, **2017**.

[5] a) B. P. Soule, F. Hyodo, K.-i. Matsumoto, N. L. Simone, J. A. Cook, M. C. Krishna, J. B. Mitchell, *Free Radical Biol. Med.* **2007**, *42*, 1632-1650; b) M. G. Lewandowski, K., *Int. J. Mol. Sci.* **2017**, *18*, 2490-2516.

[6] E. G. Bagryanskaya, S. R. A. Marque, *Chem. Rev.* **2014**, *114*, 5011-5056.

[7] K.-A. Hansen, J. P. Blinco, *J. Polym. Sci. A* **2018**, *9*, 1479-1516.

[8] a) Q. Cao, L. M. Dornan, L. Rogan, N. L. Hughes, M. J. Muldoon, *Chem. Commun.* **2014**, *50*, 4524-4543; b) A. Isogai, T. Hänninen, S. Fujisawa, T. Saito, *Prog. Polym. Sci.* **2018**, *86*, 122-148.

[9] a) S. A. Shelke, S. T. Sigurdsson, *Eur. J. Org. Chem.* **2012**, *2012*, 2291-2301; b) M. M. Haugland, J. E. Lovett, E. A. Anderson, *Chem. Soc. Rev.* **2018**, *47*, 668-680.

[10] a) J. F. W. Keana, R. J. Dinerstein, F. Baitis, *J. Org. Chem.* **1971**, *36*, 209-211; b) S. R. Harrison, R. S. Pilkington, L. H. Sutcliffe, *J. Chem. Soc. Faraday Trans. 1* **1984**, *80*, 669-689.

[11] a) D. G. Gillies, L. H. Sutcliffe, X. Wu, *J. Chem. Soc. Faraday Trans.* **1994**, *90*, 2345-2349; b) S. E. Bottle, D. G. Gillies, A. S. Micallef, D. A. Reid, L. H. Sutcliffe, *Magn. Reson. Chem.* **1999**, *37*, 730-734.

[12] a) S.-J. Hong, L. H. Piette, *Cancer Res.* **1976**, *36*, 1159-1171; b) M. F. Ottaviani, N. D. Ghatlia, S. H. Bossmann, J. K. Barton, H. Duerr, N. J. Turro, *J. Am. Chem. Soc.* **1992**, *114*, 8946-8952.

[13] S. Saha, T. Hetzke, T. F. Prisner, S. T. Sigurdsson, *Chem. Commun.* **2018**, *54*, 11749-11752.

[14] a) K. Yoshimoto, S. Nishizawa, M. Minagawa, N. Teramae, *J. Am. Chem. Soc.* **2003**, *125*, 8982-8983; b) Y. Sato, T. Ichihashi, S. Nishizawa, N. Teramae, *Angew. Chem. Int. Ed.* **2012**, *51*, 6369-6372; c) Y. Sato, Y. Toriyabe, S. Nishizawa, N. Teramae, *Chem. Commun.* **2013**, *49*, 9983-9985.

[15] a) P. Belmont, C. Chapelle, M. Demeunynck, J. Michon, P. Michon, J. Lhomme, *Bioorg. Med. Chem. Lett.* **1998**, *8*, 669-674; b) F. Thomas, J. Michon, J. Lhomme, *Biochemistry* **1999**, *38*, 1930-1937.

[16] S. A. Shelke, S. T. Sigurdsson, *Angew. Chem. Int. Ed.* **2010**, *49*, 7984-7986.

[17] a) N. R. Kamble, M. Gränz, T. F. Prisner, S. T. Sigurdsson, *Chem. Commun.* **2016**, *52*, 14442-14445; b) N. R. Kamble, S. T. Sigurdsson, *Chem. Eur. J.* **2018**, *24*, 4157-4164.

[18] a) C. D. Cox, *Infect. Immun.* **1986**, *52*, 263-270; b) M. E. Hernandez, A. Kappler, D. K. Newman, *Appl. Environ. Microbiol.* **2004**, *70*, 921-928; c) L. E. P. Dietrich, A. Price-Whelan, A. Petersen, M. Whiteley, D. K. Newman, *Mol. Microbiol.* **2006**, *61*, 1308-1321; d) L. S. Pierson, E. A. Pierson, *Appl. Microbiol. Biotechnol.* **2010**, *86*, 1659-1670; e) H. Sakhtah, A. Price-Whelan, L. E. P. Dietrich, in *Microbial phenazines: Biosynthesis, agriculture and health* (Eds.: S. Chincholkar, L. Thomashow), Springer Berlin Heidelberg, Berlin, Heidelberg, **2013**, pp. 19-42.

[19] N. Guttenberger, W. Blankenfeldt, R. Breinbauer, *Bioorg. Med. Chem.* **2017**, *25*, 6149-6166.

[20] J. B. Laursen, J. Nielsen, *Chem. Rev.* **2004**, *104*, 1663-1686.

[21] a) J. Dai, C. Punchihewa, P. Mistry, A. T. Ooi, D. Yang, *J. Biol. Chem.* **2004**, *279*, 46096-46103; b) L. Clement, Y. Danzhou, *Curr. Trends Med. Chem.* **2015**, *15*, 1385-1397.

[22] S.-T. Zhuo, C.-Y. Li, M.-H. Hu, S.-B. Chen, P.-F. Yao, S.-L. Huang, T.-M. Ou, J.-H. Tan, L.-K. An, D. Li, L.-Q. Gu, Z.-S. Huang, *Org. Biomol. Chem.* **2013**, *11*, 3989-4005.

[23] a) H. M. Hassan, I. Fridovich, *J. Bacteriol.* **1980**, *141*, 156; b) S. Sinha, X. Shen, F. Gallazzi, Q. Li, J. W. Zmijewski, J. R. Lancaster, K. S. Gates, *Chem. Res. Toxicol.* **2015**, *28*, 175-181.
[24] K. Shin-ya, K. Furihata, Y. Hayakawa, H. Seto, Y. Kato, J. Clardy, *Tetrahedron Lett.* **1991**, *32*, 943-946.
[25] a) U. Hollstein, R. J. Van Gemert, *Biochemistry* **1971**, *10*, 497-504; b) V. Kleinwächter, Z. Balcarová, K. Reinert, H. Triebel, J. Grezes, H. Bär, *Gen. Physiol. Biophys.* **1986**, *5*, 423-432; c) H. Zhou, J. Gao, Z. Chen, S. Duan, C. Li, R. Qiao, *Bioorg. Med. Chem. Lett.* **2018**, *28*, 284-288.
[26] a) A. Wohl, W. Aue, *Ber. Dtsch. Chem. Ges.* **1901**, *34*, 2442-2450; b) I. J. Pachter, M. C. Kloetzel, *J. Am. Chem. Soc.* **1951**, *73*, 4958-4961; c) H. Yang, Y. Abouelhassan, G. M. Burch, D. Kallifidas, G. Huang, H. Yousaf, S. Jin, H. Luesch, R. W. Huigens, *Sci. Rep.* **2017**, *7*, 2003.
[27] E. Bamberger, W. Ham, *Justus Liebigs Ann. Chem.* **1911**, *382*, 82-128.
[28] a) M. S. Abd El-Halim, A. S. El-Ahl, H. A. Etman, M. M. Ali, A. Fouda, A. A. Fadda, *Monatsh. Chem.* **1995**, *126*, 1217-1223; b) H. Cerecetto, M. González, M. L. Lavaggi, A. Azqueta, A. López de Cerain, A. Monge, *J. Med. Chem.* **2005**, *48*, 21-23.
[29] T. Emoto, N. Kubosaki, Y. Yamagiwa, T. Kamikawa, *Tetrahedron Lett.* **2000**, *41*, 355-358.
[30] J. K. Laha, K. S. S. Tummalapalli, A. Gupta, *Eur. J. Org. Chem.* **2013**, 8330-8335.
[31] a) A. R. Surray, *Organic Syntheses* **1955**, *Collect. Vol. 3*, 753; b) N. Vicker, L. Burgess, I. S. Chuckowree, R. Dodd, A. J. Folkes, D. J. Hardick, T. C. Hancox, W. Miller, J. Milton, S. Sohal, S. Wang, S. P. Wren, P. A. Charlton, W. Dangerfield, C. Liddle, P. Mistry, A. J. Stewart, W. A. Denny, *J. Med. Chem.* **2002**, *45*, 721-739.
[32] A. P. Jagtap, I. Krstic, N. C. Kunjir, R. Hänsel, T. F. Prisner, S. T. Sigurdsson, *Free Radical Res.* **2015**, *49*, 78-85.
[33] A. S. Micallef, R. C. Bott, S. E. Bottle, G. Smith, J. M. White, K. Matsuda, H. Iwamura, *J. Chem. Soc. Perkin Trans. 2* **1999**, 65-72.
[34] K. E. Fairfull-Smith, F. Brackmann, S. E. Bottle, *Eur. J. Org. Chem.* **2009**, 1902-1915.
[35] J. P. Blinco, J. L. Hodgson, B. J. Morrow, J. R. Walker, G. D. Will, M. L. Coote, S. E. Bottle, *J. Org. Chem.* **2008**, *73*, 6763-6771.
[36] C. D. Snyder, H. Rapoport, *J. Am. Chem. Soc.* **1972**, *94*, 227-231.
[37] E. H. Vickery, L. F. Pahler, E. J. Eisenbraun, *J. Org. Chem.* **1979**, *44*, 4444-4446.
[38] M. Hirano, S. Yakabe, H. Chikamori, J. H. Clark, T. Morimoto, *J. Chem. Res., Synop.* **1998**, 770-771.
[39] F. Gago, *Methods* **1998**, *14*, 277-292.

Entry for the Table of Contents

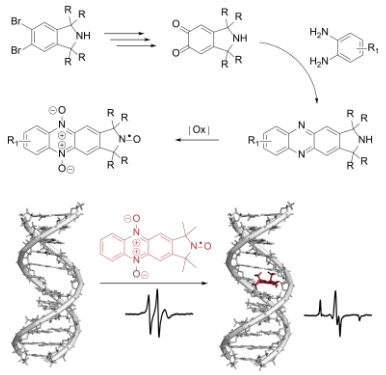

Phenazine radicals: *O*-benzoquinone isoindoline derivatives were condensed with aromatic 1,2-diamines, followed by oxidation to give phenazine-di-*N*-oxide isoindoline nitroxides. One derivative showed high binding affinity and specificity towards abasic sites in duplex DNA when the orphan base was cytosine; none of the derivatives bound to abasic sites in RNA.

Nitroxide-derived *N*-oxide phenazines for noncovalent spin-labeling of DNA

Haraldur Yngvi Juliusson and Snorri Th. Sigurdsson*

University of Iceland, Department of Chemistry, Science Institute, Dunhaga 3, 107 Reykjavik, Iceland.

**E-mail: snorrisi@hi.is*

Table of contents

^{1}H and ^{13}C NMR spectra

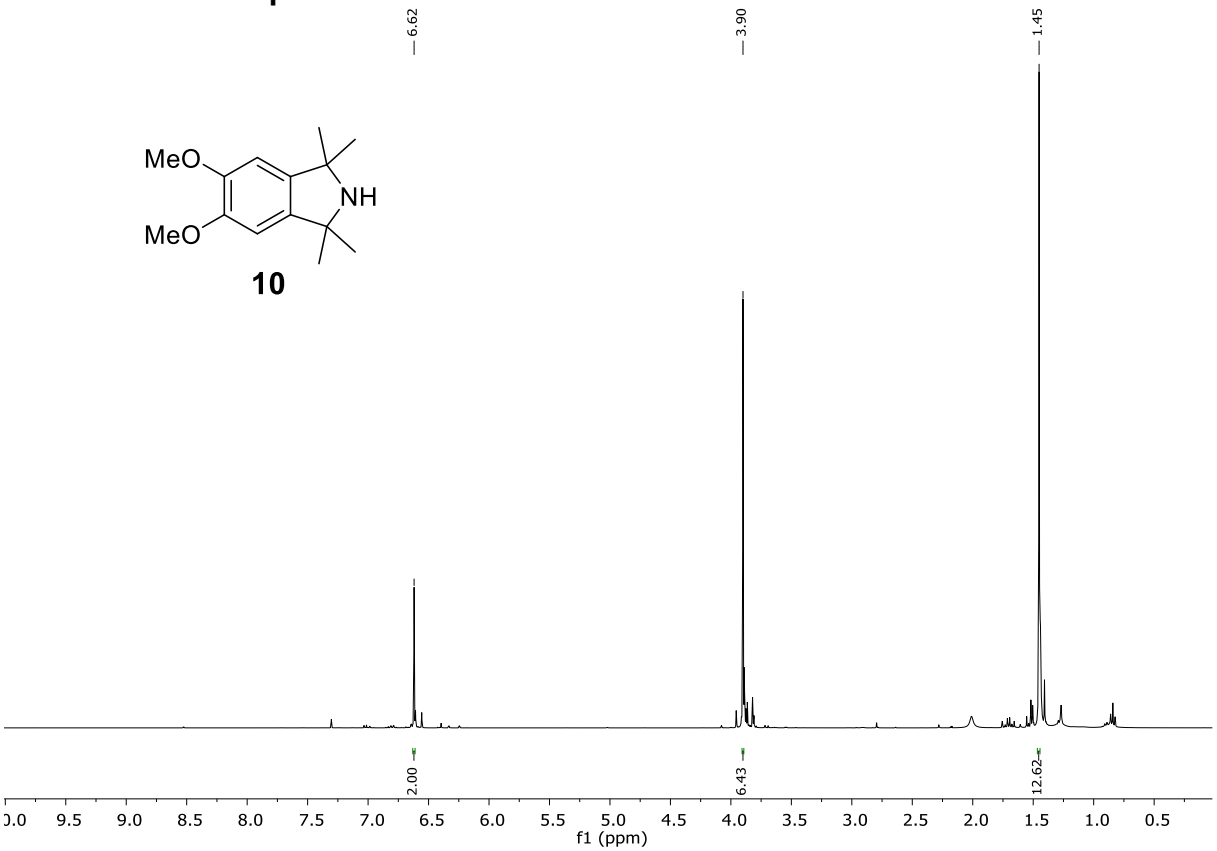

Figure S1. ^{1}H-NMR spectrum of 5,6-dimethoxy-1,1,3,3-tetramethylisoindoline (**10**).

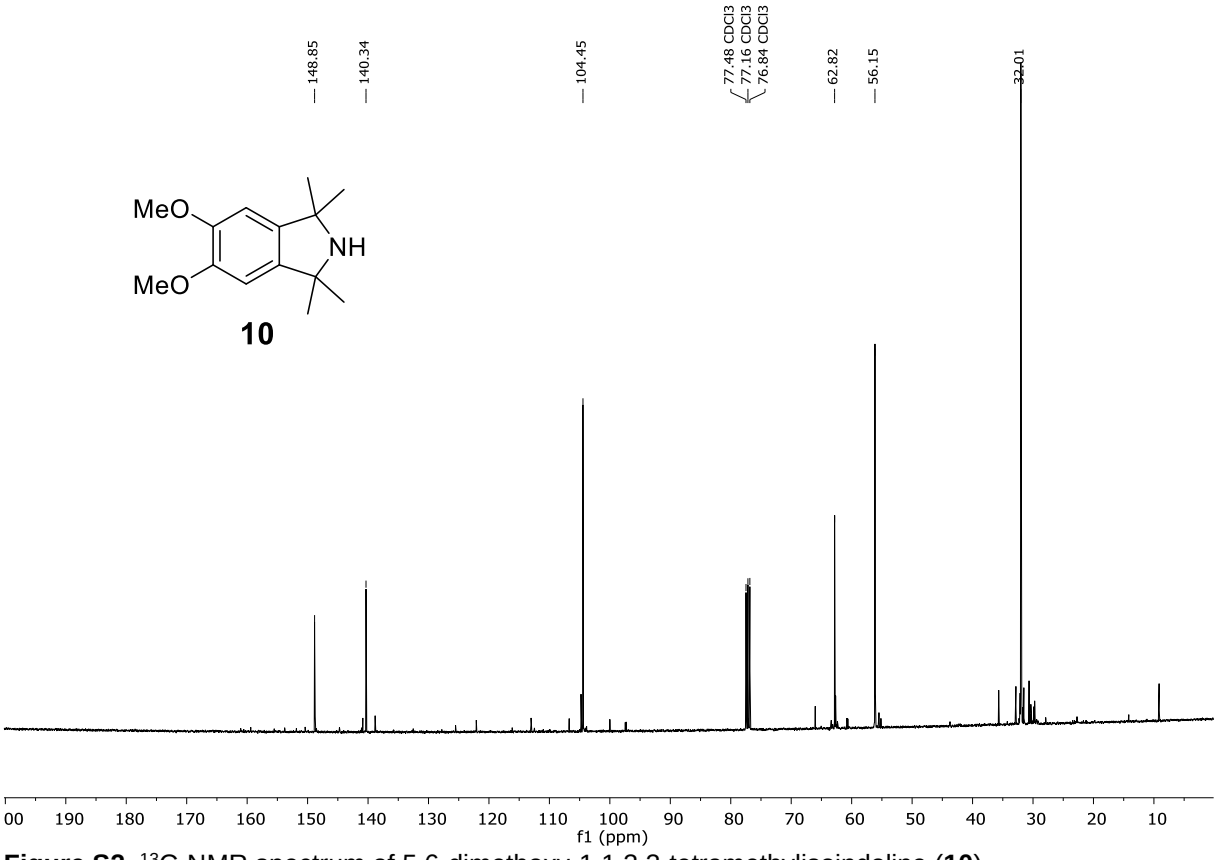

Figure S2. ^{13}C-NMR spectrum of 5,6-dimethoxy-1,1,3,3-tetramethylisoindoline (**10**).

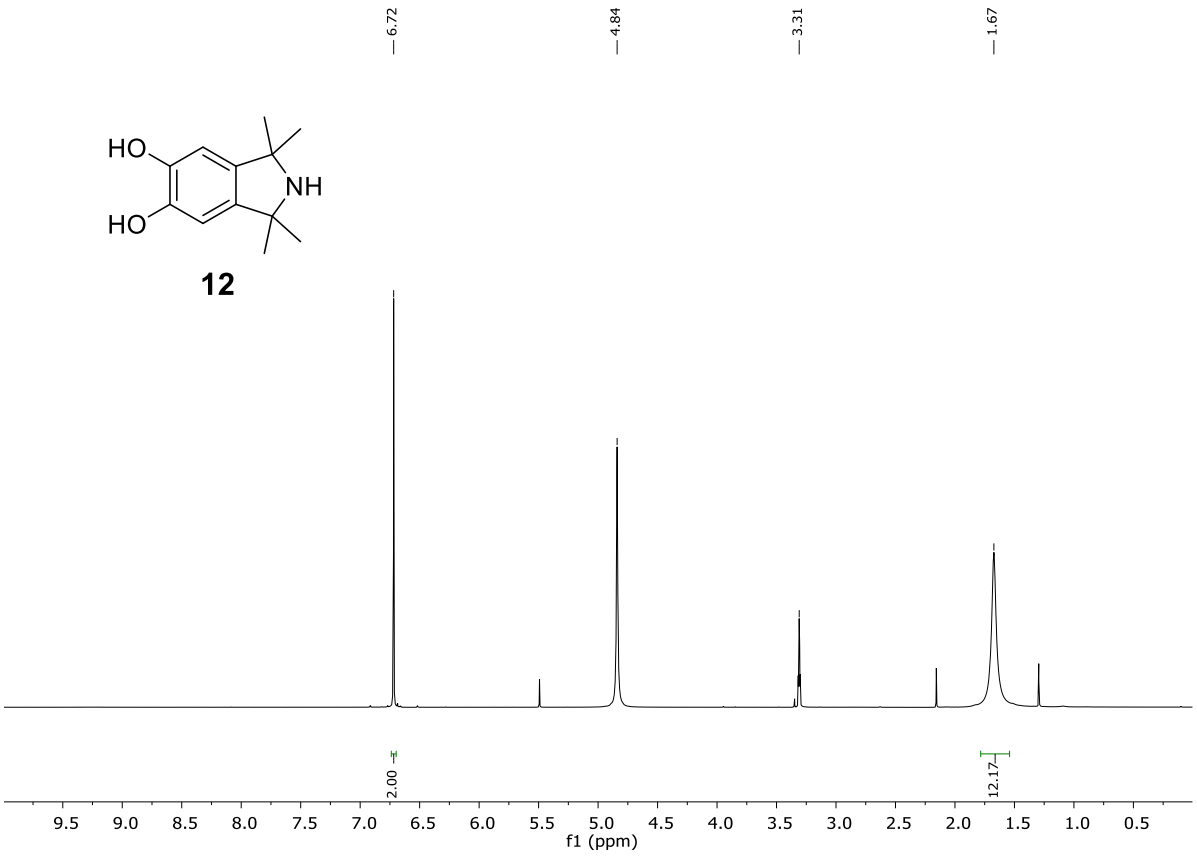

Figure S3. ^{1}H-NMR spectrum of 1,1,3,3-tetramethylisoindoline-5,6-diol (**12**).

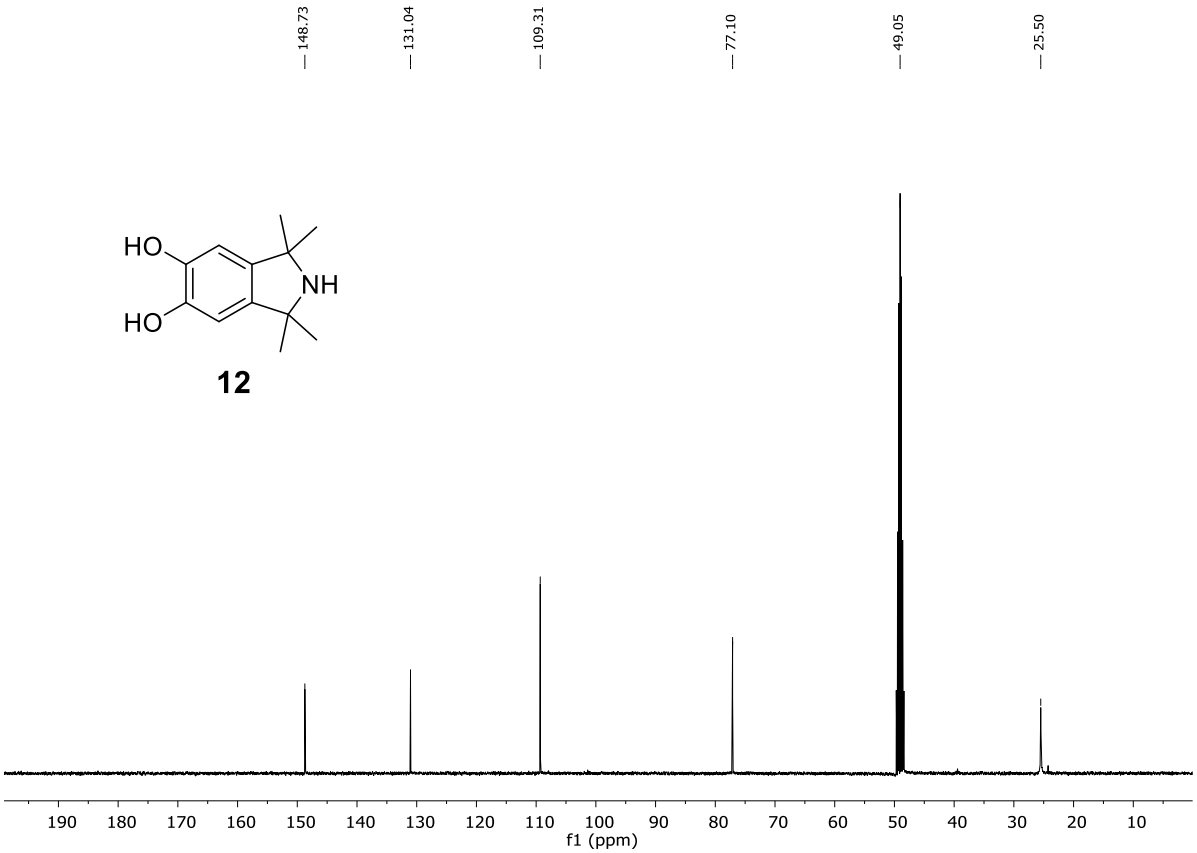

Figure S4. ^{13}C-NMR spectrum of 1,1,3,3-tetramethylisoindoline-5,6-diol (**12**).

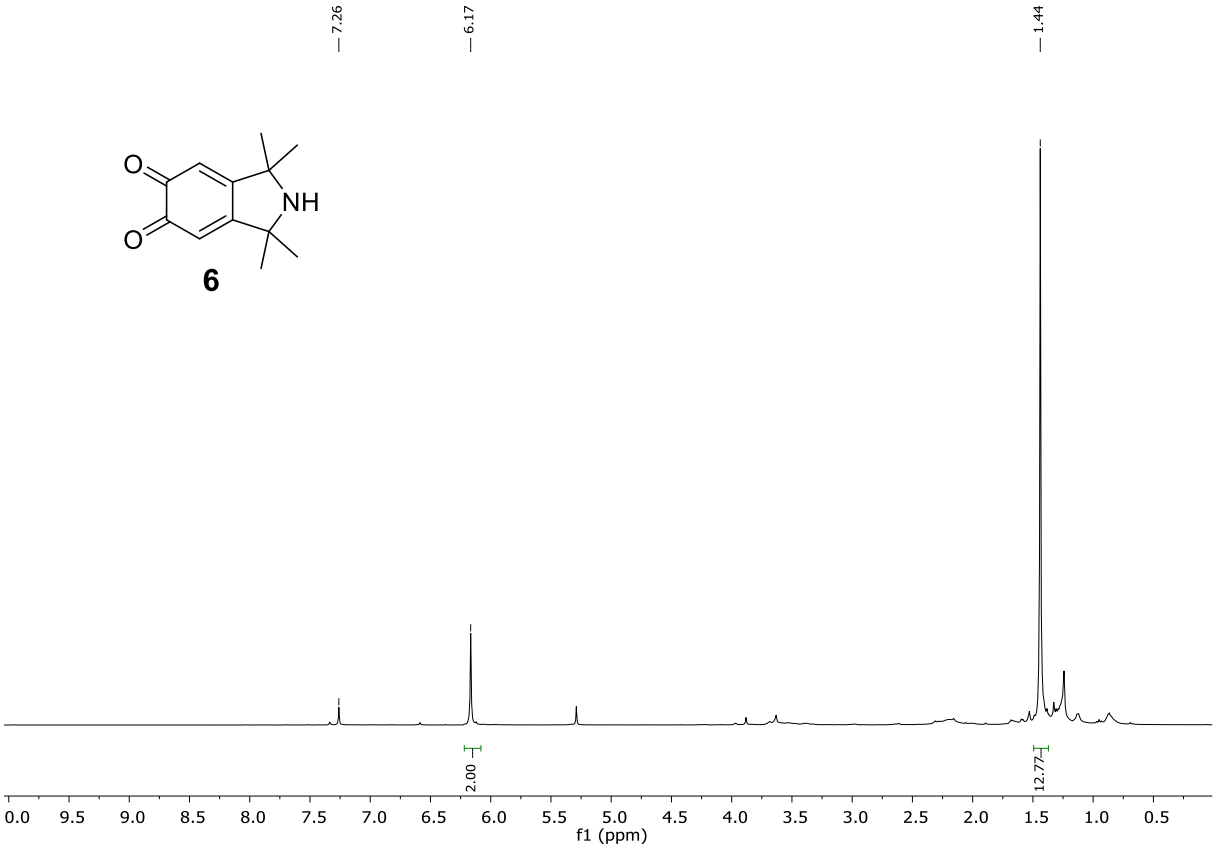

Figure S5. ^{1}H-NMR spectrum of 1,1,3,3-tetramethylisoindoline-5,6-dione (**6**).

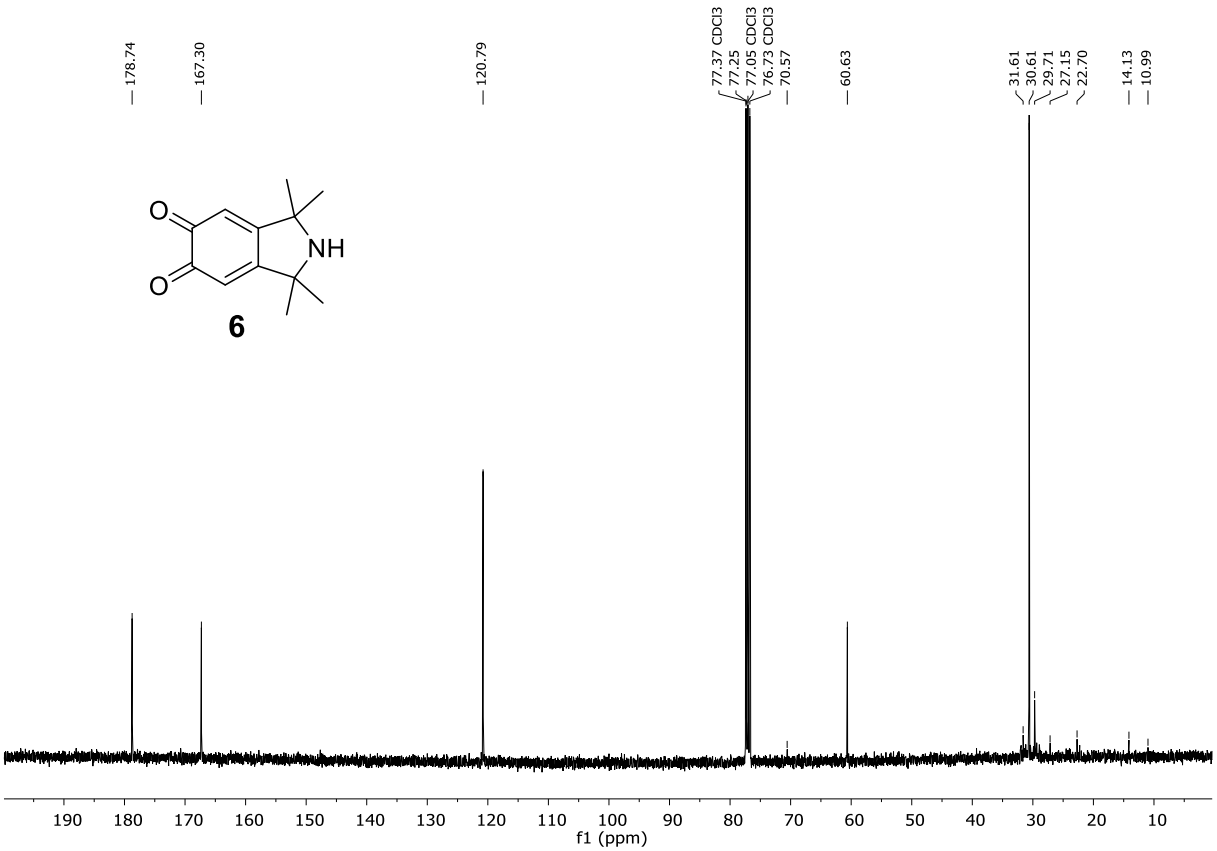

Figure S6. ^{13}C-NMR spectrum of 1,1,3,3-tetramethylisoindoline-5,6-dione (**6**).

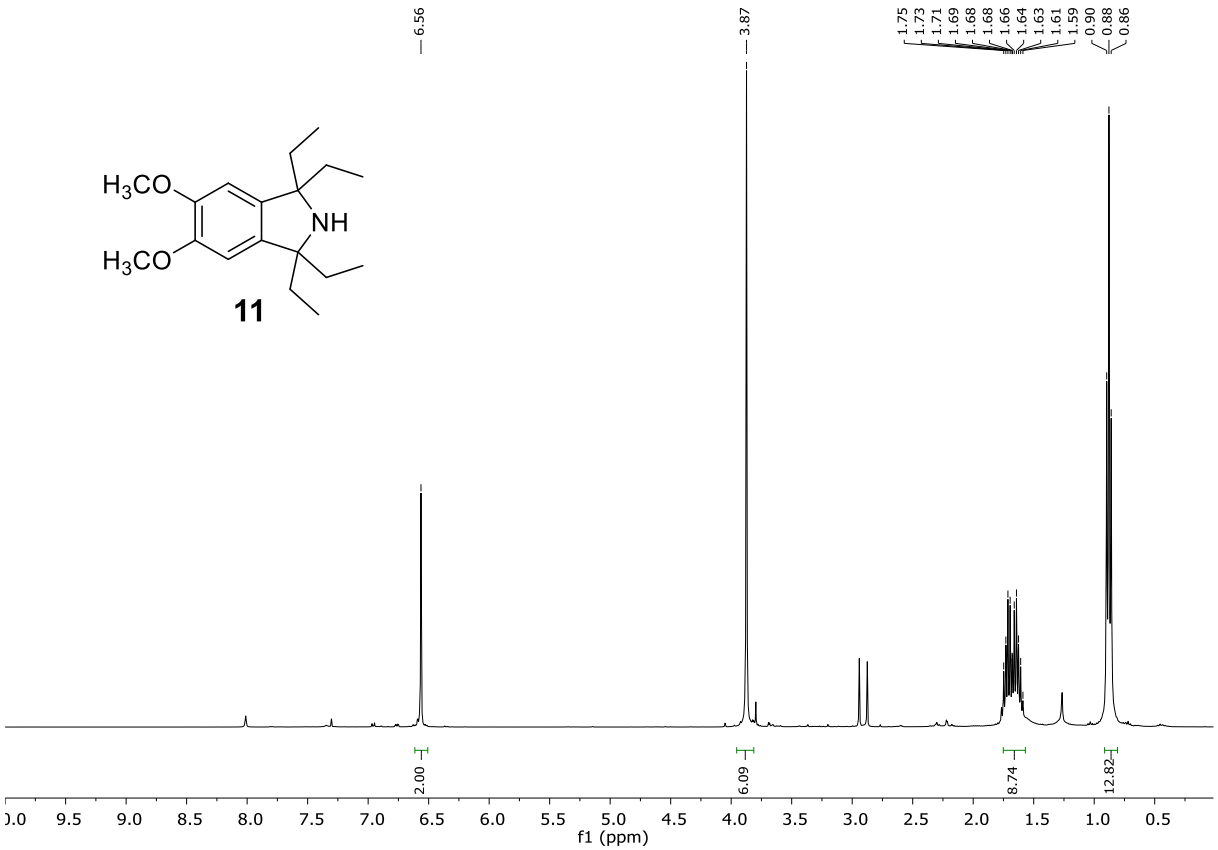

Figure S7. ^{1}H-NMR spectrum of 1,1,3,3-tetraethylisoindoline-5,6-dimethoxide (**11**).

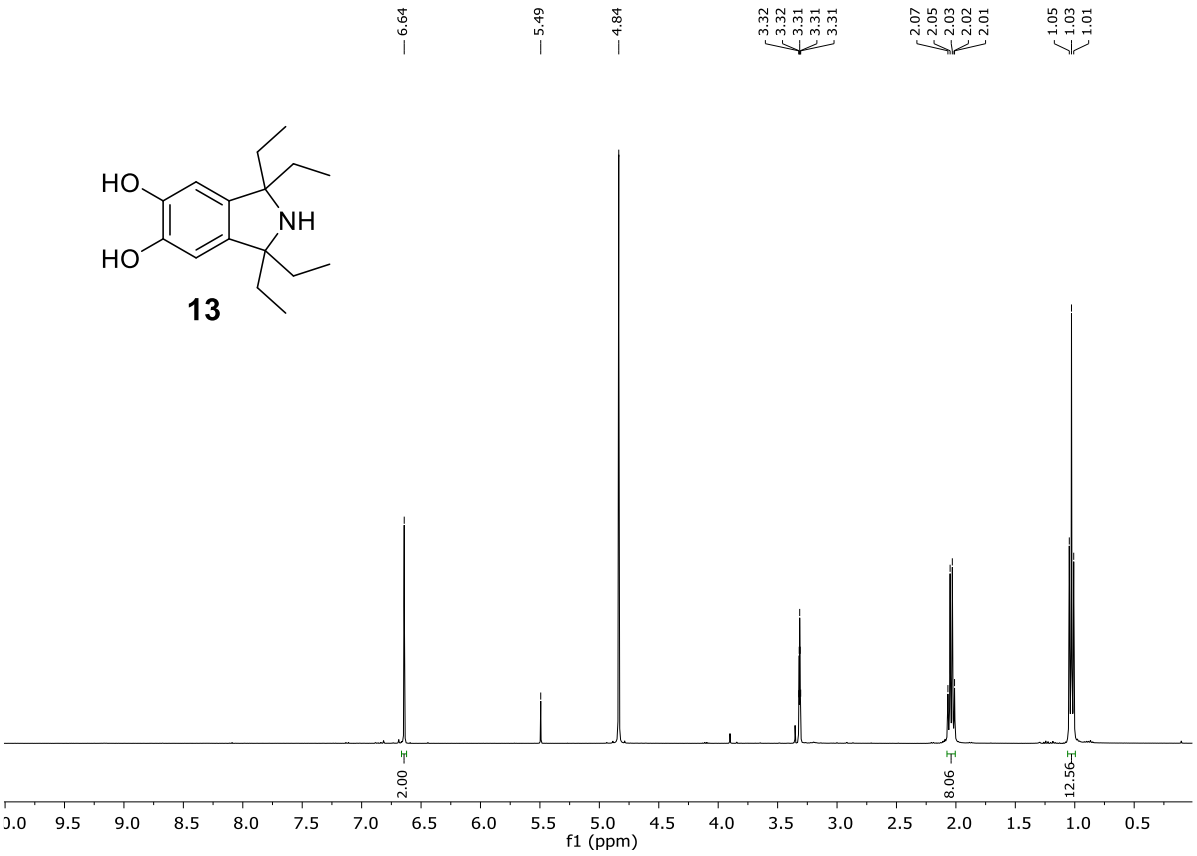

Figure S8. ^{1}H-NMR spectrum of 1,1,3,3-tetraethylisoindoline-5,6-diol (**13**).

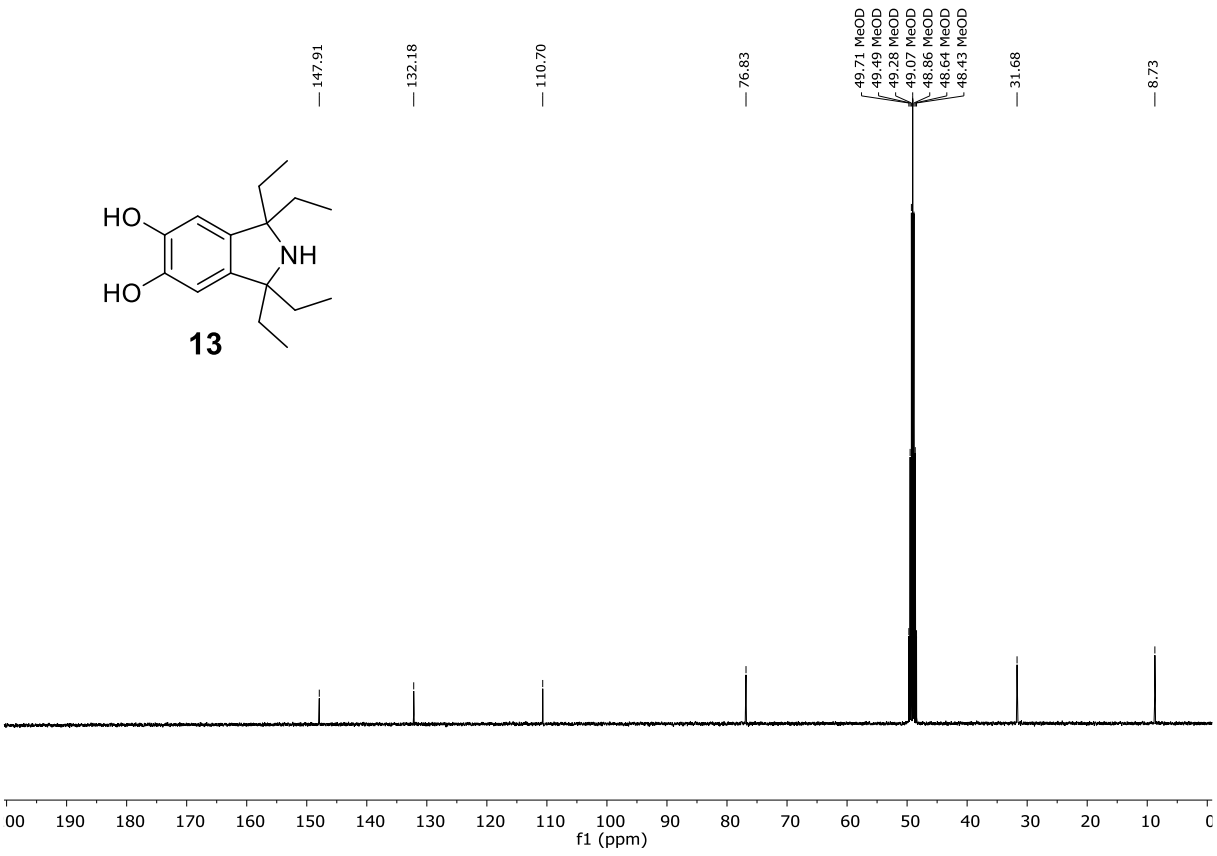

Figure S9. ^{13}C-NMR spectrum of 1,1,3,3-tetraethylisoindoline-5,6-diol (**13**).

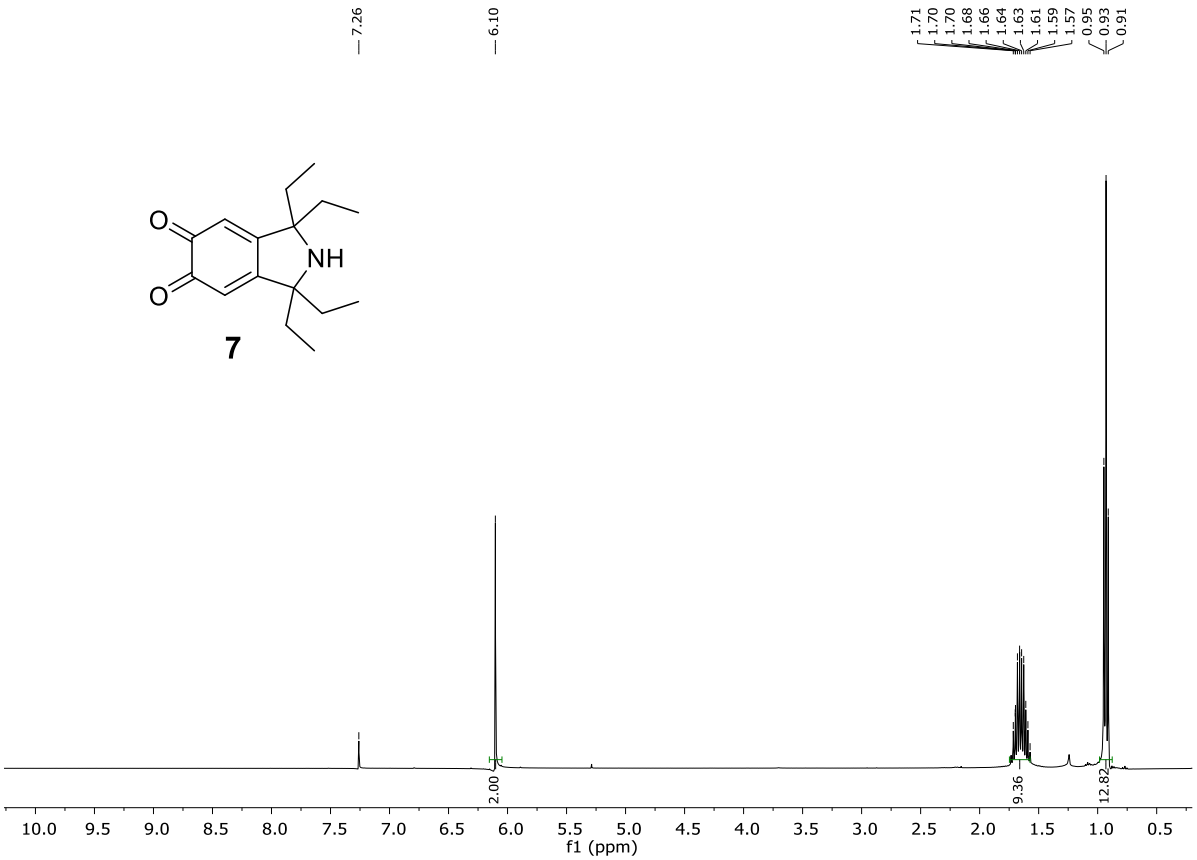

Figure S10. ^{1}H-NMR spectrum of 1,1,3,3-tetraethylisoindoline-5,6-dione (**7**).

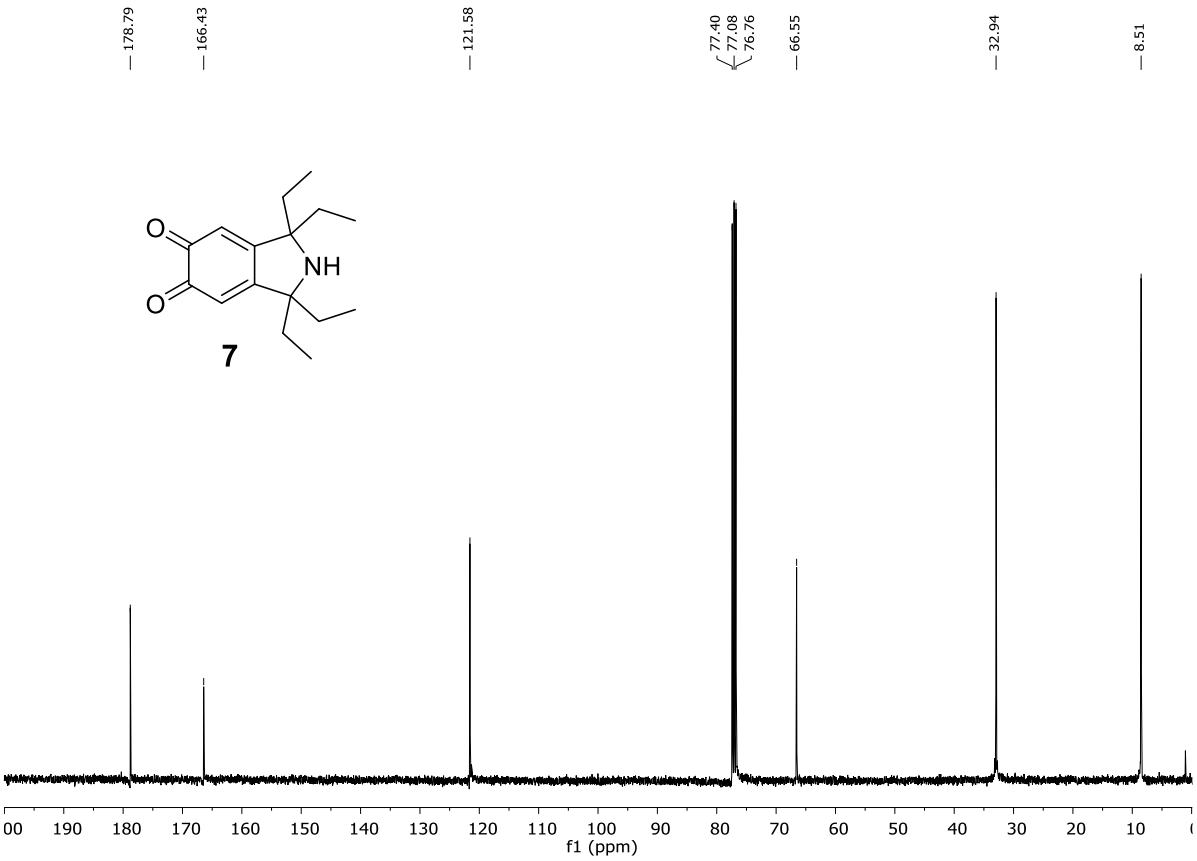

Figure S11. ^{13}C-NMR spectrum of 1,1,3,3-tetraethylisoindoline-5,6-dione (**7**).

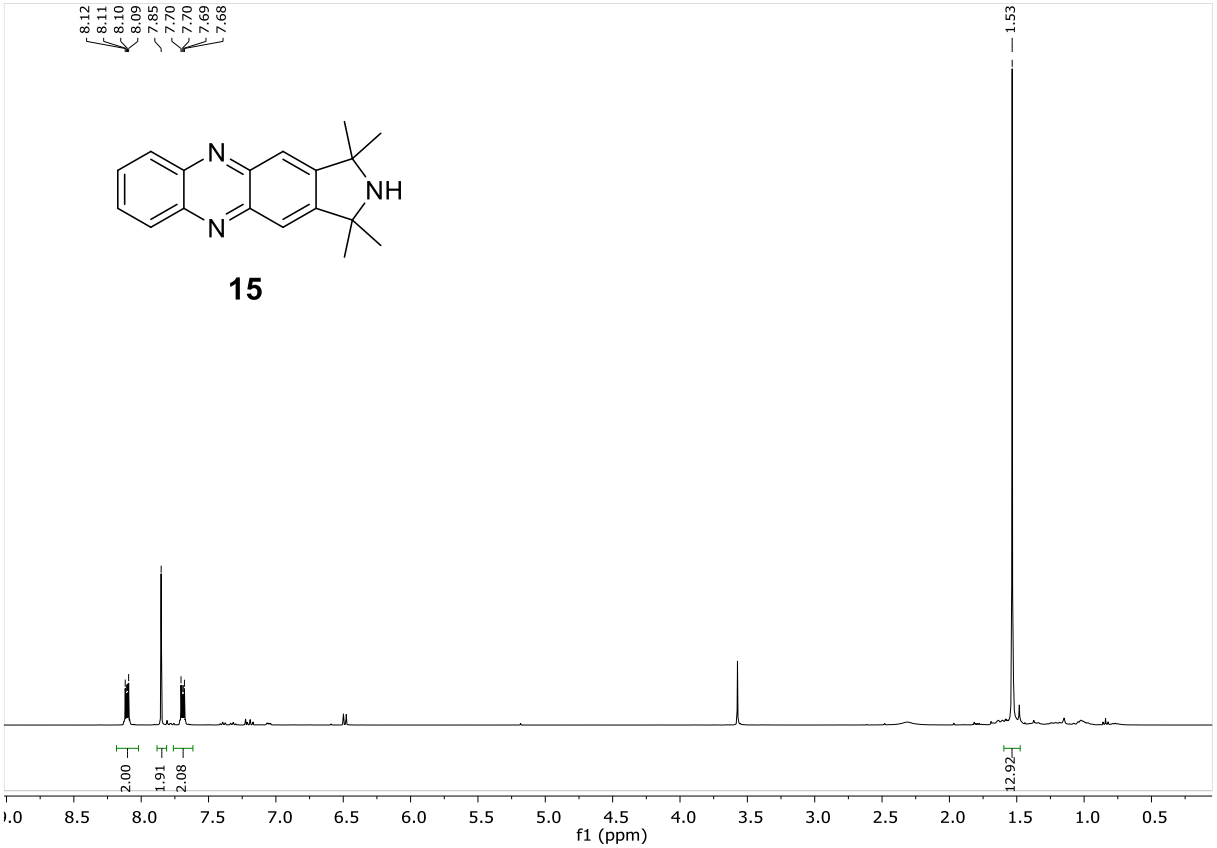

Figure S12. ^{1}H-NMR spectrum of Isoindoline phenazine **15**.

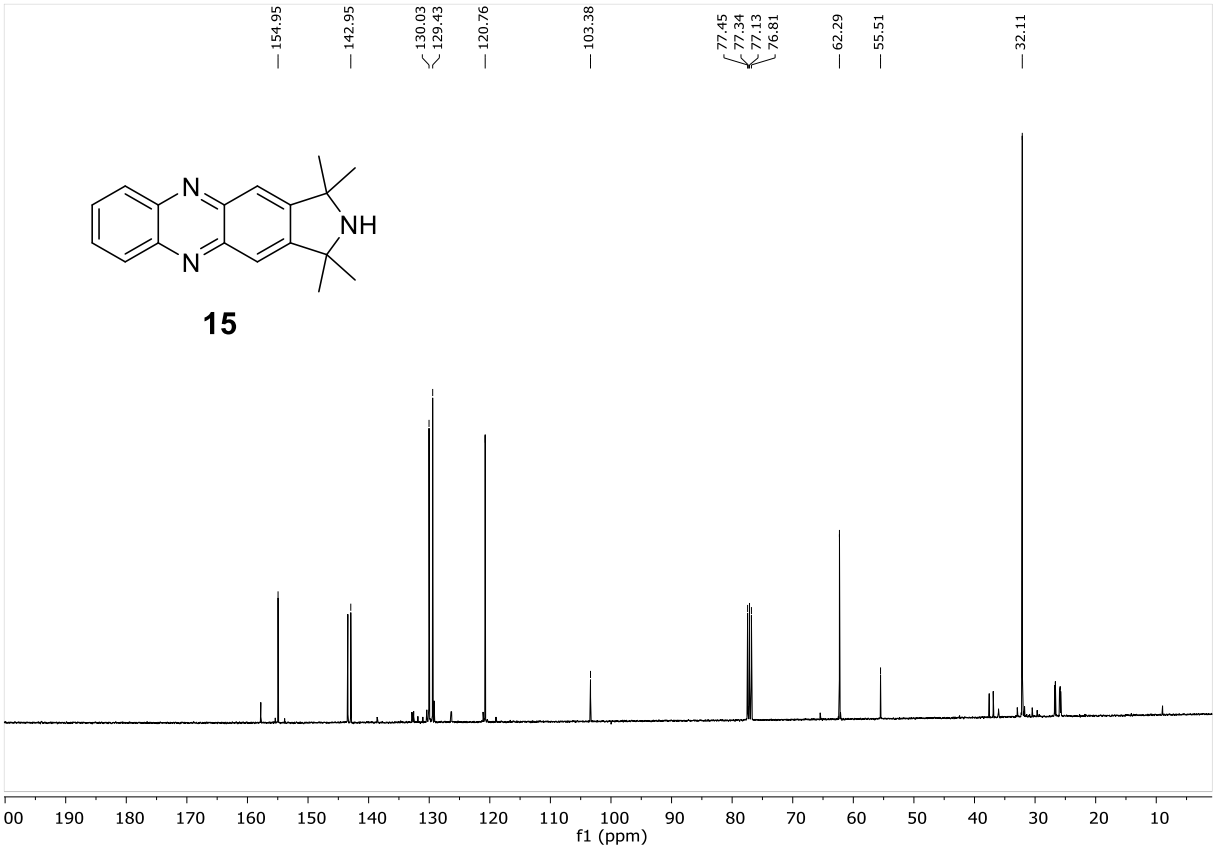

Figure S13. ^{13}C-NMR spectrum of Isoindoline phenazine derivative **15**.

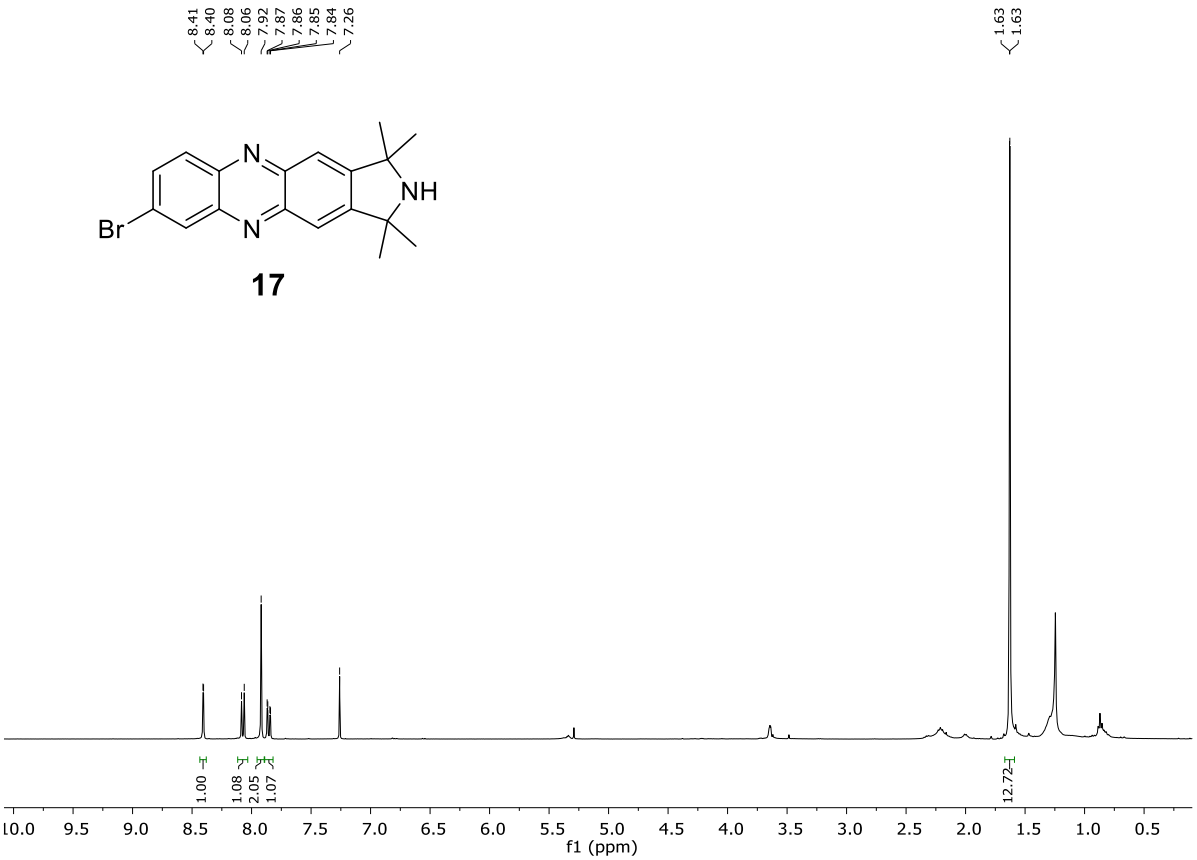

Figure S14. ^{1}H-NMR spectrum of bromo isoindoline phenazine **17.**

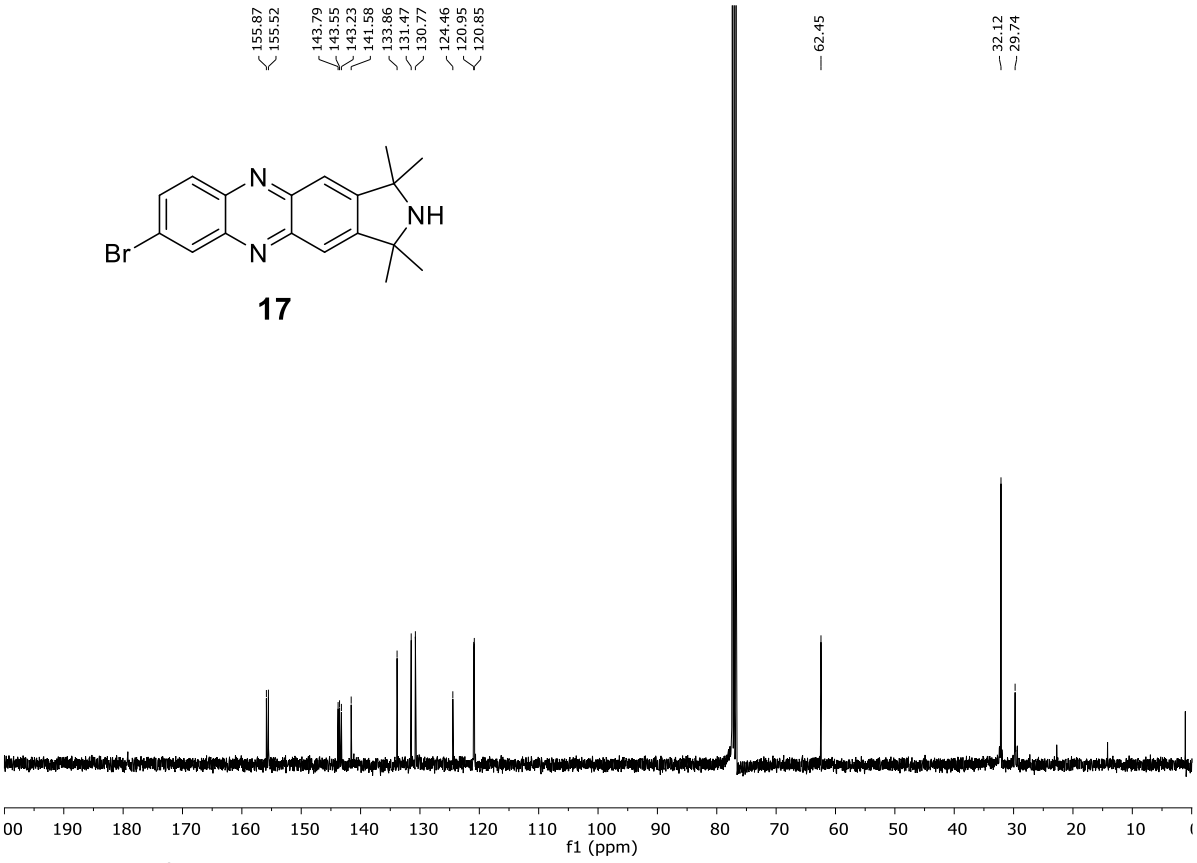

Figure S15. ^{13}C-NMR spectrum of bromo isoindoline phenazine **17.**

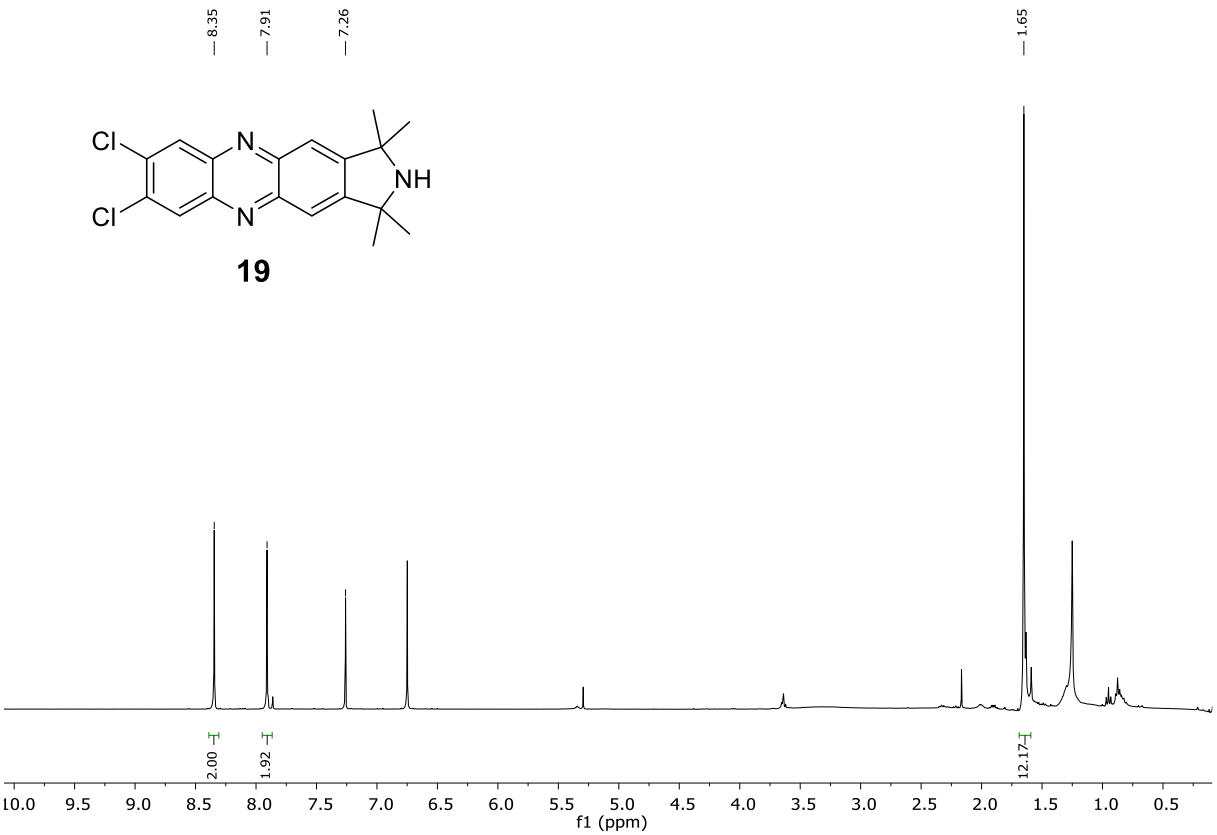

Figure S16. ^{1}H-NMR spectrum of dichloro isoindoline phenazine **19.**

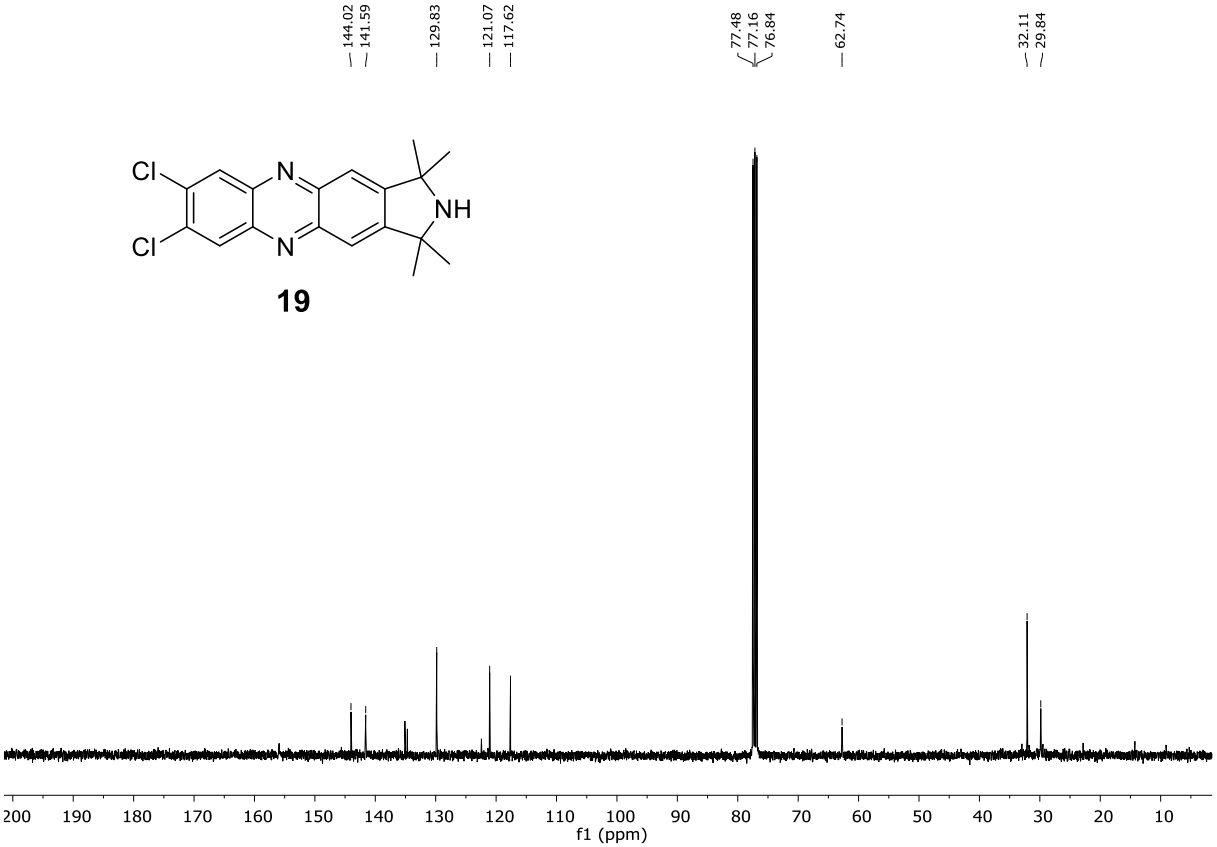

Figure S17. ^{13}C-NMR spectrum of dichloro isoindoline phenazine **19.**

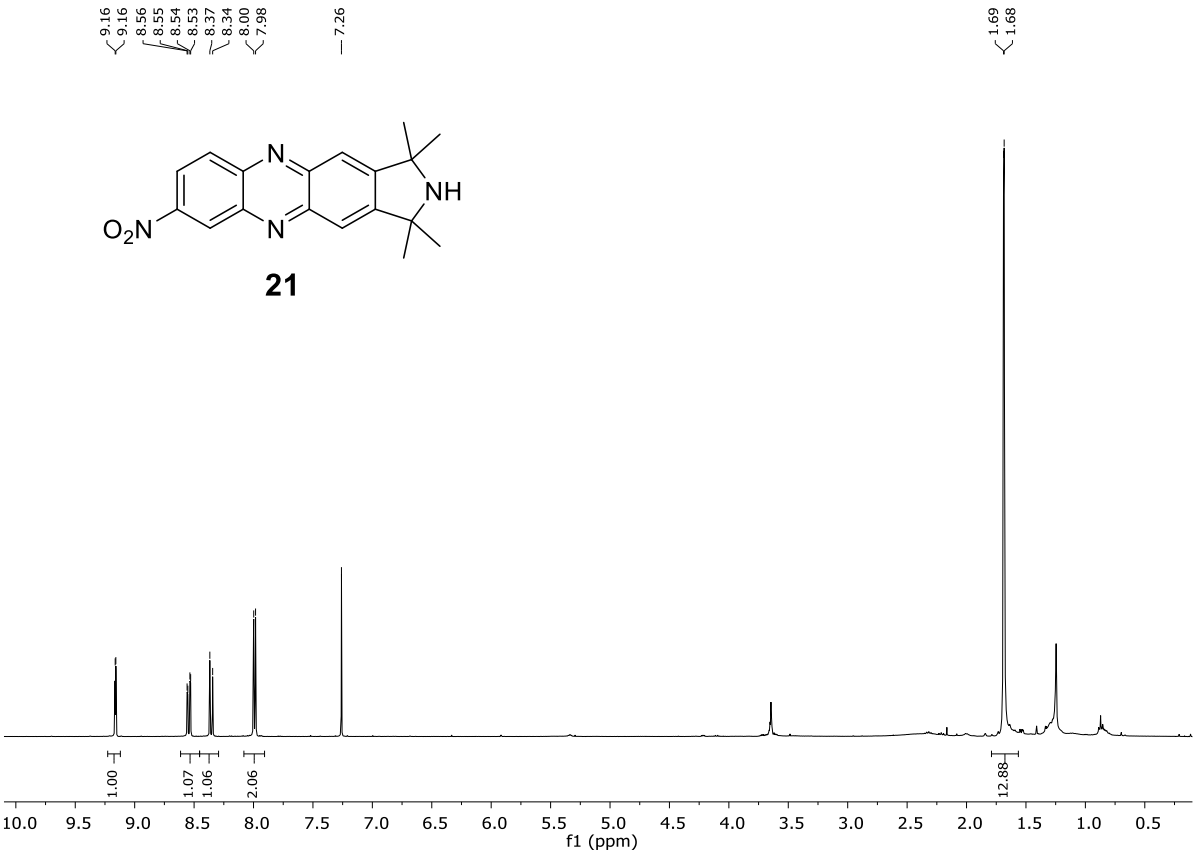

Figure S18. ^{1}H-NMR spectrum of nitro isoindoline phenazine **21**.

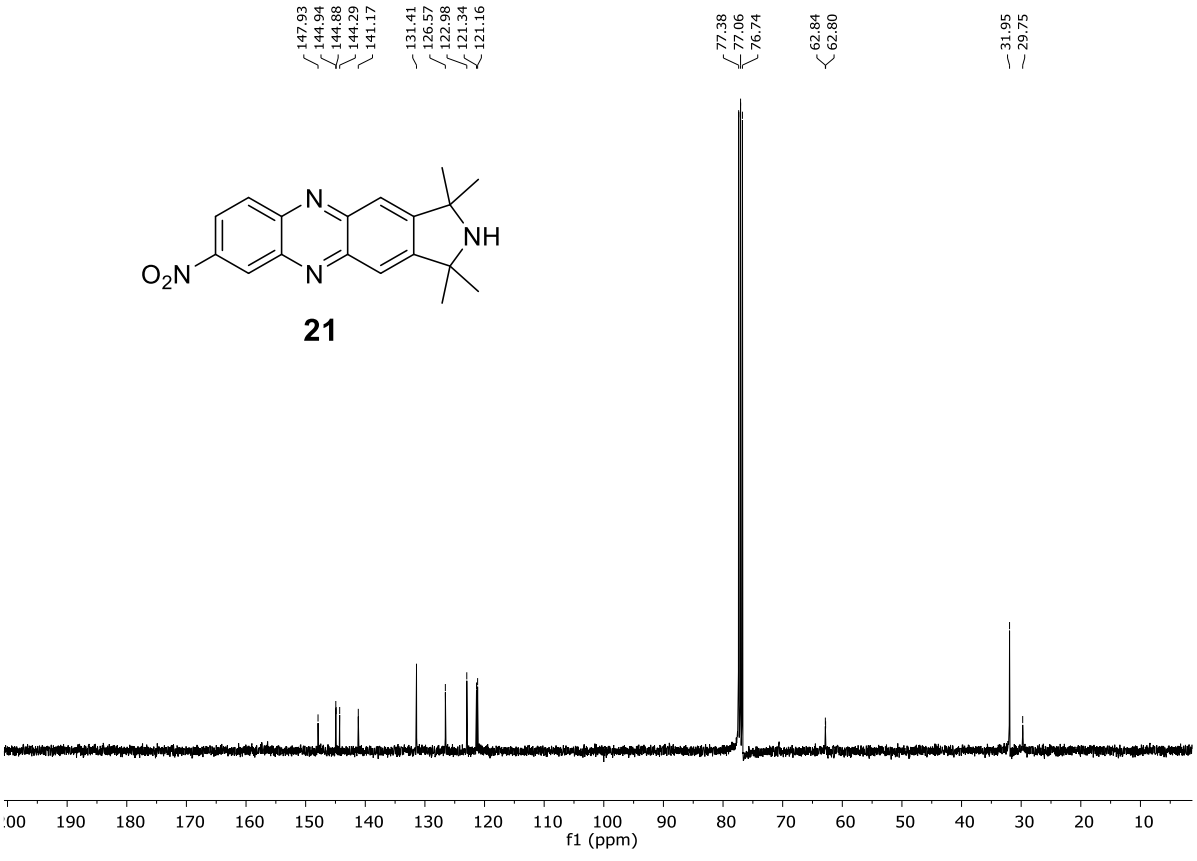

Figure S19. ^{13}C-NMR spectrum of nitro isoindoline phenazine **21**.

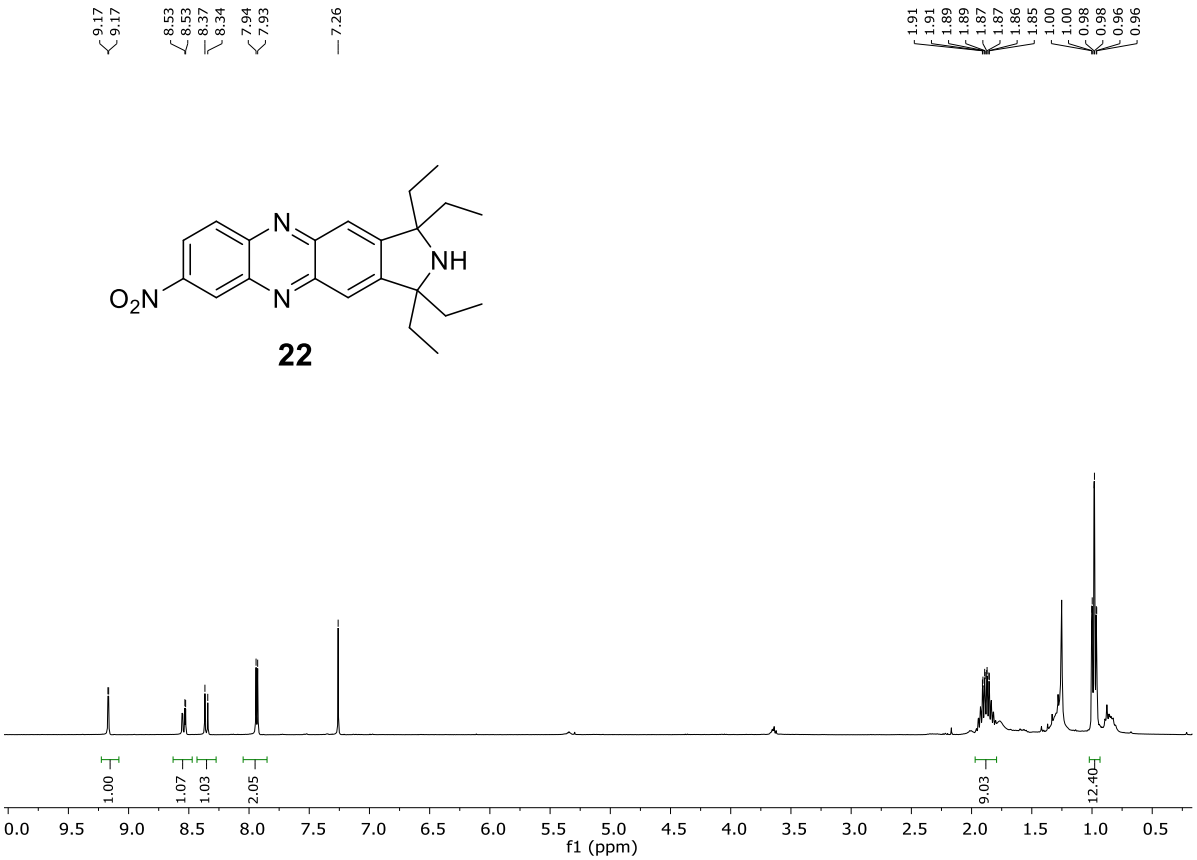

Figure S20. ^{1}H-NMR spectrum of ethylnitro isoindoline phenazine **22.**

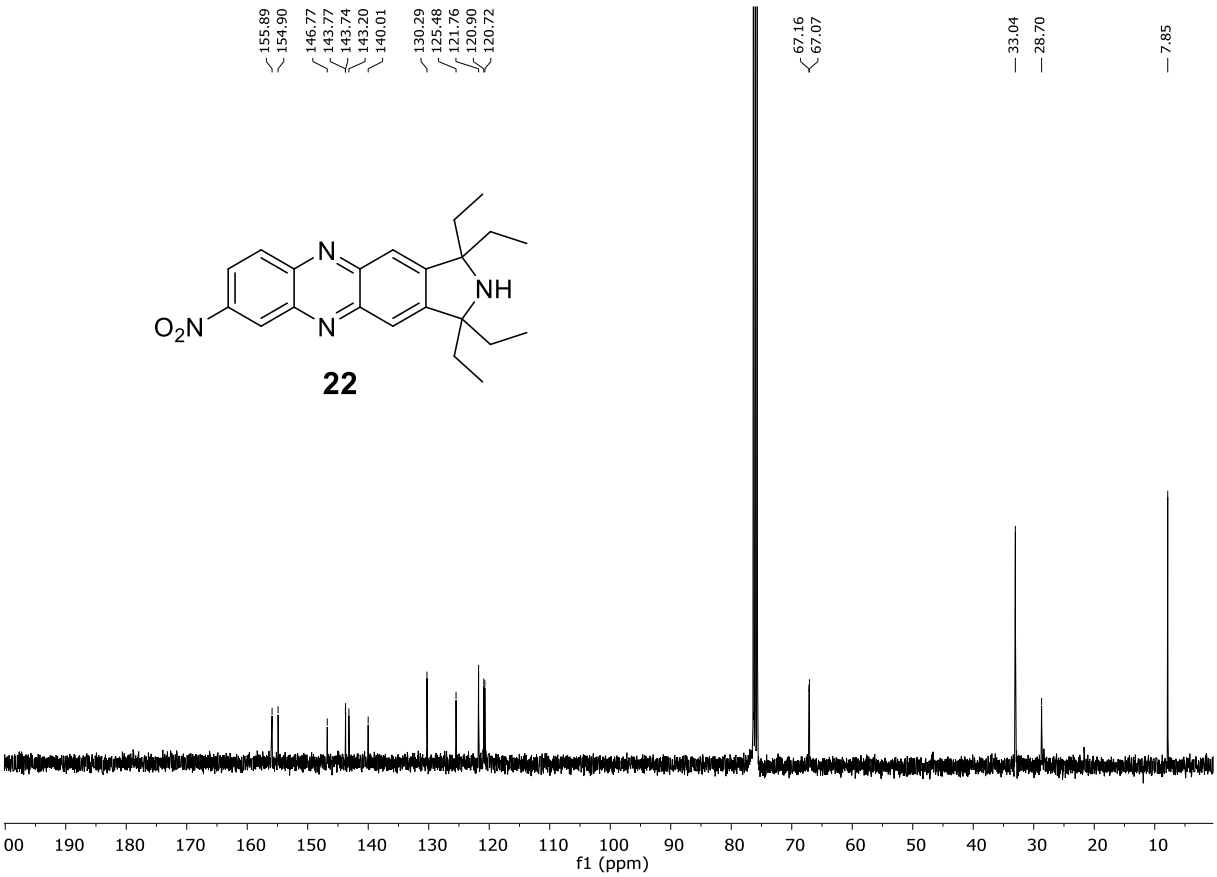

Figure S21. ^{13}C-NMR spectrum of ethylnitro isoindoline phenazine **22.**

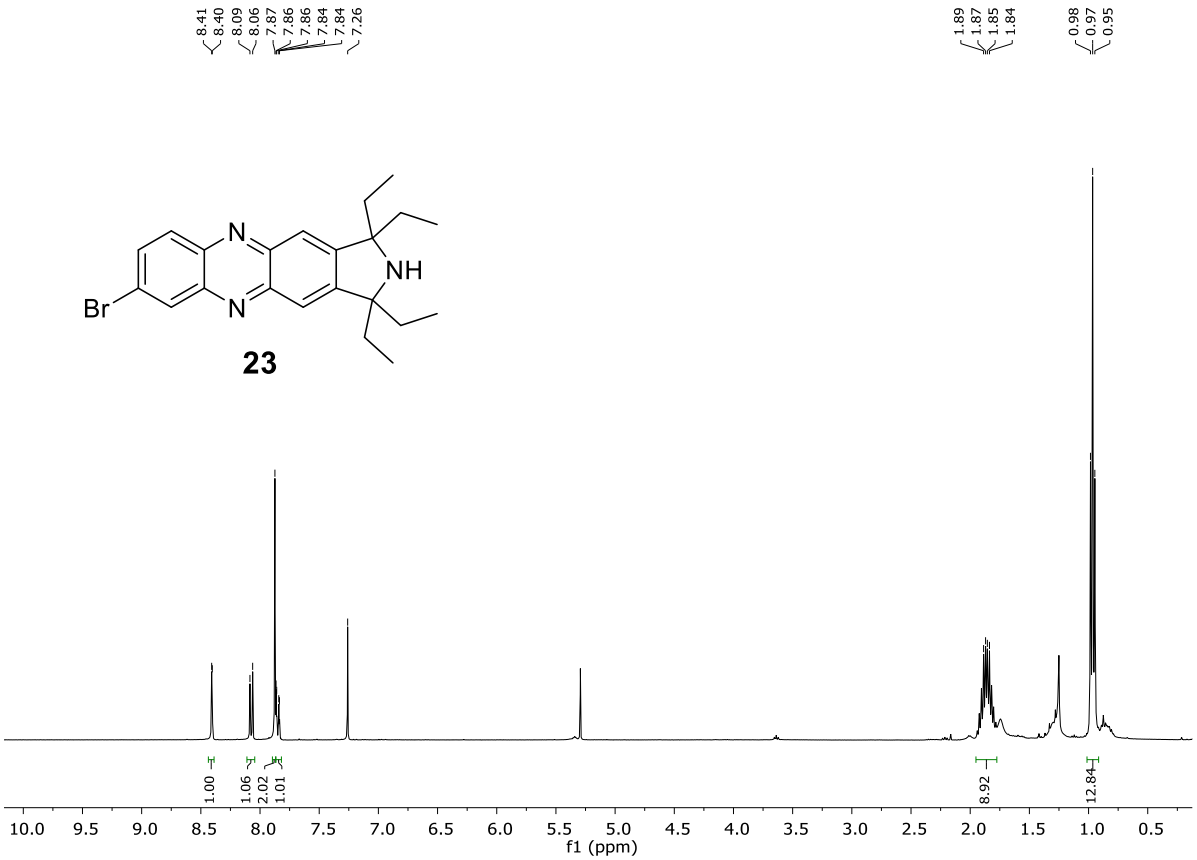

Figure S22. ^{1}H-NMR spectrum of Ethylbromo phenazine derivative **23.**

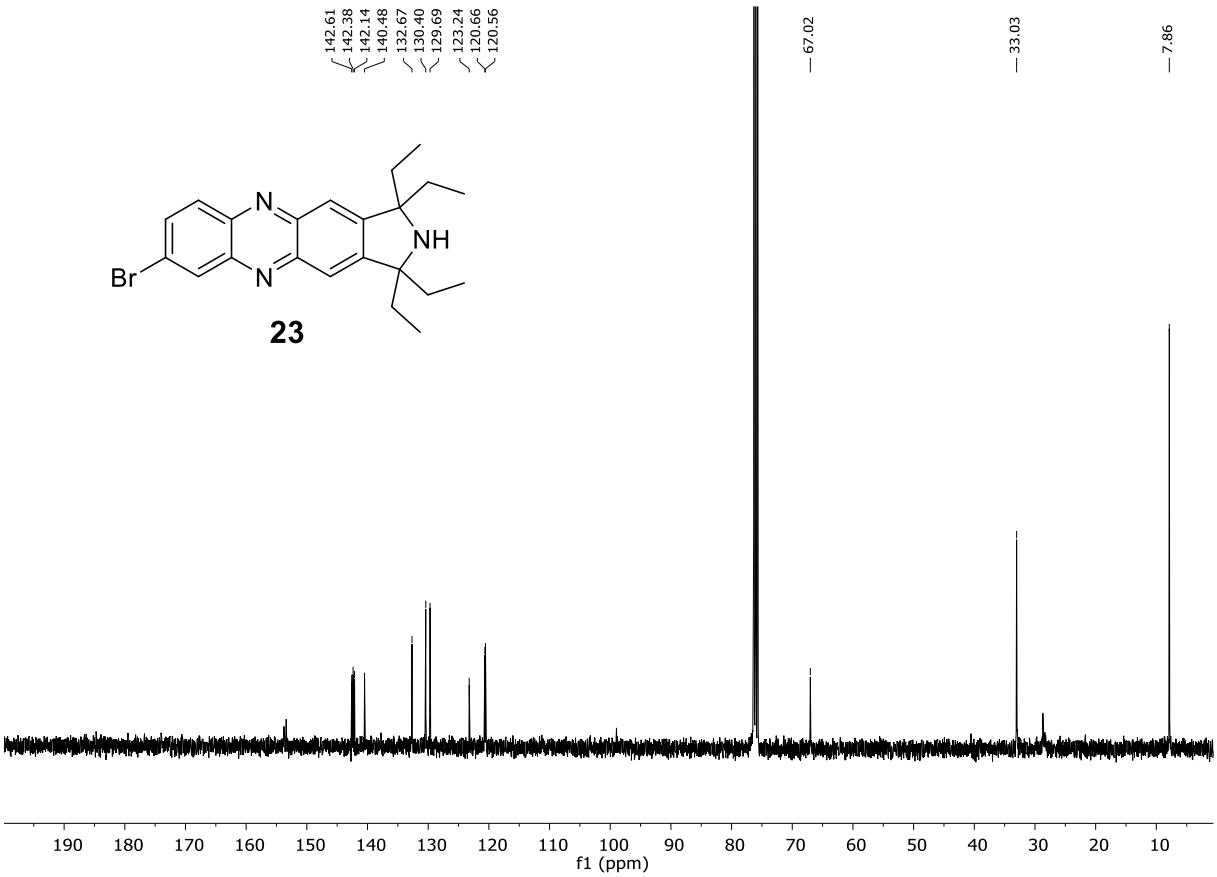

Figure S23. ^{13}C-NMR spectrum of Ethylbromo phenazine derivative **23.**

EPR spectra of Isoindoline-phenazine di-N-oxides

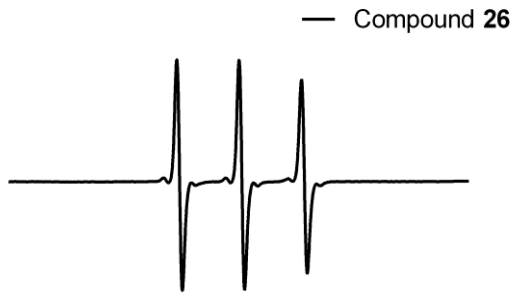

Figure S24. EPR spectrum of compound **26** in CH_2Cl_2 at 22°C.

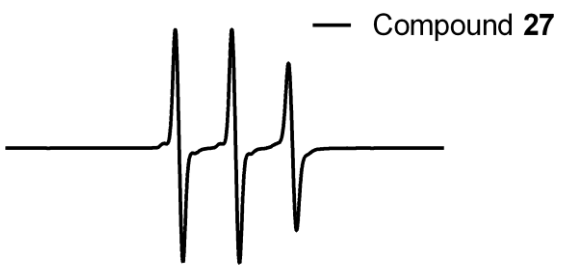

Figure S25. EPR spectrum of compound **27** in CH_2Cl_2 at 22°C.

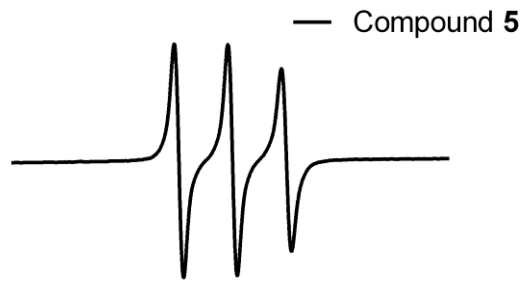

Figure S26. EPR spectrum of compound **5** in EtOH at 22°C.

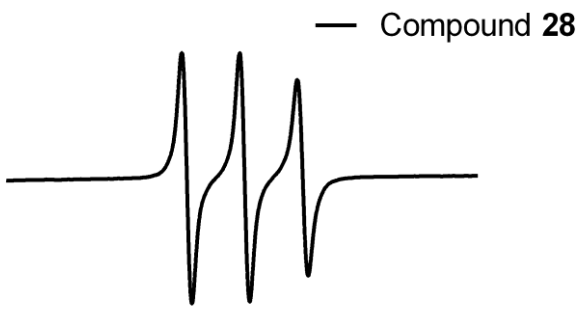

Figure S27. EPR spectrum of compound **28** in EtOH at 22°C.

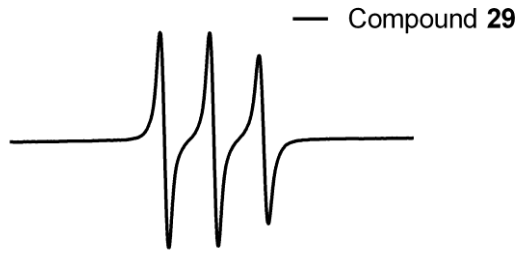

Figure S28. EPR spectrum of compound **29** in EtOH at 22°C.

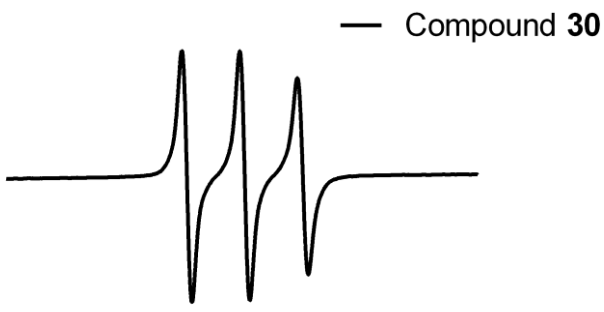

Figure S29. EPR spectrum of compound **30** in EtOH at 22°C.

Comparison of phenazines with their di-*N*-oxides by UV-vis spectroscopy

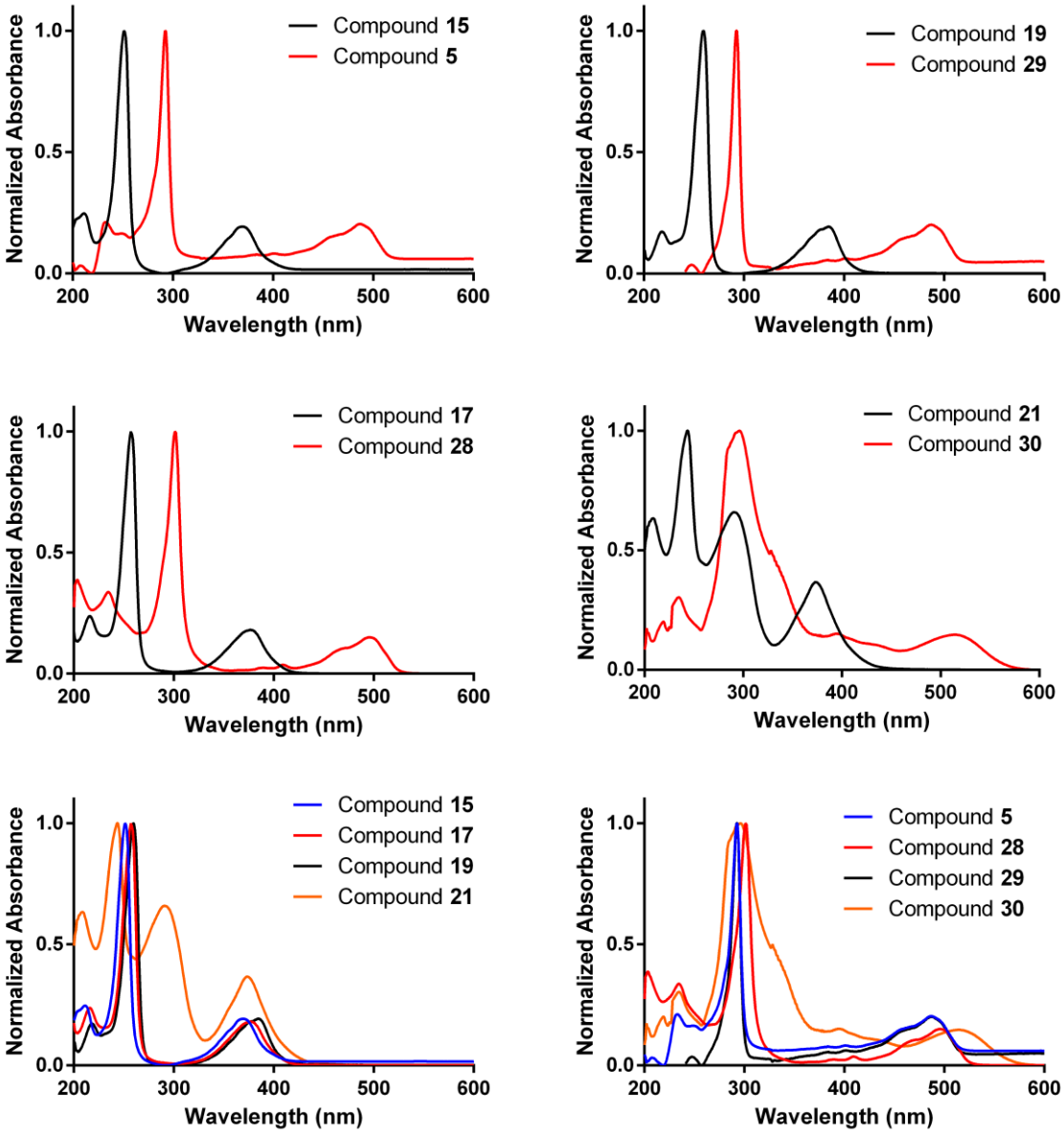

Figure S30. UV-vis spectra of the phenazine derivatives, compared to their oxidized counterparts.

Binding of *N*-oxide phenazines to RNA duplexes monitored by EPR

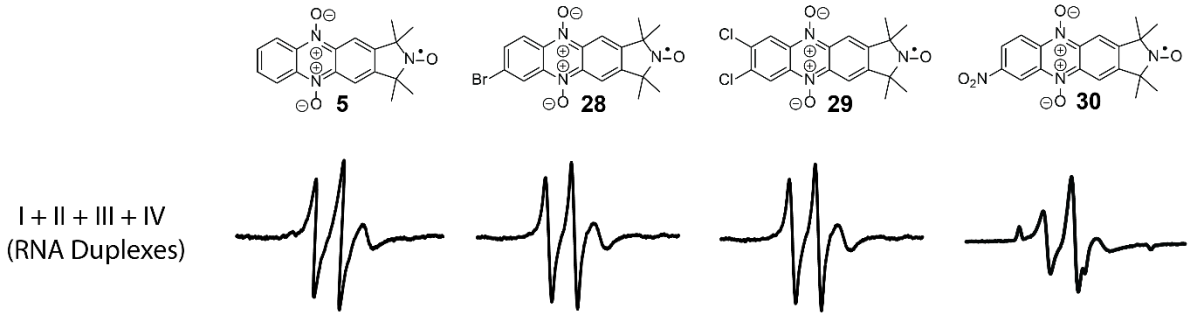

Figure S31. Evaluation of noncovalent spin labeling of abasic sites in RNA duplexes by EPR spectroscopy at -30 °C. Nitroxides **5** and **28**-**30** were screened as per the "combitorial approach" where each sample contained the spin label with four RNA duplexes, each of which contained an abasic site placed opposite to four different orphan bases, A, C, G and U. Each duplex was in twofold excess relative to the spin label. The complete RNA sequence is 5'-GACCUCG_AUCGUG-3'·5'-CACGAUXCGAGGUC)-3', where X represents the orphan base. Duplex **I** X=C, **II** X=A, **III** X=G, **IV** X=U. EPR spectra of the spin-labels (100 μM) in the presence of RNA duplexes (200 μM) were recorded in phosphate buffer (10 mM $NaHPO_4$, 100 mM NaCl, 0.1 mM Na_2EDTA, pH 7.0) containing 30% ethylene glycol and 2% DMSO at -30 °C.

Determination of dissociation constants (K_d)

An in-house MATLAB-based program was used to calculate dissociation constants (K_d).[1] The EPR spectrum of **5** and the EPR spectrum of **5** in the presence of duplex nucleic acid containing an abasic site were double-integrated[2] and normalized with respect to their area. The normalized spectrum of **5** was fractionally subtracted from the normalized spectrum of **5** in the presence of a duplex nucleic acid to get the visually best fit to a fully bound spectrum. The fraction value $\propto$ was used to calculate the dissociation constant (K_d) using the following equation:

$$K_d = \frac{[Y - (1-\propto) * \mathrm{X}][\propto * \mathrm{X}]}{(1-\propto) * \mathrm{X}}$$

Where X is the initial concentration of the spin label and Y is the initial concentration of the duplex nucleic acid that contains an abasic site.

References

[1] a) S. A. Shelke, S. T. Sigurdsson, *Angew. Chem. Int. Ed.* **2010**, *49*, 7984-7986; b) N. R. Kamble, S. T. Sigurdsson, *Chem. Eur. J.* **2018**, *24*, 4157-4164.

[2] a) A. Schick, H. Rager, *Appl. Magn. Reson.* **1993**, *4*, 367-375; b) V. N. Zinchenko, *Meas. Tech.* **1975**, *18*, 741-742.